# EXCITATORY AMINO ACID RECEPTOR-MEDIATED EVENTS IN THE BRAIN: QUANTITATIVE AUTORADIOGRAPHIC STUDIES.

SUSAN E. BROWNE, B.Sc. (HONS)

A thesis submitted for the Degree of Doctor of Philosophy
to the Faculty of Medicine, University of Glasgow

Wellcome Surgical Institute & Hugh Fraser Neuroscience Laboratories,
University of Glasgow,
Garscube Estate, Bearsden Road, Glasgow G61 1QH.



ProQuest LLC.
789 East Eisenhower Parkway
P.O. Box 1346
Ann Arbor, MI 48106 – 1346

## CONTENTS

PAGE NOS.

## CHAPTER II - METHODS

PAGE NOS.

LIST OF TABLES:

PAGE NOS.

AFTER PAGE NO.

LIST OF FIGURES:

ACKNOWLEDGEMENTS

I have thoroughly enjoyed my time in Glasgow, thanks largely to the kindness, generosity and humour of everyone at the Wellcome Surgical Institute, who all went out of their way to make me feel at home - even though I am a Sassenach!

My greatest thanks must go to Professor James McCulloch, whose immense neuroscientific knowledge and ebullient enthusiasm have served to fuel my research endeavours. I feel confident that the experimental rigour he has instilled in me will serve me well in my future career. I should also add that my extracranial circulatory system and I will certainly miss his irrepressible repartee.

I extend my thanks to Professor Murray Harper for his support and guidance throughout my studies, as well as for the provision of such excellent laboratory facilities. In addition, I would like to thank Debbie Dawson, Dr. Debbie Dewar, Gail Gartshore, Dr. Karen Horsburgh, Kenny Mackay, Dr. Mhairi Macrae, Dr. Moira McAuley, Mark McLaughlin, Tosh Patel and Dr. Brian Ross for their help in numerous aspects of laboratory work, and particularly for their efforts in forcing me to go out for the odd drink or two (hundred) over the years.

I must also acknowledge the technical assistance of the staff of the biochemical laboratories, and I thank Hayley-Jane Dingwall, Lindsay Dover, Michael Dunne, Margaret Roberts, Marion Steele, Joan Stewart and Margaret Stewart, without whose expert guidance I would probably still be toiling over a hot (?) cryostat. Thanks are also extended to Gordon Littlejohn, Dr. Joyce Ferguson, and to all the animal nurses, under the supervision of Christine

Stirton and Morag Findlay. In addition, the photographic work in this thesis was produced by Mr. Allan May of the Department of Photography, and Mrs. Ann Marie Colquhoun and Mrs. Jean Pearce provided excellent secretarial assistance.

A portion of the work comprising this thesis was performed in collaboration with Dr. Barry Everitt, Dr. Trevor Robbins and Dr. Janice Muir from the Departments of Anatomy and Experimental Psychology, University of Cambridge. I am indebted to them for performing the basal forebrain lesions and infusions, and for their scientific guidance. I would also like to thank Dr. Hirosuke Fujisawa for performing the cortical glutamate perfusions, and Dr. Kazuhiro Kusumoto for performing MCA occlusions.

My especial thanks must be extended to Lyndsay Graham who had the unenviable task of typing this thesis. I have been constantly amazed by her speed, accuracy, patience, and the fact that she put up with my demands and indecisiveness with such perpetual good humour.

Finally, I would like to thank my family and all the friends I have made during my time in Scotland. In particular, thanks to Kate, Karen, Lisa and Andrew for being the greatest of friends throughout - and especially over the last year! Most of all, many thanks to my parents, who have given me the greatest possible encouragement and support for as long as I can remember.

## SUMMARY

The effects of pharmacological and pathological manipulations of excitatory amino acid receptor-mediated events in the rat brain were investigated using quantitative *in vivo* autoradiographic procedures. [$^{14}$C]-2-Deoxyglucose *in vivo* autoradiography was used to measure local rates of cerebral glucose utilisation in discrete brain regions, following systemic administration of agents acting at AMPA and NMDA receptor subtypes, to assess physiological changes in cerebral metabolism occurring in response to pharmacological challenge. Secondly, in order to assess *in vivo* the effects of systemic administration of an agent which putatively modulates NMDA receptor activity, [$^{125}$I]-MK-801 *in vivo* autoradiography was used to measure levels of NMDA receptor activation throughout the brain. Thirdly, [$^{14}$C]-2-deoxyglucose *in vivo* autoradiography was used to assess the chronic and acute cerebral metabolic effects of manipulating discrete populations of neurones by microinjections of excitatory amino acid agonists into the basal forebrain.

### AMPA Receptor Blockade

Local cerebral glucose utilisation was examined in 50 discrete CNS regions acutely after intravenous administration of the AMPA receptor antagonists NBQX (10, 30 and 100mg/kg) and the novel agent LY-293558 (10, 30 and 100mg/kg) to conscious rats. Both agents markedly depressed glucose use throughout the brain, producing anatomically widespread, dose-dependent reductions in glucose use in the majority of regions examined. No elevations in glucose use were seen in any of the regions examined following administration of either agent.

Following NBQX (100mg/kg), statistically significant decreases in glucose use were seen in 48 of the 50 regions investigated, while significant reductions following LY-293558 (100mg/kg) occurred in 43 regions. The magnitudes of the glucose use depression seen following both NBQX (100mg/kg) and LY-293558 (100mg/kg) were as great as any previously reported with any pharmacological intervention. Rates of glucose utilisation were reduced by 50-68% in many auditory, cortical and limbic regions by the highest dose of the AMPA antagonists. For example, NBQX (100mg/kg) and LY-293558 (100mg/kg) reduced glucose use by -64% and -68% respectively in the inferior colliculus; -64% and -64% respectively in the posterior cingulate cortex; and -50% and -55% respectively in sensory motor cortex (layer IV).

The anatomical patterns of reduced glucose use following NBQX and LY-293558 were essentially similar. However, in a number of regions subtle anomalies were evident in the nature of the response to the two AMPA antagonists. For example, LY-293558 was more potent than NBQX by a factor of 2-3 in auditory structures, and in a number of limbic and cortical regions. In addition, LY-293558 at any dose failed to significantly affect glucose use in 7 of the regions examined, whereas glucose use was unchanged in 2 regions following NBQX. In one of the CNS regions examined, the superficial layer of the superior colliculus, glucose utilisation was insensitive to both NBQX and LY-293558 within the dose ranges studied.

In this study, the advantages of using the [$^{14}$C]-2-deoxyglucose autoradiography technique to map dynamic functional events *in vivo* are highlighted by its ability to discern subtle dissimilarities in the regional effects of the two AMPA antagonists. The glucose use depression produced by AMPA

receptor blockade is in marked contrast to the previously reported heterogeneous effects of competitive and non-competitive NMDA antagonists.

**NMDA Receptor Manipulation**

Local cerebral glucose utilisation was investigated in conscious rats acutely after intravenous administration of D-cycloserine (0.3, 3 and 30mg/kg), a partial agonist at the glycine regulatory site on the NMDA receptor complex. The concentration range employed was chosen on the basis of reported dose-dependent agonist and antagonist properties of D-cycloserine *in vivo*. D-Cycloserine failed to significantly alter glucose use in any of the 51 brain regions examined.

In a separate study, [$^{125}$I]-MK-801 *in vivo* autoradiography was used to assess NMDA receptor potentiation in the brain by a putative agonist dose of D-cycloserine (3mg/kg, i.v.). Results were compared with levels of [$^{125}$I]-MK-801 binding in conscious and anaesthetised rats following intravenous administration of vehicle. No significant differences in the concentrations of bound [$^{125}$I]-MK-801 were found between D-cycloserine and vehicle-treated rats, in any of the 13 CNS regions investigated, including regions with high concentrations of NMDA receptors such as the hippocampus region CA1, and posterior cingulate cortex.

In view of the apparent lack of effect of D-cycloserine on cerebral glucose use and [$^{125}$I]-MK-801 binding *in vivo*, the effects of D-cycloserine on NMDA receptor-mediated events were further investigated under pathological conditions in the rat brain. Two models of glutamate neurotoxicity were employed: the middle cerebral artery (MCA) occlusion model of focal cerebral ischaemia, and

a novel model of cortical neurotoxicity produced by intracortical glutamate perfusion. Intravenous administration of a putative agonist concentration of D-cycloserine (3mg/kg) had no significant affect on the extent of neuronal damage produced by MCA occlusion (lesion size: vehicle, 191 ± 30mm$^3$; D-cycloserine, 189 ± 40mm$^3$), or by cortical glutamate perfusion (lesion size: vehicle, 20.3 ± 1.3mm$^3$; D-cycloserine, 20.3 ± 2.1mm$^3$). The integrity of the cortical lesion model was verified by the demonstration of neuroprotection by pretreatment with the AMPA receptor antagonist NBQX (30mg/kg) (lesion size: vehicle, 14.4 ± 0.7mm$^3$; NBQX, 11.1 ± 0.7mm$^3$).

The results of these studies highlight a situation in which quantitative *in vivo* [$^{14}$C]-2-deoxyglucose and [$^{125}$I]-MK-801 autoradiography techniques fail to provide insight into the functional consequences of a pharmacological manipulation.

**Basal Forebrain Manipulations**

The chronic effects of excitotoxic basal forebrain lesions on local cerebral glucose utilisation were assessed in 49 brain regions chronically (3 weeks) after infusions of ibotenic acid, NMDA, quisqualic acid or AMPA into the nucleus basalis magnocellularis (NBM) region, which provides the major cholinergic innervation of the neocortex. No significant alterations in glucose utilisation were evident in any of the brain regions examined, including 11 cortical regions, following ibotenate, NMDA, quisqualate or AMPA-induced NBM lesions. Trends towards reduced glucose use in frontal cortical regions were evident following AMPA-induced lesions, most marked in medial prefrontal cortex (vehicle: 83 ± 3, AMPA: 67 ± 6, mean ± SEM μmol/100g/min). The lack of significant

alterations in cerebral glucose use levels 3 weeks post-lesion supports previous reports of compensatory functional adaptation following denervation in the brain, despite biochemical evidence of sustained deficiencies in other indices of functional activity (e.g. cholineacetyltransferase, ChAT activity).

In a separate series of experiments, the acute effects of basal forebrain neuronal stimulation on cerebral glucose use were investigated in conscious rats following excitatory amino acid agonist infusions into the NBM. Infusions of NMDA and AMPA resulted in significant alterations in glucose use in cortical regions innervated by NBM efferents. Glucose use was significantly reduced in 10 cortical regions following AMPA, (for example, by -27% in medial prefrontal cortex, -23% in sensory motor cortex (layer IV), and -25% in anterior cingulate cortex), and in two cortical regions following NMDA (for example, by -26% in prefrontal cortex). Both agents also induced heterogeneous alterations in glucose utilisation in a number of subcortical regions corresponding to primary and secondary striato/pallidal projection targets, including the substantia nigra (pars reticulata and pars compacta), the entopeduncular nucleus, subthalamic nucleus, and lateral habenular nucleus. The glucose use alterations in subcortical regions distal to the infusion site appear to be associated with the marked hypermetabolic effects of AMPA and NMDA in regions anatomically close to the infusion site, including striatum and globus pallidus. The effects of excitatory amino acid infusions were compared with the cerebral metabolic sequelae of infusion of the $GABA_A$ agonist muscimol into the NBM region. Muscimol did not significantly alter rates of glucose utilisation in neocortical regions, or in the vicinity of the infusion site. However, muscimol did induce heterogeneous alterations in glucose use in a number of subcortical nuclei,

including entopeduncular nucleus and substantia nigra.

The studies in this thesis serve to highlight both the strengths and weaknesses of using autoradiographic approaches to map functional events *in vivo*. In particular, it is evident that the unique opportunity afforded by the [$^{14}$C]-2-deoxyglucose technique, to assess alterations in cerebral metabolic activity in terms of local cerebral glucose use, is optimally exploited in conditions of acute pharmacological or pathological challenge where dynamic functional changes are likely to occur.

## PREFACE AND DECLARATION

This thesis presents results from autoradiographic studies in rat brain, investigating the functional consequences of manipulating glutamatergic systems within the CNS. The principal technique used was quantitative [$^{14}$C]-2-deoxyglucose autoradiography, to measure local cerebral glucose utilisation *in vivo*. [$^{125}$I]-MK-801 autoradiography was used to assess NMDA receptor activation *in vivo*. The effects of glutamatergic agents on glutamate-induced lesions were also assessed histologically.

Investigations were conducted in three broadly defined areas:

1. The effects of intravenous administration of AMPA receptor antagonists on local cerebral glucose use in the rat.
2. The effects of intravenous administration of the NMDA receptor glycine site partial agonist D-cycloserine on local cerebral glucose use, [$^{125}$I]-MK-801 binding, and on glutamate-induced neuronal damage.
3. The chronic and acute effects of basal forebrain manipulations on local cerebral glucose use.

Results from these studies are presented and discussed separately. In the final overview I have attempted to highlight the advantages and limitations of using quantitative autoradiographic techniques to assess putative functional alterations in the CNS.

This thesis comprises my own original work and has not been presented previously as a thesis in any form.

# CHAPTER I

# INTRODUCTION

# 1. THE ROLES OF GLUTAMATE WITHIN THE CNS

## 1.1 Glutamate Is The Major Excitatory Neurotransmitter In The CNS.

Glutamate is a non-essential amino acid found in abundance in the central nervous system (CNS) where it subserves a number of different roles. For many years glutamate has been known to be intimately involved in intermediary metabolism in the CNS, with roles in the Krebs Cycle (Krebs, 1935), in the detoxification of ammonia in the brain (Weil-Malherbe, 1950), as a precursor of the inhibitory neurotransmitter γ-aminobutyric acid, GABA (Roberts and Frankel, 1950), and is involved in peptide and protein synthesis (Meister, 1979). However, an increasingly large body of physiological and biochemical evidence indicates that, in addition, glutamate is the major excitatory neurotransmitter within the CNS.

A transmitter role for endogenous amino acids including glutamate and aspartate was first proposed in the 1950s following observations that these compounds could activate CNS neurones. In 1954 Hayashi found that topical application of sodium-glutamate to neocortex of dogs, monkeys and humans resulted in "clonic convulsions", while in initial electrophysiological studies Curtis et al., (1960) demonstrated that microiontophoretic application of glutamate to single spinal neurones increased their firing rate. Subsequent structure-activity relationship studies of glutamate analogues identified L-glutamate and L-aspartate as the leading candidates for endogenous excitatory neurotransmitters in the mammalian CNS (Curtis and Johnston, 1974).

Evidence supporting the concept of glutamate as a neurotransmitter in the CNS has been extensively reviewed (Di Chiara and Gessa, 1981; Fonnum,

1984; Collingridge and Lester, 1989; Monaghan et al. 1989; Headley and Grillner, 1990). Briefly, there are four main criteria which compounds must satisfy to warrant classification as a neurotransmitter. These are:-

a) Presynaptic localisation in specific neurones.

b) Release in response to physiological stimuli in concentrations high enough to evoke a post-synaptic response.

c) The existence of mechanisms to rapidly terminate transmitter activity.

d) Their actions must be compatible with those of the naturally occurring transmitter, for example in response to antagonists.

Glutamate satisfies these criteria to varying degrees, as is briefly described below.

a) Presynaptic Neuronal Location

Attempts to locate glutamate-releasing nerve terminals have been complicated by the diversity of glutamate-mediated functions within the CNS and the existence of multiple metabolic pools of glutamate. At present no precursors or synthetic enzymes are known to be specific for the transmitter pool of glutamate, and hence no reliable enzyme marker for glutamatergic terminals is yet available. However, support for a presynaptic localisation of glutamate in terminals has been provided by the demonstration of selective, adenosine triphosphate (ATP) - dependent uptake of exogenous glutamate into synaptic vesicles (Naito and Ueda, 1985). Further, the pattern of glutamate-like immunoreactivity in synaptic vesicles in neuronal terminals has been found to be similar to the previously reported distribution of high-

affinity glutamate uptake sites in rat brain (Ottersen and Storm-Mathisen, 1984b; Fonnum, 1984). More recently, the identification of carrier-mediated glutamate uptake mechanisms in neuronal terminals has further supported a presynaptic localisation of glutamate. A $Na^+$-dependent glutamate uptake carrier has been identified in presynaptic neuronal (and glial) plasma membranes, while the discovery of a $Na^+$-independent vesicular glutamate transporter has demonstrated compartmentalisation of a presumed transmitter pool of glutamate into synaptic vesicles within the presynaptic terminal, from where exocytotic vesicular release occurs (Nicholls and Attwell, 1990; see also b) and c) below).

b) Glutamate Release from Neurones by Physiological Stimuli

Substantial evidence is available that glutamate is released from neurone terminals in response to physiological stimuli (Fonnum, 1984; Greenamyre, 1986; Headley and Grillner, 1992; for review see Nicholls, 1993). Membrane depolarisation, by means of electrical or pharmacological stimulation, has been demonstrated to induce calcium ($Ca^{2+}$) -dependent glutamate release in brain slice preparations (Potashner, 1978), in isolated neurone terminal (synaptosome) preparations (for review see Nicholls and Attwell, 1990; McMahon and Nicholls, 1991), and *in vivo* by means of microdialysis techniques (Hamberger et al., 1983).

There are several examples of synaptic aspartate/glutamate release following stimulation of specific nerve pathways *in vitro*. For example,

exogenously added D-aspartate or L-glutamate is released in hippocampal slice preparations by stimulation of the Schaffer collateral pathway or the commissural pathway, and from the lateral septum in the septum-fimbria preparation (for review see Fonnum, 1984). In addition, Collins (1980) demonstrated release of endogenous amino acids after stimulation of the lateral olfactory tract in the olfactory cortical slice preparation. Glutamate release in a number of anatomical pathways has also been demonstrated *in vivo*. For example, Abdul-Ghani et al., (1979) reported glutamate release from the sensorimotor cortex after stimulation of the contralateral bronchial plexus, while Granata and Reis (1983) found that vagus nerve stimulation induced glutamate and aspartate release in the nucleus tractus solitarius region.

Early studies suggested that the amino acid transmitters were released directly from cytoplasm in nerve terminals (for review see Fonnum, 1984). However recent advances have identified a vesicular release mechanism. In 1989 Nicholls reported that prolonged depolarisation of cortical or hippocampal guinea-pig synaptosome preparations, by KCl application, resulted in $Ca^{2+}$-dependent release of 15% of the total synaptosomal glutamate content. Further studies indicated that this release occurred from a vesicular compartment by means of exocytosis, probably triggered by a high cytoplasmic calcium concentration, $[Ca^{2+}]_i$ (Nicholls and Attwell, 1990). However, there is also evidence of carrier-mediated $Ca^{2+}$-independent release of cytoplasmic glutamate occurring in circumstances of chronic plasma membrane depolarisation. Although this carrier-mediated glutamate

release, putatively due to reversal of the plasma membrane glutamate uptake carrier, is negligible during the millisecond time-course of normal physiological depolarisation, it does appear to contribute to the massive release of glutamate occurring in excitotoxic situations such as ischaemia (for review see Nicholls and Attwell, 1990; Nicholls, 1993).

There is also evidence from *in vitro* studies that a number of endogenous neurotransmitter systems may be involved in the regulation of glutamate release. For example, phorbol esters have been found to increase glutamate release from synaptosomes by 30% (Diaz-Guerra et al., 1988), while other agents including $GABA_B$, adenosine and muscarinic receptor agonists have been shown to reduce glutamate release in synaptosome preparations (Burke and Nadler, 1988; Marchi et al., 1989).

c) Rapid Termination of Neurotransmitter Activity

Mechanisms for rapid termination of transmitter activity, by removal of the excitatory amino acids from the synaptic cleft, are vital to maintain normal physiological extracellular glutamate concentrations (approximately 1μM) and hence avoid the excitotoxic effects of sustained high concentrations of glutamate. A sodium-dependent high-affinity uptake carrier is responsible for transport of L-glutamate and D- and L-aspartate, against a concentration gradient, into both presynaptic neuronal terminals and glial cells (Nicholls and Attwell, 1990; Schousboe et al., 1992). Glutamate uptake into glial cells has also been shown to be $K^+$-dependent, reduced intracellular $K^+$ or raised extracellular $K^+$

levels inhibiting uptake (Barbour et al., 1988). Neuronal glutamate uptake can be inhibited by membrane depolarisation, while glial uptake can be blocked by arachidonic acid (Barbour et al., 1989). The latter may be an important observation since there is evidence of arachidonic acid release into the extracellular space following activation of post-synaptic NMDA receptors (Dumuis et al., 1988) which could contribute to the high extracellular levels of glutamate seen in ischaemia. Inhibition of the sodium-dependent high affinity uptake system for glutamate, prolongs the excitatory action of L-glutamate (Johnston et al. 1980), confirming the importance of this uptake system in terminating glutamate's synaptic activity.

Glutamate taken up into astrocytes is converted into glutamine by glutamine synthetase (for review see Schousboe et al., 1992). Glutamine is then released from the glial cells into the extracellular space from where it is taken up into the presynaptic terminal by a low affinity $Na^+$-dependent pathway (McMahon and Nicholls, 1990). It has been postulated that glutamine is converted to cytoplasmic glutamate by mitochondrial glutaminase, although this step has yet to be confirmed. Glutamate is then transported into synaptic vesicles by a $Na^+$-independent, glutamate-specific transport system, reliant on an internal positive membrane potential which is maintained by an ATP-ase pump moving protons into the vesicle (Nicholls and Attwell, 1990).

d) Compatible Action With Endogenous Neurotransmitter

The synthesis of a number of specific agonists and antagonists has been an important factor in the identification and characterisation of glutamate receptors and glutamatergic pathways. In particular, the employment of excitatory amino acid receptor antagonists in a great number of studies has provided unequivocal support for glutamate's neurotransmitter role, by blocking post-synaptic responses to both exogenous glutamate, and the endogenous transmitter *in vivo*. As a consequence, multiple distinct post-synaptic receptor types have been identified (which will be discussed in detail in Section 1.2). Briefly, these are the ionotropic (ion channel-associated) NMDA, AMPA and kainate (KA) receptors, and the metabotropic receptor. At present, the most potent and specific antagonists have been developed for the NMDA receptor subtype. NMDA antagonists have been shown to block excitation of corticofugal fibres in the cuneate nucleus, caudate nucleus and cerebral cortex following cortical stimulation (Stone, 1979). In addition, Cotman et al. (1981) have demonstrated the existence of a number of glutamatergic pathways in the hippocampus which are differentially susceptible to blockade by different classes of glutamate receptor antagonists. Studies employing NMDA antagonists have also indicated that NMDA receptor activation is necessary for the induction and maintenance of long term potentiation (LTP), the mechanism of enhanced synaptic activity which is thought to be a critical component of learning and memory processes (Collingridge and Bliss, 1987; Ben-Ari et al., 1992).

Taken together these observations have led to glutamate being accepted as the major excitatory neurotransmitter in the mammalian CNS. In addition, evidence of the effects of lesions on high-affinity uptake and release have been useful in identifying the components of glutamatergic pathways, although the necessity of glutamate uptake for metabolic processes makes interpretation of such studies difficult (for review see Headley and Grillner, 1990).

There is still the possibility that L-aspartate and other amino acids may also contribute to excitatory transmission in the CNS. $Ca^{+}$-dependent release of endogenous L-aspartate from isolated terminal preparations has previously been demonstrated, although it constitutes at most only 10% of the amount of $Ca^{2+}$-dependent glutamate release (McMahon and Nicholls, 1990), which would be consistent with the observed specificity of the synaptic vesicle uptake carrier for L-glutamate alone (Nicholls and Attwell, 1990). Three other agents also partially fulfil the criteria for transmitters at synapses mediated by excitatory amino acid receptors. For instance, N-Acetyl-aspartylglutamate (NAAG) has been found to be selectively distributed in the CNS, with highest levels found in the spinal cord and hind brain, and lower levels in the forebrain. Evidence suggests that NAAG may be localised in presynaptic terminals, it has been shown to displace [$^{3}$H] glutamate binding in some CNS regions, and it also has identity of action with the endogenous transmitter in several pathways. In particular, NAAG has been implicated as the transmitter at the lateral olfactory tract - piriform cortex synapse, where evidence suggests glutamate and aspartate are not the principle transmitters (Ffrench-Mullen et al., 1985). Secondly, quinolinate, an

endogenous kynurenene acting primarily on NMDA receptors, also fulfils many of the criteria for neurotransmitter status, but has not yet been shown to be released by physiological stimuli (Stone and Burton, 1988). In addition, L-homocysteate has been postulated to have a neurotransmitter role on the basis that it can be released from many brain regions by veratridine-induced depolarisation (Do et al., 1986).

## 1.2 Glutamate Receptor Subtype Classification

The recent development of a large number of excitatory amino acid antagonists has led to the discovery that several distinct receptor types mediate excitatory synaptic transmission induced by glutamate and its congeners (for reviews see Collingridge and Lester, 1989; Monaghan et al., 1989; Watkins et al., 1990). To date five receptor classes have been identified, of which three are ion-channel-linked (ionotropic) receptors, named after their preferred agonists:- N-methyl-D-aspartate (NMDA), kainate (KA), and α-amino-3-hydroxy-5-methylisoxazole-4-propionic acid (AMPA). The fourth is the metabotropic receptor, which is linked to a second messenger system, and is preferentially activated by quisqualate and *trans*-1-aminocyclopentane-1,3-dicarboxylic acid (*trans*-ACPD). Finally, a putative presynaptic autoreceptor sensitive to L-2-amino-5-phosphonobutyrate (L-AP4) has been described although this receptor is the least well characterised at present. (For summary see Table 1, page 50.)

The identification of NMDA, KA and AMPA receptors arose largely from two lines of evidence:- differential sensitivity analysis (rank ordering of agonist potency in different neuronal types) and studies of

RESTING :
(Channel Closed)

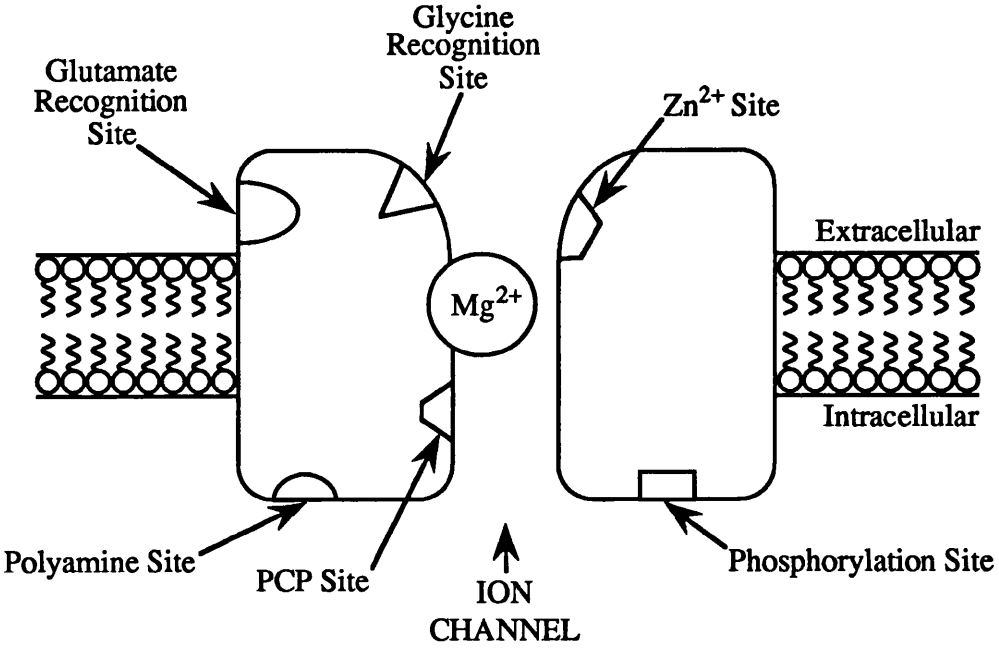


ACTIVATED :
(Channel Open)

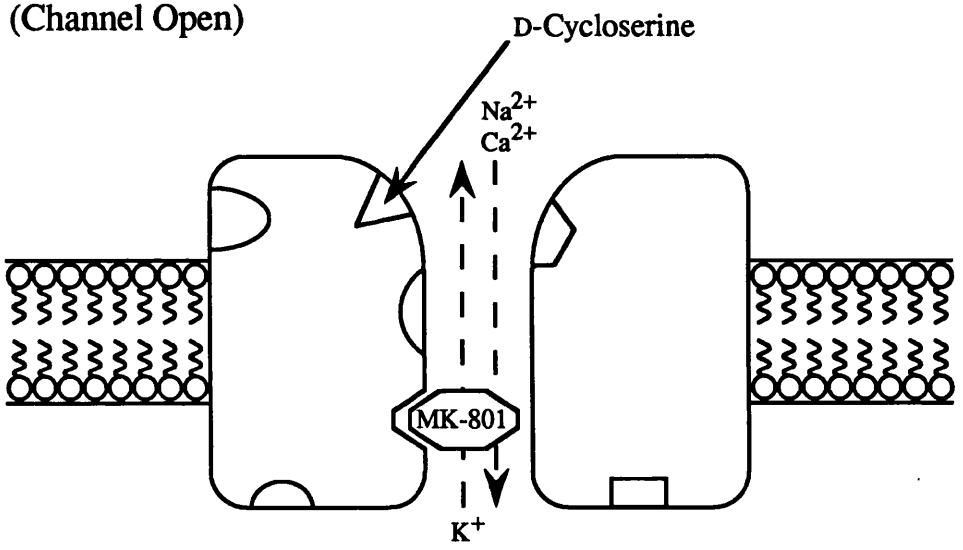


FIGURE 1: SCHEMATIC REPRESENTATION OF THE NMDA RECEPTOR-CHANNEL COMPLEX

pharmacological antagonism. The endogenous amino acids L-glutamate and L-aspartate have mixed agonist activity, glutamate acting at all receptor subtypes whereas L-aspartate is relatively selective for the NMDA receptor (for review see Mayer and Westbrook, 1987a). Stimulation of KA and AMPA receptor subtypes induces generation of fast excitatory post-synaptic potentials (EPSPs), whereas the NMDA receptor can only be activated after depolarisation and appears to be involved in amplification of excitatory responses (MacDermott and Dale, 1987). This property has led to the proposal of critical roles for NMDA receptors in the mechanisms of synaptic plasticity and induction and maintenance long-term potentiation (LTP), involvement in burst firing such as that seen in epilepsy, and a role in the induction of neuronal degeneration in certain pathological conditions.

### 1.2.1 The NMDA Receptor

The availability of high affinity agonists and antagonists, and the use of radioligand binding assays, has meant that NMDA receptors are to date the most fully characterised of the glutamate receptor subtypes (for review see Cotman and Iversen, 1987). The signal transduction and pathophysiological properties of the NMDA receptor-channel complex depend on three major characteristics of the complex:- its voltage-dependence, $Ca^{2+}$ permeability, and the existence of a number of functional domains at which receptor activity can be modulated (see Figure 1).

*Channel Properties*

NMDA receptor activation by glutamate, aspartate and related amino acids evokes a voltage-dependent conductance in neurones by opening the receptor complex-associated cation-permeable ion channel. Under physiological conditions NMDA receptor agonists induce an inward current, carried by an influx of $Na^+$ ions and balanced by an efflux of $K^+$ ions (Mayer and Westbrook, 1987a; Ascher and Nowak, 1987).

At resting membrane potentials the channel is voltage-dependently blocked by $Mg^{2+}$ which binds to a site within the channel (Mayer and Westbrook, 1987b; Ascher and Nowak, 1987; Bekkers and Stevens, 1993). This phenomenon is thought to underlie the voltage-dependency of NMDA-mediated firing (for review see MacDonald and Nowak, 1990). *In vitro* studies have demonstrated that addition of physiological concentrations of $Mg^{2+}$ to hippocampal cells in magnesium-free solutions prevents NMDA-evoked neuronal firing, unless the cell membrane is depolarised sufficiently to remove the $Mg^{2+}$ ion channel blockade (Ascher and Nowak, 1987).

The NMDA receptor channel is permeable to $Ca^{2+}$, hence linking NMDA receptor activation to a number of physiological and pathological events (MacDermott et al., 1986; Mayer and Westbrook, 1987b; Ascher and Nowak, 1988b). $Ca^{2+}$ mediates activity in a variety of intracellular biochemical processes, and $Ca^{2+}$ influx via the NMDA receptor channel (rather than through voltage-sensitive $Ca^{2+}$ channels) has been proposed to contribute to the induction of long-term potentiation (LTP) (Malenka et al., 1988), and to excitotoxic neuronal degeneration (Choi, 1987; Abele et al., 1990; see also Section 2.1).

Recent *in vitro* studies have indicated that channel activity may also be regulated by pH. Electrophysiological recordings from hippocampal neurones suggest that $H^+$ can attenuate NMDA receptor-mediated ion influx (Morad et al., 1988), while mild acidosis has been shown to abolish NMDA-activated $Ca^{2+}$ currents, and to attenuate glutamate neurotoxicity and hypoxic neuronal injury in neuronal cultures (Giffard et al., 1990; Tombaugh and Sapolsky, 1990). Consequently, the voltage-independent nature of the $H^+$ blockade has led to the proposal of a putative $H^+$ site near the external membrane surface of the NMDA receptor complex.

NMDA receptor-induced synaptic currents are characteristically slow in onset and of long duration, decaying over several hundred milliseconds. It has been speculated that this long time-course is due to constant reactivation of the receptor by residual glutamate (D'Angelo et al., 1990), however a recent study by Lester and colleagues (1990) suggests that this is not the case. Lester et al., found that the long-lasting NMDA channel activity (induced in membrane patches from cultured hippocampal neurones by application of pulses of glutamate) could be terminated instantaneously by addition of $Mg^{2+}$ but was unaltered by application of the NMDA recognition site antagonist 2-amino-5-phosphonopentanoate (AP5). These results suggest that glutamate does not constantly unbind and rebind to the recognition site, but that the long duration is directly related to the slow dissociation rate of glutamate from the receptor (Lester et al., 1990; Pan et al., 1993). Thus agonists with lower affinity for the recognition site, such as aspartate, evoke shorter duration NMDA-mediated synaptic currents. This observation may have some bearing on the understanding of pathophysiological events mediated

by EAA receptors under conditions in which the proportions of glutamate and aspartate may be disturbed (Burke and Nadler, 1988).

*Pharmacological/Regulatory Domains*

Five distinct sites with potential for pharmacological or regulatory functions have so far been identified on the NMDA receptor complex.

a) **The transmitter recognition site:** NMDA receptors are defined by their high selectivity for a number of ligands including NMDA, NMLA, aspartate and ibotenate (Collingridge and Lester, 1989; see Watkins et al., 1990), and *Gs*-2,4-methanoglutamate which is the most potent and selective NMDA receptor agonist known to date (Lanthorn et al., 1990). Competitive NMDA receptor antagonists such as 3-(2-carboxypiperazin-4-yl)propenyl-1-phosphonate (CPP-ene) and 2-amino-4-methyl-5-phosphono-3-pentanoic acid (CGP-37849) exert their inhibitory action via blockade of the transmitter recognition site (Aebischer et al., 1989; Watkins et al., 1990).

b) **The glycine regulatory site:** NMDA receptor action is enhanced by glycine, an inhibitory neurotransmitter in the CNS (for review see Foster and Kemp, 1989; Kemp and Leeson, 1993). Johnson and Ascher (1987) first showed that glycine increased the frequency of NMDA-induced channel opening in cultured neurones and suggested a mechanism of allosteric regulation of the NMDA receptor complex through a distinct glycine binding site. This co-agonist action of glycine has been shown

to be strychnine-insensitive and thus unrelated to its established role as an inhibitory neurotransmitter in the brainstem and spinal cord, which is mediated by a strychnine sensitive chloride conductance. The idea that the glycine site is an integral part of the NMDA receptor complex is supported by evidence from *in vitro* autoradiographic ligand binding studies of a high degree of co-localisation of strychnine-insensitive [$^3$H]-glycine binding sites with NMDA receptors (Monaghan and Cotman, 1985; Bristow et al., 1986), as well as with NMDA receptor channel-associated PCP binding sites labelled by [$^3$H]-MK-801 and [$^3$H]-TCP, in rat brain (Bowery et al., 1988; Maragos et al., 1988) and in human hippocampus and neocortex (Jansen et al., 1989 a and b). Following the cloning of a functional NMDA receptor subunit, Moriyoshi et al., (1991) have subsequently shown that both the transmitter- and glycine-recognition sites are colocalized on the same protein. D-Serine and D-alanine also bind with high affinity to this strychnine-insensitive glycine binding site. D-serine has subsequently become the agonist of choice in pharmacological studies of the glycine site due to its lack of affinity for both the glycine uptake system and the strychnine-sensitive glycine receptor (Johnson and Ascher, 1987).

It has recently been demonstrated that glycine binding is an absolute requirement for NMDA receptor activation. Kleckner and Dingledine (1988) found that while glycine potentiated the responses of NMDA receptors expressed in *Xenopus* oocytes, no NMDA receptor current could be elicited in the absence of glycine. Glycine enhancement of glutamate-induced synaptic responses has been further supported by

biochemical, electrophysiological and autoradiographical studies both *in vitro* and *in vivo* (Bonhaus et al., 1987; Snell et al., 1987; Wong et al., 1987; Salt et al., 1989; Thomson et al., 1989; Lester et al., 1993), and evidence from radioligand binding studies which implicates reciprocal enhancement of glutamate and glycine binding (Fadda et al., 1988; Monaghan et al., 1988; Hood et al., 1990). It has also been proposed that glycine may exert its potentiating action on NMDA receptor activity by preventing receptor desensitization during prolonged agonist exposure, via a mechanism accelerating the receptor's recovery from it desensitized state (Mayer et al., 1989).

As a consequence of the interdependence of the glycine and glutamate co-agonist sites, modulation of the glycine site has been used experimentally to manipulate NMDA receptor activity. A number of ligands which bind at the glycine site are currently available, including the broad spectrum excitatory amino acid receptor antagonists kynurenate and 7-chlorokynurenate. (+)-HA-966 (3-amino-1-hydroxypyrolid-2-one), (+)-*cis*-4-methyl-HA-966, and D-cycloserine are partial agonists at the glycine modulatory site, exhibiting dose-dependent agonist and antagonist properties (Watson et al., 1990; Emmett et al., 1991; for review see Kemp and Leeson, 1993).

c) **The PCP channel binding site:** A number of chemically dissimilar compounds have been classified as non-competitive NMDA antagonists, acting at a site functionally distinct from the transmitter recognition site. These include "dissociative anaesthetics" such as ketamine

and TCP (N-[I-thienyl]-cyclohexyl-3,4-piperidine), PCP (N-[I-phenylcyclohexyl]-piperidine; phencyclidine), and benzomorphan sigma opiates such as SKF 10047 (N-allyl-normetazocine) (Kemp et al., 1987; Lodge and Johnson, 1990). The most potent of this class of compounds is MK-801 ((+)-5-methyl-10,11-dihydro-5H-dibenzo[a,d]cyclohepten-5,10-imine maleate, dizocilpine; Clineschmidt et al., 1982; Kemp et al., 1987). Antagonism of NMDA-receptor mediated responses by these agents is voltage- and use-dependent, i.e. the receptor must first be activated by an agonist before antagonism can occur. It therefore follows that antagonism is induced by agents binding at a site inside the open NMDA receptor-associated ion channel, resulting in blockade of transmembrane ion fluxes (Honey et al., 1985; Huettner and Bean, 1988; MacDonald and Nowak, 1990).

d) **The polyamine modulatory site:** The modulatory action of polyamines on NMDA receptor activity was first identified when polyamines were found to increase the level of [$^3$H]-MK-801 binding induced by glutamate and glycine (Ransom and Stec, 1988). Subsequent studies have suggested the existence of a specific site in the NMDA receptor complex at which the polyamines spermine and spermidine act as agonists, and putrescine and arcaine are antagonists (for review see Scott et al., 1993). Further *in vitro* studies have shown that spermidine enhances NMDA-induced currents in cultured neurones (Sprosen and Woodruff, 1990), while the competitive inhibition of NMDA-evoked release of [$^3$H]-noradrenaline from brain slices induced by arcaine can be overcome by spermidine

application (Sacaan and Johnson, 1990). Spermidine has also been found to potentiate NMDA-evoked seizures *in vivo* (Singh et al. 1990). In addition, the neuroprotective drug ifenprodil appears to be a non-competitive antagonist at this polyamine site (Reynolds and Miller, 1989).

e) **The $Zn^{2+}$ binding site:** $Zn^{2+}$, a cation which is present in high concentrations in the CNS and which has been shown to be released from synaptic terminals upon excitation, non-competitively inhibits NMDA receptor activation in hippocampal and cortical neurones (Westbrook and Mayer, 1987). As a consequence of the voltage-dependent nature of $Zn^{2+}$ blockade, and the observations that $Zn^{2+}$ reduces the dissociation rates of [$^3$H]-TCP and [$^3$H]-MK-801 binding in rat cortical membranes (opposite to the effects of $Mg^{2+}$), a $Zn^{2+}$ binding site has been proposed, putatively situated within the NMDA receptor-associated channel near the extracellular surface, but distinct from the $Mg^{2+}$ site (Reynolds and Miller, 1988). However, both voltage-dependent and -independent properties of $Zn^{2+}$ action have been identified, suggesting that $Zn^{2+}$-induced blockade may involve a reduction in the frequency of channel opening (Mayer and Vyklicky, 1989). In addition, Yeh and colleagues (1990) found that $Zn^{2+}$ non-competitively inhibited [$^3$H]-glycine binding, and speculated that $Zn^{2+}$ may have a physiological role to reduce tonic activation of the NMDA receptor by glycine, thus reducing channel opening frequency. Therefore, although the exact nature of its receptor interaction is still unclear, $Zn^{2+}$ may play a role

in the regulation of NMDA receptor-mediated processes in the CNS.

Protein phosphorylation of NMDA receptors has also been implicated as an important component of modulatory control of receptor activity (for review see Raymond et al., 1993). Protein kinase-catalysed phosphorylation, at sites on the cytoplasmic domain of the receptor complex, are proposed to result in alterations in the charge and/or conformation of the receptor. Involvement of phosphorylation processes in the mechanism of synaptic plasticity underlying LTP has been proposed, on the basis of observations that protein kinase inhibitors block the induction and maintenance of LTP while, conversely, phorbol esters enhance synaptic transmission in hippocampal CA1 region (Ben-Ari et al., 1992).

*Molecular Biology of NMDA Receptors*

Molecular biological techniques have only recently yielded information on the subunit structure of NMDA receptors (for review see Seeburg, 1993). Within the last two years two subunit types have been cloned, the NRI subunit (Moriyoshi et al., 1991) which occurs in different splice forms with different pharmacological properties and the NR2 type of which four subunits (NR2A - NR2D) are known to date (Kutswada et al., 1992; Monyer, 1992; also see Seeburg, 1993). Homomeric expression of NR1 forms ion channels which exhibit characteristic NMDA receptor channel properties. These include a requirement for both glycine and a transmitter site agonist (glutamate or NMDA) to activate the channel, $Ca^{2+}$ permeability, voltage-dependent sensitivity to $Mg^{2+}$, and channel blockade by MK-801. NR2 subunits do not

appear to form receptor channels by themselves, but seem to have a modulatory role, since heteromeric NMDA receptors display different properties depending on which of the NR2 subunits is co-expressed with NR1. These effects of NR2 subunits include differences in receptor sensitivity to glycine, the strength of $Mg^{2+}$ blockade, and deactivation kinetics (Monyer et al., 1992).

Examination of the expression patterns of mRNAs encoding the NMDA receptor subunits indicates that NR1 mRNA is present in most neurones in the brain (Moriyoshi et al., 1991). In contrast, the NR2 mRNAs show distinct expression profiles, which have been suggested to underlie the differences in NMDA receptor properties in different neuronal populations (Monyer et al., 1992; Sugihara et al., 1992).

### 1.2.2 The AMPA Receptor

This ionotropic glutamate receptor subtype was originally known as the "quisqualate" receptor, since it was initially identified on the basis of excitatory neuronal responses to quisqualate and L-glutamate, which are selectively blocked by L-glutamic acid diethyl ester, GDEE (Haldeman and McLennan, 1972). Subsequently, the GDEE-sensitive excitant α-amino-3-hydroxy-5-methyl-4-isoxazole propionic acid, AMPA, has superseded quisqualate due to its much greater selectivity for this receptor (Krogsgaard-Larsen et al., 1980; Honoré et al., 1982). Characterisation of the AMPA receptor was initially hampered by the lack of selective antagonists, until the recent development of the quinoxalinediones, a class of potent non-NMDA receptor antagonists (Honoré et al., 1988). 2,3-Dihydroxy-6-nitro-7-

sulfamoyl-benzo(F)quinoxaline (NBQX) is the most potent centrally active AMPA antagonist of this class known to date (Sheardown et al., 1990). NBQX exhibits 30-fold higher affinity for AMPA receptors than for kainate receptors in the CNS, and has no affinity for NMDA receptor binding sites. Other quinoxalinediones such as 6-cyano-7-nitroquinoxaline-2,3-dione (CNQX) and 6,7-dichloroquinoxaline-2,3-dione (DNQX) also antagonise AMPA receptor-evoked responses (Honoré et al., 1988). However, these agents exhibit a much lower degree of selectivity between AMPA and kainate receptors than NBQX, being only 4-5 fold more potent inhibitors of [$^3$H]-AMPA binding than of [$^3$H]-kainate binding. In addition, CNQX and DNQX bind with low affinity at the glycine modulatory site on the NMDA receptor complex. The utility of CNQX and DNQX to block AMPA-mediated responses *in vivo* is further limited by the observation that these agents are not centrally active following systemic administration (Honoré et al., 1988).

*Channel Properties*

AMPA receptor agonists activate conductance channels which exhibit little voltage-dependence, are permeable to $Na^+$ and $K^+$, and which may be either permeable or impermeable to $Ca^{2+}$ (Mayer and Westbrook, 1987 a and b; Ascher and Nowak, 1988a; Iino et al., 1990; Miller et al., 1992; see also Section 1.2.3). Electrophysiological evidence that fast synaptic responses are blocked primarily by non-NMDA antagonists and that AMPA receptor stimulation desensitises rapidly (<1ms) suggests that AMPA receptors mediate fast depolarising responses at the majority of excitatory synapses in the CNS (for review see MacDermott and Dale, 1987; Collingridge and Lester, 1989).

*Pharmacological Regulation*

As well as the ligands already described which act at the transmitter recognition site, a number of other agents can modulate AMPA receptor activity. These include receptor antagonism by barbiturates (Simmonds and Horne, 1988), and potentiation by $Zn^{2+}$ (Koh and Choi, 1988). Recently the benzodiazepine compound GYKI-52466 (1-(4-aminophenyl)-4-methyl-7,8-methylendioxy-5H-2,3-benzodiazepine) has been shown to have non-competitive AMPA receptor antagonist properties; i.e. blockade of excitatory responses evoked by glutamate and quisqualate (but not NMDA or KA) in electrophysiological studies in the rat, and selective blockade of AMPA- and KA- (but not NMDA-) induced seizures in mice (Tarnawa, 1990; Zorumski et al., 1993; for review see Rogawski, 1993). The sites of action of these agents at the AMPA receptor complex have yet to be elucidated.

### 1.2.3 The Kainate Receptor

A third class of ionotropic glutamate receptors, preferentially activated by kainate (KA), was initially proposed on the basis that kainate-induced excitatory responses in cat spinal cord were found to be relatively insensitive to NMDA antagonists or the AMPA/quisqualate antagonist GDEE (McLennan and Lodge, 1979). Kainate and domoate are potent agonists at the transmitter recognition site, while glutamate and AMPA show only moderate activity. Receptor activation opens a cation channel permeable to $Na^+$, $K^+$ and in some circumstances $Ca^{2+}$ (Miller et al., 1992). However there is some controversy surrounding the existence of a physiologically distinct KA receptor, some investigators suggesting that KA-evoked responses are

mediated by activation of the AMPA receptor. Briefly, evidence supporting this view includes:-

a) In autoradiographic binding studies, [$^3$H]-KA binds to high and low affinity sites in rat brain membranes (Monaghan and Cotman, 1982). However, irradiation inactivation studies suggest that low affinity KA sites are identical to AMPA binding sites (Honoré et al., 1986).

b) In order to elicit an excitatory response, low micromolar KA concentrations are required, at which level KA interacts with the AMPA binding site (Mayer and Westbrook, 1987a).

c) The non-NMDA antagonists CNQX and DNQX are equipotent as antagonists of KA-, AMPA- and quisqualate-evoked increases in neuronal firing rates, suggesting that all three agonists elicit excitatory responses by activation of the same neuronal receptor (Honoré et al., 1988).

However there is also evidence that at least some KA-induced neuronal responses are independent of the AMPA receptor, including:-

d) In the rat cortical wedge, the AMPA antagonist NBQX has been reported to antagonise quisqualate- and KA-induced depolarisations differentially (Honoré et al., 1988).

e) The non-NMDA antagonists NBQX, CNQX and DNQX are more potent as inhibitors of [$^3$H]-AMPA than of [$^3$H]-KA binding in rat brain membranes (30-fold, and 4-5-fold, respectively) (Honoré et al., 1988).

f) In neuronal cultures, KA and quisqualate activate channels which show different conductance and desensitization properties (Mayer and Westbrook, 1987a; Collingridge and Lester, 1989).

g) The concentration of KA required to depolarise spinal C-fibre afferents is of the same order of magnitude as that shown to label high affinity [$^3$H]-KA binding sites in rat brain membranes (as opposed to concentrations which label the low affinity [$^3$H]-KA binding sites which have been suggested to be identical to AMPA binding sites) (see Agrawal and Evans, 1986).

h) In autoradiographic studies, the regional distribution pattern of high affinity [$^3$H]-KA binding sites is unlike those of either AMPA or NMDA receptors. In addition, the pattern of [$^3$H]-KA binding corresponds well with the brain regions which are particularly susceptible to the neurotoxic actions of KA, such as the cortex, lateral septum, and area CA3 of the hippocampus (Monaghan and Cotman, 1982; Foster and Fagg, 1984; Monaghan et al., 1989).

*Molecular Biology of Non-NMDA Receptors*

Increased insight into the characterisation of AMPA and KA receptors has been gained by recent advances in protein purification and molecular biology techniques (for review see Sommer and Seeburg, 1992; Seeburg, 1993). As a result, a number of non-NMDA receptor subunits have been cloned: GluR1 - GluR7, KAI and KAII (Hollmann et al., 1989; Keinenan et al., 1990; Bettler et al., 1992). From combinations of these subunits it is evident that multiple non-NMDA receptor subtypes exist which show differential responses to AMPA and KA, and at least one subtype appears to respond to both AMPA and KA.

High affinity AMPA, low affinity kainate receptors can be reconstituted *in vitro* by expression of one, or co-expression of any two of the four subunits termed GluR1 - GluR4, or GluRA-D. In heteromeric subunit assemblies the GluR2 subunit dictates the conductance and permeability properties of the channel, inferring channel impermeability to divalent cations including $Ca^{2+}$ (Verdoorn et al., 1991; Burnashev et al., 1992; Hollman et al., 1992). Thus, in cells expressing AMPA receptors which lack the GluR2 subunit, glutamate can activate $Ca^{2+}$ currents through AMPA receptor channels (Burnashev et al., 1992).

High-affinity kainate receptors can be generated from subunits GluR5-7, and KA1 or KA2 (Bettler et al., 1992). Homomeric configurations of GluR5 and GluR6, but not GluR7, KA1 or KA2, can form functional channels *in vitro.* However, in combination with GluR5 or GluR6, KA2 channels can be activated by AMPA as well as KA.

### 1.2.4 The Metabotropic Receptor

Agonist activation of metabotropic glutamate receptors (mGluRs) stimulates intracellular second messenger systems, via a G-protein linked receptor transduction system, which leads to inositol-triphosphate ($IP_3$)-mediated mobilisation of intracellular $Ca^{2+}$ stores (Sugiyama et al., 1987; for review see Schoepp and Conn, 1993). Quisqualate, glutamate and ibotenate are agonists at this site, while NMDA, AMPA and KA are not. Recently another glutamate analogue, DL-1-amino-1,3-cyclopentane-*trans*-dicarboxylic acid (*trans*-ACPD), has been found to be a more selective, though less potent, agonist at this site. 2-Amino-3-phosphonopropionic acid

(AP3) and AP4 appear to be weak antagonists at the metabotropic receptor.

*Molecular Biology of Metabotropic Receptors*

Within the last two years molecular biological studies have characterised a family of mGluRs consisting of at least 8 cloned receptor subtypes (mGluR1α, β, c, and mGluR2-6) (for review see Schoepp and Conn, 1993). These receptors exhibit heterogeneous functions and are coupled to multiple second messenger systems, including activation of phosphoinositide hydrolysis, activation of phospholipase C, both increases and decreases in cAMP formation, and modulation of ion channel activity. However, little is known to date about which of the cloned mGluRs mediates which second messenger response, although *in situ* localisation of mRNAs encoding different mGluRs shows contrasting distributions of the mGluR subtypes in the brain. For example, mGluR1 mRNA is concentrated in most neuronal cells throughout the CA2, CA3 and CA4 hippocampal regions and in the dentate gyrus, while mGluR5 mRNA is specifically localised in pyramidal cells of areas CA1-CA4 and granule cells of the dentate gyrus (Abe et al., 1992; Shigemoto et al., 1992). These differential distribution patterns suggest that the different mGluRs may have highly specialised cellular functions related to the specific signal-transduction mechanism they are coupled to. In general terms, mGluRs appear to be involved in acute modulation of synaptic transmission, as well as playing a role in the induction of long-lasting changes in synaptic function. For example, mGluRs have been implicated in the induction of LTP in hippocampus area CA1 (putatively by enhancing NMDA receptor currents via activation of protein kinase C, PKC; Bashir et al., 1993), and in the

lateral septal nucleus (putatively by facilitating $Ca^{2+}$ release from intracellular stores; Zheng and Gallagher, 1992).

### 1.2.5 The L-AP4 Receptor

The finding that the glutamate analogue L-2-amino-5-phosphonobutyrate (L-AP4) was a potent antagonist at subpopulations of excitatory synapses, but had no inhibitory action against the depolarising actions of glutamate, NMDA, quisqualate or KA, led to the proposal of a presynaptic L-AP4 autoreceptor (Lanthorn et al., 1984; Cotman et al., 1986). It has been hypothesised that antagonism of excitatory responses by L-AP4 results from receptor-mediated inhibition of excitatory neurotransmitter release. However, no membrane binding site for L-AP4 has as yet been identified, and the exact mechanism of L-AP4 antagonism is still to be elucidated.

### 1.2.6 The Anatomical Distribution of Excitatory Amino Acid Receptors in the CNS

Most of the information about receptor distributions in the CNS has come from ligand binding studies and, more recently, from *in situ* hybridization studies. While such methods identify the location of binding sites selective for certain ligands, it must be noted that these procedures allow no measure of functional receptor activity. However electrophysiological studies have generally supported a role for glutamate receptor activation in regions coincident with the reported distributions of excitatory amino acid binding sites. The anatomical patterns of excitatory amino acid ionotropic receptor distributions in the rat brain, based on evidence from *in vitro* autoradiographic ligand binding studies, are summarised

## TABLE 1

## EXCITATORY AMINO ACID RECEPTORS

| RECEPTOR CLASSES | AGONISTS | ANTAGONISTS | RADIOLIGANDS |
|---|---|---|---|
| **NMDA** | | | |
| *Transmitter Site* | NMDA<br>L-Glutmate<br>Methanoglutamate<br>L-Aspartate<br>Ibotenate | CPP<br>Cpp-ene<br><br>D-AP5<br>CGS-19755 | L-[$^3$H]-Glutamate<br>D-[$^3$H]-AP5<br><br>[$^3$H]-CPP<br>[$^3$H]-CGS-19755 |
| *Channel* | | PCP<br>MK-801<br>TCP<br>Ketamine<br>SKF 10047 | [$^3$H]-MK-801<br>[$^{125}$I]-MK-801<br>[$^3$H]-TCP |
| *Glycine Site* | Glycine<br>D-Serine<br>D-Alanine<br>D-Cycloserine (P) | HA-966 (P)<br>Kynurenate<br>7-Cl-Kynurenate | [$^3$H]-Glycine |
| *Polyamine Site* | Spermine<br>Spermidine | Ifenprodil | |
| **AMPA** | AMPA<br>L-Glutamate<br>Quisqualate | NBQX<br>CNQX<br>DNQX<br>LY-293558<br>GYKI-52466<br>GDEE | [$^3$H]-AMPA<br>[$^3$H]-CNQX<br>[$^3$H]-L-Glutamate |
| **KA** | KA<br>L-Glutamate<br>Domoate<br>Quisqualate | CNQX<br>DNQX | [$^3$H]-KA<br>[$^3$H]-L-Glutamate |
| **METABOTROPIC** | *trans*-ACPD<br>L-Glutamate<br>Quisqualate<br>Ibotenate | AP3<br>AP4 | |
| **L-AP4** | L-AP4<br>L-Glutamate | | |

A summary of representative agonists, antagonists and radioligands for each of the excitatory amino acid receptor classes. Agents are not necessarily ranked in order of pharmacological potency. (P): Partial agonist.
Abbreviations:
**ACPD**, 1-amino-cyclopentyl-1,3-dicarboxylate; **AMPA**, α-amino-3-hydroxy-5-methylisoxazole propionate; **AP3**, 2-amino-phosphonobutyrate; **AP4**, 2-amino-phosphonovalerate; **CNQX**, 6-cyano-7-nitro-quinoxaline-2,3-dione; **CPP**, 3-3(2-carboxypiperazin-4-yl)propyl-1-phosphate; **CPP-ene**, 3-(2-carboxypiperazin-4-yl)propenyl-1-phosphonoate; **DNQX**, 6,7-dinitro-quinoxaline-2,3-dione; **GDEE**, glutamic acid diethyl ester; **KA**, Kainate; **MK-801**, dibenzocycloheptenеimine; **NMDA**, *N*-methyl-D-aspartate; **PCP**, phencylidine; **TCP**, 1-(1-thienyl-cyclohexyl)piperidine.

below (for review see Cotman et al., 1987; Young and Fagg, 1990).

NMDA-displaceable [$^3$H]-glutamate binding sites are found throughout the brain, but predominantly in the telencephalon (Monaghan and Cotman, 1985). The general distribution of NMDA receptors in rat CNS has been confirmed by mapping the binding patterns of radiolabelled NMDA antagonists which bind at the transmitter recognition site, such as [$^3$H]-CPP and [$^3$H]-D-AP5 (Monaghan et al., 1984b; Olverman et al., 1986). Highest levels of NMDA binding sites in the brain are found in strata oriens and radiatum of the hippocampal CA1 region, while moderate levels exist in area CA3 and the dentate gyrus. These observations correlate with the proposed involvement of NMDA receptors in long term potentiation in area CA1 (Collingridge and Bliss, 1987). In cortex, highest densities of NMDA binding sites are found in frontal, anterior cingulate and pyriform cortices. In neocortical areas such as parietal cortex a laminar pattern of binding sites exists, consisting of two dense bands of NMDA binding sites corresponding to cortical layers I-III and V. In sub-cortical regions high levels of NMDA sites are found in the dorsal lateral septum, amygdala, and the basal ganglia (particularly striatum and nucleus accumbens). Other brain regions which are frequently associated with sensory functions contain moderate levels of NMDA receptors. These include visual structures such as the superior colliculus superficial layer and dorsal lateral geniculate body, auditory regions including the medial geniculate body and cochlear nucleus, and the plexiform layer of the olfactory bulb and anterior olfactory nuclei. Low levels of NMDA sites are found in regions associated with motor function including the cerebellar molecular layer, pontine nucleus and the red nucleus. Further, autoradiographic studies

show a high degree of co-localisation in the anatomical distribution patterns of NMDA-displaceable binding sites, and of ligands binding at regulatory domains on the NMDA receptor-channel complex. These include PCP site ligands (e.g. [$^3$H]-TCP and [$^3$H]-MK-801), and [$^3$H]-glycine binding to the strychnine-insensitive glycine recognition site (Bristow et al., 1986; Bowery et al., 1988; Maragos et al., 1988; Sakurai et al., 1991).

[$^3$H]-AMPA binding sites show a high degree of colocalisation with NMDA sites throughout the CNS, highest levels being found in the hippocampal complex, and in particular in strata radiatum and oriens of area CA1 (Monaghan et al., 1984a; Rainbow et al., 1984; Cotman et al., 1987). In the cortex AMPA sites are concentrated in the outer layers, and high levels are also found in striatum, nucleus accumbens, lateral septum, amygdala, anterior olfactory nuclei and the olfactory tubercle. In a few areas AMPA binding sites are more abundant than NMDA binding sites, for example in the cerebellar molecular layer and stratum pyramidale of the hippocampus. The general pattern of NMDA and AMPA receptor colocalization supports electrophysiological evidence that NMDA and AMPA receptors work in concert in mediating post-synaptic excitation, AMPA receptors being responsible for the stimulatory fast EPSP while NMDA receptors mediate a slower conductance which appears to play a modulatory role in neuronal activation, contributing to synaptic responses only under special conditions (Collingridge and Bliss, 1987; MacDermott and Dale, 1987).

Kainate binding sites, in contrast, generally do not complement NMDA distribution (Monaghan and Cotman, 1982; Unnerstall and Walmsley, 1983; Cotman et al., 1987). Kainate sites tend to predominate in regions of low

NMDA site density such as the termination zone of the mossy fibre pathway in the hippocampus (stratum lucidum). In cortex, the highest densities of kainate binding sites are found in layers V and VI. In thalamic areas, kainate sites are concentrated in the reticular nucleus and hypothalamus, whereas NMDA binding site densities are low in these regions relative to other thalamic areas. In striatum, kainate and NMDA binding site densities are similar, but NADPH-diaphorase histochemistry suggests that they are located on different cell types within the striatum (Beal et al., 1986). However, there is evidence of co-localisation of kainate and NMDA binding sites in the dentate gyrus and cerebellum.

### 1.2.7 Glutamatergic Pathways in the CNS

Evidence obtained from the distribution profiles of presynaptic markers for glutamate-containing terminals, in conjunction with observed patterns of post-synaptic excitatory amino acid receptors within the brain, indicate that endogenous excitatory amino acids, and in particular glutamate, are the major excitatory neurotransmitters in corticocortical, corticofugal and sensory systems (for review see Fonnum, 1984; Cotman et al., 1987).

Neuronal terminals employing a given transmitter can often be identified by their ability to synthesise, store, release, take up, or inactivate the transmitter. Therefore, potential markers for glutamate-secreting terminals include transmitter content, presence of the catabolic enzyme glutaminase, demonstration of $Ca^{2+}$-dependent glutamate release, and the presence of the high affinity uptake mechanism for glutamate. Histological visualisation of presynaptic markers, for example using glutamate immunocytochemistry, has

facilitated the demonstration of $Ca^{2+}$-dependent glutamate release from hippocampal neurones in response to depolarisation (see Ottersen and Storm-Mathisen, 1987). Autoradiographic mapping of the distribution of high-affinity glutamate uptake sites in the brain has also been widely used to localise glutamate-containing terminals, employing the metabolically inert glutamate analogue [$^3$H]-aspartate to label the glutamate uptake site. [$^3$H]-Aspartate autoradiography in the rat brain has demonstrated that the pattern of glutamate uptake sites is strikingly similar to the sum of the distributions of excitatory amino acid receptor subtypes throughout the CNS, with particularly high levels of uptake evident in hippocampus area CA1, strata radiatum and oriens (Ottersen and Storm-Mathisen, 1984; Taxt et al., 1984). In addition, high levels of [$^3$H]-aspartate binding are seen in the outer layers of the cerebral cortex, while slightly lower levels are seen in striatum, basal forebrain, nucleus accumbens, lateral septum, olfactory tubercles, and dorsal lateral geniculate body (Ottersen and Storm-Mathisen, 1984). Further insight into the terminal location of high-affinity glutamate uptake sites has been gained from the demonstration of down-regulation of [$^3$H]-aspartate binding in certain brain regions following deafferentation. However, the interpretation of [$^3$H]-aspartate binding as a selective marker for neuronal glutamate uptake sites should be treated with caution, following the recent demonstration that lesioning the major [$^3$H]-glutamatergic input to the superior colliculus superficial layer from the retina had no effect on levels of [$^3$H]-aspartate binding in this region. As a consequence, it was postulated that [$^3$H]-aspartate binding is not restricted solely to binding sites on presynaptic neuronal terminals, but may also label binding sites on glial cell

membranes (Browne et al., 1991).

By comparing the anatomical distribution patterns of presynaptic markers and post-synaptic receptors, and investigation of the sequelae of pathway manipulations, a number of pathways have been proposed to employ excitatory amino acids as neurotransmitters. In addition to corticocortical association fibres, linking cortical pyramidal neurones (Peinada et al., 1986), and corticofugal projections (Fonnum, 1984; Ottersen and Storm-Mathisen, 1986), sensory pathways including retinofugal projections, mossy fibre synapses in the cerebellum, and certain auditory, olfactory and somatosensory pathways have been proposed to employ glutamate as the major excitatory neurotransmitter. Evidence implicating glutamate's involvement in a number of pathways is summarised in Table 2. Further, a combination of evidence from autoradiographical, biochemical and physiological studies has indicated functional heterogeneity between two hippocampal pathways which fulfil the criteria for glutamate as a neurotransmitter. Uptake, storage and release of glutamate have been demonstrated in both the mossy fibre and Schaffer collateral pathways, while excitatory amino acid receptor antagonists have been shown to block synaptic transmission in both pathways (Cotman et al., 1986, 1987). However, autoradographic studies have revealed that the Schaffer collateral terminal field contains the highest density of NMDA receptors in the brain (which is implicated in the process of LTP in this pathway), whereas mossy fibre terminals innervate a region with the highest levels of KA receptors in the brain (Monaghan and Cotman, 1982, 1985). In addition, presynaptic L-AP4 receptors have been demonstrated on mossy fibre terminals (Cotman et al., 1986).

## TABLE 2

## MAJOR GLUTAMATERGIC PATHWAYS IN THE CNS

| | |
|---|---|
| Cortex: | |
| Cortico - Cortical | Ottersen and Storm-Mathisen (1984) |
| Cortico - Striatal | Fonnum et al. (1981) |
| Cortico - Thalamic | Fonnum et al. (1981) |
| Hippocampus: | |
| Schaffer Collateral-Commissural | Cotman et al. (1986) |
| Mossy Fiber | Taxt et al. (1984) |
| Retino-Fugal Projections | |
| (Pricipally to superior colliculus and lateral geniculate body). | Lund-Karlsen and Fonnum (1978)<br>Miller and Slaughter (1986)<br>Sillito et al. (1990) |

Selected examples from the literature of glutamatergic excitatory pathways in the CNS. For reviews, see also Fonnum (1984), Cotman et al. (1987), Collingridge and Lester (1989).

# 2. THE ROLE OF GLUTAMATE IN NEURODEGENERATION

## 2.1 Glutamate-Mediated Excitotoxicity in Neurodegeneration

Glutamate's potential toxicity to CNS neurones was first reported in 1957 when Lucas and Newhouse discovered that systemic glutamate injections led to degeneration of retinal neurones in neonatal mice. Subsequently Van Harreveld (1959) demonstrated that cortical application of glutamate in rabbits induced cortical spreading depression, and went on to propose that this effect was associated with neuronal hypoxia. These observations were supported further by investigations in which Olney (1969, 1971) showed that following systemic administration to immature rats, glutamate induced neuronal degeneration in the mature animals in areas of the brain which lack protection by the blood-brain barrier, such as the arcuate nucleus of the hypothalamus. Structure-activity studies subsequently revealed a strong correlation between the excitatory and neurotoxic potencies of different excitatory amino acid analogues, while glutamate analogues lacking excitatory activity were found to also lack neurotoxic effects. These observations suggested a convergence in the mechanisms underlying these two actions. This theory was further supported by findings that specific antagonists of glutamate-type excitation also effectively protected against glutamate-type neurotoxicity, suggesting the two events were receptor-mediated.

The neuropathological state produced acutely by glutamate and its analogues is characterised by rapid cellular swelling, most marked in dendrites (consistent with the predominantly dendritic localisation of excitatory amino acid receptors) while perikarya initially show swollen mitochondria and dilatation of endoplasmic reticulum. Subsequently, nuclear pyknosis is seen

and the cytoplasm becomes vacuolated (Olney, 1971; Olney and de Gubbareff, 1978; Olney et al., 1979).

In combination, these observations led Olney to propose the "excitotoxic" hypothesis of cell death, which states that:-

> prolonged neuronal depolarisation underlies glutamate-induced neurotoxicity, and that the toxic action of glutamate is mediated through dendrosomal synaptic receptors specialised for glutamatergic (or aspartergic) transmission.

This process is assumed to involve pathologic changes in neuronal membrane permeability and impaired ion homeostasis. Since neuronal axons, presynaptic terminals and non-neuronal cells survive a glutamatergic insult, the excitotoxic process is often termed "axon sparing".

The first direct evidence of excitotoxicity in the adult rat brain came from studies in which injections of kainic acid into striatum were found to result in neuronal death characterised by the pathological neuronal alterations described by Olney (Coyle and Schwarcz, 1976; McGeer and McGeer, 1976). Experimentally, chronic infusions of high concentrations of glutamate are required to elicit neuronal degeneration due to the attenuating effect of the high affinity uptake system for glutamate. Application of uptake inhibitors, or removal of glutamate uptake sites by axotomy have consequently been shown to enhance glutamate toxicity. Other excitotoxins which are not substrates for glutamate's uptake carrier, such as kainate, ibotenate or quisqualate, are therefore generally used experimentally.

### 2.1.1 Mechanisms of Excitotoxic Neuronal Death

The exact mechanism of glutamate-induced excitotoxic neuronal death is not yet fully understood, although evidence indicates that it is ultimately dependent on abnormally high intracellular free calcium concentrations, $[Ca^{2+}]_i$ (Siesjö et al., 1991; Miller et al., 1992).

Excitatory amino acid receptor activation induces elevations in $[Ca^{2+}]_i$ via a number of different pathways. These include $Ca^{2+}$ influx through voltage-sensitive calcium channels (VSCCs) and/or agonist-operated calcium channels (AOCCs), including channels associated with glutamate receptor subtypes; by mobilisation of intracellular $Ca^{2+}$ stores following metabotropic receptor-mediated activation of inositoltrisphosphate ($IP_3$); or alternatively by $Ca^{2+}$-induced $Ca^{2+}$ release (Siesjö, 1991; Brorson et al., 1991). Under normal physiological conditions this increase is tightly regulated by means of $Ca^{2+}$ extrusion from neurones by an ATP-dependent $Ca^{2+}/Na^+$ exchange mechanism (Mayer and Miller, 1990). These normal increases in $[Ca^{2+}]_i$ underlie basal neuronal physiological processes, such as post-synaptic excitability, membrane permeability and synaptic plasticity, and are also thought to contribute to the initiation of long-term potentiation, since $Ca^{2+}$ regulates $Ca^{2+}$-activated $K^+$ and $Cl^-$ channels in the cell membrane and can therefore directly control the membrane's electrical properties. $Ca^{2+}$ may also act as a trigger for neurotransmitter release, and is involved in regulation of gene expression. In addition, $Ca^{2+}$ activates second messenger systems within neurones and modulates the activities of various enzymes including $Ca^{2+}$-dependent phosphatases, protein kinases, proteases and lipases. Hence, $Ca^{2+}$-dependent reactions contribute to the maintenance of cell

structural elements (for review see Siesjö, 1988).

In pathological situations such as ischaemia, trauma or status epilepticus, excessive glutamate release and impaired re-uptake mechanisms result in prolonged exposure of post-synaptic receptors to the excitatory agonist, which can lead to excessive intracellular accumulation of $Ca^{2+}$. Such loss of $Ca^{2+}$ homeostasis results in "overloading" of cells with $Ca^{2+}$ and the subsequent activation of a wide range of subcellular components, which may ultimately lead to disruption of normal cellular processes. High levels of nuclear $Ca^{2+}$ activate nucleases, resulting in DNA fragmentation. Activation of proteases by high cytosolic $Ca^{2+}$ levels leads to destruction of cytoskeletal components and mitochondrial dysfunction, while alterations in the activities of other enzymes, such as lipases, results in membrane damage and the production of free radicals. The ultimate consequence of these sequelae is cell death (Siesjö, 1988; Siesjö and Bengtsson, 1989).

Over the last four years a substantial body of evidence has emerged implicating nitric oxide (NO) as a mediator of glutamate-induced neurotoxicity in the CNS. In addition to its numerous physiological functions, including mediation of smooth muscle relaxation in peristalsis and vasodilatation, NO is an intracellular messenger in the brain and the peripheral nervous system (Garthwaite, 1991; Snyder and Bredt, 1991; Dawson et al., 1993).

NO is synthesised in post-synaptic neurones in response to increased $[Ca^{2+}]_i$. $Ca^{2+}$ binding to calmodulin associated with the enzyme nitric oxide synthase (NOS), activates the enzyme to catalyse the synthesis of NO from L-arginine. Hence agonist activation of glutamate receptors, and in

particular NMDA receptors, triggers NO synthesis via the associated influx of $Ca^{2+}$ ions. The target for NO action is the soluble enzyme guanylyl cyclase which catalyses cyclic guanosine monophosphate (cGMP) production within the cell. Consequently NMDA receptor activation has been shown to increase intracellular cGMP levels (Bredt and Snyder, 1989) which in turn has an impact on various cellular functions, including regulation of protein kinases, phosphodiesterases, and ion channel activities.

The proposition that NO plays a role in mediating glutamate excitotoxicity is supported by evidence from *in vitro* studies that NOS inhibitors block the neurotoxic actions of glutamate and NMDA in neuronal cultures and brain slices, and that NOS blockade is reversible by the addition of L-arginine (Dawson et al., 1993). In addition, sodium nitroprusside (SNP), which induces spontaneous release of NO, produces cell death in neuronal cultures in a dose-dependent manner which parallels observed increases in cGMP levels, while haemoglobin (which complexes NO) and calmodulin inhibitors prevent the neurotoxic effects of both NMDA and SNP (Dawson et al., 1991, 1993). NO has also been implicated in processes of neuronal injury *in vivo*. For example, in experimental models of focal ischaemia in the rat, in which neuronal death is thought to be induced by raised extracellular glutamate levels, the NOS inhibitor N-arginine has been found to reduce or completely abolish neuronal damage (Nowicki et al., 1991; Trifiletti, 1992). Further, SNP has been found to elicit neuronal injury when injected directly into the hippocampus (Loiacona and Beart, 1992). The exact mechanism by which NO kills neurones is still unclear, although a number of reports implicate the involvement of free radicals and in particular superoxide anions

($0_2^{\cdot -}$). Superoxide and NO can combine to form peroxynitrite ($ONOO^-$), which in turn decomposes into the highly reactive free radicals $OH^{\cdot}$ and $NO_2^{\cdot}$, which may be the ultimate common mediators of NO toxicity. Evidence for the participation of superoxide anions in neurotoxicity elicited by NMDA, and by NO produced by SNP, is provided by the neuroprotective effects of superoxide dismutase, an enzyme that scavenges the superoxide anion (Dawson et al., 1993; Lafon-Cazal, 1993).

Paradoxically, under certain circumstances NO has been demonstrated to have neuroprotective properties against glutamate-induced neurotoxicity, putatively due to the ability of NO to nitrosylate the NMDA receptor complex, effectively blocking glutamatergic neurotransmission (Vige et al., 1993). Further, NOS-containing neurones have been shown to correspond to neurones that stain positively for nicotinamide adenine dinucleotide phosphate (NADPH) diaphorase (Dawson et al., 1991; Snyder and Bredt, 1991), and which have been found to be resistant to degeneration in diseases such as Alzheimer's and Huntington's diseases, to NMDA toxicity in cortical culture, and to hypoxic-ischaemic brain injury (Koh and Choi, 1988; Snyder and Bredt, 1991).

A recent report by Lipton et al. (1993), indicating that NO can exist in two distinct redox states, may provide a means of reconciling the neurotoxic and neuroprotective properties of NO. Lipton and colleagues have demonstrated that the reduced ion, nitrogen monoxide ($NO^-$) is responsible for the neurotoxic actions of NO via a reaction with superoxide anions, while the oxidized nitrosonium ion ($NO^+$) reacts with the thiol group of the NMDA receptor complex to block neurotransmission. This apparent dichotomy in

the actions of NO ions may help explain the observed resistance of NOS-containing neurones.

The proposed pathways mediating the transduction of glutamate-induced excitotoxic processes are summarised in Figure 2.

### 2.1.2 Glutamate Receptors and Excitotoxicity

*NMDA Receptor-Mediated Toxicity*

Until recently the NMDA receptor complex was thought to be the only glutamate receptor subtype involved in agonist-operated calcium channel (AOCC)-mediated $Ca^{2+}$ influx, since its associated cation channel is highly permeable to $Ca^{2+}$, $Na^{+}$ and $K^{+}$ ions (Mayer and Westbrook, 1987b). NMDA receptor activation has also been implicated in the mediation of glutamate-induced excitotoxicity in both *in vitro* (Rothman and Olney, 1987; Regan and Choi, 1991) and *in vivo* models of ischaemia and trauma (Faden and Simon, 1988; Park et al., 1988a).

**a) Acute Toxicity**

Garthwaite and Garthwaite (1990) used electron microscopy in rat brain studies to assess whether neurones become overloaded with $Ca^{2+}$ during NMDA receptor-mediated excitotoxic challenge. They demonstrated, in both cerebellar and hippocampal slice preparations, that the intracellular sites of $Ca^{2+}$ accumulation correlated well with the loci of the cytopathological changes occurring in the progression towards irreversible cell damage. The stages of neuronal damage are described thus:-

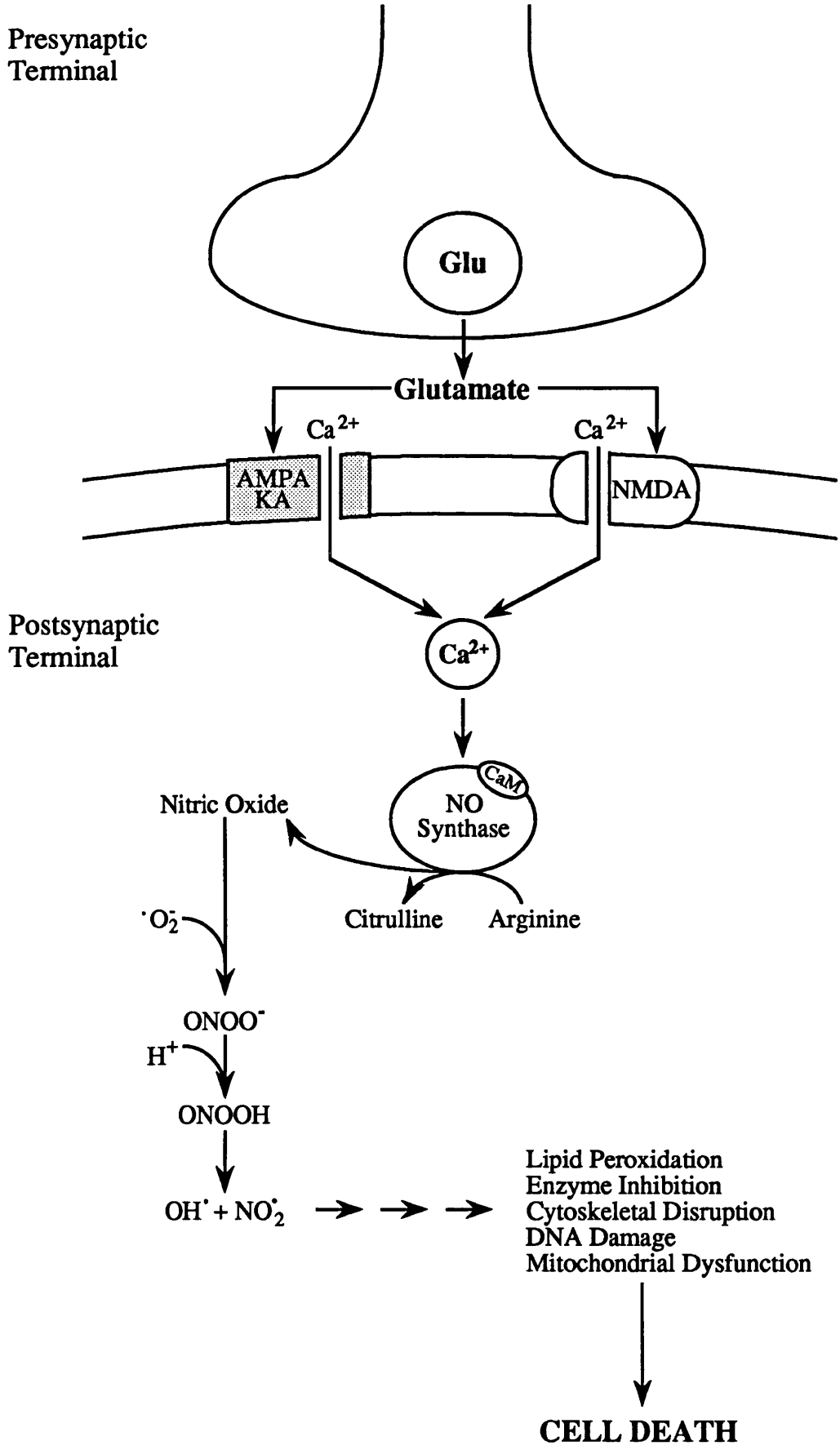


FIGURE 2: PUTATIVE MECHANISM OF GLUTAMATE EXCITOTOXICITY

(i) $Ca^{2+}$ is amassed in the Golgi apparatus, corresponding with swelling of these organelles.

(ii) $Ca^{2+}$ begins to accumulate in the nucleus, coinciding with aggregation of chromatin. If the agonist stimulation is removed at this stage cells can recover. There is insufficient $Ca^{2+}$ in cytoplasm to be detected by electron microscopy.

(iii) The onset of irreversible damage is signalled by $Ca^{2+}$ accumulation in mitochondria, which subsequently begin to swell. Large quantities of free $Ca^{2+}$ can be seen in the cytoplasm (100μM+). Removal of the agonist at this stage will not prevent neuronal necrosis.

Although the precise mechanisms elicited by high intracellular calcium levels are still unclear, the importance of its presence is illustrated by the fact that exposure of slices to NMDA in the absence of $Ca^{2+}$ prevents pathological changes occurring in the Golgi apparatus, nucleus and mitochondria, and prevents irreversible neuronal damage. Since the ionic and metabolic changes associated with NMDA receptor-mediated depolarisation still persist in these conditions, these structural alterations appear to be $Ca^{2+}$-dependent. Evidence suggests that the major route of $Ca^{2+}$ influx in the circumstances described is via AOCCs, and chiefly via the NMDA associated channel which has high $Ca^{2+}$ conductance (Mayer and Westbrook, 1987b; for review see Mayer and Miller, 1990). Stimulation of VSCCs alone, by using $K^+$ to depolarise the neurones, induced insufficient $Ca^{2+}$ influx to produce toxicity. Also

the toxicity produced in the presence of NMDA was potentiated in $Mg^{2+}$- free medium, or by simultaneously depolarising neurones with $K^+$ or kainate to overcome $Mg^{2+}$ voltage-dependent channel blockade, further suggesting the involvement of an NMDA receptor channel mediated event.

**b) Delayed Toxicity**

Following injection of NMDA into rat striatum or hippocampus *in vivo*, in amounts which are not immediately toxic, neurodegeneration occurs gradually over several hours. This delayed cell death can be inhibited by delayed administration of NMDA receptor antagonists (Foster et al., 1988).

*Non-NMDA Receptor-Mediated Toxicity*

AMPA and kainate receptor-associated ionophores have conventionally been thought to be $Ca^{2+}$-impermeable (Mayer and Westbrook, 1987a; Mayer and Miller, 1990). $Ca^{2+}$ influx has been observed after non-NMDA receptor stimulation, but in the past this $Ca^{2+}$ influx has been attributed to activation of voltage-sensitive calcium channels (VSCCs) by the membrane depolarisation which results from $Na^+$ influx through non-NMDA receptor channels (Murphy and Miller, 1989). However, an increasing body of evidence indicates that some AMPA and kainate receptor ionophores are permeable to $Ca^{2+}$.

In 1989, Murphy and Miller demonstrated that the $Ca^{2+}$ influx induced by KA in cultured striatal neurones could not be completely blocked by VSCC

blockers. In electrophysiological studies, Iino et al., (1990) and Ozawa et al. (1991) showed that a fraction of cultured hippocampal neurones expressed glutamate receptors which were permeable to $Ca^{2+}$ after stimulation by KA. They termed these receptors "type-II KA receptors", as opposed to the typical "type-I KA receptors" which are $Na^{+}$-permeable and $Ca^{2+}$-impermeable. Further, *in vitro* studies have identified the existence of $Ca^{2+}$-permeable non-NMDA receptors in rat cerebellar granule cells (Holopainen et al., 1989), rat hippocampal neurones (Ogura et al., 1990) and glial cells (Linn and Christensen, 1992).

In order to elucidate whether this non-NMDA receptor mediated $Ca^{2+}$ influx was due solely to VSCC activation, Miller and colleagues (1992) investigated the KA-induced increase in $[Ca^{2+}]_i$ in cultured cerebellar Purkinje cells in a $Na^{+}$-free medium (replacing $Na^{+}$ with the impermeant cation N-methyl-D-glucamine, NMDG). In some cells $Ca^{2+}$ influx was found to be dependent on cell depolarisation, but in the majority of cells investigated a substantial $Ca^{2+}$ influx occurred in $Na^{+}$-free conditions (Brorson et al., 1992; Miller et al., 1992). AMPA also induced $Na^{+}$-independent $Ca^{2+}$ influx, and both AMPA- and KA-induced $[Ca^{2+}]_i$ increases were found to be completely blocked by the non-NMDA receptor antagonist CNQX, but unaffected by the NMDA antagonist APV. In addition, administration of the non-specific organic VSCC blocker TA-3090, at doses sufficient to inhibit both depolarisation- and $K^{+}$-induced $Ca^{2+}$ influxes, was ineffective in blocking the $Na^{+}$-independent increase in $[Ca^{2+}]_i$ following KA stimulation ((Bleakman et al., 1991). Further, in voltage-clamped conditions KA-induced inward $Ca^{2+}$ currents were found to be unaffected by TA-3090 or the inorganic VSCC

blocker $Co^{2+}$ (Miller et al., 1992).

Further evidence of the existence of $Ca^{2+}$-permeable non-NMDA receptor-associated ionophores has come from the recent cloning of a number of non-NMDA receptor subunits, GluR1 - GluR7. Studies have revealed that when expressed in certain combinations these proteins yield glutamate receptors which are permeable to $Ca^{2+}$, as discussed in Section 2.2.3 (Keinenan et al., 1990; Hollman et al., 1992).

## 2.2 Acute Neuronal Death

Following observations that the patterns of necrosis induced by excitatory amino acid injections into discrete brain regions mimic the neuronal degeneration seen in cerebral ischaemia, it was speculated that excitatory amino acid receptors may be intrinsically involved in the acute processes of ischaemic neuronal death.

### 2.2.1 Cerebral Ischaemia

The term "cerebral ischaemia" encompasses a number of clinical situations including thrombotic stroke, which produces an irreversible focal ischaemia involving brain regions supplied by end arteries and territories with collateral supply; cardiac arrest which induces transient global ischaemia; and asphyxia which produces hypoxia and global reductions in cerebral blood flow. Interrupting the cerebral circulation prevents supply of the metabolic substrates glucose and oxygen to brain regions, which can result in neuronal death. Although neuronal viability in most parts of the brain may be reinstated if circulation is restored within a few minutes, selective neuronal

necrosis may still occur in specific brain regions (Brierley and Graham, 1984).

The etiology of the neuronal death resulting from ischaemic episodes, and other insults secondarily involving ischaemia, such as cerebral trauma and subarachnoid haemorrhage, is still not fully understood. However, it is well established that excitotoxic mechanisms are involved in ischaemic neuronal death (for review see Rothman and Olney, 1986, 1987; Siesjö, 1992). *In vivo*, microdialysis studies have demonstrated marked increases in extracellular levels of glutamate and other excitatory amino acids during global and focal ischaemic episodes (Benveniste et al., 1984; Drejer et al. 1985; Hagberg et al., 1985; Butcher et al., 1990). *In vitro* experiments suggest that increased excitatory amino acid concentrations arise from both enhanced synaptic release and from impaired reuptake of glutamate and aspartate ((Bosley et al., 1983; Drejer et al., 1985). Choi (1987) has subsequently demonstrated that the level of extracellular glutamate present after 10-30 min of ischaemia is comparable with the glutamate concentration which is toxic to neurones in culture following brief exposure (60-500μM).

Further evidence of a crucial role for excitatory amino acids in ischaemic pathology is provided by the similarity in the acute cytopathology seen following excitotoxic lesions with the changes occurring during reperfusion after transient forebrain ischaemia in the rat. The early morphology of excitotoxicity - focal dendritic swelling and mitochondrial dilatation in dendrites and perikarya - has been widely reported to be evident acutely following an ischaemic insult (Brown and Brierley, 1972; Simon et al., 1984). In addition, evidence of a role for excitatory synaptic activity in ischaemic processes is provided by the results of hippocampal deafferentation

studies. Delayed neuronal loss occurs in the CA1 zone of the hippocampus following transient global ischaemia in the rat or gerbil. However, lesioning hippocampal input pathways such as the Schaffer collateral or perforant pathways, prior to the ischaemic insult, provides partial protection against this cell loss (Wieloch et al., 1985; Onodera et al., 1986; Jorgensen et al., 1987; Buchan and Pulsinelli, 1990). In addition, evidence of the neuroprotective effects of excitatory amino acid receptor antagonists, such as MK-801 and NBQX, in animal models of focal and global ischaemia have further supported an intrinsic role for glutamate in ischaemic neuronal death (Park et al., 1988a, b; Sheardown et al., 1990; see also Section 2.2.3).

### 2.2.2 Animal Models of Cerebral Ischaemia

a) *Focal Ischaemia*

An experimental model of stroke may be achieved by permanent occlusion of the middle cerebral artery (MCA), which is the vessel most often occluded in stroke in man (Brierley and Graham, 1984).

In the rat, permanent MCA occlusion results in severely reduced blood flow in the centre of the vascular territory supplied by the MCA, in which ischaemic cell death may ultimately occur. At the periphery of this region is an area with sub-critically reduced blood flow, (the "penumbral" zone) (for review see Tamura et al., 1981b; Nedergaard, 1988; Siesjö, 1992). The MCA supplies most of the caudate nucleus and putamen, the lateral segment of the globus pallidus, much of the cerebral cortex, the insula, superior regions of the internal capsule, and adjacent white matter. Permanent MCA occlusion induces infarction

in the ischaemic core, generally involving cortical and subcortical structures supplied by the MCA. Cerebral infarction has been defined by Nedergaard (1988) as necrosis of all tissue elements within a given region, including both neuronal and glial cells, nerve fibres, and all blood vessels. Within a few hours of MCA occlusion cells at the core of the MCA territory are swollen or already lysed, chromatin is dispersed away from the nucleus and cells appear pale under light microscopic examination of stained sections, due to their inability to take up histological dyes. In the surrounding tissue with reduced blood flow, shrunken and pyknotic neurones are visible after approximately 4h. Some or all of this territory may become infarcted within 24h (Graham et al., 1993). After 24-48h most of the swollen cells will have disappeared, and small eosinophilic cells will be visible in the penumbra. At this stage the infarcted area is sharply demarcated in histologically stained sections, the transitional zone of the penumbra often being only a few millimetres wide. The nature of the lesion produced by 24h permanent MCA occlusion is illustrated in Figure 8 (Methods). However, in experimental animals eosinophilic neurones are occasionally found sporadically distributed outside the infarcted zone and penumbra. For example such cells have been identified in rat cortical mantle >1mm from the infarct following MCA occlusion (see Nedegaard, 1988).

Following transient MCA occlusion scattered areas of selective neuronal damage may be induced in the caudate/putamen. Selective neuronal injury has been defined as irreversible damage to some neurones whilst sparing other cells and preserving tissue structure

(Nedergaard, 1988). The size and distribution of neuronal damage varies with the duration of occlusion, but occlusion of 6h or more produces infarction to the same extent as permanent occlusion.

b) *Global Ischaemia*

Models of global ischaemia have been described principally in the gerbil and rat. These usually involve clamping the common carotid arteries for 5-30 min, (i.e. two- or four-vessel occlusion models; 2VO or 4VO). Transient forebrain ischaemia results in delayed degeneration of pyramidal neurones in the CA1 region of the hippocampal complex. One to 2h after the ischaemic insult acute changes such as focal dendritic swelling and mitochondrial ballooning are seen in CA1 pyramidal and other hippocampal neurones, accompanied by hypermetabolism and an increase in blood flow to this region (for review see Ginsberg, 1990). The neurones then appear to recover transiently before finally degenerating, generally 24 to 72h after the ischaemic event (Pulsinelli, 1982).

It is important to note that processes of infarction and selective neuronal injury take time to evolve. Therefore, for light microscopic histological analysis of the lesion in models of focal and global ischaemia, a sufficiently long recovery period should be allowed before quantification of infarct volume: at least 24h in cryostat-processed sections following focal ischaemia; 2-4 days following transient global ischaemia to allow for the evolution of delayed CA1 cell death.

### 2.2.3 Neuroprotection by Excitatory Amino Acid Antagonists

Excessive stimulation of glutamate receptors, due to massive increases in extracellular glutamate concentrations, appears to underlie the sequence of cellular events which lead ultimately to neuronal damage following cerebral ischaemia and traumatic head injury (Benveniste et al., 1984; Butcher et al., 1990; Bullock et al., 1992). Consequently a number of pharmacological strategies have been proposed as possible mechanisms for attenuating glutamate's neurotoxic actions. These include reduction of synthesis and release of transmitter glutamate; reducing neuronal firing rates; enhancing transmitter reuptake from the synaptic cleft; or alternatively inhibiting the post-synaptic sequelae of glutamate receptor activation, for example by inhibition of $Ca^{2+}$ influx by ion channel blockers (for review see Choi, 1990). Most notably, however, pharmacological blockade of glutamate activity at post-synaptic excitatory amino acid receptors has been found to provide marked protection against neuronal damage in models of excitotoxic and ischaemic cell death *in vitro*, and *in vivo* (including *in vivo* models of focal and global ischaemia, head injury and hypoxia) (for review see Meldrum, 1990).

The NMDA receptor subtype, in particular, has been implicated in the pathogenesis of neuronal damage, supported by a number of studies reporting the beneficial effects of NMDA receptor antagonists on the outcome of traumatic brain or spinal cord injury (Faden and Simon, 1988; for review see Bullock et al., 1992), and in ameliorating the neurochemical and behavioural deficits produced by excitotoxic lesions of discrete pathways within the brain (see Dunnett et al., 1991). However, the majority of studies demonstrating

the neuroprotective actions of excitatory amino acid antagonists *in vivo* to date have employed experimental models of focal or global ischaemia, which are briefly reviewed below.

Investigations of the effects of different excitatory amino acid receptor antagonists in experimental models of ischaemia have been complicated by many extrinsic factors which can affect the outcome of the ischaemic insult, including the animal's species, strain, sex and age; the nature of the ischaemic event (global or focal; temporary or permanent), severity and reproducibility of the experimental model used; physiological variables including temperature and cardiovascular parameters; lipophilicity of the antagonist; and the dose and route of administration of the antagonist (for review see Meldrum, 1990). As a consequence, different groups have in some cases reported contrasting effects of glutamate receptor antagonists. However, in general, NMDA receptor antagonists markedly reduce neuronal damage in focal ischaemia in the cat and rat, while AMPA antagonists appear to be more potent neuroprotectants than NMDA antagonists against the delayed hippocampal damage occurring after global ischaemia.

*Focal Cerebral Ischaemia*

The neuroprotective actions of NMDA antagonists in experimental models of focal ischaemia have been demonstrated in primate, cat, rabbit, and in the rat (Park et al., 1988a, b; Chen et al. 1991; Gill et al., 1991; for review see McCulloch, 1992). In the rat, non-competitive NMDA receptor antagonists such as PCP and MK-801 reduce ischaemic brain damage by more than 50% when administered prior to, or up to 2h after the onset of

ischaemia (Park et al., 1988b; Gill et al., 1991). In contrast, while competitive NMDA antagonists such as CPP-ene are equally effective in reducing ischaemic damage when administered prior to the ischaemic episode, most lack significant neuroprotective effects when administered 1h or more after the onset of ischaemia, putatively because of their greater hydrophilicity (and thus impaired ability to cross the blood-brain barrier) compared to non-competitive antagonists (Simon and Shiraishi, 1990; Park et al., 1991). In addition, agents acting at other modulatory sites on the NMDA receptor complex have also been found to be neuroprotective against focal ischaemia in the rat, including the glycine antagonist HA-966, the polyamine site antagonist ifenprodil and systemic administration of $Mg^{2+}$ (see McCulloch and Iversen, 1991).

A reduction in the volume of ischaemic damage induced by focal ischaemia has also been demonstrated following AMPA receptor blockade. Systemic administration of the AMPA antagonist NBQX (prior to, and after onset of ischaemia) has been shown to protect neurones against ischaemic damage in the rat, although the volume of salvaged tissue is less (approximately 30%) than that protected by NMDA antagonists (Gill et al., 1992). In addition, preliminary evidence indicates that the novel AMPA antagonist LY-293558 is neuroprotective following MCA occlusion in the cat (Bullock et al., 1993). A recent study has also indicated that the benzodiazepine non-NMDA receptor antagonist GYKI 52466 is neuroprotective against focal ischaemia in the rat (Smith and Meldrum, 1993).

*Global Cerebral Ischaemia*

In studies of global ischaemia in large animals (primates, dogs and cats) NMDA receptor antagonists are ineffective in attenuating ischaemic damage (for review see McCulloch, 1992). However, in rodents (rat and gerbil) NMDA antagonists such as MK-801 and CGS 19755 appear, in general, to reduce delayed damage to hippocampal CA1 pyramidal neurones following transient global ischaemia, although this view remains controversial as some groups have reported NMDA antagonists to be ineffective in global ischaemia models (Gill et al., 1987, 1989; Buchan et al., 1991b). Subsequently it has been suggested that the neuroprotective actions of NMDA antagonists may be due to indirect drug actions, such as hypothermia, or anticonvulsant actions (Buchan and Pulsinelli, 1990).

In contrast, the AMPA antagonist NBQX markedly reduces neuronal damage following global ischaemia in the rat and gerbil. Most notably, NBQX protects hippocampal CA1 neurones against delayed damage even when administered up to 24h after the onset of ischaemia (Sheardown et al., 1990, 1993; Buchan et al., 1991a; Diemer et al., 1992; Nellgard and Wieloch, 1992).

The reason for the different effects of NMDA and AMPA antagonists on delayed hippocampal damage following global ischaemia is not immediately apparent, especially as the CA1 region of the hippocampus is the site of highest NMDA and AMPA receptor densities in the entire brain (Cotman et al., 1987). However, following findings from molecular biological studies of different non-NMDA receptor subunits which impart different receptor characteristics, it has been suggested that the process of ischaemia might influence protein synthesis within cells, leading to a

modification in AMPA receptor structure.

Pellegrini-Giampietro and colleagues (1992) demonstrated that following transient severe ischaemia mRNA transcription in CA1 hippocampal neurones is altered, resulting in reduced production of the GLuR2 AMPA receptor subunit which maintains channel impermeability to $Ca^{2+}$. It has been postulated that if new AMPA receptor/channel complexes are synthesised in the CA1 region 12h or more after the ischaemic event, these new channels may lack the GLuR2 subunit and would therefore be permeable to $Ca^{2+}$ (Pellegrini-Giampietro et al., 1992; Pulsinelli et al., 1992). This putative modulation of mRNA may explain the unique delay in the onset of injury to CA1 neurones following transient global ischaemia, and the neuroprotective efficacy of delayed AMPA antagonist administration. The proposed changes in AMPA receptor subunit expression would precede both the histological signs of CA1 injury and the late increase in $Ca^{2+}$ uptake by CA1 neurones which has previously been demonstrated using $^{45}Ca$ autoradiography (Dienel, 1984). However further studies are required to determine if these alterations in mRNA expression are translated into functional AMPA receptors in the hippocampus following transient global ischaemia.

### 2.2.4 Cortical Glutamate Perfusion: A Novel *In Vivo* Model of Glutamate Excitotoxicity

Although animal models of cerebral ischaemia have proved to be valuable in determining the anti-ischaemic effects of agents which putatively ameliorate glutamate-mediated excitotoxicity, the nature of the experimental procedures involved means that multiple cerebrovascular and neurochemical mechanisms are disturbed in addition to the presumed primary

insult of elevated extracellular glutamate levels. Evidence suggests that these mechanisms will not only contribute to the outcome of the ischaemic insult, but will also influence anti-ischaemic drug action. For example, following MCA or carotid artery occlusion in experimental models, cerebral blood flow is reduced in the penumbral ischaemic zone, leading to impaired delivery of the metabolic substrates oxygen and glucose, reduced tissue oxygen tension, and hence disturbed energy generation. Under such circumstances the neuroprotective effects of drugs whose actions are mediated by energy-dependent mechanisms may be attenuated, while agents which improve tissue perfusion in marginal areas may reduce neuronal damage without having any direct effect on the excitotoxic process.

In an attempt to circumvent these potentially complicating factors, a novel model involving production of a glutamate-induced cortical lesion has been developed to facilitate investigations of the effects of putative neuroprotective agents against pure glutamate-induced neurotoxicity *in vivo* (Fujisawa et al., 1993a and b; Landolt et al., 1993). This method employs retrograde dialysis of glutamate into the cerebral cortex of rats to produce excitotoxic lesions in a less invasive manner than cerebral ischaemia models. The cortical lesions produced have previously been characterised and show histological alterations consistent with excitotoxic cell damage (i.e. mitochondrial and cytoplasmic swelling, pyknosis). The nature of the lesion produced by cortical glutamate perfusion is illustrated in Figure 9 (Methods).

In the past, selective excitatory amino acid receptor agonists have been widely used to produce excitotoxic lesions in the CNS rather than glutamate itself, due to their lack of affinity for the glutamate uptake carrier, and

because unlike glutamate they are not involved in CNS metabolic processes. However, in the studies of excitotoxic cortical lesions outlined in this thesis, glutamate was selected as the exogenous excitotoxin due to the apparent intrinsic involvement of endogenous glutamate in pathological processes of neuronal injury. Consequently, in an ischaemic insult, for example, the broad spectrum of glutamate-mediated actions within the CNS (including actions at all excitatory amino acid receptor subtypes and as a substrate for uptake mechanisms) potentially contribute to the overall outcome of the pathological episode (e.g. ischaemic insult).

## 2.3 Excitotoxic Cell Death in Chronic Neurodegenerative Diseases

The capacity of glutamate to induce excitotoxic lesions reminiscent of those occurring in human neurodegenerative disorders has led to the proposition that glutamate is involved in the pathogenesis of the neuronal cell death occurring in chronic diseases, such as Alzheimer's and Huntington's diseases and olivopontocerebellar atrophy. This brief analysis will concentrate on the evidence supporting a role for glutamate-mediated neurotoxicity in the neurodegenerative processes occurring in Alzheimer's Disease (AD).

### 2.3.1 Alzheimer's Disease

Alzheimer's disease (AD) is a dementing disorder manifest clinically as a progressive deterioration in memory, learning capacity, language and intellect. AD is characterised neuropathologically by the presence of large numbers of senile or neuritic plaques and neurofibrillary tangles, in

conjunction with neuronal degeneration and/or atrophy in certain brain regions, principally in associational cortex, entorhinal cortex, hippocampus and basal forebrain regions including the nucleus basalis of Meynert (nbM). In general the distribution of the histopathological markers coincides with areas of neuronal loss, high densities of plaques often being found in association areas of neocortex, hippocampus and amygdala, while high densities of tangles are similarly found in cortex, as well as in subcortical regions including the nbM, locus coeruleus and the dorsal raphé nuclei (Mann, 1988). Similarly, the psychological deficits observed in AD patients are compatible with the consequences of cortical disconnection, and dysfunction in a number of hippocampal pathways such as the entorhinal cortex - perforant pathway, thus showing some degree of correlation with the neuropathological sequelae of the disease.

Despite enormous interest in AD which has fuelled intensive research in recent years, and the subsequent proposal of numerous hypotheses concerning the etiology of this disorder, no theory has yet been able to satisfactorily explain all the facets of Alzheimer symptomatology. However, consistent abnormalities in cholinergic and glutamatergic systems within the brain have been observed in Alzheimer postmortem tissue, which has led to the proposition of two hypotheses of selective vulnerability of these neurotransmitter systems. The "cholinergic hypothesis" argues that the syndrome of dementia, the fundamental feature of this disorder, is attributable to cortical cholinergic dysfunction resulting from loss of cortical cholinergic innervation from neurones in the nbM, and cholinergic dysfunction in the hippocampus. This theory is supported by findings of reduced

cholineacetyltransferase (ChAT) and acetylcholinesterase (AChE) activities in Alzheimer hippocampus and cortex in post-mortem and biopsy studies (for review see Bartus et al., 1982; Fibiger, 1991). Additionally, neuronal loss and atrophy has been observed in cortical-projecting cholinergic magnocellular neurones of the nbM in AD patients. However recent observations of glutamatergic deficits in Alzheimer cortex and hippocampus have led to an alternative glutamate hypothesis of AD, which implicates the involvement of excitotoxic mechanisms in the pathogenesis of the disease, as is described below.

### 2.3.2 Glutamate Dysfunction in Alzheimer's Disease

Various lines of evidence indicate that glutamate-mediated excitotoxic processes are involved in the chronic neurodegeneration seen in Alzheimer's disease (AD) (for review see Greenamyre, 1986; Maragos et al., 1987; Procter et al., 1988). The neuropathology of AD includes neuronal loss in cortex and hippocampus. Glutamate is putatively the major excitatory neurotransmitter in pyramidal neurones which constitute approximately 70% of the total neuronal population of mammalian cerebral cortex and mediate cortico-cortical and cortico-fugal neurotransmission (Peinado et al., 1986). Loss of cortical pyramidal cells is a prominent feature of AD leading to suggestions that cortical glutamate dysfunction may contribute to the pathophysiological progression of the disease. Subsequently, histological studies have also demonstrated disruption of cortico-cortical association pathways and cortico-hippocampal pathways which employ glutamate as a pre-synaptic neurotransmitter in AD (Rogers and Morrison, 1985; Hymen et al., 1987).

Autoradiographic investigations of high-affinity glutamate uptake site distributions have shown marked reductions in uptake site densities in cortical and hippocampal regions (Cowburn et al., 1988) suggesting that glutamatergic presynaptic elements are severely reduced in AD. In addition, recent studies have indicated that many pyramidal neurones which contain neurofibrillary tangles also show glutamate-like immunoreactivity (see Maragos et al., 1987), while exposure of human neuronal cultures to glutamate can induce formation of paired helical filaments, which are constituents of neurofibrillary tangles suggesting a link between glutamate and cytoskeletal change in AD (De Boni and Crapper-McLachlan, 1985).

Supporting the hypothesis of glutamatergic disruption in AD there is also evidence from *in vitro* radioligand binding studies of loss of post-synaptic excitatory amino acid receptors in regions showing the neuropathological hallmarks of AD most notably in cortical and hippocampal regions (Greenamyre, 1986; Greenamyre et al. 1985, 1987; Chalmers et al., 1990; Dewar et al., 1991). Greenamyre et al., (1985) found total glutamate binding to be reduced by 34-45% in the cerebral cortex of brains from AD patients compared to levels in age-matched controls. Subsequent ligand binding studies of glutamate subtype alterations in AD postmortem tissue have in general indicated down-regulation of excitatory amino acid receptor subtypes in cortex and hippocampus. However, the diverse etiology of the disease, and the variability of the extent of progression of the disease when AD patients come to postmortem, means that the overall pattern of receptor changes is not as yet clear. For instance, while a number of groups have reported reduced NMDA receptor levels in cortical and hipppocampal regions

(Greenamyre 1986; Greenamyre et al., 1987; Chalmers et al., 1990), others have reported NMDA levels to be unaltered (Geddes et al., 1986; Cowburn et al., 1988). [$^3$H]-TCP binding to the NMDA receptor-associated ion channel has been reported to be reduced in frontal cortex and hippocampus of AD patients. In contrast, Procter et al. (1989) reported no change in [$^3$H]-MK-801 binding in the cortex of AD patients, but demonstrated a possible dissociation of the coupling between the regulatory glycine site and the PCP binding site on the NMDA receptor channel.

AMPA and KA receptor binding has been shown to be unaltered in cortical regions of AD patients relative to levels in age-matched controls (Chalmers et al., 1990). In hippocampal regions, quisqualate/AMPA binding site deficits have been reported in the CA1 region, dentate gyrus and subiculum (Greenamyre et al., 1987; Dewar et al., 1991). Down-regulation of KA receptors in the CA1 region, and reductions in metabotropic receptor levels in subiculum and CA1 have also been reported in subiculum and CA1 (Dewar et al., 1991). In conjunction with reports of the integrity of other receptor systems in these regions, including muscarinic cholinergic, benzodiazepine and $GABA_A$ binding sites, and the maintenance of normal glutamate binding levels in other brain areas, the observations from autoradiographical studies of excitatory amino acid receptor distributions in AD suggest that the pathogenesis of AD may involve regionally-specific, selective degeneration of structures innervated by glutamatergic projections.

The clinical manifestations of the disease include memory and learning impairments, processes in which glutamatergic systems are heavily implicated. For example, the hippocampus is the site of long-term

potentiation, a phenomenon mediated by NMDA receptor activity in which brief, high frequency stimulation of glutamatergic afferents leads to a long-lasting enhancement in the synaptic response, which is putatively associated with memory (Collingridge and Bliss, 1987). Thus the profound loss of glutamate receptors in cortical and hippocampal regions may explain the learning and memory deficits which are prominent in AD. In addition, behavioural studies employing lesions of glutamatergic hippocampal pathways have demonstrated learning and memory deficits in experimental animals (Morris et al., 1986; Everitt et al., 1987), thus supporting a role for glutamatergic hypofunction in the cognitive impairments characteristic of AD.

As a result of the observed role of NMDA receptors in long-term potentiation it has been suggested that positive modulation of NMDA receptor activity in AD patients may ameliorate the learning and memory impairments concomitant to the disease. Due to its well documented role in excitotoxicity, the potential of the NMDA receptor complex as a therapeutic site must be treated with caution. Therefore, manipulating the glycine co-agonist site with a partial agonist such as D-cycloserine, has been proposed as a possible route for modulating NMDA receptor activity in AD while avoiding the problems of excitotoxicity associated with excessive stimulation of the transmitter recognition site (Hood et al., 1989; Monahan et al., 1989b; Watson et al., 1990; Emmett et al., 1991; Chessell et al., 1991).

### 2.3.3 Excitotoxic Basal Forebrain Lesions - A Model of Alzheimer's Disease?

As a corollary of the observations of reduced cortical ChAT activity and concomitant loss or atrophy of neurones in the nucleus basalis of Meynert (nbM) of AD patients, it has been proposed that lesions of cholinergic basal forebrain - cortical projections in the rat might constitute an animal model of AD. Subsequently, numerous studies in the rat have reported evidence of cortical cholinergic dysfunction and impairment of performance in a variety of behavioural tests of learning and memory following both electrolytic and neurotoxic lesions of the nucleus basalis magnocellularis (NBM) basal forebrain region (for review see Dunnett et al., 1991).

The nucleus basalis magnocellularis (NBM) region in the rat, believed to be homologous with the nbM in man, consists of a group of large acetylcholinesterase (AChE) positive neurones distributed diffusely amongst cells of the ventromedial globus pallidus. NBM efferents provide the major extrinsic cholinergic innervation of cortex, contributing up to 70% of the cholinergic content of neocortex (Johnston et al., 1981). While NBM lesions induce massive cholinergic denervation in the cortex (as demonstrated by decreases in cortical ChAT and AChE activities, choline uptake and ACh release), cortical ablation or neurotoxic cortical lesions reciprocally induce retrograde degeneration of cholinesterase-positive NBM neurones (Sofroniew and Pearson, 1985) raising the possibility that in some cases the histological changes seen in AD nbM may result from retrograde degeneration.

Experimental attempts to determine the functional role of NBM neurones have to date focused primarily on the consequences of destruction of NBM efferents on performance in behavioural tasks designed to assess

different facets of cognitive function. In the absence of a selective cholinergic neurotoxin, and given the gross and non-specific nature of the cell destruction elicited by electrolytic lesions, axon-sparing excitotoxic amino acid lesions have been widely used to destroy cell bodies in the basal forebrain, including cholinergic neurones of the NBM. To this end, ibotenic acid, kainate acid (KA), quisqualic acid, AMPA and NMDA have all been employed to lesion NBM efferents (London et al., 1984; Orzi et al., 1987; Robbins et al., 1989a and b; Page et al., 1991). However, while such basal forebrain lesions have been found to impair performance in a variety of behavioural tasks which have been widely interpreted to reflect disturbances in learning and memory processes, Dunnett and colleagues have identified a dissociation in the effects of different excitatory amino acids, both in terms of cognitive deficits and accompanying cholinergic dysfunction (for review see Dunnett et al., 1991). Of the five excitotoxins cited above, AMPA and quisqualic acid appear to be the toxins of choice to lesion cholinergic NBM neurones, since they yield the greatest depletions in cortical ChAT activity while also sparing dorsal pallidal and non-cholinergic basal forebrain neurones. In the hands of different investigators, AMPA and quisqualate basal forebrain lesions have been shown to reduce cortical ChAT activity by approximately 40-70%, compared to 15-40% depletions seen following NMDA, KA and ibotenic acid lesions (Etherington et al., 1987; Dunnett et al., 1987; Robbins et al., 1989 a and b; Page et al., 1991). AMPA appears to be the most cholinergic-selective of these neurotoxins, reducing cortical ChAT activity by more than 70%, which represents near total destruction of the extrinsic cholinergic innervation of neocortex (Page et al., 1991). These

observations suggest that the excitatory amino acid input to cholinergic NBM neurones is mediated largely through AMPA receptors.

Following from these observations, doubt has been cast upon the assumption that cognitive deficits seen following excitotoxic NBM lesions are due solely to loss of cholinergic neurones since different excitatory amino acid agonists have been found to have different effects on behavioural tests of learning, memory and attention (for review see Dunnett et al., 1991). Studies have revealed that whereas ibotenic acid and NMDA lesions impair performance in tests of cognitive and mnemonic function (such as acquisition of a visual discrimination task) quisqualic acid and AMPA fail to induce deficits in the same tasks despite producing far greater reductions in cortical ChAT activity, as illustrated in Table 3. It has therefore been suggested that the functional deficits induced by ibotenic acid basal forebrain lesions in these tasks cannot be attributed to the destruction of cholinergic neurones in the NBM. Instead, these apparent "cognitive" impairments may be due to disruption of other cognitive or non-cognitive processes within the basal forebrain, arising from non-specific destruction of non-cholinergic neuronal populations. However, Robbins and colleagues (1989b) have also demonstrated that basal forebrain lesions induced by ibotenic acid, quisqualate and AMPA all impair attentional function, as assessed by a 5-choice serial reaction time task. Supporting the involvement of cholinergic systems in the attentional task examined, comparable attentional deficits have subsequently been observed in the same test paradigm following intracerebroventricular administration of the high-affinity choline uptake inhibitor hemicholinium, the effects of which can be reversed by co-

## TABLE 3
## EFFECTS OF EXCITOTOXIC BASAL FOREBRAIN LESIONS ON CORTICAL ChAT LEVELS AND COGNITIVE FUNCTION

| | IBOTENATE | QUISQUALATE | NMDA | AMPA |
|---|---|---|---|---|
| Dunnett et al. 1987 | 0.06M (2x0.5µl) | 0.12M (2x0.5µl) | 0.12M (2x0.5µl) | |
| ChAT Depletion | 41% | 50% | 39% | |
| Water Maze | +++ | - | - | |
| Passive Avoidance | +++ | +++ | +++ | |
| Etherington et al. 1987 | 0.06M (0.4µl) | 0.12M (2x0.5µl) | | |
| ChAT Depletion | 17% | 41% | | |
| Operant Delayed Matching | ++ | - | | |
| Wenk et al. 1989 | 0.025M (0.5µl) | 0.12M (0.5µl) | | |
| ChAT Depletion | 41% | 73% | | |
| T-maze Discrimination | ++ | + | | |
| Robbins et al. 1989a | 0.06M (0.4µl) | 0.12M (2x0.5µl) | | |
| ChAT Depletion | 31% | 50% | | |
| Visual Attention | ++ | ++ | | |
| Robbins et al. 1989b | 0.06M (0.4µl) | 0.12M (2x0.5µl) | | |
| ChAT Depletion | 27% | 44% | | |
| Conditional Learning | ++ | - | | |
| Riekkinen et al. 1991 | 0.07M (2x0.3µl) | 0.10M (2x0.3µl) | | |
| ChAT Depletion | 51% | 65% | | |
| Water Maze | +++ | - | | |
| Passive Avoidance | ++ | ++ | | |
| Page et al. 1991 | 0.09M (0.5µl) | | | 0.015M (0.5µl) |
| ChAT Depletion | 49% | | | 70% |
| Water Maze | +++ | | | - |
| Passive Avoidance | ++ | | | ++ |

Selected examples from the literature of differential effects of basal forebrain lesions induced by ibotenate, quisqualate, NMDA and AMPA on cortical cholineacetyltransferase (ChAT) activity, and on various tests of cognitive and attentional function. Water maze, passive avoidance, operant delayed matching, conditional learning and T-maze discrimination tasks are tests of learning and memory. Visual attentional tasks assess attentional function.
+++ major deficit; ++ moderate deficit; + mild deficit; - no deficit.

administration of the anticholinesterase physostigmine (Muir et al., 1992a). These results are therefore consistent with the hypothesis that at least some of the deficits obtained on this attentional task may be attributable to disruption of cholinergic NBM-cortical projects.

As a consequence of the use of excitatory amino acids to lesion basal forebrain-cortex projections in these experiments, it appears that NBM-cortical cholinergic neurones do not play an essential role in learning and short-term memory processes, but may be involved in attentional function. Thus, studies employing the excitotoxic properties of glutamate congeners have further challenged the "cholinergic hypothesis" of memory dysfunction in dementia and aging.

These studies serve to highlight the problems surrounding putative animal models of the deficits seen in AD patients. While it is widely accepted that the diverse symptomatology of AD generally precludes the utility of animal models such as NBM lesions, except in attempting to mimic discrete lesions which might contribute to Alzheimer pathology, investigations of NBM neurotoxic lesions have identified a mismatch between biochemical ChAT deficits and functional cognitive deficits which were previously thought to be representative of the deficits underlying dementia. In addition, such studies illustrate the utility of using excitatory amino acids to manipulate neuronal activity, and give insight into the functional organisation of anatomical pathways within the CNS.

## 3. IMAGING FUNCTIONAL ACTIVITY IN THE CNS

The development of autoradiographic radioligand binding techniques in the 1970s revolutionised experimental approaches for identifying and localising components of functional systems within the CNS (for review see Young and Fagg, 1990; London, 1993). In the past, investigations of neurotransmitter systems and functional pathways within the brain relied on biochemical, histochemical and electrophysiological techniques, such as mapping the transport of dyes or radiolabelled, fluorescent or immunofluorescent markers, measurement of the effects of discrete intracerebral interventions on levels of biochemical markers, and electrophysiological studies into the localisation of evoked electrical responses. However, the utility of these approaches is restricted by a number of fundamental drawbacks. Due to the nature of the experimental protocols involved, these procedures generally only permit investigation of isolated neuronal populations or pathways decided on *a priori*, and often necessitate the use of dissected brain tissue, therefore limiting the degree of anatomical localisation obtainable and giving little scope to evaluate the repercussions of manipulations on integrated activity throughout the CNS as a whole. In addition, while these methods may demonstrate pathways with a potential for function, they give no insight into their contribution to normal CNS activity. In contrast, *in vitro* and *in vivo* isotope labelling autoradiographic techniques allow mapping of CNS elements and functional activity, allowing visualisation and quantitation of specific radiolabelled ligand distributions in discrete structures throughout the CNS with high degrees of spatial resolution, in both normal and pathological conditions, and

with no requirement for *a priori* determination of the regions to be examined. Quantitative autoradiographic procedures have now been adapted to assess many different components of integrated cerebral functional activity both *in vitro* and *in vivo*, discussed in brief below, and provide a valuable tool to complement histochemical, biochemical and electrophysiological investigations of neurotransmitter-mediated events in the CNS (see London et al., 1993).

*In vitro* autoradiographic procedures have been applied to image the distributions of pre- and post-synaptic neuronal elements including binding sites, transmitter uptake sites and second messenger systems. For example, tritiated ligands have been widely used to map constituents of glutamatergic systems within the brain including distributions of NMDA, AMPA, kainate and metabotropic receptor-associated transmitter binding sites, receptor-associated ion channels, and high-affinity glutamate/aspartate uptake sites in both homogenate and tissue section preparations (Cotman et al., 1987; Young and Fagg, 1990; see also Section 1.1.6). Radiolabelled ligands also have a number of applications to map functional activity *in vivo*. Isotopically labelled orthograde and retrograde axoplasmic transport markers are used to map specific neuronal projections; labelled peptide substrates such as [$^{3}$H]-leucine and [$^{3}$H]-valine localise sites of protein synthesis; the distribution of activated receptor complexes may be mapped *in vivo* by radiolabelled tracers, such as the localisation of active NMDA receptors by [$^{125}$I]-MK-801 (McCulloch et al., 1992).

Initial investigations of cerebral energy metabolism *in vivo* employed the nitrous oxide method of Kety and Schmidt (1948) or adaptations of this

procedure (for review see Sokoloff, 1981). However, these procedures only measure average rates of energy metabolism throughout the brain as a whole, and consequently, while these techniques have demonstrated changes in cerebral metabolic rate following gross or diffuse changes in cerebral function (for example during anaesthesia) they are relatively insensitive to subtle or localised changes in cerebral metabolism (Sokoloff, 1981). Quantitative autoradiographic *in vivo* imaging procedures have enabled assessment of local rates of cerebral blood flow and energy metabolism in discrete brain regions, allowing non-prejudicial measurement of dynamic events simultaneously throughout the CNS.

Local rates of cerebral blood flow may be measured using [$^{14}$I]-antipyrine (Sakurada et al., 1978); and cerebral energy metabolism can be assessed in terms of local rates of cerebral glucose use (LCGU) by measuring [$^{14}$C]-2-deoxyglucose uptake in discrete brain regions (Sokoloff et al., 1977). In addition, the 2-deoxyglucose method has been modified to allow local measurement of glucose utilisation in man. Radiolabelling the 2-deoxyglucose molecule with the $\gamma$-emitter $^{18}$F allows non-invasive detection of local levels of 2-deoxyglucose in the brain using computerised positron-emission tomography (PET).

In the present thesis, the indices of cerebral functional activity in the rat, under both normal and pathological conditions, have been investigated *in vivo* using principally two quantitative autoradiographic techniques, which are described in detail below. The [$^{14}$C]-2-deoxyglucose procedure, which facilitates the measurement of cerebral metabolic rates for glucose *in vivo*, has been characterised in great detail over the last 15 years since its

development by Sokoloff and colleagues (1977). In contrast the [$^{125}$I]-MK-801 technique which maps the distribution of activated NMDA receptors *in vivo* was developed relatively recently and has yet to be extensively investigated.

## 3.1 [$^{14}$C]-2-Deoxyglucose Autoradiography Maps Cerebral Glucose Use *In Vivo*

[$^{14}$C]-2-Deoxyglucose autoradiography (Sokoloff et al., 1977) provides a unique opportunity to gain insight into functional activity within the brain as it is reflected by local rates of cerebral glucose utilisation. This autoradiographic technique permits *in vivo* localisation and quantitation of glucose use in discrete anatomical regions throughout the CNS.

The conceptual basis of the method is that, under normal physiologic conditions, aerobic catabolism of glucose constitutes the major energy-generating pathway for cerebral tissue. Since the functional activity of any CNS region is intrinsically linked directly with energy consumption within that region, and as the CNS has only a minimal capacity to store carbohydrate, then function-related energy requirements must be met by oxidative catabolism of glucose extracted from the circulating blood (Sokoloff et al., 1977; Siesjö, 1978; McCulloch, 1982).

The use of isotopically labelled 2-deoxyglucose to determine rates of cerebral glucose utilisation takes advantage of the biochemical characteristics produced by the simple modification of glucose to 2-deoxyglucose. Both molecules are transported into brain cells from the blood by the same uptake carrier at the same rate, where both undergo phosphorylation by hexokinase. However at this stage the metabolic

pathways of the two molecules diverge. While glucose-6-phosphate is further metabolised, deoxyglucose-6-phosphate metabolism ceases (at least for the 45 min duration of the experiment) and the molecule becomes essentially trapped within the neurones (Sokoloff et al. 1977). Therefore, by isotopically labelling 2-deoxyglucose with $^{14}C$, the amount of 2-deoxyglucose taken up into discrete brain structures can be measured densitometrically. By using the operational equation developed by Sokoloff and colleagues (1977), a mathematical model which takes into consideration the biochemical properties of glucose and 2-deoxyglucose, the local rate of glucose utilisation in a given structure can be calculated from the levels of glucose and [$^{14}C$]-2-deoxyglucose in the circulating arterial blood, and the autoradiographically determined level of [$^{14}C$]-2-deoxyglucose in the structure (see Methods, Section 1.1). It is therefore possible to identify structures and pathways throughout the entire CNS in which metabolic activity is altered.

Many different energy-dependent processes contribute to the rate of glucose utilisation within neurones, including transmitter synthesis, release and reuptake; the biosynthesis of macromolecules; and the maintenance of ionic gradients by ionic pumping. In addition, the different structural elements of cerebral tissue, such as the neuronal perikarya, terminals, axons and dendrites, and glial cells, will differentially contribute to glucose use within a region. It has been estimated that neurones account for approximately 75% of the total oxygen consumption in the CNS (Siesjö, 1978), while electrical activity in neuronal terminals is thought to provide the major contribution to dynamic alterations in cerebral glucose use (see Sokoloff,

1981; Kadekaro et al., 1987; Dewar and McCulloch, 1992). Studies also indicate that most of the energy generated by the brain is used for ion transport. This is based on findings that induction of an isoelectric encephalogram (EEG) by barbiturate anaesthesia reduces cerebral glucose catabolism to about 40% of its normal level (Crane et al., 1978), while concomitant inhibition of the $Na^+$, $K^+$-ATPase electrogenic pump further reduces cerebral glucose use to approximately 20% of its normal level (Astrup et al., 1981).

It should also be noted that the local rate of glucose utilisation measured in a discrete region of the brain represents the average glucose use in a heterogenous population of cell types within that structure (including afferent neurones, interneurones and glia). Hence, if different cell types within the same structure exhibit opposite alterations in [$^{14}$C]-2-deoxyglucose uptake, no overall change in deoxyglucose uptake may result, despite radical alterations in functional activity at the cellular level. In addition, increases and decreases in glucose use cannot be equated simply with neuronal excitation and inhibition, respectively. There is no evidence to suggest that the energetic requirements of post-synaptic inhibition are any different than those of excitation, particularly when reflecting that the largest component of glucose use is apparently associated with terminal activity. This view receives support from studies by Ackerman and colleagues (1984) which demonstrated increased glucose use during long-duration recurrent inhibition in the hippocampus. Thus, changes in glucose use may be used to define regions in which neuronal activity is altered. However, in pharmacological investigations these regions will not represent solely the primary sites of

drug-receptor interaction, but will reflect polysynaptic circuits in which activity is influenced by the consequences of the receptor manipulation.

A number of alternative approaches to determine local cerebral metabolic rate have previously been investigated, for example, measuring the local tissue concentrations of inert, diffusable radioactive tracers (based on methods used to determine local rates of cerebral blood flow; Landau et al., 1955; Kety, 1960), or using [$^{3}$H]- and [$^{14}$C]-deoxyglucose (Crane et al., 1978) or [$^{14}$C]-glucose (Hawkins et al., 1974) as tracer molecules. However these methods have proved unsatisfactory compared to the [$^{14}$C]-2-deoxyglucose technique of Sokoloff et al., (1977) for a number of reasons. Firstly, the use of inert radioisotopes is handicapped by the unsuitability of the radiolabelled species of the normal substrates for cerebral energy metabolism, oxygen and glucose, for measurement *in vivo*. Both oxygen and glucose are rapidly converted to carbon dioxide, which is subsequently cleared from the cerebral tissues too rapidly for accurate measurements (for review see Sokoloff et al., 1977; Sokoloff, 1981). In contrast, the method of Crane et al., (1978) measures the accumulation of deoxyglucose-6-phosphate over a brief period (4 minutes) after rapid inactivation of hexokinase. Although the short time constant makes this approach attractive, the requirement of gross tissue dissection and chromatographic detection of deoxyglucose-6-phosphate levels restrict its utility due to the limited neuroanatomical localisation possible compared with autoradiographic approaches. In addition, doubts surround the constancy of the phosphorylation coefficient in this method and it has been suggested that glucose use measures may be influenced by transient changes in local cerebral blood flow (for review see McCulloch, 1982).

Thirdly, the method described by Hawkins et al. (1974) employing radiolabelled glucose has proved to be untenable since one of the central assumptions of the technique - that isotopic equilibrium exists between glucose pools in the CNS and in arterial plasma - has been shown to be invalid (see McCulloch, 1982).

The use of the [$^{14}$C]-2-deoxyglucose *in vivo* autoradiography technique of Sokoloff and colleagues (1977) has a number of advantages over the procedures outlined above, most notably that it allows the quantification of local rates of cerebral glucose utilisation simultaneously in all components of the CNS, in conscious animals. This approach is non-prejudicial, allowing the identification of brain regions involved in functional events which may not have been predicted *a priori*. The method also attains a high degree of spatial resolution of $^{14}$C distribution, while the use of cryostat-processed brain sections allows the [$^{14}$C]-2-deoxyglucose method to be combined with ligand binding autoradiography in consecutive sections, to enable investigation of any receptor alterations in functionally altered regions. The [$^{14}$C]-2-deoxyglucose technique can therefore give novel insight into cerebral metabolic alterations occurring during physiological, pathophysiological or pharmacological challenge. A small number of the many diverse applications of this technique are reviewed briefly below.

### 3.1.1 Applications of [$^{14}$C]-2-Deoxyglucose Autoradiography

*Physiological Applications*

Simple sensory stimulation and deprivation experiments provide strong support for the utility of the [$^{14}$C]-2-deoxyglucose method for measuring local

cerebral function. Deprivation of visual stimuli, for example by orbital enucleation in the rat, results in markedly reduced glucose use in both primary neuroanatomical components of the visual system (the superior colliculus superficial layer and the dorsal lateral geniculate body) and in secondary regions (area 17 of neocortex) (Toga and Collins, 1981; Chalmers and McCulloch, 1991). In contrast, visual stimulation by diffuse light induces intensity-dependent increases in glucose use in these regions (Miyaoka et al., 1979; Toga and Collins, 1981). In addition, similar studies in monkeys have identified and characterised ocular dominance columns in striate cortex of monkeys (Kennedy et al., 1975). Thus, the [$^{14}$C]-2-deoxyglucose technique has demonstrated that altered functional activity of photoreceptors in the retina results in metabolic changes not only in the region containing the photoreceptors, but also in components of the polysynaptic pathway involved in processing visual information in the CNS.

Similarly, alterations in glucose use within polysynaptic circuits are also seen following modulation of other sensory systems. For example, electrical stimulation of the sciatic nerve in rats results in pronounced increases in glucose use in the ipsilateral dorsal horn of the lumbar spinal cord, corresponding to a local increase in terminal activity (Kadekaro et al., 1987). Auditory stimulation increases glucose use throughout the primary auditory pathway, from the cochlear nucleus to auditory cortex, while occlusion of the external auditory canals reduces glucose use in these regions (Sokoloff et al., 1977). Olfactory stimulation with various odours has also been shown to enhance glucose utilisation in certain regions of the olfactory bulb (Kauer and Cinelli, 1993). In addition, Ginsberg et al., (1987) have demonstrated in the

rat that movement of a single whisker increases glucose use in a discrete column of the somatosensory cortex. Further, marked focal increases in glucose use occur in brain areas involved in cardiovascular regulation, such as the paraventricular and supraoptic nuclei of the hypothalamus and the nucleus of the tractus solitarus, following moderate hypotension (Savaki et al., 1982). Studies like these reflect a close coupling between local functional activity and energy metabolism in the CNS. In addition, results demonstrate that metabolic responses may be used to identify CNS regions involved in specific responses to physiological stimuli.

*Pathological Manipulations*

The utility of the [$^{14}$C]-2-deoxyglucose technique to assess alterations in glucose use in pathological states is restricted in conditions involving structural damage within the CNS, such as cerebral ischaemia, due to a number of factors which will influence the viability of the measurement. These include the possibility of impeded delivery of glucose and deoxyglucose to the brain as a result of critically reduced cerebral blood flow, altered plasma glucose levels, alterations in the values of the rate constants and/or lumped constant of the model, or the establishment of non-steady state kinetics for either glucose metabolism or tissue levels of glucose and its metabolites (for review see Ginsberg, 1990). The effects of ischaemia on 2-deoxyglucose uptake are discussed further in Section 3.1.2.

In some pathophysiological convulsive states where no structural tissue damage occurs, the [$^{14}$C]-2-deoxyglucose procedure has been employed to map seizure-propagation, demonstrating massively increased glucose use in CNS

areas activated by seizures (for review see Sokoloff, 1981). It should be noted that in some seizure states such as status epilepticus, fluctuations in presumed experimental constants (such as plasma glucose levels) and neuronal damage may occur, which will have a bearing on the accuracy of glucose use calculations.

*Pharmacological Applications*

[$^{14}$C]-2-deoxyglucose autoradiography has been used in conjunction with manipulations of almost all known neurotransmitter systems within the CNS to gain insight into central drug actions. This technique is optimally exploited when investigating function-related changes in glucose use associated with receptor stimulation or blockade, when comparing the actions of agents putatively acting at the same receptor, or when contrasting the mechanisms of action of different drugs. Alternatively, the method allows different routes of drug administration to be compared, for example systemic versus direct intracerebral administration, or to investigate the temporal progression of functional events after lesioning or stimulating specific pathways within the CNS. There have been many such studies into transmitter/drug action, which have previously been extensively reviewed (see McCulloch, 1982; Kurumaji et al., 1993). A number of glucose use studies are briefly reviewed below in an attempt to highlight the many diverse, novel insights into the functional consequences of drug/receptor interactions which [$^{14}$C]-2-deoxyglucose autoradiography can provide.

Manipulations of dopaminergic systems within the CNS, after either systemic administration of dopamine agonists and antagonists or stereotaxic

lesions of dopaminergic pathways, have shown that glucose use alterations after any of these manipulations are restricted in their anatomical distribution, emphasising the selective nature of functional events which are influenced by dopaminergic activity (Brown and Wolfson, 1978; McCulloch et al., 1982a; for review see McCulloch, 1982). Systemic administration of the dopamine agonists apomorphine or amphetamine increased glucose use in regions containing dopamine receptors, including the striatum, globus pallidus, substantia nigra pars compacta and reticulata, and the subthalamic nucleus However, glucose use changes were not restricted to areas rich in dopamine receptors. Other regions devoid of dopamine receptors, but influenced by activity in extrapyramidal regions, also showed glucose use elevations (e.g. in the cerebellar hemisphere, inferior olivary nucleus, motor cortex, motor relay thalamic nuclei, and the red nucleus). Glucose use increases in all these regions were eliminated by prior administration of the dopaminergic antagonist haloperidol (McCulloch et al., 1982b).

Direct intracerebral approaches to manipulate neuronal activity within the brain, for example by lesioning dopaminergic pathways or injecting dopaminergic agents directly into discrete brain regions, have also proved useful for characterising the involvement of specific brain regions in dopaminergic activity. For example, both systemic and local striatal injection of apomorphine result in enhanced glucose use in the subthalamic nucleus (Kozlowski and Marshall, 1980). The observation that the consequences of systemic apomorphine administration in this region could be inhibited by lesioning striatal efferents suggested that activation of a striato-pallidal-subthalamic pathway is the primary cause of increased subthalamic

glucose use, rather than activation of dopaminergic receptors intrinsic to this region (Kelly et al. 1982). Similarly, the combination of systemic administration of apomorphine and lesioning of the retinal input to primary visual structures in [$^{14}$C]-2-deoxyglucose studies has aided characterisation of the involvement of retinal dopaminergic receptor activation in visual processes (Miyaoka et al., 1979; McCulloch et al., 1980). In general, procedures resulting in decreased dopaminergic activation result in glucose use reductions, whereas activating dopamine receptors (for example by apomorphine or amphetamine administration) leads to increases in glucose use (McCulloch, 1982).

In contrast, activation of receptors specific for the major inhibitory neurotransmitter, γ-aminobutyric acid (GABA), by $GABA_A$ agonists muscimol or 4,5,6,7-tetrahydroisoxazole[5,4-c]pyridin-3-ol (THIP), results in glucose use depression throughout the CNS (Kelly and McCulloch, 1982, 1984; Kelly et al., 1986). However, investigation of log dose-response curves for glucose use changes following muscimol and THIP emphasises a regional heterogeneity in the susceptibility of structures to glucose utilisation modification by these $GABA_A$ agonists (Kelly et al., 1986). In addition, the route of administration of muscimol influences the glucose use response seen. In contrast to the widespread functional depression seen following systemic administration, local activation of GABAergic mechanisms by intrastriatal injection of muscimol evokes both increases and decreases in glucose use: glucose use being reduced in the ipsilateral striatum, but elevated in striatal efferent projection targets such as the globus pallidus and substantia nigra pars reticulata (Kelly and McCulloch, 1984).

A further example of how studies of the effects of GABA agonists on cerebral glucose use have enhanced understanding of GABAergic systems in the CNS arose from the observation that systemic administration of muscimol evoked significant alterations in glucose use in the substantia nigra pars reticulata, despite this putatively being a site of essential GABA activity within the brain. Kelly and McCulloch (1987) suggested that this occurred because inhibitory striatal efferent activity in this region was already near maximal in normal conscious animals, and hence $GABA_A$ agonists would be ineffective unless the influence of this pathway was removed or reduced, for example by lesioning striatal efferents.

The contributions of excitatory neurotransmitter systems to functional activity have also been investigated, such as 5-hydroxytryptamine ($5\text{-}HT_2$, serotonin), acetylcholine and glutamate. While studies involving lesion paradigms have shed little light on 5-HT mechanisms (Cudennec et al., 1988a), electrical stimulation of serotonergic pathways has facilitated mapping of 5-HT-dependent systems (Cudennec et al., 1988b). The use of cholinergic agonists and antagonists in functional mapping investigations has highlighted the involvement of cholinergic mechanisms in pathways thought to be involved in learning and memory paradigms in the CNS (Helén and London, 1984; Kurumaji et al., 1993). Manipulations of excitatory amino acid receptor systems are reviewed below.

### 3.1.2 Glutamate and Cerebral Glucose Use

Since glutamate is the major excitatory neurotransmitter in the CNS, and its excitotoxic action is implicated in the pathogenesis of several

neurodegenerative disorders, the effects of glutamate receptor manipulations on cerebral function in both normal and pathologic conditions are of great interest. Hence the [$^{14}$C]-2-deoxyglucose autoradiography technique has been widely used to determine the cerebral metabolic consequences of glutamate receptor-mediated events in experimental animals, for example by pharmacological manipulations of excitatory amino acid receptors and in pathologic conditions associated with elevated extracellular glutamate levels such as cerebral ischaemia, subdural haematoma and excitotoxic lesions (for review see Ginsberg, 1990).

*Pharmacological Manipulations*

Due to the wide ranging metabolic and transmitter actions of glutamate in the CNS, analysis of the effects of systemic glutamate administration on glucose use presents numerous interpretational problems. However, intravenous administration of the glutamate analogue kainic acid, at a dose previously demonstrated to be neurotoxic to specific hippocampal neurones when administered systemically, has been found to massively increase glucose use in a limited number of limbic structures (in particular in hippocampal regions CA1 and CA3, the lateral septal nucleus and amygdala), whereas glucose use in other CNS regions was unaltered (Celik et al., 1979).

Due to the fact that a number of selective NMDA receptor antagonists have been available for several years, the consequences of NMDA receptor blockade on cerebral glucose use have been intensively studied. Systemic administration of NMDA antagonists results in widespread heterogeneous alterations in glucose use throughout the CNS, with pronounced differences

seen between the effects of competitive and non-competitive antagonist classes. These discrepancies are thought to reflect the different mechanisms of action of NMDA antagonists. For example, non-competitive NMDA antagonists such as MK-801 and phencyclidine (PCP) markedly increase glucose use in anatomical components of the limbic system (in particular posterior cingulate cortex and entorhinal, cortex, hippocampus, mamillary body, substantia nigra *pars compacta* and *pars reticulata*), while moderately reducing glucose use in neocortex and the inferior colliculus (Weissman et al., 1987; Nehls et al., 1988; Kurumaji et al., 1989; McCulloch and Iversen, 1991; Hargreaves et al., 1993b). The hypermetabolic sequelae of non-competitive NMDA antagonists, for instance in components of the Papez circuit, appear to reflect the use-dependent nature of NMDA receptor channel blockade in these areas (Kurumaji et al., 1989). It appears that presynaptic terminal activity is enhanced during non-competitive channel blockade in an attempt to overcome the blockade by elevating synaptic glutamate concentrations.

In contrast to the non-competitive NMDA antagonists, which generally produce similar patterns of glucose use alterations, competitive antagonists display heterogeneous effects on glucose use. For example, CPP and AP7 induce few overt glucose use changes, but CPP-ene reduces glucose use in sensory regions including auditory and visual structures, while not markedly affecting glucose use in limbic regions (Chapman et al., 1989; Kurumaji et al., 1989). In addition, the AP7 analogue CGP-39551 (2-amino-4-methyl-5-phosphono-3-pentanoic acid 1-ethyl ester), a potent orally active competitive NMDA antagonist, induces large increases in glucose use in

limbic regions, the extrapyramidal system and olfactory regions, whilst not affecting sensory regions (Chapman et al., 1991). These heterogeneous patterns of glucose use changes evoked by competitive NMDA antagonists may represent some degree of affinity of these agents for other receptor classes, or alternatively may reflect the proposed existence of sub-populations of NMDA receptors within the brain (Sakurai et al., 1993; Seeburg, 1993). Selective, centrally active AMPA receptor antagonists have, in contrast, only recently become available. The consequences of AMPA receptor blockade on local rates of cerebral glucose utilisation are addressed in this thesis.

*Pathologic Conditions*

Following experimental focal ischaemia induced by MCA occlusion, glucose use is greatly diminished in the ischaemic core in the caudate nucleus, while a transient increase in glucose utilisation has been demonstrated in a zone around the periphery of the infarcted tissue (Shiraishi and Simon, 1990; for review see Ginsberg, 1990). This enhanced [$^{14}$C]-2-deoxyglucose uptake in the ischaemic penumbra was previously speculated to be due to anaerobic glycolysis, since double-labelling studies of local cerebral glucose use and cerebral blood flow (CBF) have demonstrated that areas of increased glucose use coincided with regions in which local CBF was markedly depressed (Ginsberg, 1990). Thus, the cerebrometabolic sequelae of ischaemic damage are in marked contrast to the association between glucose use and CBF in normal, non-ischaemic brain, where local levels of metabolism and blood flow are generally tightly coupled. However, an

increasing body of evidence supports the concept that this hypermetabolic response represents excitatory activity in penumbral neurones induced by abnormally high levels of glutamate release (Shiraishi and Simon, 1990). After global forebrain ischaemia, [$^{14}$C]-2-deoxyglucose autoradiographic studies in rat and gerbil have demonstrated general glucose use depression 1h post-ischaemia, (with the exception of the hippocampus) which persists for up to 48h in parietal cortex and caudate. In hippocampal regions (in particular, CA1), marked, though transient increases in glucose use are seen (Pulsinelli et al., 1982). This intense increase in the rate of 2-deoxyglucose uptake in the hippocampus coincides with the period of early postischaemic reperfusion and reported electrical hyperactivity in neurones, and is followed by delayed neuronal death in CA1 2-3 days later.

Subdural haematoma in the rat, which results in a zone of focal ischaemic damage in areas of cortex and striatum immediately underlying the haematoma, has also been shown to have a marked, but transient effect on cerebral metabolism around the lesion site (see Bullock et al., 1992). Glucose use is transiently increased in the periphery of the ischaemic zone, persisting for 2-4h after induction of the haematoma. However, the most striking change in functional activity occurs bilaterally in the hippocampi, where glucose use increases of approximately 142% have been detected in ipsilateral CA1 2h post-haematoma, disappearing by 4h post-lesion.

Excitotoxic lesions induced by direct intracerebral injections of excitatory amino acid agonists have been shown to result in reduced 2-deoxyglucose uptake in the lesion core. However, it should be noted that in damaged tissue reduced uptake does not necessarily represent decreased

metabolic rate (as discussed in Section 3.1.1). Nevertheless, decreases in 2-deoxyglucose uptake have been observed following a number of different interventions, including in the striatum following intra-striatal injections of kainic acid (Wooten and Collins, 1982; Kelly et al., 1982), in the amygdala following kainate lesions (Tremblay et al., 1983), and in the entorhinal cortex 14 days after ibotenate lesions of this region (Kurumaji and McCulloch, 1990a). In the latter study, the NMDA antagonist MK-801 was shown to profoundly alter the cerebral metabolic responses to entorhinal lesions in CNS regions innervated by the putatively glutamatergic projection arising from the entorhinal cortex. In contrast, intrahippocampal injections of the NMDA antagonist MK-801 result in elevated glucose utilisation in hippocampal regions 8-10 days post-lesion (Kurumaji and McCulloch, 1990b).

## 3.2 Imaging NMDA Receptor Activation *In Vivo* With [$^{125}$I]-MK-801

[$^{125}$I]-MK-801 autoradiography maps the distribution of activated NMDA receptor-channel complexes throughout the CNS (McCulloch et al., 1992; also see Wallace et al., 1992). The theoretical basis for this technique is that the NMDA antagonist MK-801 binds non-competitively at a site within the NMDA receptor-associated cation channel. At resting membrane potentials this channel is voltage-dependently blocked by $Mg^{2+}$. Therefore membrane depolarisation is required to remove this blockade, facilitating receptor activation by agonist binding at the cell surface recognition site, leading to channel opening. Thus, MK-801 binding within the channel only occurs when the NMDA receptor complex is activated (see Figure 1) (Kemp et al., 1987).

Since MK-801 is highly lipophilic and readily crosses the blood-brain barrier, it is postulated that, following intravenous injection of tracer levels of [$^{125}$I]-MK-801, subsequent autoradiographic detection and measurement of the [$^{125}$I] radiolabel in discrete brain regions will allow quantitative mapping of [$^{125}$I]-MK-801 binding, putatively reflecting the extent of NMDA receptor activation throughout the CNS. In order to take into account the degree of non-specific [$^{125}$I]-MK-801 binding within the brain, densitometric measures of isotope levels in forebrain structures are compared with cerebellar isotope levels, which act as a measure of non-specific binding due to the paucity of NMDA receptors in this region (McCulloch et al., 1992).

The specificity of [$^{125}$I]-MK-801 for the NMDA receptor ionophore has been investigated by co-administration of pharmacological doses of "cold" MK-801 and tracer doses of [$^{125}$I]-MK-801 in experimental animal models of focal ischaemia following MCA occlusion (McCulloch et al., 1992). Compelling evidence implicates the involvement of NMDA receptors in the neuropathologic processes of ischaemic brain damage, since NMDA receptor antagonists ameliorate ischaemic damage in experimental models of focal cerebral ischaemia, brain trauma and subdural haematoma (see McCulloch and Iversen, 1992). McCulloch and colleagues (1992) demonstrated in the rat, following MCA occlusion, that cold MK-801 displaced [$^{125}$I]-MK-801 binding in pathologically damaged tissue within the ischaemic core. [$^{125}$I]-MK-801 was not readily displaced in non-ischaemic tissue. It has previously been shown that extracellular levels of amino acids such as glutamate and aspartate are elevated during an ischaemic insult (Benveniste et al., 1984; Drejer et al., 1985; Butcher et al., 1990), and these elevations are thought to

In previous studies assessing [$^{125}$I]- and [$^{3}$H]-MK-801 binding *in vivo*, non-specific binding has been determined by displacement of the radioligand by an excess of cold MK-801 (Wallace et al., 1992; McCulloch et al., 1992). This approach was not used in the present study, which employed a tracer dose of [$^{125}$I]-MK-801, since the required concentration of cold MK-801 would be sufficient to be pharmacologically active *in vivo*, blocking the NMDA receptor ionophore, and would therefore interfere with the action of D-cycloserine under investigation. As a consequence, levels of [$^{125}$I]-MK-801 binding in the cerebellum were used in the present study as an estimate of non-specific binding since the cerebellum contains a low density of NMDA receptors relative to forebrain structures. However, it is recognised that this does not constitute an accurate measure of non-specific binding. As a consequence, in this thesis [$^{125}$I]-MK-801 binding levels are referred to as "total" binding in forebrain structures relative to cerebellar levels. In studies employing displacement of radiolabelled MK-801, non-specific binding has been found to constitute approximately 50% of total binding (Wallace et al., 1992). The differences in the ability of cold MK-801 to displace [$^{125}$I]-MK-801 binding in normal and damaged tissue reported by McCulloch et al., (1992) appear to reflect the large signal to noise ratio seen in [$^{125}$I]-MK-801 autoradiograms.

underlie excitotoxic cell death in ischaemia. Thus, the observation of [$^{125}$I]-MK-801 binding in conditions of increased glutamate-induced receptor stimulation, and therefore enhanced channel opening, suggests that [$^{125}$I]-MK-801 is binding at abnormally activated NMDA receptors. These observations suggest that [$^{125}$I]-MK-801 is mapping a dynamic process involved in the evolution of ischaemic brain injury *in vivo*, a view further supported by findings that [$^{125}$I]-MK-801 binding in ischaemic tissue declines over time, reflecting the progression of the ischaemic pathology from reversible to irreversible neuronal changes. However, [$^{125}$I]-MK-801 uptake was not reduced by cold MK-801 in non-ischaemic tissue where normal levels of NMDA activation exist, leading to uncertainty about the utility of using [$^{125}$I]-MK-801 as an *in vivo* ligand in the normal CNS.

It has therefore been suggested that [$^{125}$I]-MK-801 autoradiography may be valuable in elucidating the functional competency of NMDA receptors *in vivo* during a pathological challenge, such as ischaemia. This technique provides an opportunity to map dynamic activation of NMDA receptors both in animal models (McCulloch et al., 1992; Wallace et al., 1992) and in man (McCulloch et al., 1991).

In the present thesis the [$^{125}$I]-MK-801 *in vivo* binding technique has been used to try to elucidate whether NMDA receptor activation occurs in the CNS following putative stimulation of the NMDA receptor complex. Experiments are described which assess dynamic changes in NMDA receptors following administration of D-cycloserine, a ligand at the glycine modulatory site on the NMDA receptor complex at a putative agonist dose (see Section 4.3).

## 4. AIMS OF THESIS

This thesis will investigate what insight can be gained into the consequences of glutamate receptor manipulations on cerebral function by the use of quantitative autoradiographic techniques to map functional events *in vivo.*

The experiments described employ three different approaches to manipulate the activities of glutamate receptor subtypes, namely blockade of AMPA receptor activity, modulation of NMDA receptor activity by a glycine site partial agonist, and modification of neuronal activity in a circumscribed region of the CNS by direct intracerebral injections of excitatory amino acid receptor agonists. The analytical techniques used allow examination of aspects of the functional consequences of manipulations which putatively influence glutamate's roles in the CNS as a neurotransmitter, and as a neurotoxin.

### 4.1 AMPA Receptor Blockade

Glutamate-induced neurotoxicity is implicated in the pathology of neurodegenerative disorders such as ischaemia. In the last ten years, much effort has been exerted in attempts to ameliorate the excitotoxic properties of glutamate by manipulating excitatory amino acid receptor activities. Most work, to date, has focused on modulation of the NMDA receptor due to the availability of potent NMDA receptor antagonists. However, while NMDA receptor antagonists such as MK-801 and CPP-ene are undoubtedly potent neuroprotectants, their clinical utility is restricted by their adverse effects on brain function. NMDA receptor antagonists have been found to

induce morphological cell changes including cytoplasmic swelling in certain regions of the CNS, notably in the posterior cingulate cortex (Olney et al., 1989, 1991; Hargreaves et al. 1993). These changes, which are similar to excitotoxic neuronal pathology, may progress to cell death. Previous [$^{14}$C]-2-deoxyglucose autoradiography studies have highlighted hypermetabolic sequelae of NMDA receptor blockade in regions associated with abnormal morphometric cell changes and altered gene expression, (Park et al., 1988a and b; Kurumaji et al., 1989; Hargreaves et al., 1993). In addition NMDA antagonists are associated with psychosis and memory loss. Grotta (1994) Therefore, it is important to identify alternative anti-ischaemic strategies which avoid the adverse metabolic effects of NMDA antagonists.

Attention has recently turned to trying to ameliorate excitotoxicity at non-NMDA receptors. In particular, AMPA receptor activity has come under increased scrutiny following reports that the fast excitatory post-synaptic potential (EPSP) mediated by AMPA receptors underlies neuronal excitation, and the identification of several mechanisms of AMPA receptor involvement in $Ca^{2+}$ influx, (which are postulated to be the ultimate cause of cell death). Subsequently, various non-NMDA antagonists have been shown to be neuro-protective in both *in vitro* and *in vivo* models of excitotoxicity and ischaemia. To date, the most potent AMPA receptor antagonists described are NBQX and the novel agent LY-293558.

*NBQX*: A quinoxalinedione analogue, 2,3-dihydroxy-6-nitro-7-sulfamoyl-benzo(F)quinoxaline (NBQX) is the most potent AMPA antagonist of this class as yet reported. In binding studies in rat cortical membranes NBQX

**AMPA**

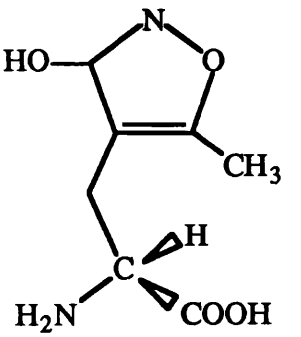


**NBQX**

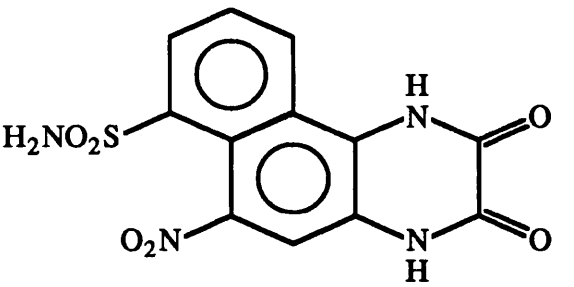


**LY-293558**
**(-) Isomer**

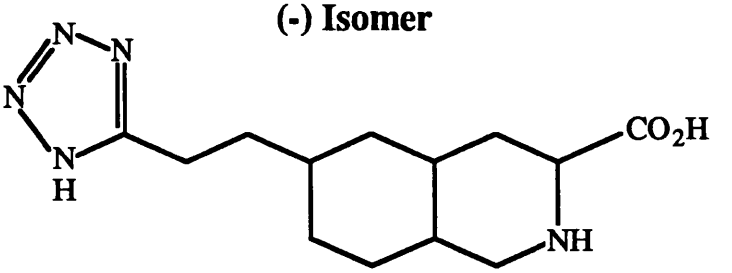


FIGURE 3: AMPA RECEPTOR LIGANDS

competitively inhibited [$^3$H]AMPA binding with an $IC_{50}$ of 150nM compared to an $IC_{50}$ of 4.8μM for displacement of [$^3$H]-KA binding. In addition, NBQX has no affinity for the transmitter recognition site or the glycine regulatory site on the NMDA receptor complex (Sheardown et al., 1990). NBQX has been found to be neuroprotective in both *in vitro* (Sheardown et al., 1990), and *in vivo* models of global ischaemia in the gerbil (Sheardown et al., 1990) and the rat (Buchan et al., 1991a; Nellgard and Wieloch, 1992; Diemer et al., 1993; Sheardown et al., 1993), and in a model of focal ischaemia in the rat (Gill et al., 1992). The potent neuroprotective action of NBQX against the delayed selective neuronal death seen in the hippocampus following transient global ischaemia contrasts markedly with the limited neuroprotection seen after NMDA antagonists (Buchan et al., 1991a and b; Sheardown et al. 1993).

*LY-293558*: Initial studies have demonstrated that the novel AMPA antagonist (-)-6-(2-(1H-tetrazol-5-yl)ethyl)-1,2,3,4,4a,5,6,7,8,8a-decahydroisoquinoline-3-carboxylate ((-)LY-293558) selectively displaces [$^3$H]AMPA binding in rat cortical membranes with an $IC_{50}$ of 1.35 μM. In electrophysiological studies in the cortical slice assay LY-293558 was found to reduce depolarisations due to 40μM AMPA with an $IC_{50}$ of 1.78μM (Ornstein et al., 1993). Previous investigations into the racemic amino acid analogue, LY-215490, have revealed neuroprotective actions of this agent *in vivo*. LY-215490 is anticonvulsant in a maximal electroshock (MES) seizure assay in mice, and blocks rigidity in mice induced by the AMPA receptor agonist ATPA (see Ornstein et al., 1993). Observations that LY-215490 is less potent than its (-) isomer, LY-293558, in displacing [$^3$H]AMPA binding in

rat cortical membranes ($IC_{50}$ of 4.81μM) and in antagonizing AMPA-induced depolarisations in a cortical slice assay ($IC_{50}$ of 6.0μM) (Ornstein et al., 1993) have led to the suggestion that LY-293558 will also have potent neuroprotective effects *in vivo*. Although investigations into the neuroprotective actions of LY-293558 are limited to date, initial studies in the MCA occlusion model of ischaemia in the cat (Bullock et al., 1993) support a neuroprotective role for LY-293558 *in vivo*.

AIM NUMBER 1: To assess the consequences of AMPA receptor blockade on cerebral function in the conscious rat. The study will employ [$^{14}$C]-2-deoxyglucose *in vivo* autoradiography to compare and contrast the effects of systemic administration of NBQX and LY-293558 on local cerebral glucose utilisation, and to determine whether AMPA receptor blockade at neuroprotective doses induces adverse metabolic alterations similar to those elicited by NMDA antagonists.

## 4.2 NMDA Receptor Manipulation by a Glycine Site Partial Agonist

It has been proposed that dysfunction in the mechanism of long-term potentiation (LTP) in hippocampal neurones may underlie the memory and learning impairments manifested in the dementia associated with Alzheimer's disease (AD). Following reports that NMDA receptor activation is necessary for the induction of LTP in the hippocampus, and the detection of NMDA receptor deficits in hippocampal regions of AD brain, it has been postulated that positive modulation of NMDA receptors may ameliorate the cognitive deficits seen in this disease. One putative method of enhancing NMDA

receptor activity is by agonist stimulation of the glycine modulatory site on the NMDA receptor complex. D-Cycloserine (D-4-amino-3-isoxaxoldione), a partial agonist at the glycine regulatory site on the NMDA receptor complex, has been proposed as a possible candidate to enhance NMDA receptor activation in situations of glutamatergic dysfunction. D-Cycloserine has been in clinical use for many years as an antimycobacterial agent, but a neurobiological action has only recently been recognised following observations that it readily crosses the blood-brain barrier. Subsequent studies have indicated that D-cycloserine exhibits partial agonist properties at the glycine co-agonist site on the NMDA receptor complex: D-cycloserine displaces strychnine-insensitive [$^3$H]-glycine binding in both rodent and human brain tissue (Monahan et al., 1989b; Procter et al., 1991), and has also been shown to dose-dependently enhance [$^3$H]-TCP binding at the NMDA receptor-associated ionophore (Hood et al., 1989). However, the maximal extent of [$^3$H]-TCP binding enhancement by D-cycloserine is less than that produced by pure glycine site agonists such as glycine and serine, while D-cycloserine actually antagonises glycine-induced enhancement of [$^3$H]-TCP binding (Hood et al., 1989). In addition, partial agonist actions of D-cycloserine have been identified in its regulation of cGMP activity in Xenopus oocytes (Watson et al., 1990) and in mouse cerebellum (Emmett et al., 1991) (see Figure 4). Further, putative agonist doses of D-cycloserine (0.1-10mg/kg) have been shown to positively modulate NMDA activity, enhancing performance in behavioural tests of learning in the rat (Monahan et al., 1989b).

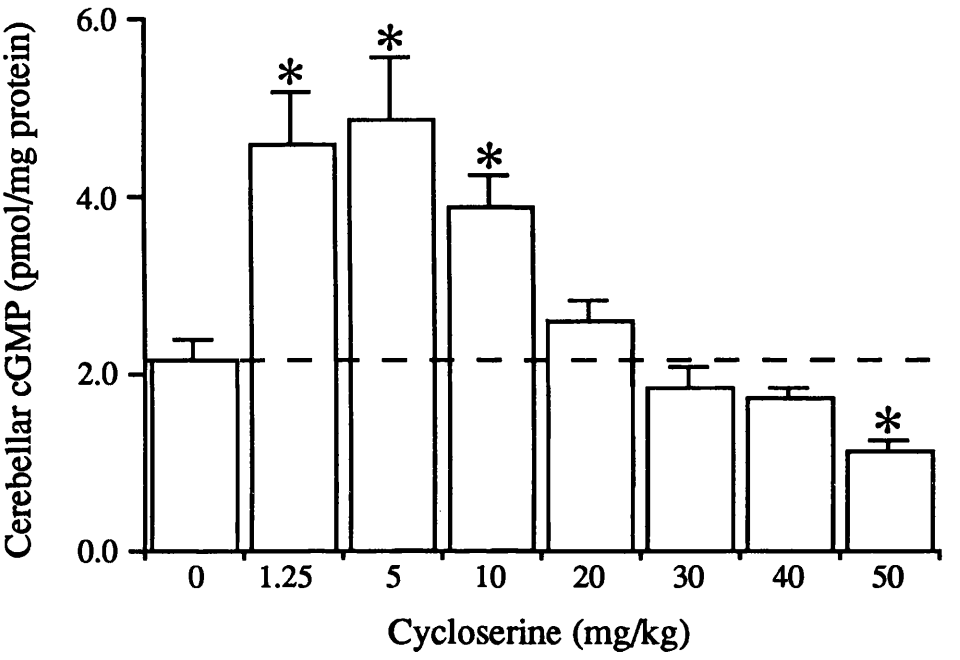


FIGURE 4: EFFECTS OF D-CYCLOSERINE ON CEREBELLAR cGMP LEVELS : PARTIAL AGONISM *IN VIVO*

Cyclic guanosine monophosphate (cGMP) levels were measured in mouse cerebellum 30 min after parenteral injections of D-cycloserine (1.25 - 50 mg/kg), to assess NMDA receptor - mediated activity *in vivo*. D-Cycloserine produced biphasic dose-response effects on cGMP levels, low doses (1.25 - 10 mg/kg) augmenting NMDA receptor activity, while a higher dose (50 mg/kg) significantly reduced cGMP levels ($*p < 0.05$, t - test). In addition, the maximal *in vivo* agonist effects of D-cycloserine on cerebellar cGMP were approximately 40 - 50% of those of a full agonist such as D-serine (Wood *et al.*, 1989). Thus, the observed effects of D-cycloserine on cerebellar cGMP levels are consistent with partial agonist modulation of NMDA receptor activity. (After Emmett *et al.*, 1991).

AIM NUMBER 2: To investigate the consequences of NMDA receptor modulation by the glycine site partial agonist D-cycloserine on cerebral function in normal and pathologic states in the rat. Four approaches will be used to examine the effects of D-cycloserine on glutamatergic processes within the brain:-

(i) *Local Cerebral Glucose Utilisation*: [$^{14}$C]-2-deoxyglucose autoradiography will be used to map any alterations in local rates of glucose metabolism in the CNS acutely after systemic administration of D-cycloserine (0.3, 3 and 30mg/kg). The dose range examined encompasses concentrations of D-cycloserine which have previously been reported to exhibit agonist and antagonists properties *in vivo*.

(ii) *[$^{125}$I]-MK-801 Binding In Vivo*: [$^{125}$I]-MK-801 *in vivo* autoradiography will be used to investigate the effects of a putative agonist dose of D-cycloserine (3mg/kg) on NMDA receptor activation in the conscious rat CNS. Results will be compared with levels of [$^{125}$I]-MK-801 binding in conscious and halothane-anaesthetised controls.

(iii) *Focal Cerebral Ischaemia*: The effects of putative potentiation of NMDA receptor activity on the volume of ischaemic damage will be investigated in the MCA occlusion model following administration of a reported agonist dose of D-cycloserine (3mg/kg).

(iv) *Cortical Glutamate Perfusion*: The consequences of NMDA receptor modulation on excitotoxic cell death will be examined in the anaesthetised rat by investigating the effects of a putative agonist dose of D-cycloserine (3mg/kg) on the volume of neuronal damage produced by cortical glutamate perfusion. In order to validate this

approach, the neuroprotective actions of the AMPA receptor antagonist NBQX will be investigated in the same model.

### 4.3 Intracerebral Manipulations of Basal Forebrain Activity

The cholinergic innervation of the neocortex arising from the basal forebrain can be manipulated by excitatory amino acid-induced activation of basal forebrain neurones, including magnocellular cholinergic neurones of the nucleus basalis magnocellularis (NBM).

Previous *in vivo* studies into the contribution of cholinergic NBM efferents to cerebral function, employing behavioural tests of cognitive function in conjunction with biochemical analyses of cholinergic markers following excitotoxic basal forebrain lesions, have indicated a separation in the effects of NMDA and non-NMDA receptor agonists (Dunnett et al., 1987; Etherington et al., 1987; Robbins et al., 1989a,b; Page et al., 1991; see also Table 3). Evidence suggests that AMPA and quisqualate are more selective for cholinergic neurones than ibotenate and NMDA (Page et al. 1991; for review see Dunnett et al., 1991). However, a number of factors limit the utility of behavioural paradigms to assess alterations in cerebral function, most notably that these studies allow examination of only one functional pathway within the brain, decided *a priori.*

Autoradiographic techniques have also been used previously to map the effects of basal forebrain lesions on cerebral function throughout the entire CNS. Such studies have included assessment of glucose use alterations by [$^{14}$C]-2-deoxyglucose *in vivo* autoradiography in the rat and [$^{3}$H]-2-deoxyglucose binding in rat brain homogenates following unilateral and

bilateral excitotoxic NBM lesions, (Lamarca and Fibiger, 1984; London et al., 1984; Orzi et al., 1988; Soncrant et al., 1992), and positron emission tomography (PET) following electrolytic nbM lesions in the baboon (Kiyosawa et al., 1989). All investigators reported initial reductions in glucose utilisation in cortical areas which receive NBM projections 3-4 days after unilateral lesions, the extent of functional depression correlating with the degree of ChAT depletion in the cortex. Bilateral NBM lesions produced widespread metabolic depression throughout the CNS. However, within 4 weeks of unilateral lesions (and 4 months of bilateral lesions) glucose use in cortical regions had returned back to basal levels, despite sustained depletions in presynaptic cholinergic markers in the cortex, and persistent impairment of conditioned behaviour. It should be noted that previously reported [$^{14}$C]-2-deoxyglucose studies have investigated only the effects of kainic acid (Lamarca and Fibiger, 1984) or ibotenic acid (London et al., 1984; Orzi et al., 1988; Soncrant et al., 1992) lesions of NBM efferents in the rat, whereas the consequences of AMPA- or quisqualic acid-induced lesions on cortical function, which are putatively more selective for cholinergic NBM neurones, have not previously been examined by *in vivo* autoradiographic methods.

The observations of metabolic recovery following excitotoxic basal forebrain lesions suggest that the [$^{14}$C]-2-deoxyglucose autoradiography technique may not be a particularly sensitive method of distinguishing subtle differences in the effects of different excitatory amino acid agonists at chronic time points post-lesion. An alternative approach is to measure the effects on cerebral glucose use of neuronal stimulation directly after receptor activation by excitatory amino acid agonists.

A complementary approach to manipulate the activity of basal forebrain cholinergic neurones is via modulation of the inhibitory GABAergic input to these neurones (Sarter et al., 1990). Glutamic acid decarboxylase (GAD)-immunoreactive terminals have been shown to synapse on magnocellular cholinergic neurones in the NBM (Zaborszky et al., 1986). Evidence indicates that these GABAergic projections arise from the nucleus accumbens (Page et al., 1991) and possibly also from neurones intrinsic to the basal forebrain (Zaborszky et al., 1986). This GABAergic innervation of cholinergic neurones appears to have a regulatory role, deduced from observations of altered cholinergic activity in the cortex following pharmacological manipulations of basal forebrain neuronal populations with GABAergic agents. Injections of the $GABA_A$ agonist muscimol directly into the basal forebrain have been found to decrease cortical ACh turnover (Wood, 1985), to reduce cortical ACh release (Casamenti et al., 1986), and to decrease high affinity choline uptake in cortex (Wenk, 1984).

The consequences of manipulating GABAergic input to the basal forebrain on functional activity in the CNS have previously been assessed *in vivo* by using behavioral tests of cognition and attention (Muir et al., 1992b). The aims of these studies were to compare the acute sequelae of manipulating GABA-ergic input to the basal forebrain with those following excitatory amino acid-induced activation of basal forebrain neurones. The results demonstrated that muscimol infusion into the NBM region impaired animals' responses in a five-choice serial reaction time task, indicating a deficit in attentional function reminiscent of the effects of AMPA, quisqualate and ibotenate infusions. This muscimol-induced deficit could be reversed by administration of the cholinomimetic agent physostigmine.

However, like ibotenic acid, muscimol also impaired acquisition of a passive avoidance task, which is postulated not to be cholinergic in nature (Dunnett et al., 1991). These results suggest that the functional consequences of $GABA_A$ receptor stimulation in the basal forebrain indicate non-selective actions on both cholinergic and non-cholinergic neuronal populations.

AIM NUMBER 3: To compare and contrast the effects of different excitatory amino acids on functional activity within the basal forebrain. [$^{14}$C]-2-deoxyglucose *in vivo* autoradiography will be used to map functional events in the CNS in conscious rats following manipulations of glutamatergic input to the NBM region of the basal forebrain by two different approaches:-

(i) *Chronic*: Local rates of cerebral glucose utilisation will be measured approximately 3 weeks after unilateral infusions of ibotenate, NMDA, AMPA and quisqualate into the NBM basal forebrain region.

(ii) *Acute*: The consequences of agonist stimulation of different glutamate receptor subtypes in the basal forebrain on cerebral function throughout the brain will be assessed acutely (15 min) after unilateral infusions of NMDA and AMPA into the NBM region. Results will be compared with the effects of indirect manipulation of basal forebrain neuronal activity by intracerebral administration of the $GABA_A$ agonist muscimol.

# CHAPTER II

# METHODS

# 1. AUTORADIOGRAPHIC TECHNIQUES

In this section, the quantitative autoradiographic techniques employed in the present thesis will be described. The following sections, 2-4, will deal with the specific experimental investigations to which these techniques were applied.

## 1.1 *In Vivo* [$^{14}$C]-2-Deoxyglucose Autoradiography

### 1.1.2 Theory

There are two basic principles which provide the conceptual basis for the utility of the [$^{14}$C]-2-deoxyglucose technique as an experimental measure to give insight into cerebral function *in vivo*. Firstly, under normal physiological conditions the energy requirements of cerebral tissue are derived almost exclusively from the oxidative catabolism of glucose (Sokoloff et al., 1977; Siesjö, 1978). The CNS has a low capacity to store carbohydrates, and therefore functional energy requirements must be met by glucose supplied continuously from the cerebral circulation. Second, since functional activity is intimately related to cerebral metabolic rate (Sokoloff et al., 1977), regional measurement of local rates of glucose phosphorylation gives direct insight into local levels of functional activity within the CNS.

The [$^{14}$C]-2-deoxyglucose autoradiography technique measures rates of cerebral energy metabolism in anatomically discrete regions of the CNS in vivo, in terms of local rates of cerebral glucose utilisation (LCGU; Sokoloff et al., 1977). The technique takes advantage of the biochemical characteristics resulting from a simple modification of the glucose molecule, by replacement of a hydroxyl group on the second carbon atom of glucose with

a hydrogen atom, to become 2-deoxyglucose.

Glucose and 2-deoxyglucose are transported from blood into the CNS by the same saturable carrier. In cerebral tissue glucose and 2-deoxyglucose compete for the hexokinase enzyme which phosphorylates both, or for the carrier molecule for transport back to plasma. At this point the two agents' metabolic pathways diverge. Glucose-6-phosphate is subsequently metabolised via the glycolytic and tricarboxylic acid pathways and therefore does not accumulate within cerebral tissues. In contrast, deoxyglucose-6-phosphate is not a substrate for glucose-6-phosphate isomerase or glucose-6-phosphate dehydrogenase. Therefore its catabolism ceases at this point (at least within the 45 min experimental period; Sokoloff et al., 1977) and deoxyglucose-6-phosphate becomes essentially "trapped" within the cerebral tissue. Thus the rate of deoxyglucose-6-phosphate accumulation in any cerebral region over a given time is equivalent to the rate of 2-deoxyglucose phosphorylation by hexokinase, and hence may be directly related to the rate of glucose phosphorylation since deoxyglucose is taken up and phosphorylated by cells at a definable rate relative to glucose.

Sokoloff and colleagues (1977) have developed a theoretical model (Figure 5) whereby the rate of cerebral glucose utilisation (Ri) can be calculated using an operational equation in terms of the concentration of [$^{14}$C]-2-deoxyglucose (Cp*) and glucose (Cp) in arterial plasma during the experimental period, and the total concentration of $^{14}$C tracer (Ci) within a given cerebral region at the end of the experimental procedure (Figure 6). In deriving this equation the following assumptions are made:-

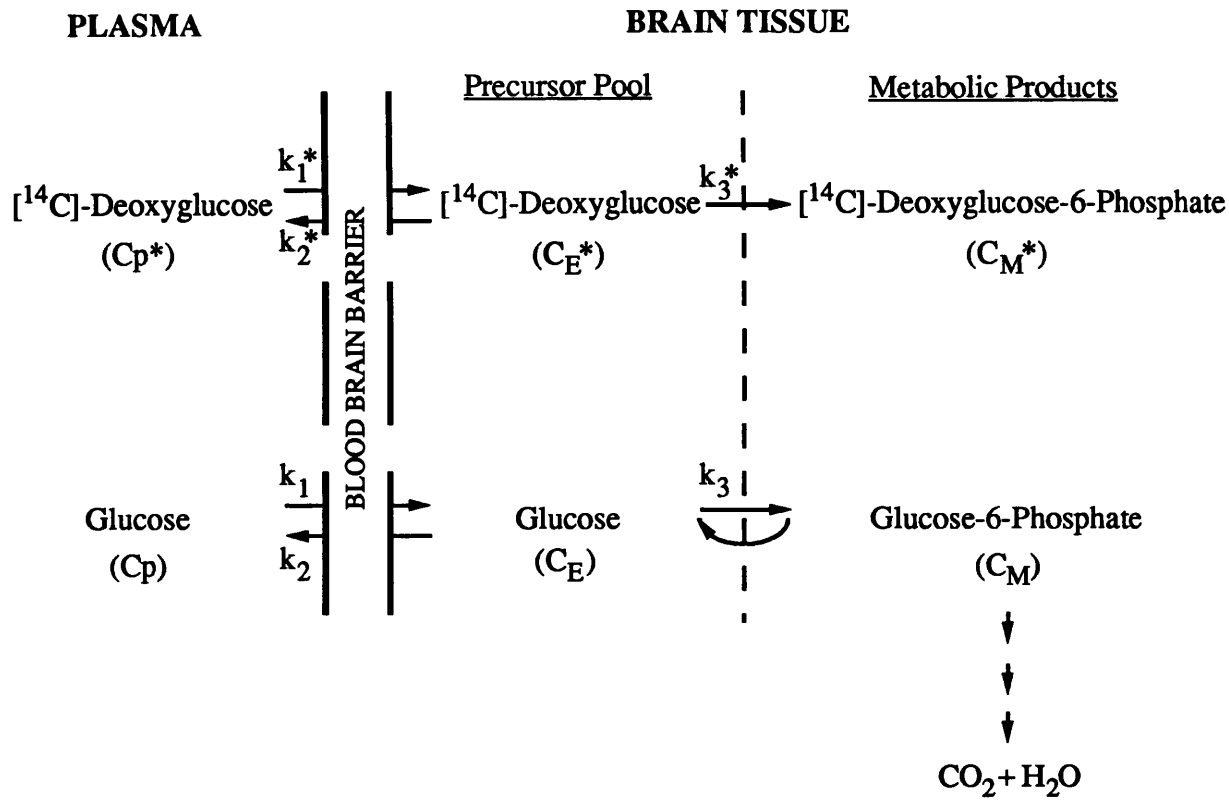


Total Tissue $^{14}C$ Concentration, $C_i^* = C_E^* + C_M^*$

FIGURE 5: THEORETICAL MODEL OF DEOXYGLUCOSE UPTAKE IN THE BRAIN

Cp* and Cp represent the concentrations of [ $^{14}C$] - deoxyglucose and glucose in arterial plasma, whilst $C_E^*$ and $C_E$ represent their respective concentrations in the tissue precursor pool. $C_M^*$ represents the concentration of [$^{14}C$] - deoxyglucose-6-phosphate in the tissue. The constants $k_1^*$, $k_2^*$ and $k_3^*$ represent the rate constants for carrier-mediated [ $^{14}C$] - deoxyglucose uptake and its subsequent phosphorylation by hexokinase; $k_1$, $k_2$ and $k_3$ are the equivalent rate constants for glucose. The possibility of glucose-6-phosphate hydrolysis by glucose-6-phosphatase is indicated by the curved arrow (after Sokoloff *et al.*, 1977).

$$\mathbf{Ri} = \frac{Ci^*(T) - k_1^* e^{-(k_2^* + k_3^*)T} \int_0^T Cp^* e^{(k_2^* + k_3^*)t} dt}{K \bullet \left[ \int_0^T (Cp^*/Cp)\, dt - e^{-(k_2^* + k_3^*)T} \bullet \int_0^T (Cp^*/Cp)\, e^{(k_2^* + k_3^*)t} dt \right]}$$

FIGURE 6: THE OPERATIONAL EQUATION

The rate of glucose utilisation, **Ri**, in any region of cerebral tissue is calculated from the total tissue concentration of $^{14}C$ in that region (Ci*) measured densitometrically at the end of the experiment (time T); from the concentrations of [$^{14}C$]-2-deoxyglucose and glucose in the plasma (Cp* and Cp respectively) at given times (t) throughout the experiment; from the rate constants for deoxyglucose transport to and from plasma and tissue precursor pools, and for phosphorylation of deoxyglucose by hexokinase ($k_1^*$, $k_2^*$ and $k_3^*$); and from the lumped constant, K. K is composed of the ratio of tissue distribution volumes for deoxyglucose and glucose; the fraction of glucose which, once phosphorylated, will be further metabolised via the glycolytic pathway; and the Michaelis-Menten constants and maximal velocities of hexokinase for both deoxyglucose and glucose (Sokoloff *et al.*, 1977).

1) Carbohydrate metabolism is in steady state, with a constant plasma glucose concentration and a constant rate of cerebral glucose consumption throughout the duration of the procedure.

2) Each tissue compartment where measurement is made is homogenous, where concentrations of [$^{14}$C]-2-deoxyglucose and glucose are uniform and exchange directly with plasma at constant rates.

3) [$^{14}$C]-2-Deoxyglucose and [$^{14}$C]-2-deoxyglucose-6-phosphate are present only in tracer concentrations and are pharmacologically inactive.

4) [$^{14}$C]-2-Deoxyglucose-6-phosphate, and any metabolites, remain trapped within the cerebral tissue for the duration of the sampling period.

The rate constants $K_1$*, $K_2$* and $K_3$* define the distribution of tracer between plasma and brain tissue compartments. The "lumped constant", K, "corrects" for the relative preference of the glucose transport and enzyme systems for glucose, as opposed to 2-deoxyglucose. The constants used are not measured in each experiment, but are those previously determined in the rat by Sokoloff and colleagues in the original description of the technique (Sokoloff et al., 1977).

### 1.1.2 Methodological Considerations

The stability of the lumped constant, K, in the operational equation, which allows the rate of deoxyglucose phosphorylation to be converted to that

of glucose, has been the subject of debate since it has been found to alter in certain extreme experimental circumstances such as seizure, ischaemia, tumours and severe hypoglycaemia and hyperglycaemia (for review see Gjedde, 1982). However, in the vast majority of neuropharmacological applications of the [$^{14}$C]-2-deoxyglucose technique it is very unlikely that local alterations in the lumped constant will complicate the interpretation of measured glucose utilisation rates (Sokoloff et al., 1977). In cases of hypoglycaemia, plasma glucose concentrations of less than 5mM have been found to result in an overestimation of the cerebral metabolic rate, while in hyperglycaemic animals glucose use may be underestimated (Schuier et al., 1990). Consequently, in the experiments described in this thesis, plasma glucose concentrations were measured prior to initiating the procedure, and no animal was used if its pre-experiment glucose level was below 6mM or exceeded 15mM. In animals undergoing stereotactic surgery and subsequent recovery, an initial loss in body weight often followed surgery. Animals generally recovered body weight rapidly (within approximately 4 days), but no animal underwent subsequent [$^{14}$C]-2-deoxyglucose autoradiography before its pre-surgery body weight had been equalled or surpassed.

Potential errors in calculating glucose utilisation may arise from uncertainty of the rate constants $K_1$*, $K_2$* and $K_3$* which define the distribution of tracer between plasma and tissue compartments, and which may vary under different physiological conditions. Uncertainties are minimised by allowing sufficient time for [$^{14}$C]-2-deoxyglucose clearance from plasma, so that the exponential terms containing the rate constants fall to levels too low to significantly influence the result (Mori et al., 1990).

In designing the experimental protocol, it is also necessary to take into consideration the activity of another CNS enzyme, glucose-6-phosphatase. Both glucose-6-phosphate and deoxyglucose-6-phosphate are substrates for hydrolysis by glucose-6-phosphatase to yield glucose and deoxyglucose. Hence, if glucose-6-phosphate activity were significant within the duration of the experiment, its action would seriously undermine the use of [$^{14}$C]-2-deoxyglucose technique as a determinant of local cerebral glucose utilisation (Hawkins and Miller, 1987). However, neurochemical studies provide no evidence that glucose-6-phosphatase is present in the CNS in concentrations sufficient to interfere with the use of [$^{14}$C]-2-deoxyglucose as a tracer if the experimental period is limited to less than 1h (Nelson et al., 1987).

A further limiting factor to the procedure is the restraint of animals which is necessary for blood sampling. The experimental period should be kept short to limit the effects of stress induced in the animal, such as elevated plasma glucose levels.

In order to minimise the impact of these potential complicating factors, an experimental period of 45 min was used in the studies of cerebral glucose use described in this thesis. This period has been deemed long enough to allow plasma and tissue glucose and [$^{14}$C]-2-deoxyglucose levels to equilibrate, and hence minimise any uncertainties in the rate constants employed, while being short enough to minimise any [$^{14}$C]-2-deoxyglucose-6-phosphate depletion from the cerebral tissue due to glucose-6-phosphatase activity (Sokoloff et al., 1977; Mori et al., 1990).

### 1.1.3 Surgical Preparation of Animals for [$^{14}$C]-2-Deoxyglucose Measurement

Rats were placed in a perspex chamber and anaesthestised with 5% halothane in a nitrous oxide and oxygen gas mixture (70%/30%). Anaesthesia was subsequently maintained by administering 0.5 - 1% halothane in the gas mixture via a face mask. Femoral vessels were exposed bilaterally by blunt dissection through small incisions in the skin at each side of the animal's groin. Polyethylene catheters (Portex: external diameter 0.96mm; internal diameter 0.58mm; 15cm long) containing heparinised saline (10 IU/ml) were inserted 2cm into both femoral arteries and veins, and tied off using silk thread. The incision sites were infiltrated with a local anaesthetic gel (xylocaine, 2%) and sutured closed. The wounds were covered with gauze pads held in place by tape. Animals were then enveloped in a surgical stocking and a plaster of Paris bandage (Gypsona: 7.5cm side) applied around the pelvis and lower abdomen to immobilise the animals, taking care not to restrict thoracic movements. The plaster was taped to a lead brick to support the animal. With the rats thus restrained, halothane anaesthesia was discontinued and the rats allowed to recover for at least 2h before further manipulation. One femoral artery was connected to a pressure transducer (P23ID Gould Stratham, Model 2202) to measure arterial pressure throughout the [$^{14}$C]-2-deoxyglucose procedure. Core temperature was measured by means of a rectal temperature probe, rats being maintained normothermic by means of heating lamps.

### 1.1.4 The [$^{14}$C]-2-Deoxyglucose Procedure

The local rates of cerebral glucose utilisation were measured in conscious rats using the [$^{14}$C]-2-deoxyglucose technique in accordance with the previously published experimental procedures (Sokoloff et al., 1977), and the methodological considerations discussed above (Section 1.1.2).

The procedure was initiated by the intravenous administration of a pulse of [$^{14}$C]-2-deoxyglucose (125μCi/kg in 0.7ml saline) injected at a constant rate over 30 sec. Over the subsequent 45 min, 14 timed arterial blood samples (approximately 100μl) were taken and immediately centrifuged. Plasma aliquots were then assayed to determine $^{14}$C and glucose concentrations, by means of liquid scintillation analysis and by semi-automated glucose oxidase enzyme assay (Beckman), respectively. Further arterial blood samples were taken at predetermined intervals before and after isotope administration, for analysis of $pCO_2$, $pO_2$ and pH using a blood gas analyser (168pH/Blood Gas System, Corning). Forty-five min after isotope administration the rats were killed by decapitation and their brains removed, frozen in isopentane at -43°C and processed for quantitative autoradiography (see Section 1.4.2.).

## 1.2 *In Vivo* [$^{125}$I]-MK-801 Autoradiography

### 1.2.1 Theory

[$^{125}$I]-MK-801 autoradiography provides a means of measuring NMDA receptor activation *in vivo* (McCulloch et al., 1992). The basic principle for the technique is that the non-competitive NMDA receptor antagonist MK-801 can only gain access to its binding site within the receptor-associated channel when the NMDA receptor has been activated, since under resting

conditions the channel is voltage-dependently blocked. It has been postulated that autoradiographic analysis of the distribution of [$^{125}$I]-labelled MK-801 following intravenous injection will reflect the pattern of MK-801 binding within the brain and hence the pattern of activated NMDA receptors either in resting conditions, or following pathologic, physiologic or pharmacologic manipulations of glutamatergic activity within the CNS. Subsequently, altered levels of [$^{125}$I]-MK-801 binding have been detected in the region of ischaemic infarct in experimental models of focal cerebral ischaemia in the rat (McCulloch et al., 1992).

### 1.2.2 Surgical Preparation of Animals for [$^{125}$I]-MK-801 Measurement

Rats were placed in a perspex chamber and anaesthetised with 5% halothane in a nitrous oxide and oxygen gas mixture (70%/30%). Anaesthesia was subsequently maintained by administering 0.5 - 1% halothane in the gas mixture via a face mask. Femoral vessels were exposed bilaterally by blunt dissection through small incisions through the skin in each side of the animal's groin. Polyethylene catheters (Portex: external diameter 0.96mm; internal diameter 0.58mm; 15cm long) containing heparinised saline (10 IU/ml) were inserted 2cm into both femoral arteries and veins, and tied off using silk thread. The incision sites were infiltrated with local anaesthetic gel (xylocaine, 2%), sutured closed, and the wounds covered with gauze pads held in place by tape. Animals to be anaesthetised during the [$^{125}$I]-MK-801 procedure underwent no further manipulation. Animals to be conscious during the autoradiographic procedure were enveloped in a surgical stocking and a plaster of Paris bandage (Gypsona: 7.5cm side) applied around the pelvis and

lower abdomen to immobilise the animals while not restricting thoracic movements, and the plaster taped to a lead brick for support. With the rats thus restrained, halothane anaesthesia was discontinued and the rats allowed to recover for at least 2h before further manipulation. In all animals, arterial blood pressure was measured throughout the procedure by a pressure transducer (P23ID Gould Stratham, Model 2202) connected to one femoral artery catheter. Core temperature was measured by means of a rectal temperature probe and rats maintained normothermic by heating lamps.

### 1.2.3 The [$^{125}$I]-MK-801 Procedure

[$^{125}$I]-MK-801 content in discrete brain regions was measured in conscious and halothane-anaesthetised rats using a modification of the previously described [$^{125}$I]-MK-801 *in vivo* autoradiographical technique of McCulloch et al. (1992).

The procedure was initiated by the intravenous injection of a pulse of [$^{125}$I]-MK-801 (500uCi/kg in 0.7ml saline) at a constant rate over 30 sec. Over the subsequent 120 min, 15 timed arterial blood samples (approximately 100µl) were taken and immediately centrifuged. 20µl Plasma aliquots were then assayed to determine [$^{125}$I] and glucose concentrations, by means of liquid scintillation analysis and by semi-automated glucose oxidase enzyme assay (Beckman) respectively. Arterial blood samples were also taken at predetermined intervals before and after isotope administration for analysis of $pCO_2$, $pO_2$ and pH using a blood gas analyser (168pH/Blood Gas System, Corning). 120 min after isotope administration the rats were killed by decapitation and their brains processed for quantitative autoradiography as

outlined in section 1.4.3).

## 1.3 *In Vitro* [$^3$H] Ligand Binding Autoradiography

### 1.3.1 Theory

*In vitro* ligand binding autoradiography is based on the principle that radiolabelled ligands, which are highly selective for particular recognition sites, emit energy which will produce a photographic image when placed in contact with radiation-sensitive film. The optical density of the image is related to the amount of radioligand bound, and hence to the density of binding sites in any given area, and can be quantified by reference to calibrated radioactive standards. Thus *in vitro* autoradiography techniques allow anatomical mapping of the distribution of ligand binding sites within the CNS with a high degree of spatial resolution, and sensitive quantification of ligand binding densities in discrete brain regions.

### 1.3.2 [$^3$H]-PK-11195 Autoradiography

The *in vitro* ligand binding experiment described in this thesis employed the tritiated ligand, [$^3$H]-PK-11195. [$^3$H]-PK-11195 binds with high affinity to peripheral-type benzodiazepine binding sites (Benavides et al., 1983; 1987) which are located predominantly on glial cells within the CNS. Hence the pattern of [$^3$H]-PK-11195 binding within the brain gives an indication of the distribution of glial cells. In the present thesis, [$^3$H]-PK-11195 binding was carried out in rat brain sections taken from animals in which local cerebral glucose use had previously been measured using the [$^{14}$C]-2-deoxyglucose technique.

*In vitro* [$^{3}$H]-PK-11195 binding was performed according to the technique of Benavides et al., (1983), and is summarised in Figure 7. Rats were killed by decapitation and their intact brains dissected out, frozen by immersion in isopentane at -43°C for 10 min, and cut into 20μm-thick coronal sections using a cryostat microtome. Triplicate tissue sections (2 for total, and 1 for non-specific ligand binding), taken at 200μM intervals throughout the CNS and adjacent to those sections used in contemporaneous [$^{14}$C]-2-deoxyglucose studies, were thaw-mounted onto gelatin-subbed slides and stored at -20°C. Prior to ligand binding, sections were dried in air at room temperature. Since [$^{3}$H]-PK-1195 *in vitro* autoradiography was carried out in brain sections which had previously been labelled *in vivo* by [$^{14}$C]-2-deoxyglucose, it was essential that the [$^{14}$C] was eluted from the slide-mounted sections prior to incubation with [$^{3}$H]-PK-1195. Therefore, sections were washed twice for 30 sec in Tris/HCl buffer (170mM, 24°C) prior to preincubation for [$^{3}$H]-PK-11195 autoradiography (Chalmers and McCulloch, 1991a). Any low residual levels of [$^{14}$C] remaining in sections will contribute to the non-specific binding signal determined in the [$^{3}$H]-ligand binding studies (Chalmers and McCulloch, 1991a).

Sections were incubated in Tris/HCl buffer (170mM, pH 7.4) containing [$^{3}$H]-PK-11195 (1nM) for 30 min at 24°C (total binding). Non-specific binding (ligand binding to sites other than the desired recognition sites such as other tissue constituents, or glass) was determined by incubating adjacent sections with [$^{3}$H]-PK-11195 (1nM) under the same incubation conditions with the addition of an excess of unlabelled PK-11195 (3μM) to competitively displace the isotopically-labelled ligand. After incubation, sections were washed twice

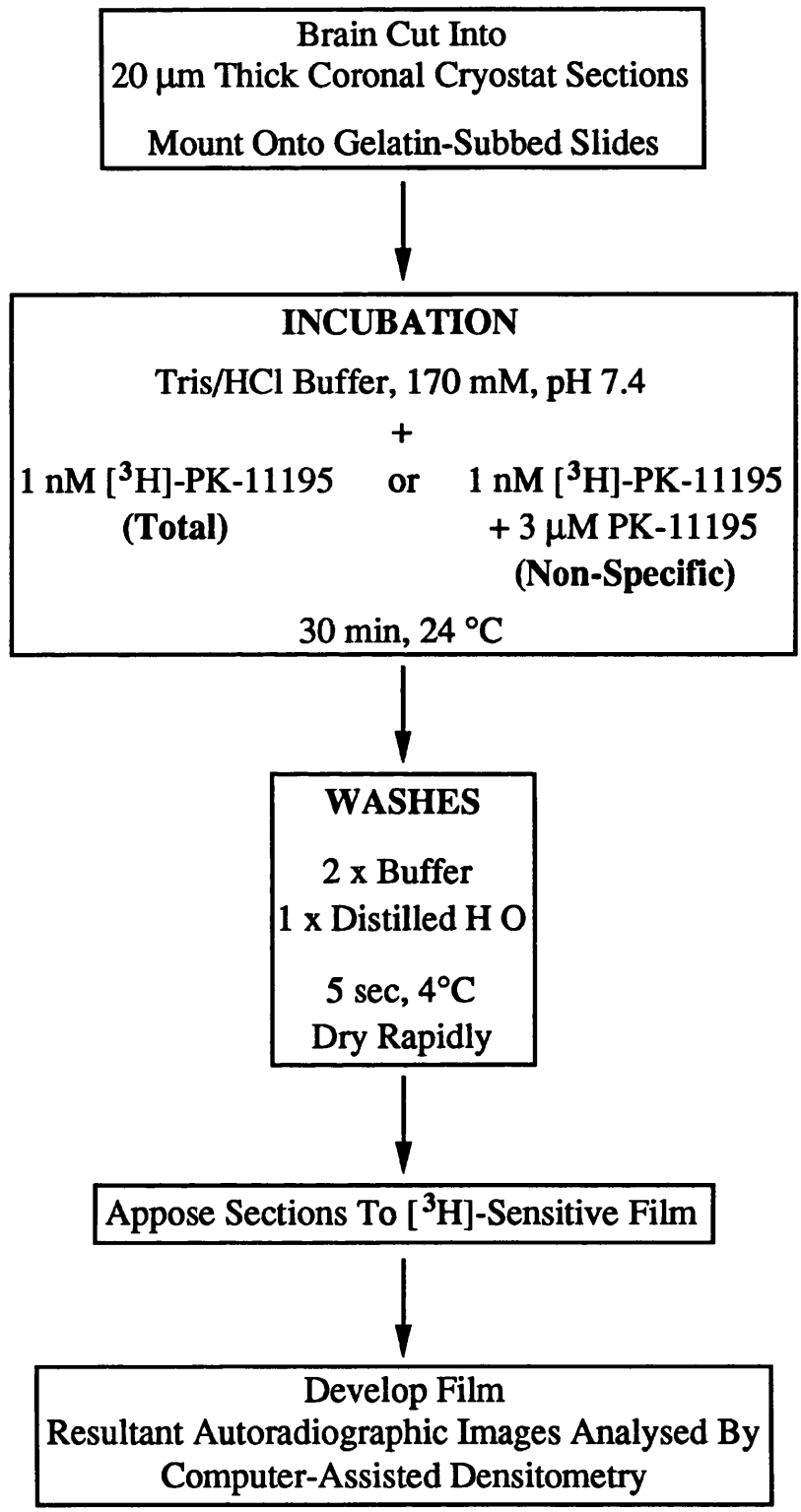


FIGURE 7: [$^3$H]-PK-11195 BINDING PROTOCOL

for 5 sec in buffer (4°C) to remove any unbound isotope, dipped in distilled water (4°C), and then dried rapidly in a stream of air. Autoradiograms were generated according to the procedure outlined in section 1.4.4. In this thesis total [$^3$H]-PK-11195 binding autoradiograms were used for qualitative assessment of the distribution of peripheral-type benzodiazepine receptors in the CNS after excitotoxic basal forebrain lesions.

Several extrinsic factors may influence the amount of ligand binding to sections. These include temperature of incubation and rinsing, differences in the buffer medium (such as pH or salt concentrations), or differences in the specific activity or concentration of the radiolabelled ligand in the incubation medium. In order to minimise the contributions of these factors, binding studies for all animals in the experimental series were carried out on the same day.

The concentration of [$^3$H]-PK-11195 used was similar to the equilibrium dissociation constant (Benavides et al., 1983; $K_D \sim$ 1nM), allowing sensitive detection of small changes in the numbers of binding sites.

## 1.4 Experimental Analysis

### 1.4.1 Liquid Scintillation Analysis

Liquid scintillation analysis was an essential component of [$^{14}$C]-2-deoxyglucose and [$^3$H] ligand binding autoradiography protocols. To determine the plasma history of [$^{14}$C]-2-deoxyglucose over the 45 min experimental period, for use in calculation of the plasma integral, a 20µl plasma aliquot from each arterial sample was pipetted into a scintillation vial containing 1ml distilled water. Pipettes were repeatedly flushed with water to expel any

residual radioactivity. Prior to [$^3$H] ligand binding procedures, the concentration of the radioligand in the incubation medium was determined by pipetting 10µl aliquots into 1ml distilled water in scintillation vials. The procedure was repeated in triplicate.

Scintillation fluid (10mls; Ecoscint, National Diagnostics, New Jersey, U.S.A.) was added to each vial, and vials shaken thoroughly. Radioactivity was counted in a refrigerated scintillation counter (Packard Tricarb, 1900CA) using the external standards channel-ratio method (Peng, 1977) with a standard calibration curve for quench correction. Mean values for disintegrations per minute (dpm) were calculated from triplicate counts.

### 1.4.2 Preparation of [$^{14}$C]-2-Deoxyglucose Autoradiograms

At the end of the 45 min experimental period, rats were decapitated and their brains removed intact. Whole brains were frozen by immersion in isopentane pre-cooled to -43°C, for 10 min. The time from decapitation to brain freezing did not exceed 5 min. The frozen brains were mounted onto swivel headed microtome chucks with plastic embedding matrix (Lipshaw) over solid $CO_2$, and stored at -20°C for a maximum of 2 days (-80°C for longer periods if necessary), before being cut into 20µm-thick coronal cryostat sections. Triplicate sections were collected at predetermined levels, routinely at 200µm intervals throughout the brain. Cutting schedules varied in different experiments depending on regions of special interest. Sections were thaw-mounted onto heated glass coverslips and then dried rapidly on a hotplate at 60°C. The coverslips were then glued onto thin card. Autoradiograms were generated by exposing the brain sections along with

precalibrated epoxy resin $^{14}C$ standards (concentration range 44-1880nCi/g tissue equivalents) to $^{14}C$-sensitive X-ray plates (Kodak GRL), in light-tight cassettes for 16-24 days. The duration of exposure was estimated from the calculated plasma integral value for each animal in order to optimise the optical density range of the resultant autoradiograms, to facilitate densitometric processing. Films were processed using a standard Kodak automatic processor.

### 1.4.3 Preparation of [$^{125}I$]-MK-801 Autoradiograms

At the end of the 120 min experimental period, rats were decapitated, their brains removed intact and frozen in isopentane at -43°C for 10 min. The time from decapitation to freezing did not exceed 5 min. Frozen brains were mounted onto swivel-headed microtome chucks with plastic embedding matrix (Lipshaw) over solid $CO_2$ and stored at -20°C (for 2 days maximum) before being cut into 20µm-thick coronal cryostat sections. Four sets of duplicate sections were collected at 5 predetermined regions of interest, at the levels of cerebellum hemisphere, medial geniculate body, hippocampus, posterior cingulate cortex, and striatum. At each coronal level, one pair of sections were thaw-mounted onto heated glass coverslips for immediate autoradiography, and the remaining pairs thaw-mounted onto gelatin-subbed slides for washing prior to autoradiography. Sections were dried rapidly on a hotplate at 60°C. Sections were washed in cold (4°C) Tris/acetate buffer (170mM, pH 7.2) for periods of 15, 30 or 60 min. After washing, sections were air dried. Coverslips and slides were then glued onto thin card and autoradiograms generated by exposing the brain sections along with

precalibrated $^{125}I$ standards (concentration range 1,490 - 42,000nCi/g) to $^{125}I$-sensitive film (Kodak GRL) in light-tight cassettes for 3-12 weeks. The duration of exposure was estimated from the calculated plasma integral for $^{125}I$ and the known half-life of $^{125}I$ (60 days). Films were processed using a standard Kodak automatic processor.

### 1.4.4 Preparation of [$^{3}H$]-PK-11195 Binding Autoradiograms

Tissue sections labelled with [$^{3}H$]-PK-11195 were mounted securely on card along with a set of precalibrated tritium standards (1060-17720nCi/mg tissue equivalents). The brain sections and standards were apposed to tritium-sensitive film (Hyperfilm, Amersham) in light-tight cassettes for 14 days. At the end of the exposure time films were manually developed in Kodak D-19 developer for 5 min at 17°C, with intermittent agitation. Development was stopped by a 30 sec rinse in deionised water at 20°C. After fixing for 10 min at 20°C in Kodak Kodafix, films were washed in running filtered water for 40 min, rinsed in deionised water, and then suspended in a drying cabinet overnight.

### 1.4.5 Quantification of Autoradigrams

Analysis of resultant [$^{14}C$]-2-deoxyglucose, [$^{125}I$]-MK-801 and [$^{3}H$]-PK-11195 autoradiograms was performed using a computer-assisted image analysis system (Quantimet 970, Cambridge Instruments). Films were analysed densitometrically for radioisotope content in discrete brain regions by grey level comparison with precalibrated standards.

Optical density measurements of autoradiograms were made under

constant low lighting provided by four 24W lamps, the light intensity being computer controlled. Autoradiographic images were captured by a video camera fitted with a zoom lens (2.5x), and digitised into an array of image points (pixels), each with a grey level value in the range 0-255 (grey level = 1 corresponds to optical density = 2.41; grey level = 255 corresponds to optical density = 0). The image analyser was calibrated against an opaque object (maximum optical density) and a Kodak neutral density filter (optical density = 1.0) to allow grey level values of each pixel to be converted into optical density values, and against the film background to facilitate reproducible measurements.

Following calibration, the optical densities of the images produced by the pre-calibrated standards were measured, generating a calibration curve of optical density versus isotope concentration and thus allowing subsequent quantification of tissue isotope concentrations in discrete brain regions. Optical density measurements were made by placing a measuring frame over each anatomical region of interest. The size of the measuring frame was variable (9-900 pixels/frame) but was kept constant for each anatomical region between animals. For each anatomical region of interest, the image analyser calculated the mean of optical density values made in 3-6 sections per animal. In rat studies of systemic drug administration, optical density measurements were made bilaterally for each region. In rat studies involving intracerebral interventions, optical density measurements were made separately in the ipsilateral and contralateral hemispheres for each region. Structures in rat brain were defined anatomically with reference to a stereotaxic atlas (Paxinos & Watson, 1986).

### 1.4.6 Data Analysis

The statistical design to be employed in analysis of each experiment was decided *a priori*. In studies involving analysis of multiple treatment groups, appropriate Bonferroni correction factors were applied to significance levels in order to take into consideration the impact of comparing more than two sets of data. Due to the complexities of the statistical designs applied to different experiments in this thesis, statistical analysis will be addressed in greater detail with respect to individual experimental protocols.

## 2. ANIMAL STUDIES I

## GLUTAMATE RECEPTOR MANIPULATIONS: *IN VIVO* AUTORADIOGRAPHIC STUDIES FOLLOWING SYSTEMIC DRUG ADMINISTRATION

### 2.1 General

In the following section, experiments are described in which *in vivo* autoradiographic procedures were performed after systemic administration of pharmacologically active agents. In two series of animals [$^{14}$C]-2-deoxyglucose autoradiography was performed to assess the effects of glutamatergic agents on local rates of cerebral energy metabolism. In a third series of animals [$^{125}$I]-MK-801 autoradiography was performed to assess the effect of an agent on NMDA receptor activation *in vivo*.

#### 2.1.1 Animals

The subjects of these experiments were male adult Sprague Dawley rats, 270-400g. Prior to drug administration and autoradiography the animals were housed 2 or 3 to a cage, in natural daylight conditions, at a room temperature of approximately 21°C, with food and water available *ad libitum*.

### 2.2 [$^{14}$C]-2-Deoxyglucose Autoradiography

#### 2.2.1 Drug Administration

Prior to drug administration rats were surgically prepared for [$^{14}$C]-2-deoxyglucose autoradiography as described in section 1.1.3. The deoxyglucose procedure was performed according to the protocol outlined in section 1.1.4 after intravenous administration of one of the following agents:-

1) **NBQX or LY-2935598**

The AMPA receptor antagonists NBQX (10, 30 or 100mg/kg) or LY-293558 (10, 30 or 100mg/kg) were administered by intravenous injection via the femoral vein catheter, in a volume of 2ml/kg at a constant rate over 2 min, 15 min prior to administration of [$^{14}$C]-2-deoxyglucose. Control animals similarly received an intravenous injection of vehicle (5.5% glucose, pH 8.0 with NaOH; 2ml/kg) 15 min prior to isotope injection.

2) **D-Cycloserine** binding site on the NMDA receptor complex.

The NMDA receptor-glycine site partial agonist D-cycloserine (0.3, 3 or 30mg/kg) was administered by intravenous injection via the femoral vein catheter, in a volume of 1ml/kg at a constant rate over 2 min, 15 min prior to isotope injection. Control animals similarly received intravenous injections of vehicle (sterile saline: 1ml/kg).

2.2.2 Data Analysis

**NBQX and LY-293558**

Local cerebral glucose utilisation (LCGU) values measured in each of 50 CNS regions following intravenous administration of NBQX (10, 30 or 100mg/kg) or LY-293558 (10, 30 or 100mg/kg) were compared with the LCGU values of corresponding regions in control animals.

One way analysis of variance (ANOVA) was used initially to identify anatomical regions in which significant alterations in glucose utilization occurred, followed by independent *t*-tests to identify the drug groups

producing significant changes relative to control values in these regions. A Bonferroni correction factor of 6 was applied to probability values, to take into consideration the multiple comparisons between treatment and control groups.

The degree of responsiveness of each of the 50 regions investigated to each of the 2 drugs, NBQX (10, 30, 100mg/kg) and LY-293558 (10, 30, 100mg/kg) was then assessed by application of an arithmetic function which encompasses the entire dose-response data available for each region. A rank ordering of these regional responses was derived from the function, $f$ :-

$$f = \Sigma (x_c - x_{Ti})^2$$

where $x_c$ is the mean of $log_e$ (glucose use) for the control group members, and $x_{Ti}$ is the mean of $log_e$ (glucose use) for the $i^{th}$ dose of the treatment group in question, T, i.e. either NBQX or LY-293558 (Kelly et al., 1986).

The advantage of using this method to compare drug actions is primarily that this arithmetic function takes into account all of the dose-response data generated by the 2-deoxyglucose technique, thus removing the bias of *posthoc* selection of a single "representative" dose. In addition, the use of log data minimises the distortion created by differences in the magnitude of the basal rates of glucose use in different regions, while squaring of the function permits comparison of bidirectional events if applicable. The validity and reliability of this approach has been described previously (Kelly et al. 1986). The $f$ values were calculated for each drug in each region. Frequency distribution profiles were thus generated for both drugs, and NBQX and LY-293558 activities were compared by application of Pearson's correlation analysis.

**D-Cycloserine**

Local cerebral glucose use values measured in each of 51 CNS regions following intravenous administration of D-cycloserine (0.3, 3 or 30mg/kg) were compared with the glucose use values of corresponding regions in control animals. One way analysis of variance (ANOVA) was used initially to identify anatomical regions in which significant glucose use alterations occurred, followed by independent *t*-tests (2-tailed) between treatment and control groups, with a Bonferroni correction factor of 3 for multiple comparisons.

## 2.3 [$^{125}$I]-MK-801 Autoradiography

### 2.3.1 Drug Administration

Prior to drug administration animals were prepared for the autoradiography procedure as described in section 1.2.2. The [$^{125}$I]-MK-801 autoradiography procedure was performed according to the protocol outlined in section 1.2.4, isotope being injected intravenously 15 min after intravenous administration of D-cycloserine (3mg/kg) (1ml/kg volume). Control animals similarly received an intravenous injection of vehicle (sterile saline; 1ml/kg) 15 min prior to isotope injection.

### 2.3.2 Data Analysis

Total bound [$^{125}$I]-MK-801 was measured in 13 discrete CNS regions from rat brain sections washed in buffer for 0, 15, 30 or 60 min, following intravenous administration of D-cycloserine (3mg) to conscious rats. Values were compared with total bound [$^{125}$I]-MK-801 in corresponding regions of vehicle-injected control animals (anaesthetised and conscious). Due to the

paucity of NMDA receptors in the cerebellum molecular layer, radioisotope concentration in this region served as a within animal measure of non-specific binding. The ratio of total [$^{125}$I]-MK-801 bound in each of the 12 forebrain structures, relative to total [$^{125}$I]-MK-801 bound in the cerebellum hemisphere molecular layer, was calculated for each wash period. Ratios for each structure were then compared between all treatment groups for each wash time, initially using one way analysis of variance (ANOVA) to identify any regions in which the extent of [$^{125}$I]-MK-801 binding significantly differed between groups, followed by independent *t*-tests (2-tailed) with a Bonferroni correction factor of 2 for multiple comparisons.

## 3. ANIMAL STUDIES II

## GLUTAMATE NEUROTOXICITY *IN VIVO*: EFFECTS OF AMPA AND NMDA RECEPTOR MANIPULATIONS

### 3.1 General

Experiments are described which utilise two models of glutamate-induced neuronal damage in the rat:- the middle cerebral artery (MCA) occlusion model of focal cerebral ischaemia, and a novel model of cortical neuronal cell death induced by glutamate perfusion. In the following section the surgical procedures involved to produce these models are described. The experimental routines described involved manipulation of glutamatergic receptor activities by two pharmacologically active agents, NBQX and D-cycloserine, which act at AMPA and NMDA excitatory amino acid receptor subtypes respectively, to analyse any modification in the pattern or extent of neuronal damage produced in these models.

#### 3.1.1 Animals

The subjects of these experiments were male adult Sprague Dawley rats, 300-400g. Prior to experiments animals were housed in cages in groups of 2 or 3 under natural daylight conditions, at a room temperature of approximately 21°C, with food and water available *ad libitum*. In the 24h survival experiments described, animals were returned to these conditions post-surgery, but were housed individually in cages lined with absorbent pads, and were regularly examined to check their post-operative recovery.

## 3.2 Middle Cerebral Artery Occlusion

### 3.2.1 Background

Permanent occlusion of one middle cerebral artery (MCA) produces focal cerebral ischaemia in a discrete region of ipsilateral cerebral cortex and striatum, characterised 24h post-occlusion by neuronal cell death, pyknosis, vacuolation of the neuropil, and oedema. A typical lesion produced by MCA occlusion is illustrated in Figure 8. Glutamate has been implicated in the production of ischaemic cell damage, as extracellular concentrations of glutamate are markedly elevated in ischaemic brain tissue as a consequence of both enhanced neuronal glutamate release, and impaired glutamate uptake into glia and neurones (Benveniste et al., 1984; Drejer et al., 1985; Hagberg et al., 1987; Butcher et al., 1990). In addition, glutamate receptor antagonists have been found to markedly reduce neuronal damage in experimental models of ischaemic cell death (Gill et al., 1991; Park et al., 1988b; Choi, 1990).

### 3.2.2 Procedure

Rats were placed in a perspex chamber and anaesthetised initially with 5% halothane in a nitrous oxide-oxygen gas mixture (70%:30%). Anaesthesia was maintained thereafter with 0.5-1% halothane in the gas mixture administered via a plastic face mask. The surgical procedure involved, firstly, exposure of the skull by a longitudinal midline incision in the scalp. The animals then underwent subtemporal craniectomy and exposure of the left MCA, under an operating microscope at high magnification. The exposed artery was occluded from its origin to the point where it crosses the inferior

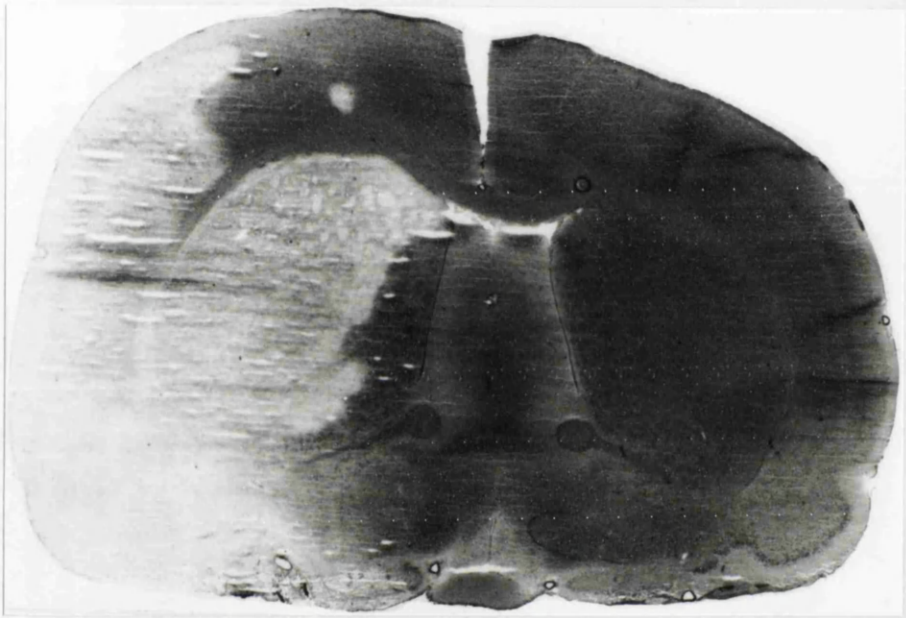

FIGURE 8: FOCAL ISCHAEMIC LESION

A representative coronal rat brain section stained with haematoxylin and eosin, illustrating a typical lesion produced by permanent occlusion of the left middle cerebral artery (MCA), 24h post-occlusion. The region of ischaemic infarct is evident as an area of pallor with a discrete boundary, affecting ipsilateral striatum and cortex. Within this region there is histological evidence ischaemic damage, including cellular swelling, shrunken nuclei, vacuolisation, and neuronal loss. In addition, the ipsilateral hemisphere appears swollen.

cerebral vein, by microbipolar coagulation. This surgical division of the artery with extensive coagulation results in large, consistent ischaemic lesions in the cerebral cortex and basal ganglia. Body temperature was monitored throughout by a rectal thermometer and animals maintained normothermic by means of heating lamps.

Following MCA occlusion the scalp wound was sutured closed, anaesthesia discontinued, and the animals allowed to regain consciousness. Twenty-four hours after occlusion the rats were decapitated, their brains removed intact, frozen by immersion in isopentane at -43°C and processed for histological lesion assessment (see section 2.3.4).

### 3.2.3 Drug Administration

**D-Cycloserine** (3mg/kg) was administered by subcutaneous injection (1ml/kg) 15 min after MCA occlusion, and again 3h later. Control animals received subcutaneous injections of sterile saline vehicle (1ml/kg) at the same time points.

## 3.3 Cortical Glutamate Neurotoxicity

### 3.3.1 Background

Glutamate perfusion into the cortex of intact rat brain *in vivo*, via a microdialysis probe, results in the generation of a well-defined lesion around the probe, as illustrated in Figure 9 (Fujisawa et al., 1993a and b; Landolt et al., 1993). In contrast to the MCA occlusion model of ischaemic neuronal injury, this intervention has been shown to minimally affect cerebral blood flow and energy supply, and hence to produce lesions putatively due solely to

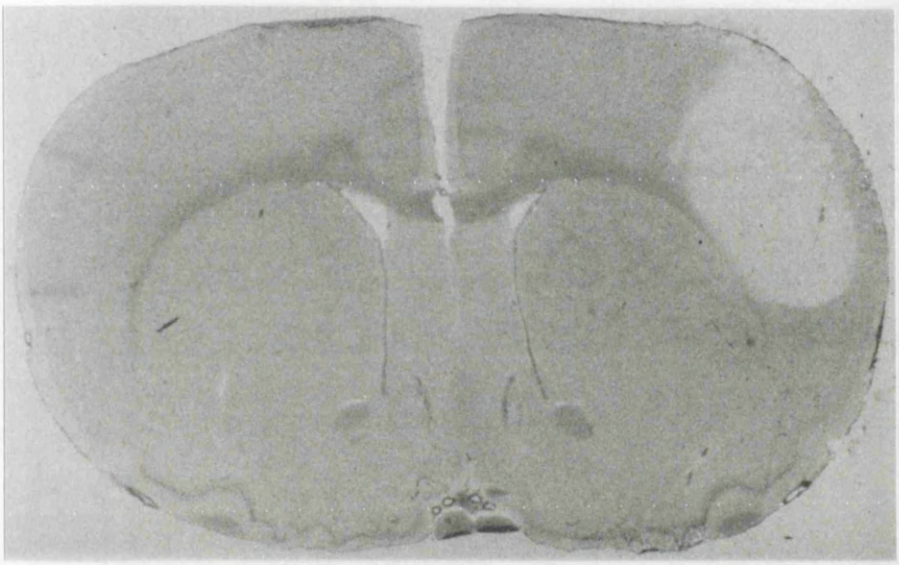

FIGURE 9: CORTICAL GLUTAMATE LESION

A representative coronal rat brain section stained with haematoxylin and eosin, illustrating a typical lesion produced by perfusion of glutamate (0.5M) into the right cerebral cortex. Section shown is at the same plane as the dialysis probe. Glutamate perfusion produced a pale lesion with a clear boundary around the dialysis probe, in the cortex. Shrinkage of neurones and neuropil, triangulation of the nucleus, and swelling of perineuronal astrocytes were evident in the area of pallor. No histological abnormalities were evident in brain regions remote from the dialysis probe.

the presence of glutamate in the extracellular space. Another advantage of this procedure is that it is less invasive than other *in vivo* models of glutamate toxicity, such as the MCA occlusion model.

### 3.3.2 Surgical Preparation of Animals

Animals were placed in a perspex chamber and anaesthetised with 5% halothane in a nitrous oxide-oxygen gas mixture (70%:30%). Anaesthesia was maintained with 1% halothane by use of a face mask while a tracheostomy was performed, and thereafter rats were ventilated mechanically by means of a pump, with a nitrous oxide-oxygen gas mix (70%:30%) containing 0.5-1% halothane. The femoral vessels were exposed bilaterally by blunt dissection via small incisions made either side of the groin. Polyethylene catheters (Portex: external diameter 0.96mm; internal diameter 0.58mm; 15cm long) containing heparinised saline (10 IU/ml) were inserted 2cm into both femoral arteries and one femoral vein. The catheters were tied in place with silk thread and the wounds sutured closed. One arterial catheter was connected to a pressure transducer (P23ID Gould Stratham, Model 2202) for continuous monitoring of arterial pressure. Core temperature was monitored by a rectal thermometer, and animals were maintained normothermic by means of heating blankets and lamps. Arterial $pCO_2$, $pO_2$ and pH were monitored throughout the subsequent procedures by blood gas analysis (168pH/Blood Gas System, Corning). The stroke volume of the ventilator was adjusted to maintain arterial carbon dioxide tension at approximately 35mmHg, and adequate arterial oxygenation ($pO_2$ > 90mmHg) throughout the experiment.

### 3.3.3 Glutamate Perfusion

The anaesthetised and ventilated animals were mounted into a Kopf stereotaxic frame (Clark Electromedical, London, U.K.). The right parietal skull and Bregma were exposed by making a longitudinal midline incision in the scalp, reflecting the skin and clearing any connective tissue from the skull surface. The stereotaxic coordinates for placement of the microdialysis probe, taken from the stereotaxic atlas of Paxinos and Watson (1986), relative to Bregma were:- Anterior-Posterior +0.0mm; Lateral +4.0mm; Ventral -3.5mm below dura; incisor bar set +5mm above the interaural line. The position of probe placement was marked in ink on the skull surface and a burr hole made through the skull with a high-speed dental drill. After incising the arachnoid dura, a microdialysis probe (Carnegie Medicin, Sweden, membrane length 3mm; outside diameter 0.5mm) was lowered into the cortex at an angle of 15° to the sagittal plane.

Monosodium glutamate (0.5M) was dissolved in mock cerebrospinal fluid, CSF (NaCl, 135mM; KCl, 1mM; $KH_2PO_4$, 2mM; $CaCl_2$, 1.2mM; $MgCl_2$, 1mM; pH 7.4). After placement in the cortex, the microdialysis probe was perfused with mock CSF for bewteen 30 and 60 min and thereafter with 0.5M glutamate at a flow rate of 1.5µl/min for 90 min using a Carnegie Medicin 100 infusion pump (Biotech Instruments, Luton, U.K.). Following 90 min of glutamate perfusion, the microdialysis probe was removed from the cortex and the scalp wound closely sutured. The animals were decapitated 150 min later (4h after the start of glutamate perfusion), their brains dissected out intact, frozen by immersion in isopentane at -43°C and processed for histological lesion assessment (see section 3.4).

### 3.3.4 Drug Administration

In two series of animals the following pharmacologically active agents were administered by intravenous injection via the femoral vein catheter at a constant rate over 2 min. Glutamate perfusion was initiated 30 min after drug or vehicle administration.

1) **NBQX**

Dual injections of NBQX were administered at a dose of 30mg/kg (2ml/kg volume) 30 min prior to and 30 min after the start of glutamate perfusion. Control animals similarly received dual intravenous injections of vehicle (5.5% glucose, pH 8.0 with NaOH; 2ml/kg).

2) **D-Cycloserine**

D-Cycloserine was administered at a dose of 3mg/kg (1ml/kg volume). Control animals received an intravenous injection of vehicle (sterile saline; 1ml/kg).

## 3.4 Experimental Analysis

### 3.4.1 Histological Processing of Brain Tissue

The frozen brains were mounted onto swivel-headed microtome chucks with plastic embedding matrix (Lipshaw) and cut into 20μm-thick coronal cryostat sections. Three consecutive sections were picked up onto gelatin-subbed slides at 200μm intervals throughout the forebrain for haematoxylin and eosin staining. A fourth adjacent section was similarly collected for cresyl-violet staining for light microscopic verification of the lesion.

### 3.4.2 Quantification of Lesion/Infarct Volumes

At 24h following MCA occlusion, or 4h after glutamate perfusion, the region of infarcted tissue could be clearly identified in sections stained with haematoxylin and eosin (see Figures 8 and 9). The infarcted area could be defined as a sharply delineated region of pallor, bordered by normal, densely stained tissue. The volumes of brain damage were measured by computer-assisted densitometry (Quantimet 920, Cambridge Instruments, U.K.). The haematoxylin and eosin stained sections were placed under the video camera which projected the section image onto the monitor screen. The regions of lesion or ischaemic infarct were easily identified as areas of low optical density relative to the intact brain. The boundary of the lesion/ischaemic region was delineated manually on the screen using the computer "mouse". The densitometer calculated the area of the delineated region. Area measurements were made on each of the triplicate sections at each level throughout the brain, and mean area calculated. Hence the total volume of lesion/ischaemic tissue per specimen was calculated from the area measurements and the known distance between each coronal level (260μm). In MCA occluded animals, the volumes of ipsilateral and contralateral hemispheres were similarly calculated from densitometric measurement of hemipsheric areas at each coronal level and the known distance between each coronal plane. Knowledge of hemispheric volume allowed analysis of any drug-induced swelling effect. Sections were analysed "blind", i.e. sections were coded by a colleague to prevent knowledge of the treatment group they belonged to during the densitometric analysis.

### 3.4.3 Data Analysis

**MCA Occlusion - D-Cycloserine**

The hemispheric volume and volume of infarcted cerebral tissue in MCA occluded animals after systemic administration of D-cycloserine (3mg/kg) were compared with hemispheric volume and infarct volume in MCA occluded animals after vehicle injection (controls) using Student's unpaired *t*-test (1-tailed for infarct comparison, 2-tailed for hemipsheric volume comparison).

**Glutamate Perfusion**

1) **D-Cycloserine**

The volume of the glutamate-induced lesion in animals receiving D-cycloserine (3mg/kg) was compared with lesion volume in vehicle-injected control animals using one way analysis of variance (ANOVA), followed by an independent *t*-test (2-tailed). In a contemporaneous study employing the same control group, the effect of another pharmacologically active agent on glutamate-induced cerebral damage was also investigated. Consequently, a Bonferroni correction factor of 2 was applied to *t*-test probability values to take into consideration the multiple control-vehicle group comparisons.

2) **NBQX**

The volume of tissue damage resulting from glutamate perfusion of the cortex following intravenous administration of NBQX (2 x 30mg/kg) was compared with the lesion volume produced by glutamate perfusion following systemic administration of vehicle, using ANOVA,

followed by an indpendent *t*-test (2-tailed). In contemporaneous experiments, using the same group of control animals, the effects of 3 other agents on the extent of glutamate-induced damage were also investigated which were not part of the present study (Fujisawa et al., 1993a). Consequently, a Bonferroni correction factor of 4 was applied to the *t*-test probability values to take into consideration the multiple treatment-vehicle comparisons.

## 4. ANIMAL STUDIES III

## BASAL FOREBRAIN INTERVENTIONS: EFFECTS ON LOCAL CEREBRAL GLUCOSE USE

### 4.1 General

The chronic effects of excitotoxic basal forebrain lesions, and the acute effects of excitatory amino acid and GABA agonist infusions into the basal forebrain on local cerebral glucose utilisation were investigated using the [$^{14}$C]-2-deoxyglucose *in vivo* autoradiography technique. Stereotactic surgical procedures were employed to infuse the agonists into the nucleus basalis magnocellularis (NBM) region of the basal forebrain. In addition, [$^{3}$H]-PK-11195 *in vitro* autoradiography was performed in sections taken from animals which had received basal forebrain lesions, to gain insight into the location and extent of glial proliferation associated with chronic excitotoxic lesions.

#### 4.1.1 Animals

The subjects of these experiments were male, adult, hooded Lister rats, 250-300g pre-operative weights (Olac, Bicester, U.K.). Prior to surgery animals were allowed to acclimatise to their surroundings for 5 days and nights. In holding, both prior to and following surgery, rats were individually housed under natural daylight conditions, with room temperature maintained at approximately 21°C, and food and water provided *ad libitum*. The animals weights and general physiological condition were checked daily to ensure the rats recovered normally from surgery.

## 4.2 Surgical Preparation of Animals

### 4.2.1 Stereotactic Lesions of the NBM: Chronic Glucose Use Measurement

Rats were anaesthetised by an intraperitoneal injection of Avertin (tribromoethanol in tertiary amyl alcohol; 1ml/kg body weight). Once unconscious animals were not handled for 15 min, and were then placed in a stereotactic frame (David Kopf, Tujunga, CA, U.S.A.). A longitudinal midline incision was made into the scalp and the skin reflected to expose the skull. Burr holes were made through the skull, bilaterally at the appropriate stereotactic coordinates for infusion, using a high speed dental drill. 30-Gauge stainless steel cannulae (Cooper's Needleworks Ltd., U.K.) attached to 5µl microsyringes (Hamilton) were lowered through the burr holes into the NBM region of the basal forebrain at the following stereotactic coordinates (relative to Bregma):-AP +1.0mm; L ±3.2mm; V -7.2mm from dura; incisor bar set +5mm above interaural line (coordinates taken from the stereotaxic atlas of Paxinos & Watson, 1986; see Robbins et al., 1989a and b). Quisqualic acid (0.09M), α-amino-3-hydroxy-5-methyl-4-isoxazole propionic acid (AMPA; 0.015M), N-methyl-D-aspartate (NMDA; 0.09M) and ibotenic acid (0.09M) or sterile phosphate buffered saline vehicle (0.2M, pH 7.2) were then infused unilaterally into the NBM in a volume of 0.5µl, at a constant rate over 3 min. The cannula was left in place for a further 3 min to allow the infusate to diffuse away from the infusion site and prevent "back-tracking" up the needle tract. The needle placement in the contralateral hemisphere, with no infusion served as a "sham" operation. Following cannulae removal the scalp wound was sutured closed with silk thread and the animals allowed to recover from anaesthesia. Glucose/saline (5ml) was administered subcutaneously to

compensate for loss of body fluids during recovery from anaesthesia.

Following surgery, animals survived for 21-24 days, at which time the rats underwent [$^{14}$C]-2-deoxyglucose *in vivo* autoradiography according to the procedures outlined in sections 1.1.3 and 1.1.4. At the end of the procedure the rats' brains were processed for quantitative autoradiography (see section 1.4) and [$^{3}$H]-PK-11195 *in vitro* autoradiography (see section 1.3.2).

### 4.2.2 Stereotactic Agonist Infusions into the NBM: Acute Glucose Use Measurement

Rats were anaesthetised with Avertin (1ml/kg body weight, i.p.), placed in a Kopf stereotactic frame and the skull exposed, as described in section 4.2.1. Burr holes were made through the skull bilaterally, at the appropriate stereotactic coordinates, using a high-speed dental drill. Stainless steel guide cannulae (23 gauge; Cooper's Needleworks Ltd., U.K.) were implanted bilaterally into the basal forebrain, terminating 1.2mm above the injection sites. The stereotaxic coordinates for injections targeted on the NBM relative to Bregma were:- Anterior-Posterior (A-P) + 1.0mm; Lateral (L) ± 3.2mm; and Ventral (V) -7.2mm from dura (guide cannulae inserted to -6.0mm from dura); incisor bar set +5mm above the interaural line taken from the stereotaxic atlas of Paxinos and Watson (1986) (Muir et al., 1992). Two stainless steel screws were place in the skull anterior and posterior to the guide cannulae and the entire assembly covered in dental acrylic. In order to keep the cannulae patent a stainless steel stylet, cut to the same length as the guide cannulae, was inserted into each. Animals were then removed from the frame and allowed to regain consciousness. Glucose/saline solution

(5ml) was administered subcutaneously to compensate for loss of body fluids while the animals were recovering from the effects of anaesthesia. Ten to fourteen days were allowed for post-operative recovery prior to further manipulation.

The excitatory amino acid agonists AMPA (0.0015M), NMDA (0.009M) and the GABA agonist muscimol (0.03mM) were dissolved (1ml/kg) in sterile phosphate buffer vehicle (2M, pH 7.2). Aliquots were made in advance and stored, frozen at -20°C, for a maximum of 1 week.

On the day of the agonist infusion the rats were prepared for [$^{14}$C]-2-deoxyglucose autoradiography as described in section 1.1.3. Agonist perfusion was initiated at least 2h after animals had regained consciousness following halothane anaesthesia. The stylets were removed from both guide cannulae and a 30-gauge cannula was inserted into each outer guide tube, to protrude 1.2mm below the base of each guide cannula. Each injection cannula was attached to a 5µl Hamilton syringe. AMPA, NMDA or muscimol, in a volume of 1µl, were injected unilaterally into the right hemisphere at a constant rate of 0.5µl/min by means of a perfusion pump controlling the Hamilton syringes. In all animals, vehicle (1µl) was simultaneously infused into the contralateral hemisphere. Injection cannulae were left in place for a further 2 min before removal.

The [$^{14}$C]-2-deoxyglucose procedure was initiated 15 min after completion of agonist infusion, according to the protocol outlined in section 1.1.4. At the end of the procedure the rat's brains were removed and processed for quantitative autoradiography (as described in section 1.4).

## 4.3 Quantification of Lesion Volume and Histological Analysis

[$^3$H]-PK-11195 binds to peripheral-type benzodiazepine binding sites which are situated predominantly on glial cells within the CNS. Hence the extent of increased [$^3$H]-PK-11195 binding evident after an intracerebral intervention putatively gives insight into the location and extent of gliosis occurring as a result of that intervention.

The volume of brain tissue showing an increased density of [$^3$H]-PK-11195 binding after excitotoxic lesions, relative to the levels of binding in the contralateral non-lesioned hemisphere was assessed in each animal by computer-assisted densitometry. [$^3$H]-PK-11195 autoradiograms were positioned under the video camera and section images analysed from the monitor screen. In [$^3$H]-PK-11195 binding autoradiograms, regions of enhanced [$^3$H]-PK-11195 binding were easily identified due to the greatly increased optical density of the film relative to "normal" cerebral tissue in the non-lesioned hemisphere. The densitometric paradigm used involved measuring the optical density of the blackest region of "normal" brain tissue in a section outwith the infusion site, to give a maximal optical density limit for "background". It was then possible to programme the densitometer to detect regions with an optical density greater than this value (set individually for each animal film) and hence quantify the area in which [$^3$H]-PK-1195 binding was abnormally increased. By using the computer "mouse" to delineate a region of the section encompassing the infusion site and lesion, the densitometer then calculated the area of tissue within this region with an optical density greater than the previously set background limit, corresponding to the area of [$^3$H]-PK-11195 binding. It was important to

exclude regions of normally high glial content from this region of measurement (for example, the ventricles). Mean area values were calculated from duplicate adjacent sections, at 200μm intervals throughout the extent of the lesion. Hence the volume of tissue in which increased [$^3$H]-PK-11195 binding was evident following agonist infusions could be calculated from the area measurements and knowledge of the distance between successive sections.

The position of the lesions was verified by histological analysis of cresyl-violet stained sections, taken at 260μm intervals throughout the brain, and adjacent to sections used for autoradiography.

## 4.4 Data Analysis

### 4.4.1 Chronic NBM Lesions

Local cerebral glucose use values were measured bilaterally in 49 CNS regions in animals which had received unilateral infusions of NMDA, ibotenic acid, quisqualic acid, AMPA or vehicle into the NBM region of the basal forebrain. A needle was inserted into the corresponding region of the contralateral hemisphere to provide a "sham-operated" control hemisphere. Statistical analysis involved, firstly, analysis of glucose use values for structures in the contralateral, sham-operated hemispheres between all treatment groups, (using one way analysis of variance (ANOVA), followed by independent *t*-tests with Bonferroni correction for multiple comparisons). No significant differences in contralateral glucose use values were evident between vehicle- and treatment-infused groups. Subsequent interhemispheric comparison of glucose utilisation values for each structure in the vehicle-

infused (control) animals, using Student's paired *t*-test, demonstrated no significant differences between rates of glucose use in vehicle-infused and sham-operated hemispheres. Consequently, glucose use values in the vehicle-infused (ipsilateral) hemisphere of control animals were used as control values for subsequent comparison with values in the ipsilateral hemisphere of agonist-infused animals, initially using ANOVA to identify any regions showing alterations in glucose use, followed by independent *t*-tests with a Bonferroni correction factor of 4 for multiple comparisons.

### 4.4.2 Acute NBM Infusions

Local rates of cerebral glucose utilisation were measured bilaterally in 52 CNS regions in animals which had received unilateral infusions of AMPA, NMDA or muscimol into the NBM region of the basal forebrain, with simultaneous infusions of vehicle into the corresponding region of the contralateral hemisphere. The statistical analysis involved, firstly, comparison of glucose use values for each structure of the contralateral (vehicle-infused) hemisphere, between all three treatment groups, using one way analysis of variance (ANOVA) followed by independent *t*-tests. No significant differences in glucose use values between treatment groups were identified in any of the regions investigated. Therefore, subsequent analyses of any alterations in glucose use in the ipsilateral (agonist-infused) hemispheres used the contralateral hemisphere as "control" values, comparing ipsilateral and contralateral glucose use values within treatment groups using Student's paired *t*-test.

## 5. MATERIALS

[$^{14}$C]-2-Deoxy-D-glucose (50-60mCi/mmol) was obtained from Amersham. (+)-3-[$^{125}$I]-MK-801 (2200Ci/mmol) and [$^{3}$H]-PK-11195 (86Ci/mmol) were obtained from New England Nuclear. N-Methyl-D-aspartic acid (NMDA), α-amino-3-hydroxy-5-methyl-4-isoxazole propionic acid (AMPA), quisqualic acid, ibotenic acid, muscimol, PK-11195, D-cycloserine and Tris buffer base (Tris[hydroxymethyl]amino-methane) were all obtained from Sigma Chemical Company. 2,3-Dihydroxy-6-nitro-7-sulfamoyl-benzo(F) quinoxaline (NBQX) was obtained from Novo Nordisk and LY-293558 from Eli Lilly.

# CHAPTER III

# RESULTS

# 1. EFFECTS OF AMPA RECEPTOR BLOCKADE ON CEREBRAL GLUCOSE USE

The effects of systemic administration of the AMPA receptor antagonists NBQX (10, 30 and 100mg/kg) and LY-293558 (10, 30 and 100mg/kg) on local cerebral glucose utilisation were assessed, in conjunction with measurements of physiological parameters and observation of overt behaviour, to gain insight into the functional consequences of AMPA receptor blockade.

## 1.1 General Observations

Intravenous administration of the AMPA-receptor antagonists NBQX (10, 30, 100mg/kg) and LY-293558 (10, 30, 100mg/kg) resulted in marked alterations in the overt behaviour of the rats (which varied drug- and dose-dependently in rate of onset and duration) and changes in the measured respiratory parameters, but had no sustained effect on the cardiovascular system. All physiological measurements are presented in Table 4.

Prior to drug administration the partially restrained rats were generally quiescent, with intermittent periods of spontaneous head and forelimb movements, grooming and sniffing. All rats responded appropriately to noise and visual stimulation. Following the administration of NBQX and LY-293558 rats became heavily sedated, apparently unconscious, staring straight ahead with a rigid body posture, no movement of head or forelimbs, and signs of CNS depression characterised by loss of responsiveness to auditory and visual stimuli. The rate of onset of this state was slower after LY-293558 administration than after NBQX. Rats became sedated within 1 min of receiving NBQX (100mg/kg), and 1-5 min after NBQX (10 or

30mg/kg). Rats receiving LY-293558 (100mg/kg) became sedated 1-5 min post-administration, while the rate of onset of sedation was slower after lower doses of LY-293558 (4-20 min after 10mg/kg and 3-10 min after 30mg/kg). Following NBQX (100mg/kg) or LY-293558 (100mg/kg) rats remained sedated for the duration of the experiment. Following lower doses, animals showed signs of recovery within 30 min of NBQX (10mg/kg) or LY-293558 (10mg/kg), and within 40 min of NBQX (30mg/kg) or LY-293558 (30mg/kg). Recovery was exemplified by the return of responsiveness to auditory and visual stimuli, and movements of head and forelimbs. During recovery from sedation, animals exhibited abnormal motor activity characterised by intermittent periods of jerky head movements, neck arching, facial twitching, gnawing and grinding of teeth, which persisted for the remainder of the experimental period. Similar atypical movements were seen in all animals after LY-293558 administration, prior to the onset of sedation occurring. In contrast, control animals remained fully conscious, lively and alert throughout the experimental period.

NBQX and LY-293558 both evoked dose-dependent increases in arterial $CO_2$ tension ($pCO_2$) and decreases in arterial oxygen tension ($pO_2$) over the time course of the experiments (Figures 10 and 11). The respiratory depressant effects of LY-293558 were more marked than those of NBQX. Control animals showed no significant alterations in $PCO_2$ and $PO_2$ during the 1h experimental period.

The cardiovascular effects of each agent were restricted to the period immediately following injection, with neither drug inducing a sustained significant change in arterial blood pressure over the 60 min experimental

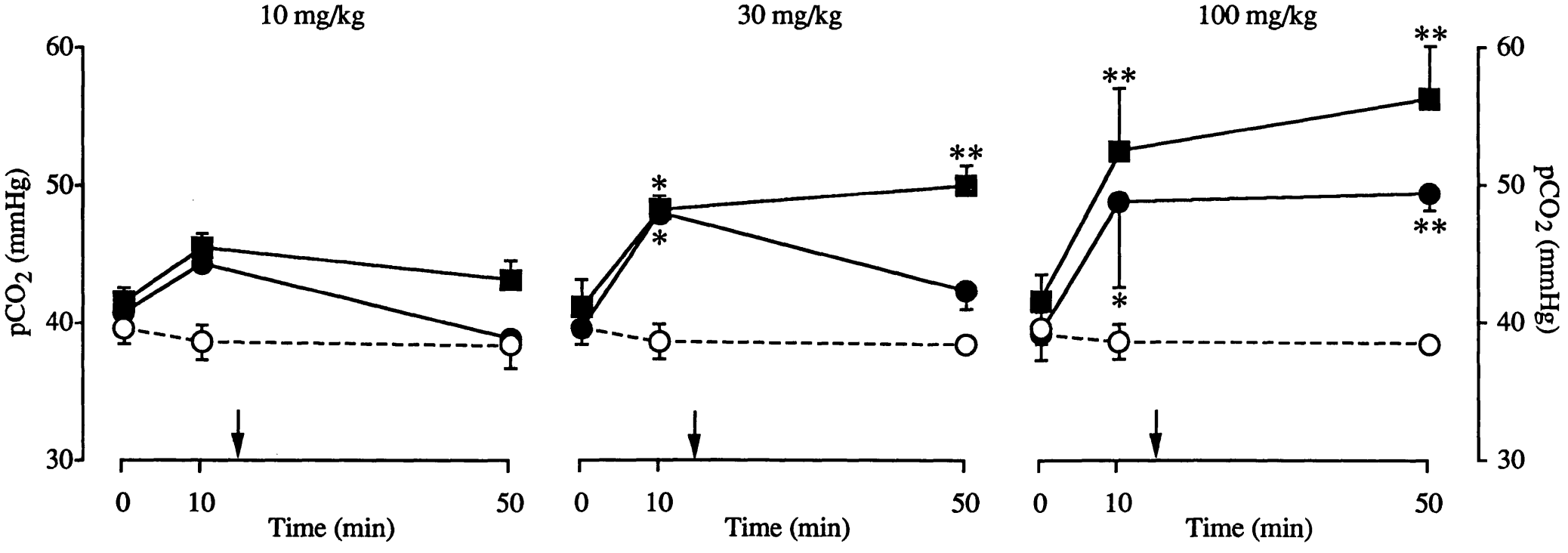


FIGURE 10: ARTERIAL CARBON DIOXIDE TENSION FOLLOWING NBQX AND LY-293558 ADMINISTRATION

Data presented as mean ± SEM (n = 6). * $p < 0.05$, ** $p < 0.01$, significant difference relative to contemporaneous value in control animals (ANOVA, followed by Student's unpaired t-test). Arrows indicate the start of the [$^{14}$C]-2-deoxyglucose measurement, 15 min after drug or vehicle injection.

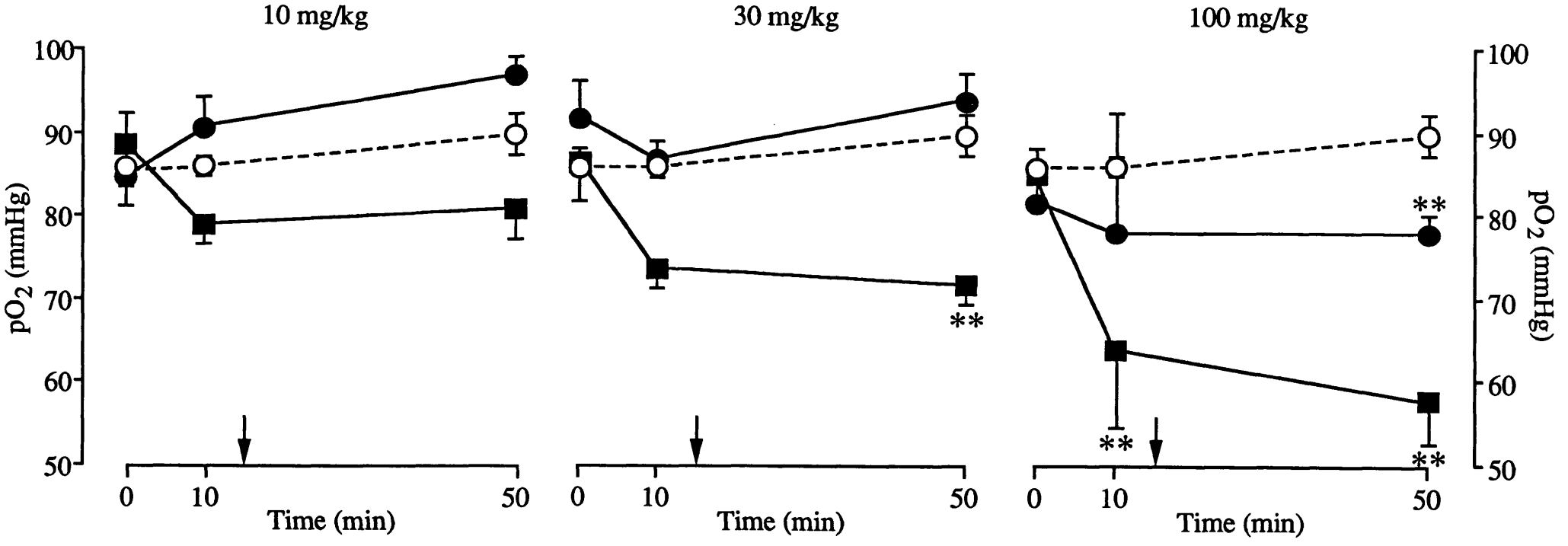


FIGURE 11: ARTERIAL OXYGEN TENSION FOLLOWING NBQX AND LY-293558 ADMINISTRATION

Data presented as mean ± SEM (n = 6). * $p < 0.05$, ** $p < 0.01$, significant difference relative to contemporaneous value in control animals (ANOVA, followed by Student's unpaired t-test). Arrows indicate the start of the [$^{14}$C]-2-deoxyglucose measurement, 15 min after drug or vehicle injection.

period. However, NBQX (100mg/kg) and LY-293558 (100mg/kg) had contrasting effects on mean arterial blood pressure acutely after injection. NBQX (100mg/kg) produced a transient decrease in arterial pressure (-12 ± 9mmHg, mean ± SEM), maximal by 1 min post-administration and persisting for up to 5 min. Lower doses of NBQX had negligible effects on blood pressure. In contrast, LY-293558 induced a dose-dependent pressor effect. LY-293558 (100mg/kg) markedly increased arterial pressure (+33 ± 9mmHg, mean ± SEM, $p<0.05$) maximal by 1 min post-injection and which returned to pre-injection levels within 6 min. In animals receiving lower doses of LY-293558, transient but non-significant increases in blood pressure occurred following 30mg/kg (+19 ± 6mmHg) and 10mg/kg (+15 ± 4mmHg), evident by 1 min post-injection and persisting for up to 6 min. In control animals, vehicle injection had no effect on arterial pressure.

Plasma glucose levels were significantly increased 50 min after NBQX (100mg/kg) relative to control values. In contrast LY-293558 had no significant effects on plasma glucose levels over the time course of the experiments. Trends towards reduced body temperature were evident in some animals following both NBQX and LY-293558, however the use of heating lamps throughout the experimental period makes interpretation of drug-related temperature effects difficult.

## TABLE 4

## PHYSIOLOGICAL VARIABLES FOLLOWING INTRAVENOUS ADMINISTRATION OF NBQX AND LY-293558 TO CONSCIOUS RATS

| | TIME AFTER DRUG (min) | CONTROL | NBQX (mg/kg) | | | LY-293558 (mg/kg) | | |
|---|---|---|---|---|---|---|---|---|
| | | | 10 | 30 | 100 | 10 | 30 | 100 |
| Rectal Temperature | 0 | 37.0±0.1 | 36.5±0.2 | 37.0±0.2 | 37.2±0.1 | 36.6±0.2 | 37.0±0.3 | 37.2±0.3 |
| (°C) | 10 | 37.0±0.1 | 36.0±0.3* | 36.8±0.1 | 36.7±0.3 | 36.9±0.1 | 36.5±0.2 | 36.8±0.3 |
| | 50 | 36.9±0.1 | 36.1±0.5 | 36.7±0.3 | 35.9±0.7 | 36.4±0.2 | 36.6±0.3 | 36.0±0.1 |
| Mean Arterial | 0 | 130 ± 3 | 137 ± 2 | 123 ± 4 | 134 ± 8 | 117 ± 4 | 130 ± 4 | 130 ± 5 |
| Blood Pressure | 10 | 130 ± 3 | 140 ± 6 | 125 ± 3 | 121 ± 5 | 132 ± 5 | 131 ± 7 | 137 ± 10 |
| (mmHg) | 50 | 130 ± 2 | 142 ± 5 | 128 ± 5 | 133 ± 7 | 119 ± 5 | 120 ± 10 | 135 ± 20 |
| Arterial Plasma | 0 | 8.3±0.5 | 7.3±0.3 | 8.4±0.7 | 9.6±0.4 | 8.2±0.7 | 7.1±0.5 | 8.1±0.8 |
| Glucose (mM) | 50 | 9.3±0.6 | 10.4±0.6 | 10.9±1.3 | 17.1±3.0 ** | 9.9±0.7 | 8.2±1.7 | 7.3±0.3 |
| $pCO_2$ | 0 | 40 ± 1 | 41 ± 2 | 40 ± 1 | 39 ± 2 | 41 ± 1 | 41 ± 2 | 42 ± 2 |
| (mmHg) | 10 | 39 ± 1 | 44 ± 1 | 48 ± 1* | 49 ± 6* | 45 ± 1 | 48 ± 1* | 53 ± 5** |
| | 50 | 39 ± 2 | 39 ± 2 | 42 ± 1 | 50 ± 1** | 43 ± 1 | 50 ± 1** | 56 ± 4** |
| $pO_2$ | 0 | 86 ± 2 | 85 ± 3 | 92 ± 4 | 82 ± 4 | 89 ± 3 | 87 ± 4 | 85 ± 3 |
| (mmHg) | 10 | 86 ± 1 | 91 ± 3 | 87 ± 2 | 78 ±14 | 79 ± 2 | 74 ± 2 | 64 ± 7** |
| | 50 | 90 ± 2 | 97 ± 2 | 94 ± 3 | 78 ± 2** | 81 ± 3 | 72 ± 2** | 58 ± 4** |
| Number of Animals | | 9 | 5 | 5 | 4 | 5 | 5 | 4 |

Data are presented as mean ± SEM. Data represent values at times 0, 10 and 50 min following intravenous administration of NBQX, LY-293558 or vehicle (controls). *$p<0.05$, **$p<0.01$ for statistical difference between drug-treated and control animals at each time point (ANOVA, followed by Student's unpaired *t*-test with Bonferroni correction).

## 1.2 Local Cerebral Glucose Utilisation

### 1.2.1 General

Intravenous administration of NBQX (10, 30 and 100mg/kg) and LY-293558 (10, 30 and 100mg/kg) resulted in marked, widespread, dose-dependent reductions in local cerebral glucose utilisation throughout the CNS. The glucose use alterations associated with systemic administration of NBQX or LY-293558 in the 50 CNS regions investigated are presented in Tables 5 - 9 (see also Figures 12 and 13).

Following intravenous administration of NBQX (10mg/kg), none of the 50 regions examined displayed significant alterations in glucose use. Following NBQX (30mg/kg), glucose use was significantly reduced in 17 of the 50 regions investigated, and NBQX (100mg/kg) significantly reduced glucose use in 48 of the 50 regions. In contrast, intravenous administration of LY-293558 (10mg/kg) produced significant reductions in glucose use in 7 of the 50 regions examined. Following LY-293558 (30mg/kg) glucose use was significantly reduced in 34 of the 50 regions investigated, while LY-293558 (100mg/kg) significantly reduced glucose use in 43 of the 50 regions. No significant elevation in glucose use was observed in any of the brain regions examined following any dose of either drug.

Administration of the highest dose of either agent, NBQX (100mg/kg) or LY-293558 (100mg/kg), resulted in extremely large magnitude reductions in glucose use in several CNS regions, in particular in a number of cortical, auditory and limbic regions where glucose use was decreased by up to 68% (see Figures 12 and 13). For example, in the superior olivary nucleus glucose use was reduced from 114 ± 6 μmol/100g/min in control animals to 44 ± 6 and

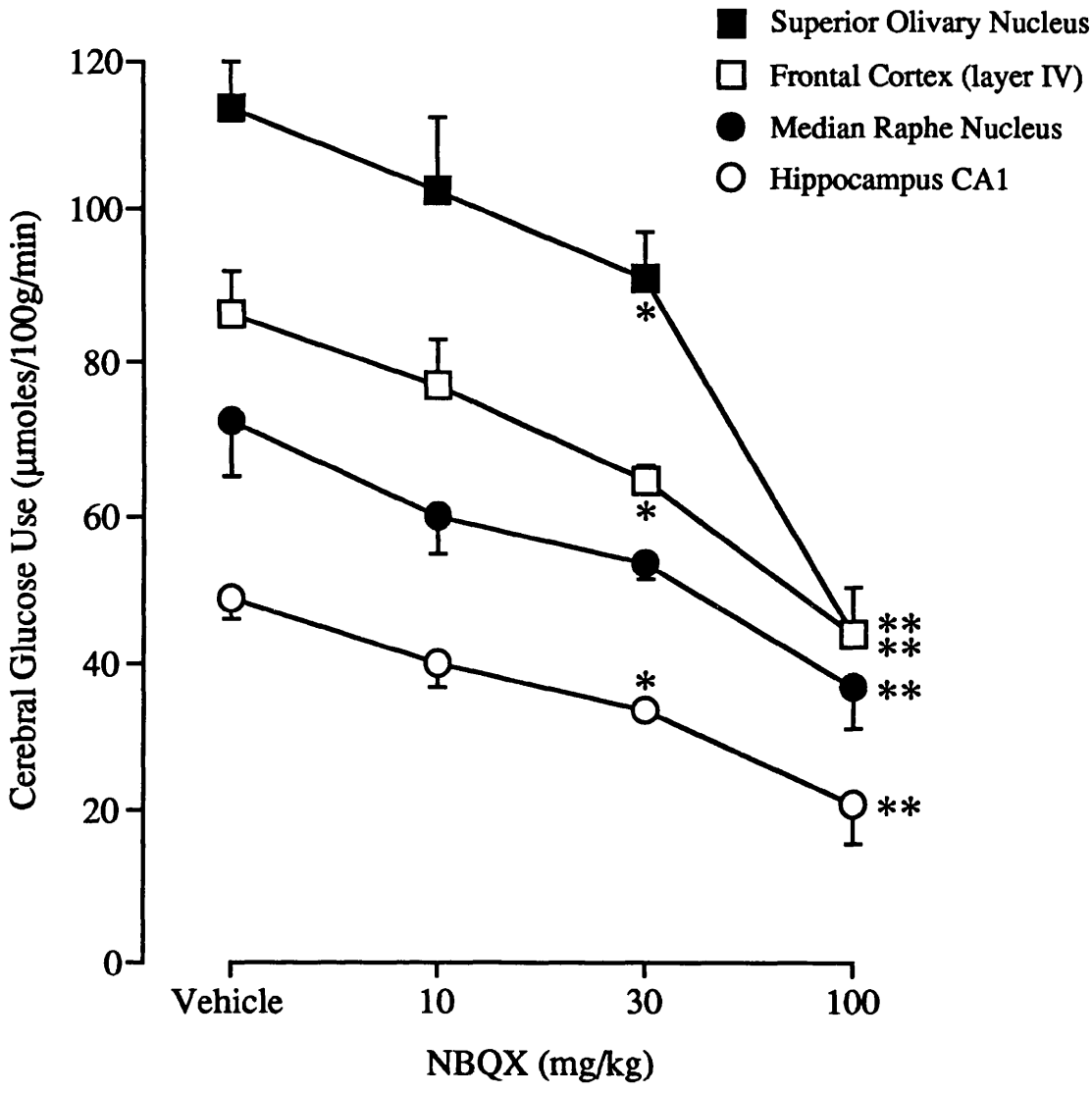


FIGURE 12: NBQX AND CEREBRAL GLUCOSE USE

Representative dose-response curves illustrating the effects of intravenous administration of NBQX (10, 30 or 100 mg/kg) or vehicle on local cerebral glucose utilisation. Data presented as mean ± SEM.

Note the general similarities between the dose-dependent glucose use reductions in the four brain regions illustrated, although glucose use was depressed to a proportionately greater extent by NBQX (100 mg/kg) in the superior olivary nucleus than in the limbic and cortical regions.

*$p<0.05$, **$p<0.01$ (ANOVA, followed by Student's unpaired *t*-test with Bonferroni correction).

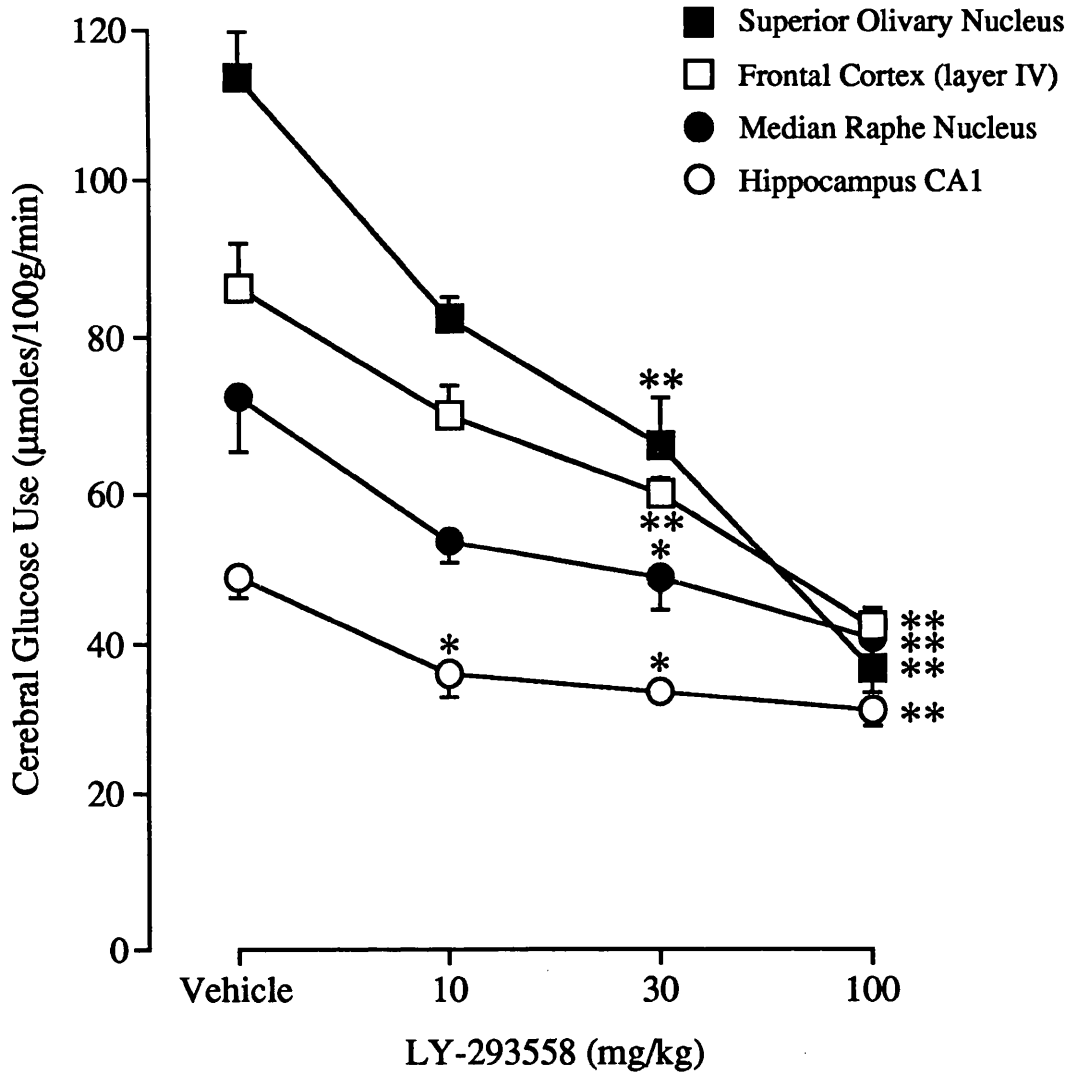


FIGURE 13: LY-293558 AND CEREBRAL GLUCOSE USE

Representative dose-response curves illustrating the effects of intravenous administration of LY-293558 (10, 30 or 100 mg/kg) or vehicle on local cerebral glucose utilisation. Data presented as mean ± SEM.

Note the general similarities between the dose-dependent glucose use reductions in the four brain regions illustrated, although glucose use was depressed to a proportionately greater extent by LY-293558 (100 mg/kg) in the superior olivary nucleus than in the limbic and cortical regions.

*$p<0.05$, **$p<0.01$ (ANOVA, followed by Student's unpaired *t*-test with Bonferroni correction).

37 ± 3 μmol/100g/min following NBQX (100mg/kg; -61%) and LY-293558 (100mg/kg; -68%) respectively.

In the cerebral cortex, both AMPA antagonists markedly reduced glucose utilisation in all regions investigated (Table 6). The laminar pattern of glucose use seen in sensory motor and frontal cortex of control animals was conserved following antagonist administration, layer IV exhibiting greater glucose use than other lamina. In neocortical and allocortical regions the reductions in glucose use seen after NBQX and LY-293558 were both qualitatively and quantitatively similar, with the exception of cingulate cortical regions which exhibited markedly greater glucose use reductions following either NBQX or LY-293558 than other cortical regions. For example, in the posterior cingulate cortex glucose use was reduced from 89 ± 7 μmol/100g/min in control animals to 31 ± 5 and 32 ± 1 μmol/100g/min following NBQX (100mg/kg; -65%) and LY-293558 (100mg/kg; -64%) respectively. No significant elevation in glucose use was observed in any of the brain regions examined following any dose of either drug.

In the majority of regions investigated NBQX and LY-293558 produced qualitatively similar patterns of glucose use alterations, both agents inducing more or less uniform dose-dependent reductions in glucose use, as is demonstrated by the similarities between dose-response curves for glucose use alterations in response to NBQX and LY-293558, illustrated in Figures 12 and 13. However, a small number of regions exhibited heterogeneous responses to NBQX and LY-293558. The observation of anomalous responses to NBQX and LY-293558 in some brain regions is underlined by the fact that NBQX (100mg/kg) produced significant reductions in glucose use in 48 out of the 50

regions examined whereas LY-293558 (100mg/kg) significantly affected only 43 regions. For example, in the olfactory tubercle NBQX (100mg/kg) produced a significant reduction in glucose use, from 99 ± 7 μmol/100g/min in control animals to 52 ± 5 μmol/100g/min (-47%, $p<0.01$), whereas LY-293558 (100mg/kg) produced a much smaller magnitude reduction in the same region (to 73 ± 6μmol/100g/min, -26%, $p>0.05$). The insensitivity of the olfactory tubercle to glucose use alteration by LY-293558, relative to the marked reduction produced by NBQX, is readily apparent from visual inspection of the autoradiograms (see Figure 14).

Other brain regions examined in which glucose use was insensitive to any dose of LY-293558 were the superficial layer of the superior colliculus, olfactory amygdala, substantia nigra pars compacta and pars reticulata, medial habenular nucleus and cerebellar white matter (see Tables 5, 7, 8 and 9). Glucose use in the superior colliculus superficial layer and inferior olivary nucleus was insensitive to change by NBQX at any dose (see Tables 5 and 8). In one region, the superficial layer of the superior colliculus, glucose utilisation was not significantly altered by either NBQX or LY-293558 (controls = 72 ± 5 μmol/100g/min; NBQX (100mg/kg) = 56 ± 6 μmol/100g/min; LY-293558 (100mg/kg) = 66 ± 4 μmol/100g/min). The lack of effect of NBQX (100mg/kg) and LY-293558 (100mg/kg) on glucose use in the superior colliculus superficial layer, relative to the marked glucose use reductions in other brain regions, is clearly evident from visual inspection of the autoradiograms (see Figure 15).

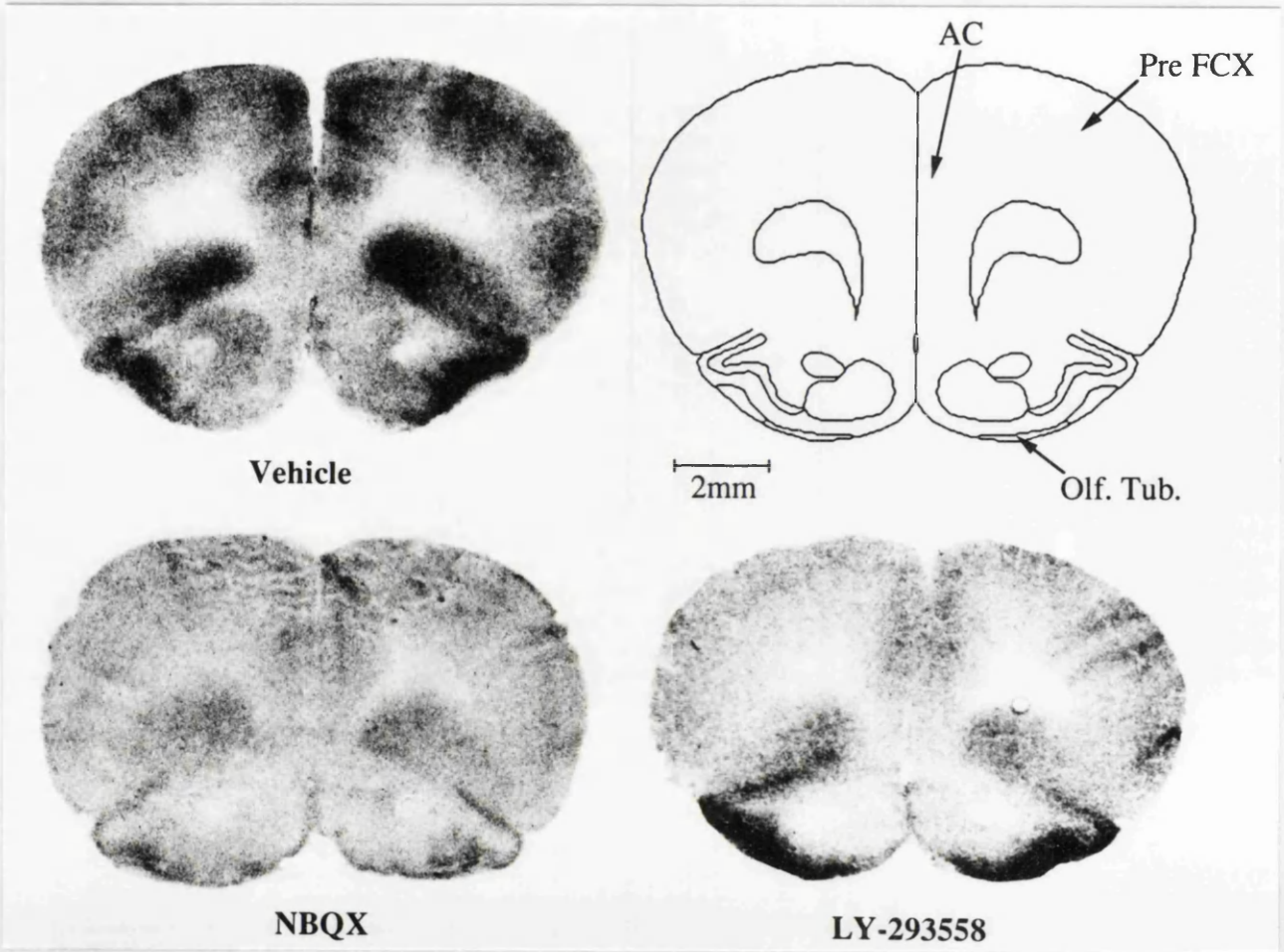


FIGURE 14: GLUCOSE USE IN THE OLFACTORY TUBERCLE IS INSENSITIVE TO LY-293558

Representative autoradiograms illustrating local cerebral glucose use following intravenous administration of NBQX (100 mg/kg), LY-293558 (100 mg/kg) or vehicle (control). Note the insensitivity of glucose use in the olfactory tubercle (Olf. Tub.) to alteration by LY-293558, in contrast to the reduced glucose use in the olfactory tubercle following NBQX, and the marked glucose use depression in other cerebral regions following AMPA receptor blockade. *Abbreviations:* PreFCX: prefrontal cortex; AC: anterior cingulate cortex.

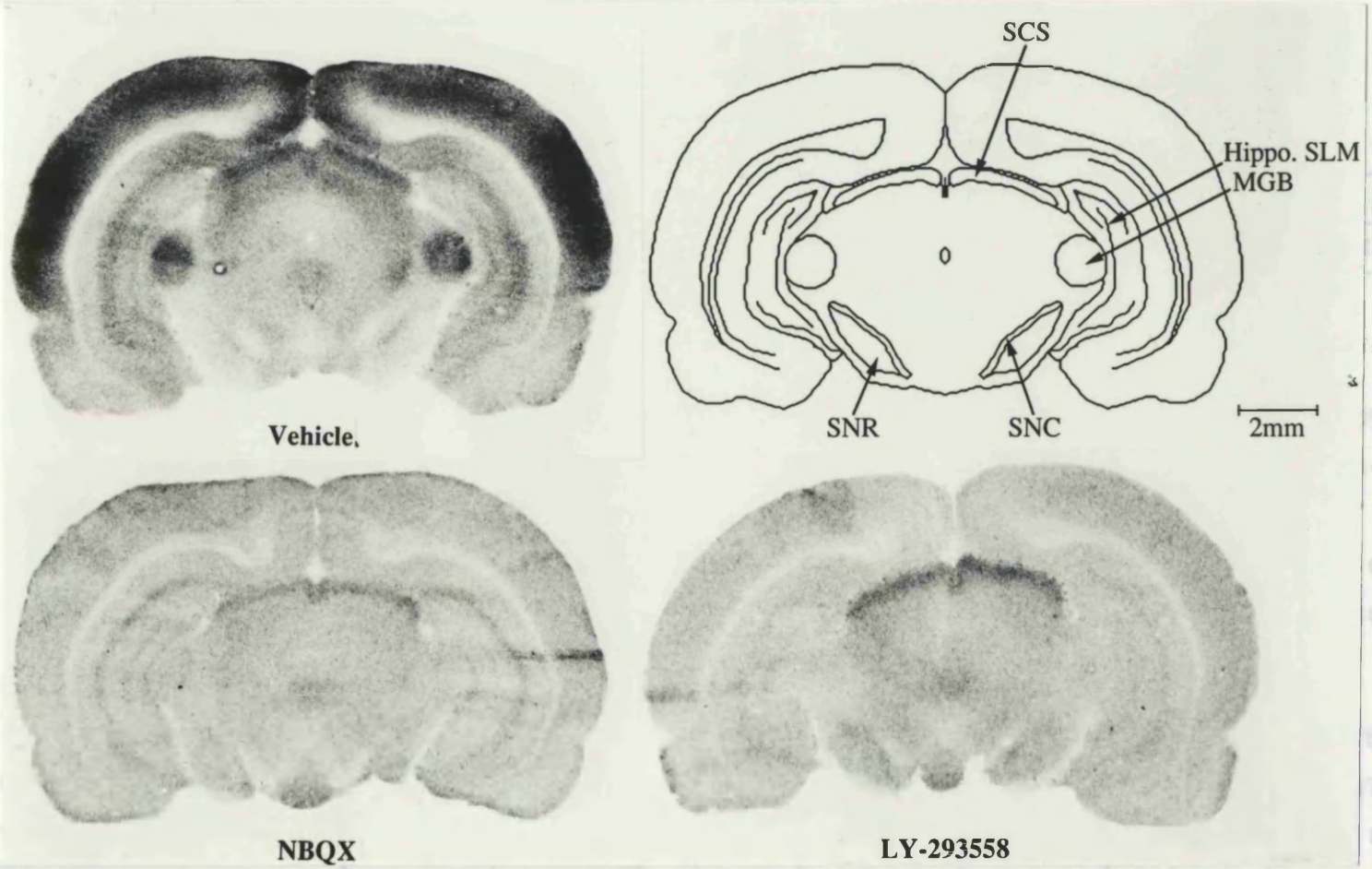


FIGURE 15: GLUCOSE USE IN THE SUPERIOR COLLICULUS IS INSENSITIVE TO AMPA RECEPTOR BLOCKADE

Representative autoradiograms illustrating local cerebral glucose use following intravenous administration of NBQX (100 mg/kg), LY-293558 (100 mg/kg) or vehicle (control). Note the insensitivity of glucose use in the superior colliculus superficial layer (SCS) to alteration by NBQX or, most notably, by LY-293558, in contrast to the marked glucose use reductions in other cerebral regions. *Abbreviations:* MGB: medial geniculate body; SNC: substantia nigra pars compacta; SNR: substantia nigra pars reticulata; Hippo. SLM: hippocampus molecular layer.

## TABLE 5
## GLUCOSE UTILISATION FOLLOWING ADMINISTRATION OF NBQX AND LY-293558: PRIMARY VISUAL AND AUDITORY AREAS

| | | NBQX (mg/kg) | | | LY-293558 (mg/kg) | | | *f* VALUE | |
|---|---|---|---|---|---|---|---|---|---|
| **STRUCTURE** | **CONTROL** | **10** | **30** | **100** | **10** | **30** | **100** | **NBQX** | **LY-293558** |
| Primary Visual System | | | | | | | | | |
| Visual Cortex, Layer IV | 76 ± 5 | 69 ± 5 | 56 ± 4* | 41 ± 4** | 60 ± 2 | 48 ± 5** | 37 ± 2** | 0.474 | 0.768 |
| Dorsal Lateral Geniculate Body | 64 ± 5 | 63 ± 6 | 55 ± 3 | 32 ± 4** | 52 ± 4 | 45 ± 2* | 34 ± 2** | 0.489 | 0.505 |
| Thalamus: Lateral Posterior | 78 ± 8 | 72 ± 4 | 60 ± 4 | 39 ± 5** | 59 ± 5 | 46 ± 2** | 40 ± 3** | 0.534 | 0.706 |
| Superior Colliculus: | | | | | | | | | |
| Superficial Layer | 72 ± 5 | 64 ± 4 | 59 ± 4 | 56 ± 6 | 68 ± 2 | 67 ± 5 | 66 ± 4 | 0.116 | 0.011 |
| Deep Layer | 67 ± 6 | 58 ± 4 | 54 ± 5 | 39 ± 5** | 57 ± 3 | 51 ± 3 | 42 ± 3** | 0.338 | 0.278 |
| Primary Auditory System | | | | | | | | | |
| Auditory Cortex, Layer IV | 119 ± 10 | 98 ± 9 | 84 ± 4* | 43 ± 3** | 82 ± 4** | 64 ± 4** | 40 ± 3** | 1.118 | 1.599 |
| Medial Geniculate Body | 86 ± 8 | 75 ± 7 | 70 ± 3 | 31 ± 5** | 61 ± 4* | 49 ± 4** | 31 ± 2** | 1.087 | 1.379 |
| Inferior Colliculus | 141 ± 9 | 126 ± 11 | 114 ± 6 | 53 ± 6** | 112 ± 6 | 87 ± 7** | 46 ± 4** | 1.011 | 1.523 |
| Superior Olivary Nucleus | 114 ± 6 | 103 ± 10 | 91 ± 6* | 44 ± 6** | 82 ± 3** | 66 ± 6** | 37 ± 3** | 1.020 | 1.682 |
| Cochlear Nucleus | 110 ± 6 | 108 ± 5 | 92 ± 5 | 67 ± 20** | 87 ± 5 | 69 ± 3** | 52 ± 5** | 0.395 | 0.833 |
| | n = 9 | n = 5 | n = 5 | n = 4 | n = 5 | n = 5 | n = 4 | | |

Data are presented as mean ± SEM (µmol/100g/min.) *p<0.05, **p<0.01, significant difference relative to control values (ANOVA, followed by Student's unpaired *t*-test with Bonferroni correction). *f* values were derived from the NBQX and LY-293558 data presented, as described in Section 1.2.2.

## TABLE 6

## GLUCOSE UTILISATION FOLLOWING ADMINISTRATION OF NBQX AND LY-293558: CEREBRAL CORTEX

| | | NBQX (mg/kg) | | | LY-293558 (mg/kg) | | | *f* VALUE | |
|---|---|---|---|---|---|---|---|---|---|
| STRUCTURE | CONTROL | 10 | 30 | 100 | 10 | 30 | 100 | NBQX | LY-293558 |
| Sensory Motor Cortex: | | | | | | | | | |
| Layer I-III | 75 ± 6 | 61 ± 8 | 59 ± 2 | 37 ± 4** | 63 ± 2 | 55 ± 2* | 37 ± 3** | 0.594 | 0.576 |
| Layer IV | 86 ± 7 | 75 ± 5 | 66 ± 2* | 43 ± 5** | 69 ± 3 | 60 ± 3** | 39 ± 2** | 0.550 | 0.743 |
| Layer V-VI | 71 ± 6 | 67 ± 7 | 53 ± 1 | 33 ± 4** | 59 ± 2 | 51 ± 2* | 31 ± 3** | 0.627 | 0.733 |
| Parietal Cortex: | | | | | | | | | |
| Layer IV | 84 ± 7 | 77 ± 6 | 63 ± 1* | 41 ± 7** | 66 ± 5 | 56 ± 2** | 38 ± 2** | 0.629 | 0.789 |
| Frontal Cortex: | | | | | | | | | |
| Layer I-III | 77 ± 6 | 69 ± 4 | 58 ± 2* | 40 ± 2** | 64 ± 3 | 54 ± 2* | 40 ± 3** | 0.470 | 0.535 |
| Layer IV | 86 ± 6 | 77 ± 6 | 64 ± 2* | 44 ± 2** | 70 ± 4 | 60 ± 2** | 42 ± 3** | 0.515 | 0.633 |
| Layer V-VI | 71 ± 6 | 64 ± 5 | 52 ± 2* | 35 ± 3** | 59 ± 3 | 51 ± 2* | 33 ± 2** | 0.529 | 0.615 |
| Posterior Cingulate Cortex | 89 ± 7 | 80 ± 6 | 64 ± 4* | 31 ± 5** | 67 ± 4* | 44 ± 2** | 32 ± 1** | 1.186 | 1.525 |
| Anterior Cingulate Cortex | 99 ± 9 | 80 ± 6 | 64 ± 2** | 44 ± 4** | 75 ± 4* | 60 ± 2** | 41 ± 2** | 0.814 | 0.987 |
| Prefrontal Cortex: | | | | | | | | | |
| Layer IV | 88 ± 8 | 80 ± 6 | 64 ± 5* | 44 ± 4** | 71 ± 3 | 63 ± 5* | 40 ± 2** | 0.525 | 0.727 |
| | n = 9 | n = 5 | n = 5 | n = 4 | n = 5 | n = 5 | n = 4 | | |

Data are presented as mean ± SEM (µmol/100g/min.) *p<0.05, **p<0.01, significant difference relative to control values (ANOVA, followed by Student's unpaired *t*-test with Bonferroni correction). *f* values were derived from the NBQX and LY-293558 data presented, as described in Section 1.2.2.

## TABLE 7

## GLUCOSE UTILISATION FOLLOWING ADMINISTRATION OF NBQX AND LY-293558: OLFACTORY AREAS

| | | NBQX (mg/kg) | | | LY-293558 (mg/kg) | | | *f* VALUE | |
|---|---|---|---|---|---|---|---|---|---|
| STRUCTURE | CONTROL | 10 | 30 | 100 | 10 | 30 | 100 | NBQX | LY-293558 |
| Primary Olfactory Cortex: | | | | | | | | | |
| Layer I | 60 ± 4 | 51 ± 3 | 47 ± 4 | 28 ± 6** | 55 ± 3 | 48 ± 2 | 36 ± 3** | 0.700 | 0.310 |
| Olfactory Tubercle | 99 ± 7 | 92 ± 8 | 76 ± 6 | 52 ± 5** | 86 ± 4 | 93 ± 5 | 73 ± 6 | 0.453 | 0.096 |
| Olfactory Amygdala | 39 ± 2 | 34 ± 4 | 34 ± 2 | 26 ± 5* | 36 ± 3 | 33 ± 2 | 31 ± 1 | 0.275 | 0.089 |
| Entorhinal Cortex: | | | | | | | | | |
| Layer I | 58 ± 4 | 47 ± 2 | 44 ± 4* | 29 ± 4** | 48 ± 2 | 43 ± 3* | 34 ± 2** | 0.625 | 0.375 |
| | n = 9 | n = 5 | n = 5 | n = 4 | n = 5 | n = 5 | n = 4 | | |

Data are presented as mean ± SEM (µmol/100g/min.) *p<0.05, **p<0.01, significant difference relative to control values (ANOVA, followed by Student's unpaired *t*-test with Bonferroni correction). *f* values were derived from the NBQX and LY-293558 data presented, as described in Section 1.2.2.

## TABLE 8
## GLUCOSE UTILISATION FOLLOWING ADMINISTRATION OF NBQX AND LY-293558: EXTRAPYRAMIDAL AND SENSORY-MOTOR AREAS

| | | NBQX (mg/kg) | | | LY-293558 (mg/kg) | | | *f* VALUE | |
|---|---|---|---|---|---|---|---|---|---|
| **STRUCTURE** | **CONTROL** | 10 | 30 | 100 | 10 | 30 | 100 | **NBQX** | **LY-293558** |
| Striatum: | | | | | | | | | |
| Dorsolateral | 77 ± 6 | 72 ± 4 | 57 ± 0* | 36 ± 6** | 67 ± 3 | 58 ± 3* | 40 ± 5** | 0.663 | 0.468 |
| Ventromedial | 67 ± 6 | 59 ± 7 | 48 ± 2 | 34 ± 6** | 53 ± 2 | 51 ± 4 | 36 ± 1** | 0.566 | 0.429 |
| Globus Pallidus | 42 ± 3 | 41 ± 5 | 33 ± 2 | 19 ± 3** | 37 ± 2 | 34 ± 2 | 29 ± 2* | 0.783 | 0.197 |
| Substantia Nigra: | | | | | | | | | |
| Pars Compacta | 53 ± 4 | 47 ± 3 | 44 ± 2 | 30 ± 3** | 49 ± 3 | 49 ± 4 | 40 ± 3 | 0.332 | 0.075 |
| Pars Reticulata | 46 ± 4 | 37 ± 4 | 35 ± 3 | 28 ± 1** | 37 ± 2 | 37 ± 2 | 34 ± 3 | 0.318 | 0.136 |
| Thalamus: | | | | | | | | | |
| Mediodorsal | 80 ± 8 | 75 ± 7 | 64 ± 2 | 42 ± 6** | 62 ± 5 | 60 ± 3 | 43 ± 5** | 0.437 | 0.470 |
| Ventrolateral | 61 ± 5 | 54 ± 4 | 48 ± 1 | 29 ± 4** | 46 ± 4 | 43 ± 2* | 33 ± 2** | 0.641 | 0.532 |
| Ventromedial | 91 ± 10 | 78 ± 6 | 68 ± 2 | 41 ± 9** | 66 ± 3 | 58 ± 4* | 48 ± 2** | 0.716 | 0.573 |
| Subthalamic Nucleus | 67 ± 4 | 66 ± 3 | 64 ± 4 | 48 ± 8* | 64 ± 5 | 59 ± 4 | 45 ± 2* | 0.137 | 0.164 |
| Inferior Olivary Nucleus | 65 ± 6 | 57 ± 4 | 53 ± 2 | 46 ± 8 | 60 ± 6 | 50 ± 3 | 43 ± 2* | 0.173 | 0.210 |
| Cerebellar Nuclei | 95 ± 5 | 86 ± 4 | 80 ± 3 | 64 ± 4** | 83 ± 3 | 72 ± 5** | 65 ± 3** | 0.185 | 0.218 |
| Cerebellar hemisphere: | | | | | | | | | |
| Granular Layer | 48 ± 4 | 40 ± 3 | 34 ± 1* | 27 ± 4** | 37 ± 2 | 31 ± 2** | 30 ± 2** | 0.490 | 0.389 |
| Molecular Layer | 48 ± 3 | 42 ± 3 | 37 ± 3* | 29 ± 2** | 41 ± 2 | 34 ± 2** | 32 ± 2** | 0.343 | 0.306 |
| Cerebellar White Matter | 29 ± 3 | 26 ± 3 | 21 ± 1 | 15 ± 3** | 25 ± 2 | 21 ± 2 | 20 ± 2 | 0.570 | 0.255 |
| | n = 9 | n = 5 | n = 5 | n = 4 | n = 5 | n = 5 | n = 4 | | |

Data are presented as mean ± SEM (µmol/100g/min.) *p<0.05, **p<0.01, significant difference relative to control values (ANOVA, followed by Student's unpaired *t*-test with Bonferroni correction). *f* values were derived from the NBQX and LY-293558 data presented, as described in Section 1.2.2.

## TABLE 9

## GLUCOSE UTILISATION FOLLOWING ADMINISTRATION OF NBQX AND LY-293558: LIMBIC SYSTEM AND OTHER BRAIN AREAS

| | | NBQX (mg/kg) | | | LY-293558 (mg/kg) | | | *f* VALUE | |
|---|---|---|---|---|---|---|---|---|---|
| STRUCTURE | CONTROL | 10 | 30 | 100 | 10 | 30 | 100 | NBQX | LY-293558 |
| Hippocampus: | | | | | | | | | |
| CA1 | 49 ± 3 | 40 ± 3 | 34 ± 1* | 21 ± 5** | 36 ± 3* | 34 ± 1* | 31 ± 3** | 1.047 | 0.394 |
| CA3 | 50 ± 4 | 46 ± 3 | 38 ± 2 | 23 ± 5** | 40 ± 4 | 37 ± 2 | 32 ± 4** | 0.798 | 0.327 |
| Molecular Layer | 66 ± 5 | 55 ± 4 | 50 ± 5 | 34 ± 6** | 52 ± 4 | 46 ± 3* | 37 ± 3** | 0.559 | 0.501 |
| Dentate Gyrus | 52 ± 4 | 44 ± 4 | 35 ± 3* | 25 ± 6** | 39 ± 4 | 35 ± 2* | 31 ± 3** | 0.798 | 0.445 |
| Lateral Habenular Nucleus | 82 ± 7 | 79 ± 5 | 70 ± 8 | 48 ± 7** | 68 ± 2 | 53 ± 4* | 54 ± 6* | 0.312 | 0.359 |
| Medial Habenular Nucleus | 55 ± 4 | 53 ± 1 | 50 ± 3 | 37 ± 6** | 49 ± 2 | 43 ± 2 | 47 ± 3 | 0.164 | 0.095 |
| Mamillary Body | 80 ± 6 | 61 ± 9 | 64 ± 4 | 43 ± 7** | 62 ± 5 | 51 ± 2** | 45 ± 2** | 0.555 | 0.545 |
| Median Raphe Nucleus | 72 ± 7 | 60 ± 5 | 53 ± 2 | 37 ± 6** | 53 ± 3 | 49 ± 4* | 41 ± 4** | 0.546 | 0.491 |
| Dorsal Raphe Nucleus | 72 ± 5 | 65 ± 4 | 58 ± 4 | 44 ± 5** | 61 ± 3 | 50 ± 2** | 51 ± 1* | 0.295 | 0.240 |
| Hypothalamus | 40 ± 4 | 35 ± 3 | 33 ± 1 | 21 ± 4** | 33 ± 2 | 32 ± 1 | 26 ± 2* | 0.447 | 0.221 |
| Thalamus: | | | | | | | | | |
| Anteroventral | 87 ± 9 | 73 ± 2 | 68 ± 4 | 40 ± 9** | 61 ± 5* | 50 ± 3** | 37 ± 2** | 0.672 | 1.065 |
| Anteromedial | 83 ± 8 | 73 ± 5 | 65 ± 2 | 40 ± 6** | 63 ± 3 | 58 ± 4* | 39 ± 1** | 0.562 | 0.665 |
| | n = 9 | n = 5 | n = 5 | n = 4 | n = 5 | n = 5 | n = 4 | | |

Data are presented as mean ± SEM (µmol/100g/min.) *p<0.05, **p<0.01, significant difference relative to control values (ANOVA, followed by Student's unpaired *t*-test with Bonferroni correction). *f* values were derived from the NBQX and LY-293558 data presented, as described in Section 1.2.2.

### 1.2.2 Comparison of Effects of NBQX and LY-293558: "*f*" Ranking Analysis

The anatomical patterns of glucose use changes produced by NBQX and LY-293558 were broadly similar throughout the CNS, with approximately two thirds of the regions investigated showing similar sensitivities to both agents (as illustrated in Figure 16). However, a number of regional anomalies are apparent between the effects of the two drugs (see Figures 17 and 18). Further insight into the differences between glucose use responses to NBQX and LY-293558 can be gained by examination of the "*f*" ranking function values generated in each region independently for the effects of either NBQX (10, 30 and 100mg/kg) and LY-293558 (10, 30 and 100mg/kg) (as outlined in Methods, Section 2.2.2). Briefly, the "*f*" function is an arithmetic function which provides an index of the degree of responsiveness of each CNS region investigated to each of the two drugs, taking into consideration the entire dose-response data available following administration of multiple drug doses (Kelly et al., 1986). The "*f*" ranking function:-

$$f = \Sigma (x_c - x_{T_i})^2$$

where $x_c$ is the mean of $\log_e$ (glucose use) for control group members, and $x_{T_i}$ is the mean of $\log_e$ (glucose use) for the $i^{th}$ dose of the treatment group in question, T, i.e. either NBQX (10, 30, 100mg/kg) or LY-293558 (10, 30, 100mg/kg). *f* values for each of the 50 CNS regions investigated are presented in Tables 5-9.

Application of the "*f*" function allowed regional responses to NBQX or LY-293558 to be rank ordered, to compare inter-regional differences in responsiveness of the two drugs using an approach which takes into account the entire data group available. The hierarchies of regional sensitivies are presented in Tables 10a and 10b.

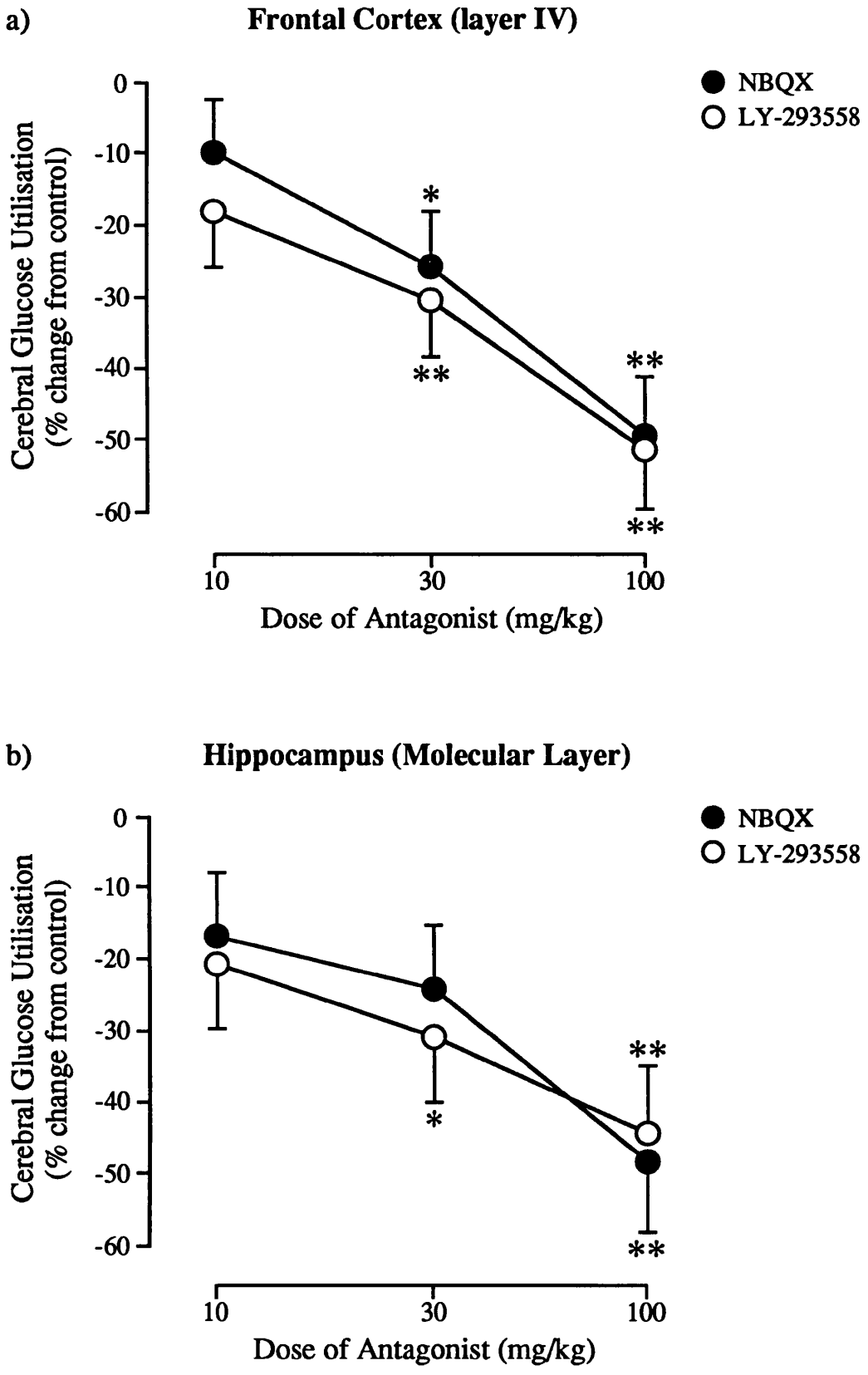


FIGURE 16: AMPA ANTAGONISTS AND CEREBRAL GLUCOSE USE: HOMOGENEOUS EFFECTS OF NBQX AND LY-293558

Data presented as mean ± SEM percentage change in glucose utilisation relative to glucose use in control (vehicle-treated) animals. * $p < 0.05$, ** $p < 0.01$ (ANOVA, followed by Student's unpaired t-test with Bonferroni correction). Note the similarities in the magnitudes of glucose use reductions induced by NBQX and LY-293558 in (a) frontal cortex and (b) hippocampus molecular layer.

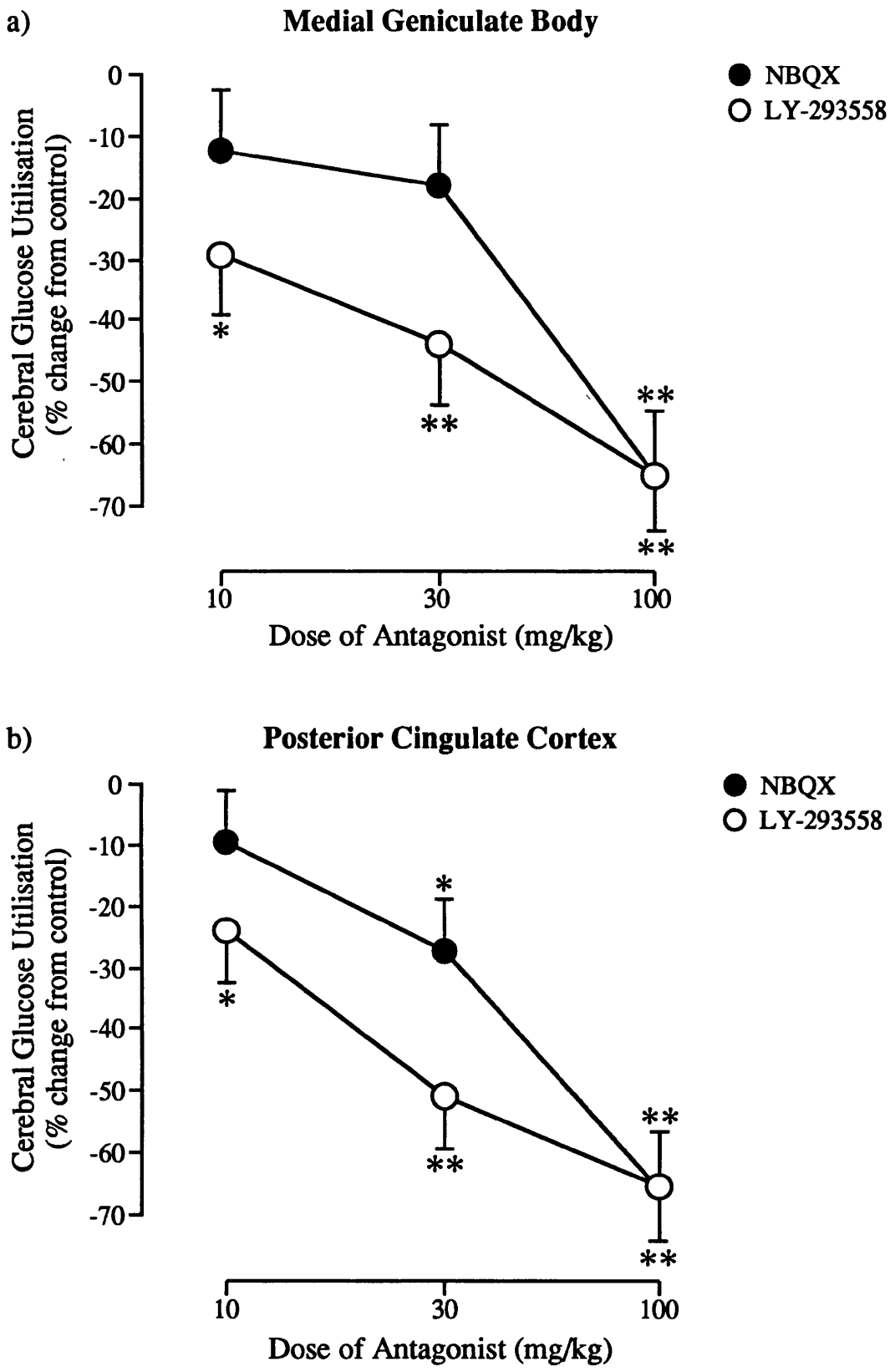


FIGURE 17: AMPA ANTAGONISTS AND CEREBRAL GLUCOSE USE : HETEROGENEOUS EFFECTS OF NBQX AND LY-293558

Data presented as mean ± SEM percentage change in glucose utilisation relative to glucose use in control (vehicle-treated) animals. * $p < 0.05$, ** $p < 0.01$ (ANOVA, followed by Student's unpaired t-test with Bonferroni correction). Note the greater potency of LY-293558 than NBQX in these representative auditory (a) and limbic (b) regions.

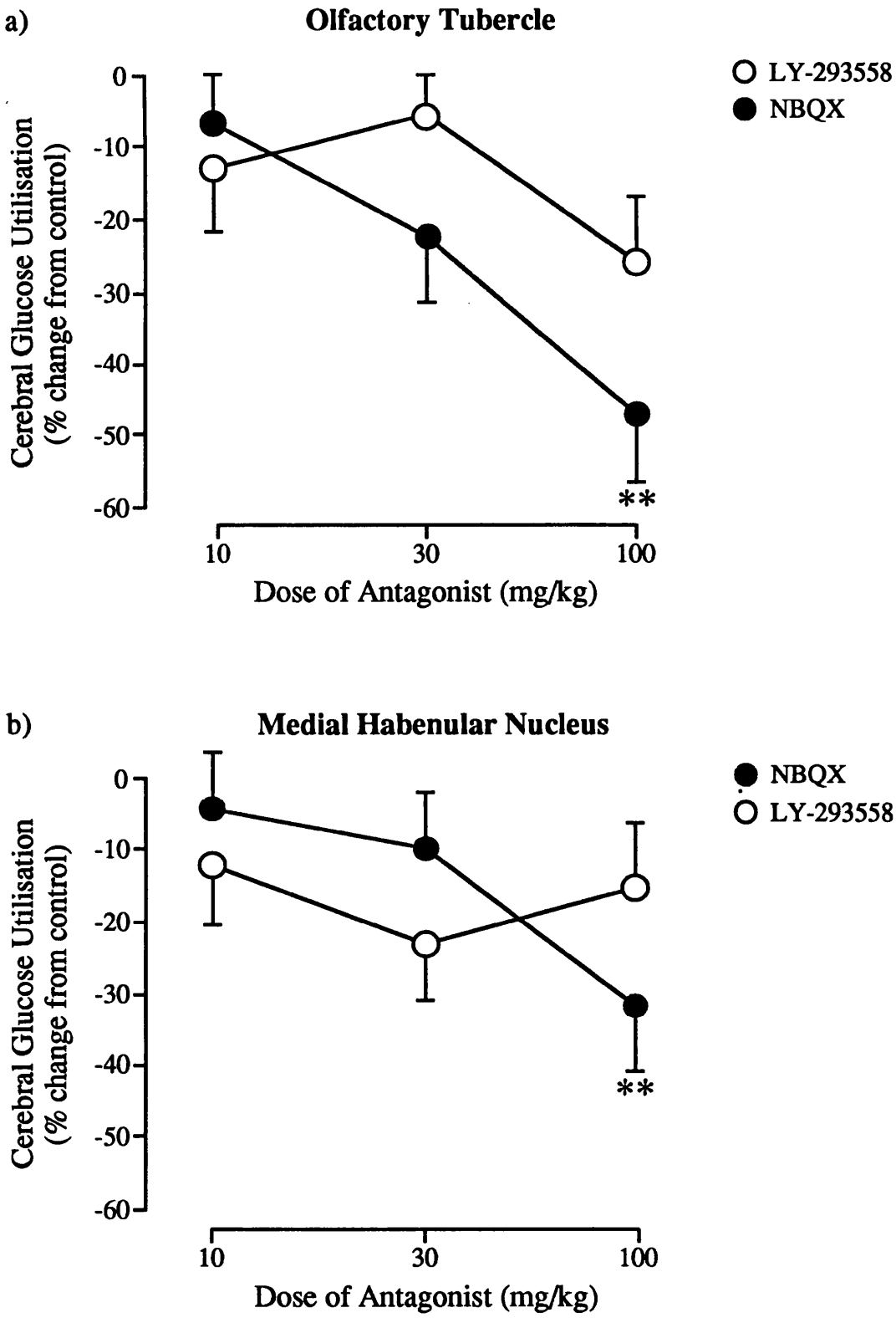


FIGURE 18: AMPA ANTAGONISTS AND CEREBRAL GLUCOSE USE : HETEROGENEOUS EFFECTS OF NBQX AND LY-293558

Data presented as mean ± SEM percentage change in glucose utilisation relative to glucose use in control (vehicle-treated) animals. * $p < 0.05$, ** $p < 0.01$ (ANOVA, followed by Student's unpaired t-test with Bonferroni correction). Note the relative insensitivities of (a) the olfactory tubercle and (b) the medial habenular nucleus to glucose use depression by LY-293558, compared to the effects of NBQX.

**LEGEND TO TABLES 10a AND 10b:**
**HIERARCHY OF REGIONAL RESPONSIVENESS TO NBQX (10a) AND TO LY-293558 (10b)**

The effects of NBQX and LY-293558 on local cerebral glucose use in each of the 50 brain regions investigated are ranked in order of decreasing magnitude of effect, according to the regional calculated $f$ values. The "$f$ " function takes into consideration all the dose-response data available for a given region, and hence reflects the overall sensitivity of the region to glucose use alteration by NBQX or LY-293558 (for derivation of the "$f$ " function, see Methods, Section 2.2.2). Regions have been arbitrarily classified into four groups:-

Extremely Sensitive regions, classified as $f > 0.08$. The $f$ values for these regions lie outwith the normal distribution of $f$ values for either drug. Extremely sensitive regions generally displayed glucose use reductions of >55% after the highest dose (100mg/kg) of either agent.

Sensitive regions, $0.5 < f < 0.8$. Sensitive regions generally displayed glucose use reductions of >50% after the highest dose (100mg/kg) of either agent.

Moderately Sensitive regions, $0.3 < f < 0.5$. Moderately sensitive regions generally displayed 30-50% reductions in glucose use after the highest dose (100mg/kg) of either agent.

Minimally Sensitive regions, $f < 0.3$. Minimally sensitive regions displayed glucose use reductions of <30% after the highest dose (100mg/kg) of either agent. Included in this group are regions in which glucose use was not significantly altered after any dose of NBQX or LY-293558, although all regions showed a trend towards decreased glucose use. These insensitive regions are identified by *.

## TABLE 10a

## HIERARCHY OF RESPONSIVENESS TO NBQX

| EXTREMELY SENSITIVE | SENSITIVE | MODERATELY SENSITIVE | MINIMALLY SENSITIVE |
|---|---|---|---|
| Posterior Cingulate Cortex | Dentate Gyrus | Cerebellar Hemisphere - Granular Layer | Dorsal Raphe Nucleus |
| Auditory Cortex | Hippocampus-CA3 | Dorsal Lateral Geniculate Body | Olfactory Amygdala |
| Medial Geniculate Body | Globus Pallidus | Visual Cortex | Cerebellar Nuclei |
| Hippocampus-CA1 | Thalamus - Ventromedial | Frontal Cortex (I-III) | Medial Habenula |
| Superior Olivary Body | Primary Olfactory Cortex | Olfactory Tubercle | Subthalamic Nucleus |
| Inferior Colliculus | Thalamus - Anteroventral | Hypothalamus | Inferior Olivary Nucleus * |
| Anterior Cingulate Cortex | Striatum - Dorsolateral | Thalamus - Mediodorsal | Superior Colliculus - Superficial Layer * |
| | Thalamus - Ventrolateral | Cochlear Nuclei | |
| | Parietal Cortex (IV) | Cerebellar Hemisphere - Molecular Layer | |
| | Sensory Motor Cortex (V-VI) | Superior Colliculus - Deep Layer | |
| | Entorhinal Cortex | Substantia Nigra Pars Compacta | |
| | Sensory Motor Cortex (I-III) | Substantia Nigra Pars Reticulata | |
| | Cerebellar White Matter | Lateral Habenular Nucleus | |
| | Striatum - Ventromedial | | |
| | Thalamus - Anteromedial | | |
| | Hippocampus - Molecular Layer | | |
| | Mamillary Body | | |
| | Sensory Motor Cortex (IV) | | |
| | Median Raphe Nucleus | | |
| | Thalamus - Lateral Posterior | | |
| | Frontal Cortex (V-VI) | | |
| | Prefrontal Cortex (IV) | | |
| | Frontal Cortex (IV) | | |

## TABLE 10b

## HIERARCHY OF RESPONSIVENESS TO LY-293558

| EXTREMELY SENSITIVE | SENSITIVE | MODERATELY SENSITIVE | MINIMALLY SENSITIVE |
|---|---|---|---|
| Superior Olivary Nucleus | Parietal Cortex (IV) | Median Raphe Nucleus | Superior Colliculus - Deep Layer |
| Auditory Cortex | Visual Cortex (IV) | Thalamus - Mediodorsal | Cerebellar White Matter * |
| Posterior Cingulate Cortex | Sensory Motor Cortex (IV) | Striatum - Dorsolateral | Dorsal Raphe Nucleus |
| Inferior Colliculus | Sensory Motor Cortex (V-VI) | Dentate Gyrus | Hypothalamus |
| Medial Geniculate Body | Prefrontal Cortex (IV) | Striatum - Ventromedial | Cerebellar Nuclei |
| Thalamus - Anteroventral | Thalamus - Lateral Posterior | Hippocampus-CA1 | Inferior Olivary Nucleus |
| Anterior Cingulate Cortex | Thalamus - Anteromedial | Cerebellar Hemisphere - Granular Layer | Globus Pallidus |
| Cochlear Nuclei | Frontal Cortex (IV) | Entorhinal Cortex | Subthalamic Nucleus |
| | Frontal Cortex (V-VI) | Lateral Habenular Nucleus | Substantia Nigra Pars Reticulata * |
| | Sensory Motor Cortex (I-III) | Hippocampus-CA3 | Olfactory Tubercle * |
| | Thalamus - Ventromedial | Primary Olfactory Cortex | Medial Habenular Nucleus * |
| | Mamillary Body | Cerebellar Hemisphere - Molecular Layer | Olfactory Amygdala * |
| | Frontal Cortex (I-III) | | Substantia Nigra Pars Compacta * |
| | Thalamus - Ventrolateral | | Superior Colliculus - Superficial Layer * |
| | Dorsal Lateral Geniculate Body | | |
| | Hippocampus - Molecular Layer | | |

By examination of the "*f*" ranking hierarchies it is apparent that areas which were particularly sensitive to LY-293558 were, in general also highly sensitive to NBQX (see also Figure 16), while those least affected by LY-293558 were also least susceptible to NBQX. Regions in which glucose use was particularly sensitive to NBQX, typically displaying reductions in glucose use of 50% or more at 100mg/kg and *f* values in excess of 0.5 (Table 10a), included primary auditory areas, cerebral cortex, limbic regions (including cingulate cortex and the hippocampal formation), basal ganglia and thalamic regions. Regions in which glucose use was particularly sensitive to LY-293558, displaying glucose use reductions of 50% or more at 100mg/kg and *f* values in excess of 0.5 (Table 10b), included primary auditory areas, the cerebral cortex (in particular cingulate cortex) and thalamus.

However, examination of frequency distribution profiles of *f* values for NBQX and LY-293558 (Figure 19) and correlation analysis of *f* values (Figure 20), reveals differences in glucose use responses to the two agents in a small number of regions. The regional *f* values in NBQX-treated animals are normally distributed around the mean, reflecting the relatively homogenous anatomical pattern of depressant effects of NBQX on local cerebral glucose use (Figure 19a). This observation is supported by examination of the magnitudes of glucose use reductions throughout the brain (Tables 5-8). In contrast, the anatomical pattern of local cerebral glucose use depression produced by LY-293558, although widespread, was more heterogeneous than the pattern of effects produced by NBQX. This is evident from the skewed distribution of LY-293558 *f* values (Figure 19b), the range of glucose use reductions across different brain regions (Tables 5-9), and the failure of a

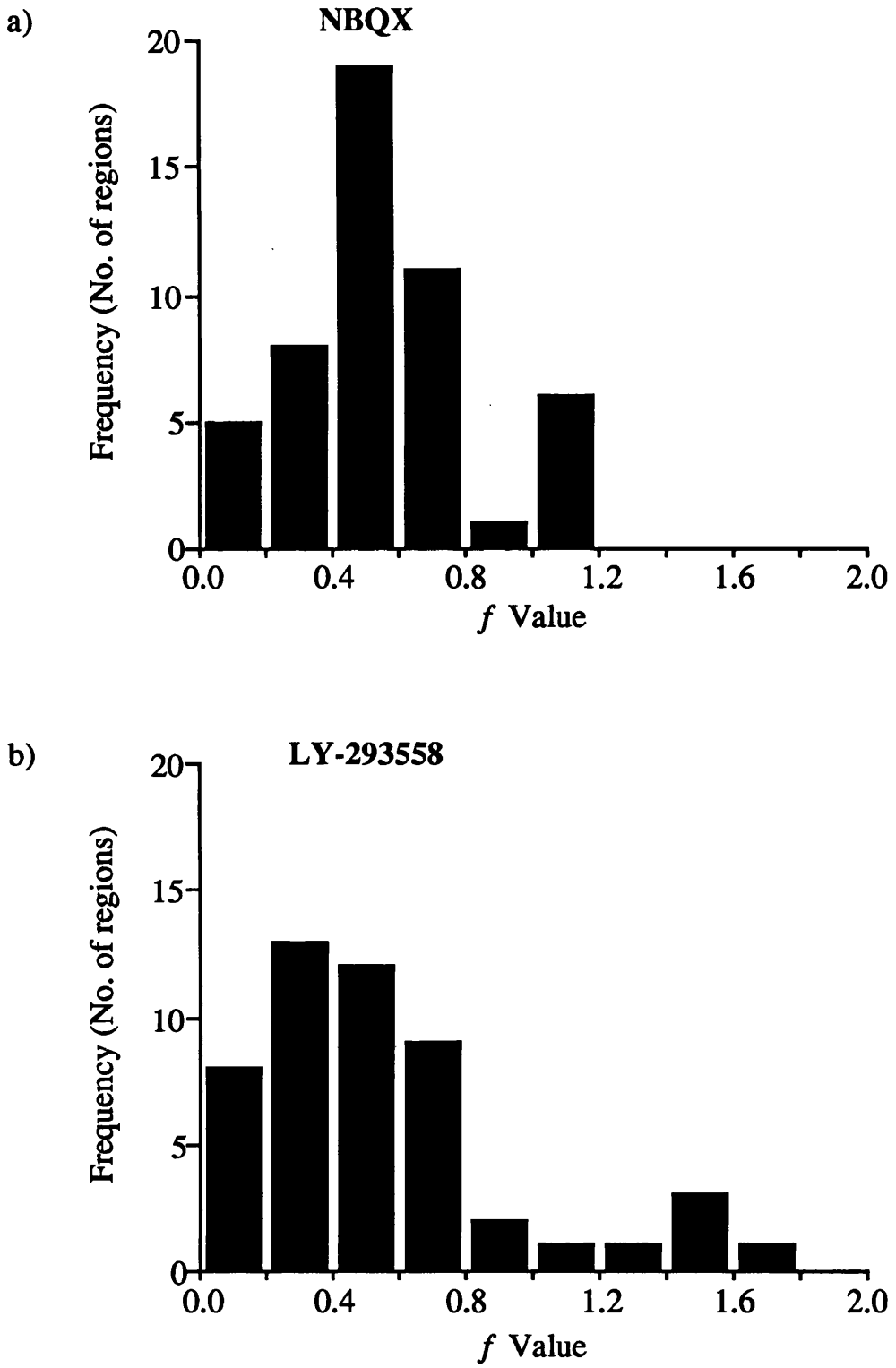


FIGURE 19: FREQUENCY DISTRIBUTIONS OF *f* VALUES FOR NBQX AND LY-293558

*"f"* Function values reflect the sensitivity of individual regions to drug treatment. Following the administration of NBQX (a) the distribution of *f* values was relatively regionally homogeneous, regions being normally distributed around an *f* value of 0.5. In contrast, the regional response to LY-293558 (b) was more heterogeneous, with a wider range of *f* values and a skewed distribution.

greater number of brain regions to achieve accepted statistical significance following LY-293558 (100mg/kg) than after NBQX (100mg/kg).

Comparison of the *f* values for NBQX with those for LY-293558 in each region using Pearson's product moment correlation analysis generated a coefficient value (*r*), of 0.758 reflecting a high degree of association between *f* values across all the CNS regions investigated (illustrated in Figure 20a). This correlation analysis confirms the broad similarity between regional responses to the two agents.

However, within a subset of regions the *f* value for LY-293558 greatly exceeded the value for NBQX, reflecting enhanced sensitivity of these regions to glucose use depression by LY-293558, as illustrated in Figure 20b. This subset of regions was not randomly distributed in the CNS, but comprised mainly two functional systems - the primary auditory system and thalamocortical regions, including all neocortical and suprarhinal cortical areas ($r = 0.895$). The increased potency of LY-293558 relative to NBQX in the medial geniculate body and posterior cingulate cortex is evident from examination of Figure 17 .

Within all other brain areas examined, including limbic, primary visual, olfactory, sensory motor and extrapyramidal regions, NBQX and LY-293558 were generally equipotent (showing a relatively low degree of correlation, $r = 0.5$; Figure 20c) with the exception of a small number of regions which showed slightly greater susceptibility to NBQX than to LY-293558. These regions included the substantia nigra (pars reticulata and pars compacta), cerebellar white matter, medial habenular nucleus, olfactory amygdala and olfactory tubercle (see Figures 14 and 18).

LEGEND TO FIGURE 20:

The relationship between the responsiveness of glucose utilisation in 50 brain regions to NBQX and LY-293558. Each data point represents the "*f* " value generated from analysis of the entire dose-response curve of a single structure in reponse to NBQX and LY-293558. "*f* " values were compared using Pearson's product-moment correlation analysis.

a) The overall correlation coefficient, r, for all regions investigated is 0.758, indicating a high degree of association between the regional effects of NBQX and LY-293558.

b) A subset of regions, comprising primary auditory regions, cerebral cortex and thalamus, showed a particularly high degree of association, with a correlation coefficient of 0.895 and a slope of 1.44. In these regions, glucose use was more susceptible to depression by LY-293558 than NBQX.

c) Residual areas exhibited a lower degree of association, with a correlation coefficient of 0.586 and a slope of 0.38.

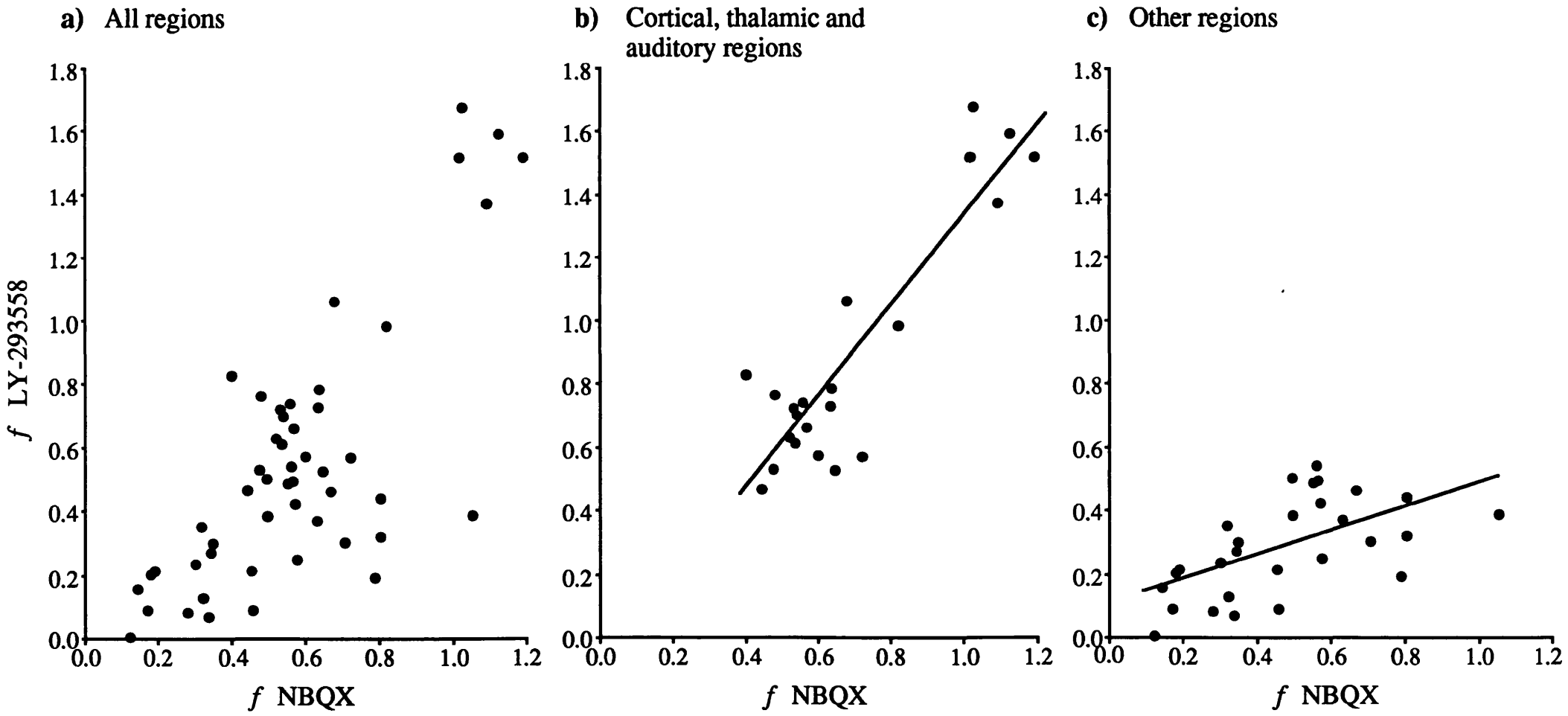


FIGURE 20: RELATIONSHIP BETWEEN *f* VALUES FOR GLUCOSE USE AFTER NBQX AND LY-293558

## 2. MANIPULATION OF NMDA RECEPTOR ACTIVITY BY D-CYCLOSERINE

Four different approaches were used to gain insight into the effects of putative NMDA receptor modulation by the glycine site partial agonist D-cycloserine, on aspects of CNS function under both normal and pathological conditions in the rat. The four strategies employed were:-

(i) Investigation of the effects of systemic administration of D-cycloserine (0.3, 3 and 30mg/kg) on local cerebral glucose utilisation in conscious rats, using the [$^{14}$C]-2-deoxyglucose *in vivo* autoradiography technique.

(ii) Investigation of the effects of systemic administration of a putative agonist dose of D-cycloserine (3mg/kg) on [$^{125}$I]-MK-801 binding in the conscious rat brain, to gain insight into the consequences of putative glycine site stimulation on NMDA receptor activation in the CNS. Results were compared with levels of [$^{125}$I]-MK-801 binding in both conscious and halothane-anaesthetised control animals.

(iii) Investigation of the effect of systemic administration of a putative agonist dose of D-cycloserine (3mg/kg) on lesion volume in the MCA occlusion model of focal cerebral ischaemia.

(iv) Investigation of the effect of systemic administration of a putative agonist dose of D-cycloserine (3mg/kg) on the volume of lesion produced by intracortical perfusion of glutamate. The effects of D-cycloserine were compared with the effects of a well characterised neuroprotective dose of the AMPA receptor antagonist NBQX (30mg/kg) on lesion size in the same model, assessed in a separate group of experiments.

## 2.1 Local Cerebral Glucose Utilisation

### 2.1.1 General Observations

Intravenous administration of D-cycloserine (0.3, 3 and 30mg/kg) to conscious rats had no effect on overt behaviour, or the measured respiratory or cardiovascular parameters throughout the 1h experimental period. All physiological measurements are presented in Table 11.

The partially restrained animals were generally quiescent throughout, with intermittent periods of spontaneous head and forelimb movements, grooming and sniffing following either D-cycloserine (0.3, 3 and 30mg/kg) or vehicle administration. Both drug and vehicle-treated rats remained conscious and alert during the experiments. There were no significant differences in the measured respiratory parameters ($pCO_2$ and $pO_2$) or plasma glucose concentrations between control and drug-treated animals of the time course of the experiments. The statistical analysis employed (ANOVA, followed by Student's unpaired *t*-test) indicated that mean arterial blood pressure in the group of animals which received D-cycloserine (0.3 and 3mg/kg) was significantly higher at the start of the experiment than in control animals, while there were no significant differences between treatment groups 50 min after drug or vehicle administration. However, from subsequent paired *t*-test analysis within treatment groups, no significant differences were evident within treatment groups between blood pressure levels prior to, and 50 min after administration of vehicle or D-cycloserine (0.3, 3 or 30mg/kg) (Student's paired *t*-test, $p>0.05$). This observation indicates that there is no evidence that D-cycloserine significantly alters mean arterial blood pressure over the duration of the experiment.

## TABLE 11

## PHYSIOLOGICAL VARIABLES FOLLOWING INTRAVENOUS ADMINISTRATION OF D-CYCLOSERINE TO CONSCIOUS RATS

| | TIME AFTER DRUG (min) | | D-CYCLOSERINE (mg/kg) | | |
|---|---|---|---|---|---|
| | | CONTROL | 0.3 | 0.3 | 0.3 |
| Rectal Temperature (°C) | 0 | 37.1 ± 0.2 | 36.9 ± 0.1 | 36.6 ± 0.2 | 36.7 ± 0.2 |
| | 50 | 36.5 ± 0.3 | 36.7 ± 0.2 | 37.0 ± 0.1 | 36.6 ± 0.1 |
| Mean Arterial Blood Pressure (mmHg) | 0 | 137 ± 1 | 128 ± 2* | 129 ± 2* | 138 ± 2 |
| | 50 | 120 ± 7 | 120 ± 4 | 122 ± 7 | 128 ± 6 |
| Arterial Plasma Glucose (mM) | 0 | 8.2 ± 0.3 | 8.8 ± 0.2 | 8.6 ± 0.4 | 8.1 ± 0.5 |
| | 50 | 9.6 ± 0.4 | 11.7 ± 0.5 | 10.4 ± 1.0 | 10.1 ± 0.8 |
| $pCO_2$ (mmHg) | 0 | 39 ± 1 | 41 ± 1 | 41 ± 1 | 42 ± 1 |
| | 50 | 40 ± 1 | 39 ± 2 | 39 ± 1 | 40 ± 1 |
| $pO_2$ (mmHg) | 0 | 100 ± 2 | 96 ± 3 | 96 ± 4 | 95 ± 4 |
| | 50 | 97 ± 3 | 97 ± 5 | 95 ± 4 | 99 ± 4 |
| Number of Animals | | 6 | 6 | 6 | 6 |

Data are presented as mean ± SEM. Data represent values immediately prior to (0 min) and 50 min after intravenous administration of D-cycloserine or vehicle (controls). * $p>0.05$, ** $p<0.01$ for statistical difference between values in control and drug-treated rats at each time point (ANOVA, followed by Student's unpaired *t*-test with Bonferroni correction).

2.1.2 Glucose Utilisation

The glucose utilisation values associated with the intravenous administration of D-cycloserine (0.3, 3 and 30mg/kg) are presented in Tables 12-15. Glucose utilisation was not significantly altered in any of the 51 CNS regions investigated following any dose of D-cycloserine, relative to values in the corresponding regions of control animals.

Examination of the glucose use values measured after D-cycloserine (0.3, 3 and 30 mg/kg) indicates that the degree of variance in glucose use values within treatment groups is extremely low (see Figures 21 and 22, Tables 12-15). This observation suggests that significant dose-dependent glucose use changes are not being masked by intra-group variability, and supports the evidence of no effect of D-cycloserine (0.3, 3 or 30mg/kg) on local cerebral glucose utilisation in the 51 CNS regions examined. The lack of effect of D-cycloserine on cerebral metabolic rate in limbic (Figure 21) and cerebellar regions (Figure 22) is of particular interest in light of the high concentrations of NMDA receptors present in limbic regions (in particular in hippocampus), the marked effects of the non-competitive NMDA antagonist MK-801 on glucose use in regions such as the posterior cingulate cortex, and the previously reported stimulatory effect of D-cycloserine (3mg/kg) on cGMP activity in the cerebellum.

It should be noted that the statistical design adopted *a priori* involved initial identification of regions in which glucose use was altered by any dose of D-cycloserine by analysis of variance (ANOVA), followed by Student's unpaired *t*-test with Bonferroni correction for multiple treatment groups. However, no significant glucose use alterations were detected by analysis of variance in any of the 51 brain regions examined. Therefore, to gain insight into regions in

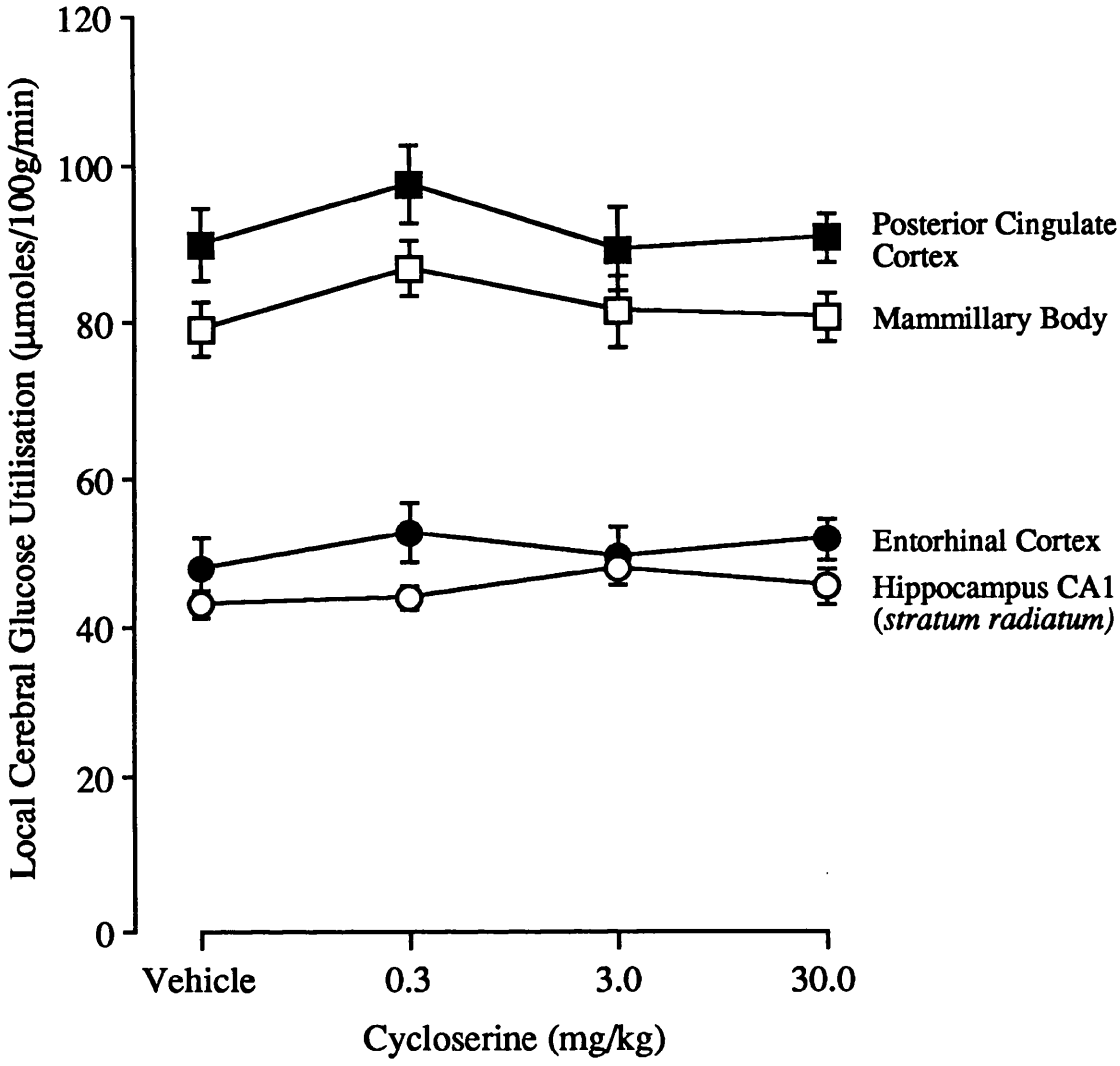


FIGURE 21: D-CYCLOSERINE AND GLUCOSE USE I : LIMBIC REGIONS

Representative dose-response curves illustrating the effects of intravenous administration of D-cycloserine (0.3, 3 or 30 mg/kg) or vehicle on local cerebral glucose utilisation. Data presented as mean ± SEM (µmoles/100g/min).

Note the lack of any significant dose-dependent effects of D-cycloserine on glucose use in these limbic structures, in which NMDA receptor activity is thought to play an important role in functional activity.

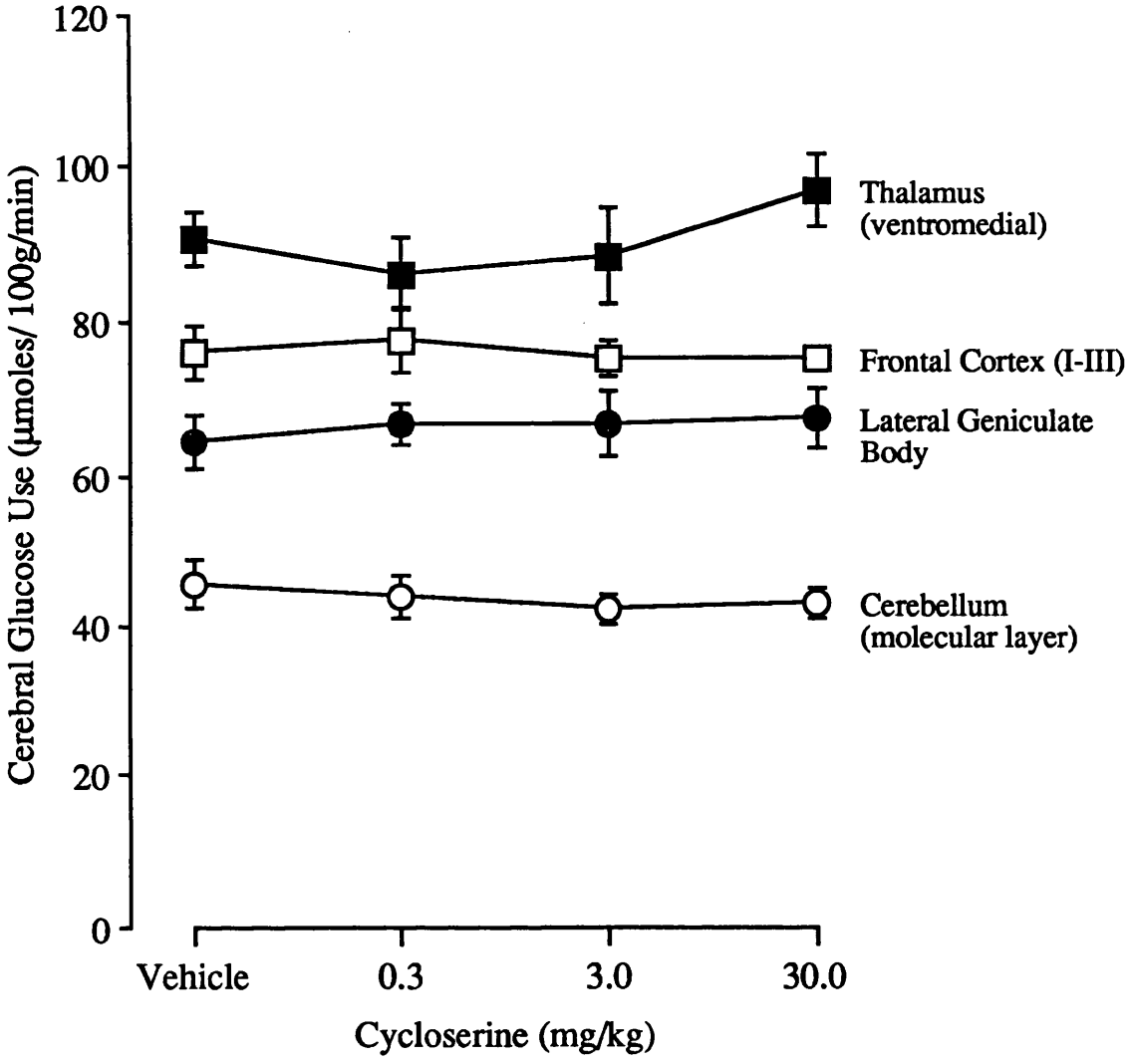


FIGURE 22: D-CYCLOSERINE AND GLUCOSE USE II

Representative dose-response curves illustrating the effects of intravenous administration of D-cycloserine (0.3, 3 or 30 mg/kg) or vehicle on local cerebral glucose utilisation. Data presented as mean ± SEM (µmoles/100g/min).

Note the lack of any significant dose-dependent effects of D-cycloserine on glucose use in the thalamus, frontal cortex and lateral geniculate body - structures in which ligand binding studies have previously identified high densities of NMDA receptor binding sites . In contrast, the cerebellum (molecular layer) contains relatively low levels of NMDA receptor binding sites (Monaghan and Cotman, 1986).

which glucose use showed some sensitivity towards alteration by D-cycloserine, a less conservative statistical approach was employed, involving application of independent *t*-tests (Student's unpaired *t*-test, 2-tailed) between control and treatment groups, with no Bonferroni correction. Using this approach, trends towards reduced glucose utilisation were observed in:- cerebellar white matter following D-cycloserine (0.3mg/kg) (controls = 34 ± 2, D-cycloserine = 28 ± 2 μmol/100g/min); and following D-cycloserine (3mg/kg) in the cochlear nucleus (controls = 106 ± 5, D-cycloserine = 81 ± 8 μmol/100g/min), and superior olivary nucleus (controls = 123 ± 5, D-cycloserine = 104 ± 5 μmol/100g/min).

In contrast, trends towards increased glucose use were observed in:- the lateral habenular nucleus after D-cycloserine (0.3mg/kg) (controls = 87 ± 4, D-cycloserine = 100 ± 4 μmol/100/min); and following D-cycloserine (0.3 and 30mg/kg) in hippocampus CA1 stratum oriens (controls = 46 ± 1, D-cycloserine (0.3mg/kg) = 52 ± 2 μmol/100g/min, D-cycloserine (30mg/kg) = 53 ± 3 μmol/100g/min).

It should be emphasised that these small magnitude glucose use changes do not represent statistically significant alterations in cerebral metabolic rate following systemic administration of D-cycloserine.

## TABLE 12

## GLUCOSE UTILISATION FOLLOWING D-CYCLOSERINE ADMINISTRATION: PRIMARY VISUAL AND AUDITORY REGIONS

| | | D-CYCLOSERINE (mg/kg) | | |
|---|---|---|---|---|
| STRUCTURE | CONTROL | 0.3 | 3.0 | 30 |
| Primary Visual System | | | | |
| Visual Cortex, Layer IV | 69 ± 2 | 77 ± 4 | 71 ± 4 | 72 ± 3 |
| Dorsal Lateral Geniculate Body | 64 ± 4 | 66 ± 3 | 67 ± 4 | 68 ± 4 |
| Thalamus: Lateral Posterior | 81 ± 3 | 74 ± 3 | 80 ± 6 | 84 ± 4 |
| Superior Colliculus: | | | | |
| Superficial Layer | 69 ± 3 | 76 ± 5 | 67 ± 4 | 71 ± 3 |
| Deep Layer | 70 ± 2 | 73 ± 3 | 69 ± 5 | 71 ± 2 |
| Primary Auditory System | | | | |
| Auditory Cortex, Layer IV | 102 ± 8 | 121 ± 7 | 120 ± 6 | 108 ± 5 |
| Medial Geniculate Body | 99 ± 7 | 99 ± 5 | 99 ± 5 | 94 ± 3 |
| Inferior Colliculus | 136 ± 7 | 140 ± 8 | 134 ± 8 | 141 ± 8 |
| Superior Olivary Nucleus | 123 ± 5 | 111 ± 10 | 104 ± 5 | 108 ± 6 |
| Cochlear Nucleus | 107 ± 5 | 88 ± 13 | 81 ± 8 | 88 ± 14 |
| | n = 6 | n = 6 | n = 6 | n = 6 |

Data are presented as mean ± SEM (μmol/100g/min.) There were no significant differences between treatment groups relative to control values (ANOVA, $p>0.05$).

## TABLE 13

## GLUCOSE UTILISATION FOLLOWING D-CYCLOSERINE ADMINISTRATION: CEREBRAL CORTEX

| | | D-CYCLOSERINE (mg/kg) | | |
|---|---|---|---|---|
| STRUCTURE | CONTROL | 0.3 | 3.0 | 30 |
| Sensory Motor Cortex: | | | | |
| Layer I-III | 76 ± 5 | 79 ± 5 | 79 ± 4 | 76 ± 3 |
| Layer IV | 87 ± 4 | 88 ± 6 | 88 ± 5 | 85 ± 3 |
| Layer V-VI | 74 ± 4 | 65 ± 4 | 67 ± 3 | 66 ± 4 |
| Parietal Cortex: | | | | |
| Layer IV | 81 ± 3 | 81 ± 3 | 79 ± 4 | 84 ± 4 |
| Frontal Cortex: | | | | |
| Layer I-III | 76 ± 4 | 78 ± 4 | 75 ± 2 | 75 ± 2 |
| Layer IV | 89 ± 4 | 89 ± 4 | 85 ± 4 | 85 ± 3 |
| Layer V-VI | 70 ± 3 | 64 ± 4 | 67 ± 4 | 67 ± 3 |
| Posterior Cingulate Cortex | 90 ± 5 | 98 ± 5 | 90 ± 5 | 91 ± 3 |
| Anterior Cingulate Cortex | 88 ± 4 | 93 ± 4 | 92 ± 4 | 84 ± 7 |
| Prefrontal Cortex: | | | | |
| Layer IV | 81 ± 3 | 82 ± 7 | 82 ± 3 | 81 ± 3 |
| | n = 6 | n = 6 | n = 6 | n = 6 |

Data are presented as mean ± SEM (μmol/100g/min.) There were no significant differences between treatment groups relative to control values (ANOVA, $p>0.05$).

## TABLE 14

## GLUCOSE UTILISATION FOLLOWING D-CYCLOSERINE ADMINISTRATION: LIMBIC AND OLFACTORY REGIONS

| | | D-CYCLOSERINE (mg/kg) | | |
|---|---|---|---|---|
| STRUCTURE | CONTROL | 0.3 | 3.0 | 30 |
| Hippocampus: | | | | |
| Molecular Layer | 61 ± 3 | 65 ± 3 | 64 ± 5 | 65 ± 3 |
| CA1 Stratum Radiatum | 44 ± 2 | 44 ± 2 | 48 ± 2 | 46 ± 3 |
| CA1 Stratum Oriens | 46 ± 2 | 52 ± 2 | 47 ± 4 | 53 ± 3 |
| CA3 | 45 ± 2 | 46 ± 3 | 45 ± 3 | 50 ± 3 |
| Dentate Gyrus | 48 ± 3 | 50 ± 2 | 48 ± 3 | 51 ± 2 |
| Median Raphe Nucleus | 77 ± 2 | 79 ± 3 | 82 ± 3 | 76 ± 3 |
| Dorsal Raphe Nucleus | 74 ± 3 | 74 ± 3 | 71 ± 3 | 71 ± 3 |
| Lateral Habenular Nucleus | 87 ± 4 | 100 ± 4 | 82 ± 7 | 96 ± 4 |
| Medial Habenular Nucleus | 62 ± 2 | 65 ± 3 | 56 ± 4 | 62 ± 3 |
| Mamillary Body | 79 ± 4 | 87 ± 3 | 82 ± 5 | 81 ± 3 |
| Hypothalamus | 39 ± 1 | 41 ± 3 | 38 ± 3 | 41 ± 2 |
| Olfactory Amygdala | 37 ± 2 | 40 ± 5 | 35 ± 2 | 38 ± 2 |
| Primary Olfactory Cortex | 54 ± 3 | 57 ± 3 | 55 ± 4 | 58 ± 3 |
| Entorhinal Cortex | 48 ± 4 | 52 ± 4 | 49 ± 4 | 52 ± 3 |
| | n = 6 | n = 6 | n = 6 | n = 6 |

Data are presented as mean ± SEM (μmol/100g/min.) There were no significant differences between treatment groups relative to control values (ANOVA, $p<0.05$).

## TABLE 15

## GLUCOSE UTILISATION FOLLOWING D-CYCLOSERINE ADMINISTRATION: EXTRAPYRAMIDAL AND SENSORY-MOTOR AREAS

| | | D-CYCLOSERINE (mg/kg) | | |
|---|---|---|---|---|
| STRUCTURE | CONTROL | 0.3 | 3.0 | 30 |
| Striatum: | | | | |
| Dorsolateral | 82 ± 5 | 88 ± 5 | 87 ± 6 | 87 ± 5 |
| Ventromedial | 81 ± 4 | 81 ± 5 | 77 ± 5 | 83 ± 5 |
| Globus Pallidus | 43 ± 1 | 45 ± 3 | 43 ± 3 | 45 ± 2 |
| Nucleus Accumbens | 65 ± 2 | 71 ± 4 | 60 ± 4 | 72 ± 5 |
| Substantia Nigra: | | | | |
| Pars Compacta | 55 ± 3 | 60 ± 3 | 54 ± 2 | 57 ± 2 |
| Pars Reticulata | 37 ± 2 | 43 ± 2 | 42 ± 1 | 40 ± 2 |
| Thalamus: | | | | |
| Mediodorsal | 87 ± 2 | 86 ± 3 | 87 ± 6 | 91 ± 3 |
| Ventrolateral | 63 ± 1 | 62 ± 2 | 60 ± 4 | 65 ± 3 |
| Ventromedial | 91 ± 4 | 86 ± 5 | 88 ± 6 | 98 ± 5 |
| Anteriodorsal | 87 ± 6 | 80 ± 3 | 87 ± 4 | 84 ± 4 |
| Anteriomedial | 92 ± 5 | 87 ± 7 | 87 ± 5 | 88 ± 3 |
| Subthalamic Nucleus | 62 ± 4 | 64 ± 3 | 64 ± 3 | 67 ± 3 |
| Inferior Olivary Nucleus | 63 ± 4 | 67 ± 6 | 59 ± 3 | 65 ± 4 |
| Cerebellar Nucleus | 98 ± 6 | 102 ± 6 | 94 ± 3 | 94 ± 5 |
| Cerebellar Hemisphere: | | | | |
| Granular Layer | 51 ± 2 | 55 ± 4 | 48 ± 2 | 50 ± 2 |
| Molecular Layer | 46 ± 3 | 44 ± 3 | 42 ± 2 | 43 ± 2 |
| Cerebellar White Matter | 34 ± 2 | 28 ± 2 | 31 ± 2 | 30 ± 2 |
| | n = 6 | n = 6 | n = 6 | n = 6 |

Data are presented as mean ± SEM (µmol/100g/min.) There were no significant differences between treatment groups relative to control values (ANOVA, $p<0.05$).

## 2.2 [$^{125}$I]-MK-801 *In Vivo* Autoradiography

### 2.2.1 General Observations

The physiological variables in the conscious and anaesthetised (ventilated) rats, measured immediately prior to intravenous administration of D-cycloserine (3mg/kg) or vehicle, are presented in Table 16. The measured respiratory parameters ($pO_2$ and $pCO_2$), temperature, and mean arterial blood pressure were deemed to be within acceptable limits at the commencement of experiments, indicating that rats were not adversely stressed. Within each of the three treatment groups, mean arterial blood pressure did not significantly alter over the 120 min experimental period.

### 2.2.2 [$^{125}$I]-MK-801 Binding

Total bound [$^{125}$I]-MK-801 was measured in 13 CNS regions from coronal rat brain sections washed for 0, 15, 30 or 60 min to remove unbound ligand. Data are presented in Tables 17-20. Within each of the treatment groups (anaesthetised vehicle, conscious vehicle (controls), and conscious D-cycloserine), there were no significant differences between levels of [$^{125}$I]-MK-801 bound in any of the 13 brain regions examined. Hence, D-cycloserine (3mg/kg) had no apparent significant effect on the extent of [$^{125}$I]-MK-801 binding to the NMDA receptor-associated channel, *in vivo*.

Washing the brain sections revealed regional heterogeneity in the densities of [$^{125}$I]-MK-801 binding sites, with highest levels present in the hippocampus CA1 (in conscious controls after a 60 min wash, [$^{125}$I]-MK-801 bound = 1.74 ± 0.38 pmol/g tissue). Relatively high levels of binding were found in hippocampus, CA3, dentate gyrus, thalamus (ventrolateral), cortex

(sensory motor, auditory and cingulate) and the medial geniculate body. Lowest levels of binding were seen in the hypothalamus and cerebellar hemisphere (in conscious controls after a 60 min wash, [$^{125}$I]-MK-801 bound = 0.49 ± 0.15 pmol/g tissue). The effects of washing on [$^{125}$I]-MK-801 binding are illustrated in the autoradiograms in Figure 23. By washing the brain sections it is evident that a much higher proportion of the [$^{125}$I]-MK-801 measured in unwashed sections represents total bound [$^{125}$I]-MK-801 in hippocampus CA1 than in cerebellar hemisphere:- conscious control rats, CA1: unwashed = 3.34 ± 0.90, 60 min wash = 1.74 ± 0.38 pmol/g tissue; cerebellar hemisphere; unwashed = 1.73 ± 0.51, 60 min wash = 0.49 ± 0.15 pmol/g tissue.

Since the cerebellar hemisphere contains few NMDA receptors, comparison of levels of [$^{125}$I]-MK-801 binding in brain regions relative to levels in the cerebellar hemisphere, gives a clearer indication of the heterogeneous distribution of [$^{125}$I]-MK-801 binding sites *in vivo*. The calculated ratios of [$^{125}$I]-MK-801 bound in each structure relative to cerebellar levels, are presented in Tables 21-24. Figures 24-26 illustrate the effect of washing on the [$^{125}$I]-MK-801 binding ratios in four representative structures. These figure underline the high concentration of [$^{125}$I]-MK-801 binding sites in hippocampus CA1 region, which indicates a high level of NMDA receptor activation in this region relative to other brain regions. D-Cycloserine (3mg/kg) had no significant effect on the [$^{125}$I]-MK-801 binding ratios, relative to cerebellar levels, in any of the brain structures examined.

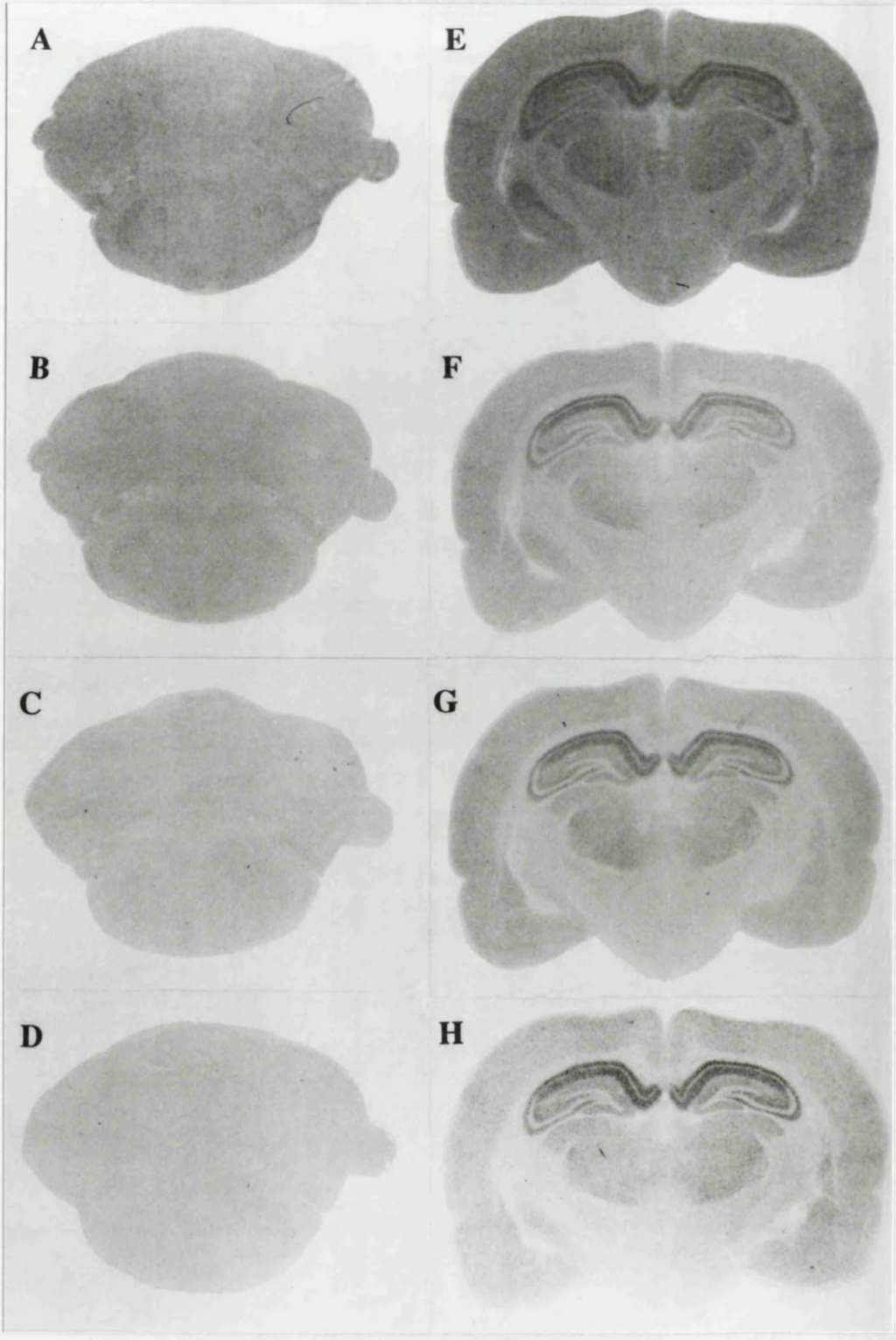


FIGURE 23: [$^{125}$I]-MK-801 BINDING *IN VIVO*

Representative autoradiograms illustrating [$^{125}$I]-MK-801 in rat brain, at the level of the cerebellum (A, B, C and D), and hippocampus (E, F, G and H), in serial sections washed for 0 (A, E), 15 (B, F), 30 (C, G) and 60 min (D, H). Note the gradual reduction in optical density of the cerebellar sections with increased duration of wash, reflecting elution of the radioligand (A - D). The level of [$^{125}$I] -MK-801 also declines with washing in cortex, thalamus and hypothalamus, but is relatively conserved in hippocampus CA1 region (E-H).

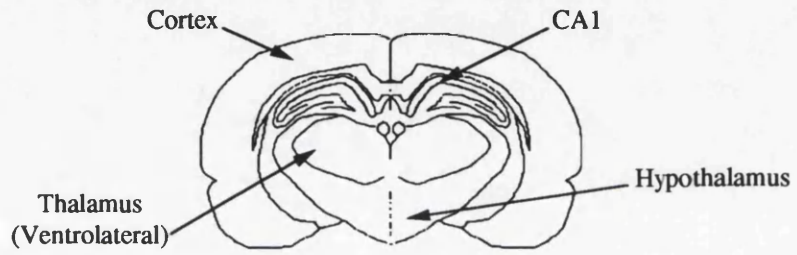

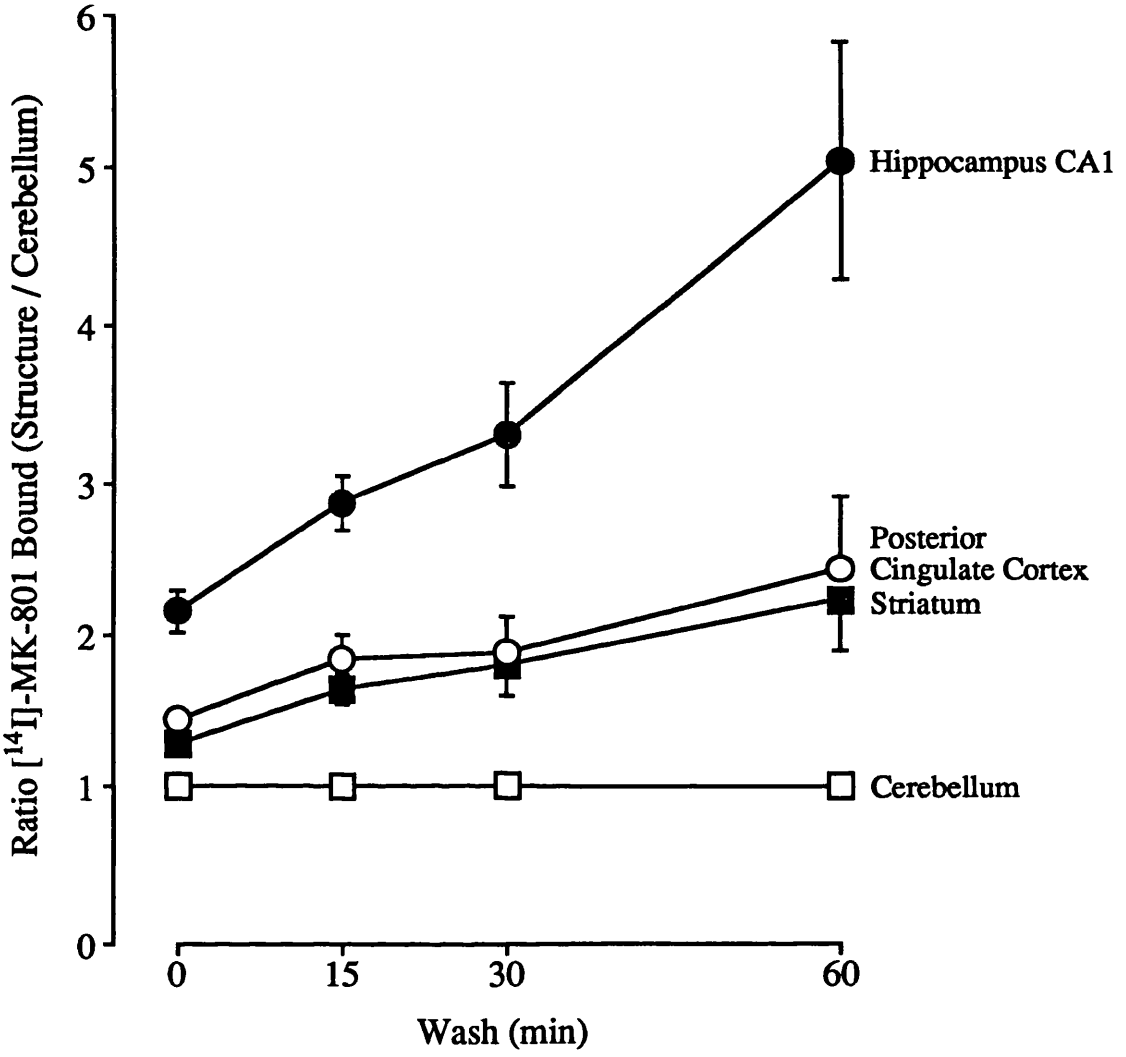


FIGURE 24: EFFECTS OF WASHOUT ON [$^{125}$I]-MK-801 BINDING RATIOS: ANAESTHETISED CONTROLS

Data represent ratios of the concentrations of [$^{125}$I]-MK-801 detected in hippocampus CA1, posterior cingulate cortex and striatum relative to levels in the cerebellar hemisphere, following intravenous administration of vehicle to conscious rats. Tissue sections were washed for 0, 15, 30 or 60 min. Data presented as mean ± SEM.

The marked increase in the ratio of [$^{125}$I]-MK-801 in hippocampus CA1 region with increased duration of wash, reflects the greater density of MK-801 binding sites in CA1 relative to the cerebellum. In contrast, [$^{125}$I]-MK-801 ratios for striatum and posterior cingulate cortex indicate that these regions contain moderate levels of MK-801 binding sites compared to levels in CA1, but approximately 2-fold greater binding site densities than in the cerebellum.

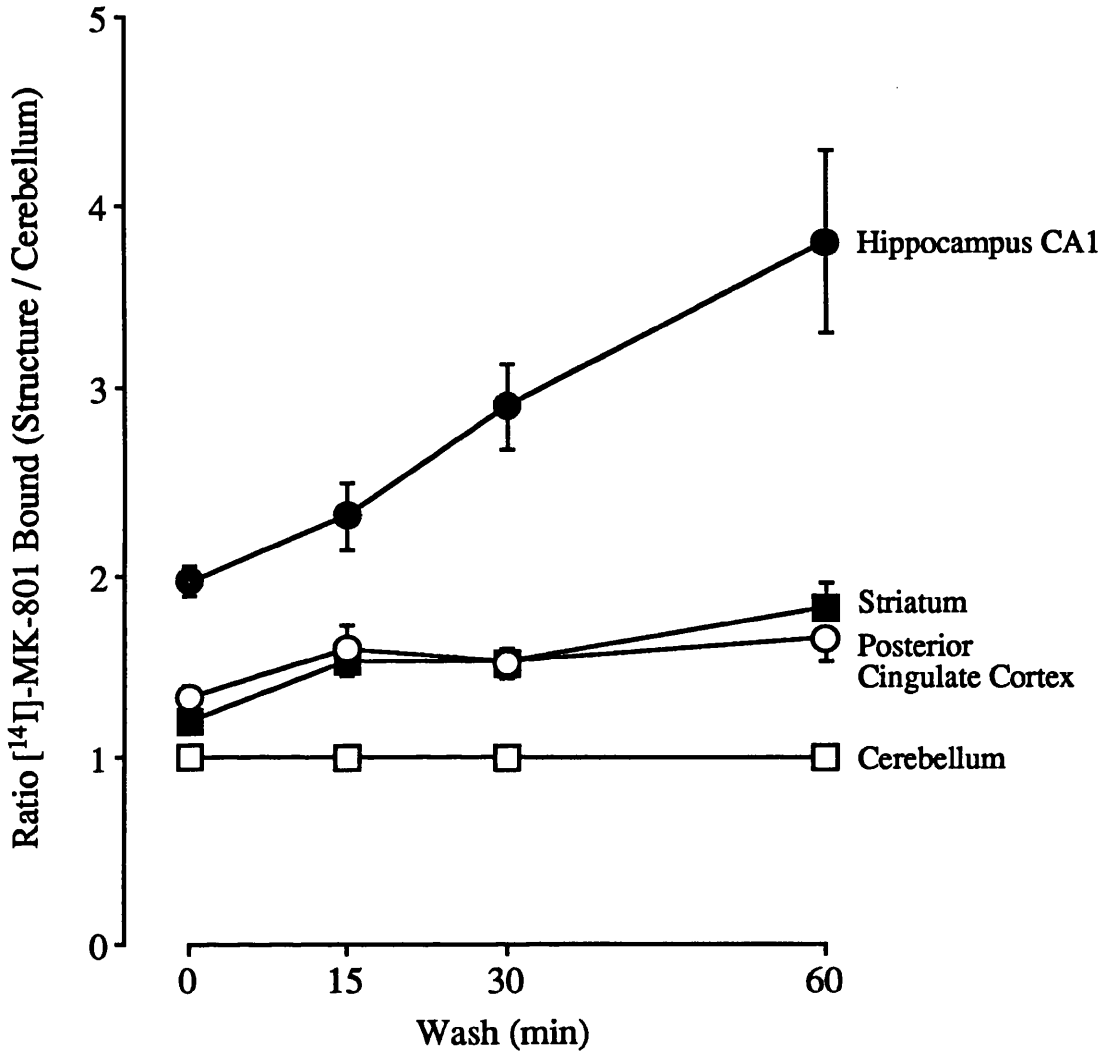


FIGURE 25: EFFECTS OF WASHOUT ON [$^{125}$I]-MK-801 BINDING RATIOS: CONSCIOUS CONTROLS

Data represent ratios of the concentrations of [$^{125}$I]-MK-801 detected in hippocampus CA1, posterior cingulate cortex and striatum relative to levels in the cerebellar hemisphere, following intravenous administration of vehicle to conscious rats. Tissue sections were washed for 0, 15, 30 or 60 min. Data presented as mean ± SEM.

There were no significant differences between the calculated [$^{125}$I]-MK-801 binding ratios in conscious and anaesthetised control animals, for any of the CNS regions examined.

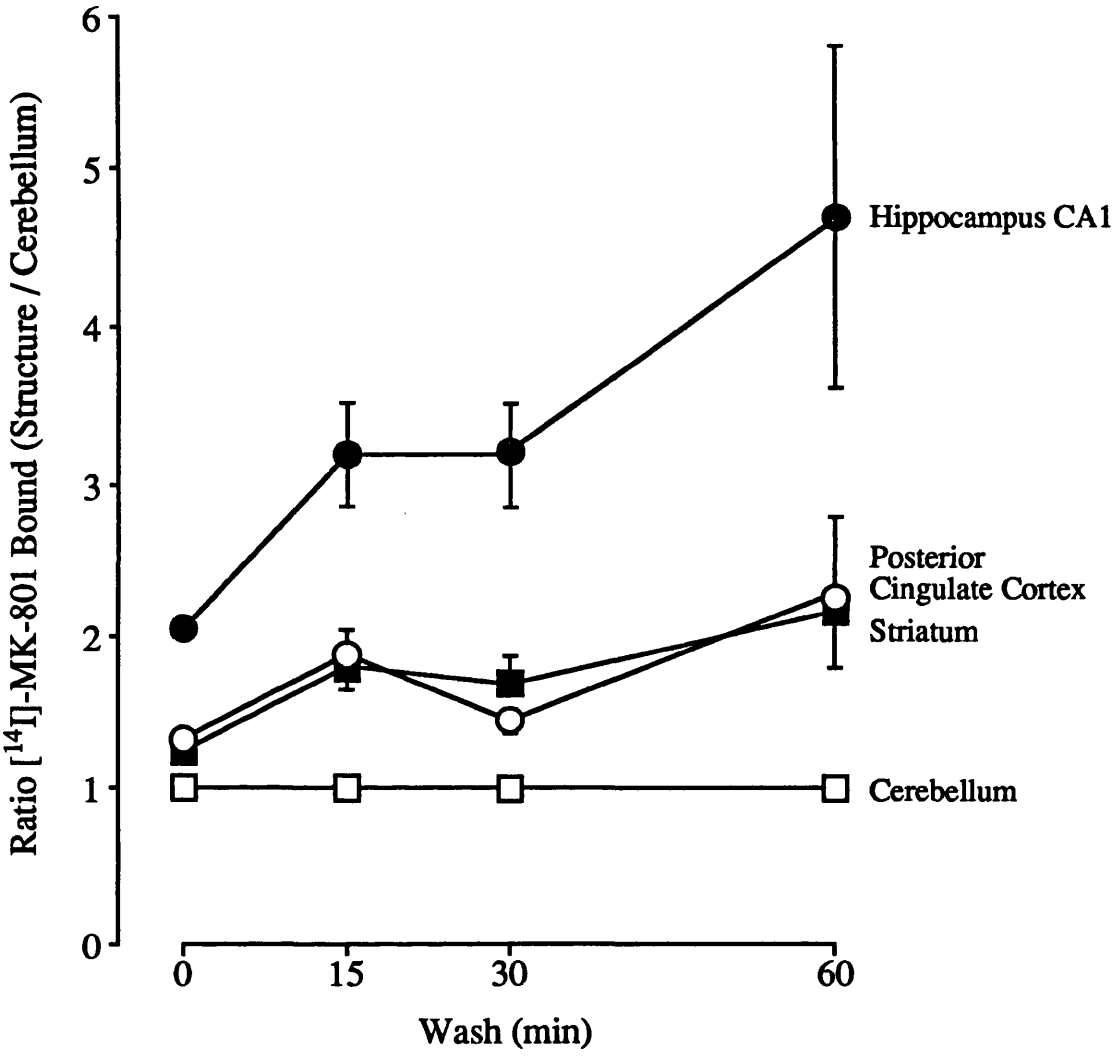


FIGURE 26: EFFECTS OF WASHOUT ON [$^{125}$I]-MK-801 BINDING RATIOS: D-CYCLOSERINE IN CONSCIOUS RATS

Data represent ratios of the concentrations of [$^{125}$I]-MK-801 detected in hippocampus CA1, posterior cingulate cortex and striatum relative to levels in the cerebellar hemisphere, following intravenous administration of D-cycloserine (3 mg/kg) to conscious rats. Tissue sections were washed for 0, 15, 30 or 60 min. Data are presented as mean ± SEM.

D-Cycloserine had no effect on [$^{125}$I]-MK-801 binding ratios, relative to ratios in conscious or anaesthetised control animals, in any of the regions examined.

## TABLE 16

## PHYSIOLOGICAL VARIABLES FOLLOWING INTRAVENOUS ADMINISTRATION OF D-CYCLOSERINE OR VEHICLE TO CONSCIOUS OR ANAESTHETISED RATS

| | TIME AFTER DRUG (min) | ANAESTHETISED VEHICLE | CONSCIOUS VEHICLE | CONSCIOUS D-CYCLOSERINE (3mg/kg) |
|---|---|---|---|---|
| Rectal Temperature (°C) | 0 | 37.1 ± 0.2 | 36.9 ± 0.1 | 37.2 ± 0.2 |
| Mean Arterial Blood Pressure (mmHg) | 0 | 69 ± 1 | 140 ± 7 | 137 ± 3 |
| | 120 | 74 ± 3 | 140 ± 6 | 138 ± 7 |
| $pCO_2$ (mmHg) | 0 | 35.9 ± 1.8 | 40.2 ± 1.7 | 39.9 ± 0.6 |
| $pO_2$ (mmHg) | 0 | 144.2 ± 12.1 | 100.1 ± 5.7 | 85.4 ± 3.0 |
| Number of Animals | | 6 | 5 | 5 |

Data are presented as mean ± SEM. Data represent values immediately prior to (0 min) intravenous administration of D-cycloserine (3mg/kg) or vehicle (saline). Mean blood pressure was measured immeditely prior to (0 min) and 120 min after drug or vehicle administration. There were no apparent significant differences between blood pressure values within treatment groups at 0 and 120 min (ANOVA, $p>0.05$).

## TABLE 17

## [$^{125}$I]-MK-801 BINDING IN RAT BRAIN SECTIONS: UNWASHED

| STRUCTURE | [125I]-MK-801 BOUND (pmol/g) | | |
|---|---|---|---|
| | ANAESTHETISED VEHICLE (n=6) | CONSCIOUS VEHICLE (n=6) | CONSCIOUS D-CYCLOSERINE (n=5) |
| Medial Geniculate Body | 1.72 ± 0.70 | 2.43 ± 0.72 | 1.50 ± 0.72 |
| Auditory Cortex Layer IV | 1.78 ± 0.71 | 2.28 ± 0.66 | 1.63 ± 0.79 |
| Hippocampus: CA1 | 2.71 ± 1.07 | 3.34 ± 0.90 | 2.36 ± 1.16 |
| CA3 | 2.54 ± 0.98 | 3.18 ± 0.92 | 2.17 ± 1.09 |
| Dentate Gyrus | 1.83 ± 0.73 | 2.33 ± 0.65 | 1.62 ± 0.79 |
| Hypothalamus | 1.42 ± 0.58 | 1.95 ± 0.54 | 1.25 ± 0.60 |
| Thalamus: Ventrolateral | 1.77 ± 0.75 | 2.51 ± 0.72 | 1.74 ± 0.78 |
| Posterior Cingulate Cortex | 1.81 ± 0.71 | 2.30 ± 0.64 | 1.58 ± 0.76 |
| Sensory Motor Cortex : Superficial Layers | 1.72 ± 0.67 | 2.11 ± 0.59 | 1.51 ± 0.73 |
| Deep Layers | 1.70 ± 0.67 | 2.17 ± 0.61 | 1.51 ± 0.73 |
| Lateral Septum | 2.22 ± 0.91 | 2.75 ± 0.73 | 1.86 ± 0.90 |
| Striatum | 1.62 ± 0.64 | 2.08 ± 0.61 | 1.54 ± 0.73 |
| Cerebellar Hemisphere | 1.28 ± 0.49 | 1.73 ± 0.51 | 1.17 ± 0.58 |

Data are presented as mean ± SEM. Data represent total bound [$^{125}$I]-MK-801 (pmol/g tissue) measured in unwashed sections following intravenous administration of D-cycloserine (3mg/kg) to conscious rats, or vehicle (saline) to conscious and anaesthetised rats. There were no significant differences between treatment groups in any of the regions examined (ANOVA, followed by Student's *t*-test with Bonferroni correction).

## TABLE 18

## [$^{125}$I]-MK-801 BINDING: 15 MINUTE WASH

| STRUCTURE | [125I]-MK-801 BOUND (pmol/g) | | |
|---|---|---|---|
| | ANAESTHETISED VEHICLE (n=6) | CONSCIOUS VEHICLE (n=6) | CONSCIOUS D-CYCLOSERINE (n=5) |
| Medial Geniculate Body | 1.65 ± 0.70 | 1.33 ± 0.33 | 0.78 ± 0.46 |
| Auditory Cortex Layer IV | 1.73 ± 0.70 | 1.15 ± 0.25 | 0.78 ± 0.46 |
| Hippocampus: CA1 | 2.82 ± 1.10 | 1.74 ± 0.35 | 1.45 ± 0.81 |
| CA3 | 2.17 ± 0.86 | 1.50 ± 0.32 | 1.11 ± 0.63 |
| Dentate Gyrus | 2.03 ± 0.81 | 1.30 ± 0.25 | 0.98 ± 0.55 |
| Hypothalamus | 1.11 ± 0.45 | 0.77 ± 0.14 | 0.55 ± 0.31 |
| Thalamus: Ventrolateral | 1.70 ± 0.73 | 1.33 ± 0.28 | 0.95 ± 0.43 |
| Posterior Cingulate Cortex | 1.83 ± 0.75 | 1.27 ± 0.32 | 0.86 ± 0.50 |
| Sensory Motor Cortex : Superficial Layers | 1.67 ± 0.68 | 1.16 ± 0.25 | 0.80 ± 0.45 |
| Deep Layers | 1.61 ± 0.68 | 1.16 ± 0.27 | 0.78 ± 0.43 |
| Lateral Septum | 1.63 ± 0.71 | 1.23 ± 0.33 | 0.79 ± 0.44 |
| Striatum | 1.63 ± 0.68 | 1.19 ± 0.27 | 0.83 ± 0.46 |
| Cerebellar Hemisphere | 0.96 ± 0.43 | 0.83 ± 0.24 | 0.40 ± 0.27 |

Data are presented as mean ± SEM. Data represent total bound [$^{125}$I]-MK-801 (pmol/g tissue) measured in sections washed for 15 min following intravenous administration of D-cycloserine (3mg/kg) to conscious rats, or vehicle (saline) to conscious and anaesthetised rats. There were no significant differences between treatment groups in any of the regions examined (ANOVA, followed by Student's *t*-test with Bonferroni correction).

## TABLE 19

## [$^{125}$I]-MK-801 BINDING: 30 MINUTE WASH

| STRUCTURE | [125I]-MK-801 BOUND (pmol/g) | | |
|---|---|---|---|
| | ANAESTHETISED VEHICLE (n=6) | CONSCIOUS VEHICLE (n=6) | CONSCIOUS D-CYCLOSERINE (n=5) |
| Medial Geniculate Body | 1.72 ± 0.70 | 1.34 ± 0.33 | 0.82 ± 0.49 |
| Auditory Cortex Layer IV | 1.91 ± 0.71 | 1.09 ± 0.23 | 0.84 ± 0.52 |
| Hippocampus: CA1 | 3.31 ± 1.19 | 1.97 ± 0.45 | 1.58 ± 1.01 |
| CA3 | 2.30 ± 0.85 | 1.45 ± 0.33 | 1.12 ± 0.69 |
| Dentate Gyrus | 2.21 ± 0.82 | 1.32 ± 0.29 | 1.09 ± 0.67 |
| Hypothalamus | 0.98 ± 0.40 | 0.68 ± 0.15 | 0.57 ± 0.30 |
| Thalamus: Ventrolateral | 1.80 ± 0.76 | 1.28 ± 0.29 | 0.99 ± 0.44 |
| Posterior Cingulate Cortex | 1.79 ± 0.76 | 1.10 ± 0.28 | 0.74 ± 0.41 |
| Sensory Motor Cortex : Superficial Layers | 1.66 ± 0.67 | 1.00 ± 0.22 | 0.81 ± 0.45 |
| Deep Layers | 1.66 ± 0.68 | 0.97 ± 0.24 | 0.77 ± 0.43 |
| Lateral Septum | 1.67 ± 0.77 | 1.06 ± 0.29 | 0.74 ± 0.36 |
| Striatum | 1.71 ± 0.71 | 1.05 ± 0.66 | 0.84 ± 0.46 |
| Cerebellar Hemisphere | 0.93 ± 0.38 | 0.68 ± 0.16 | 0.37 ± 0.20 |

Data are presented as mean ± SEM. Data represent total bound [$^{125}$I]-MK-801 (pmol/g tissue) measured in sections washed for 30 min, following intravenous administration of D-cycloserine (3mg/kg) to conscious rats, or vehicle (saline) to conscious and anaesthetised rats. There were no significant differences between treatment groups in any of the regions examined (ANOVA, followed by Student's *t*-test with Bonferroni correction).

## TABLE 20

## [$^{125}$I]-MK-801 BINDING: 60 MINUTE WASH

| STRUCTURE | [125I]-MK-801 BOUND (pmol/g) | | |
|---|---|---|---|
| | ANAESTHETISED VEHICLE (n=6) | CONSCIOUS VEHICLE (n=6) | CONSCIOUS D-CYCLOSERINE (n=5) |
| Medial Geniculate Body | 1.40 ± 0.58 | 1.14 ± 0.29 | 0.77 ± 0.44 |
| Auditory Cortex Layer IV | 1.47 ± 0.57 | 0.94 ± 0.21 | 0.77 ± 0.44 |
| Hippocampus: CA1 | 3.00 ± 1.10 | 1.74 ± 0.38 | 1.41 ± 0.87 |
| CA3 | 2.07 ± 0.75 | 1.19 ± 0.25 | 0.99 ± 0.61 |
| Dentate Gyrus | 2.05 ± 0.80 | 1.18 ± 0.26 | 0.96 ± 0.55 |
| Hypothalamus | 0.74 ± 0.32 | 0.56 ± 0.13 | 0.41 ± 0.21 |
| Thalamus: Ventrolateral | 1.52 ± 0.65 | 1.08 ± 0.28 | 0.83 ± 0.37 |
| Posterior Cingulate Cortex | 1.39 ± 0.56 | 0.81 ± 0.21 | 0.71 ± 0.39 |
| Sensory Motor Cortex : Superficial Layers | 1.32 ± 0.52 | 0.80 ± 0.16 | 0.69 ± 0.37 |
| Deep Layers | 1.23 ± 0.49 | 0.78 ± 0.17 | 0.66 ± 0.36 |
| Lateral Septum | 1.18 ± 0.59 | 0.81 ± 0.20 | 0.66 ± 0.25 |
| Striatum | 1.23 ± 0.53 | 0.87 ± 0.27 | 0.68 ± 0.34 |
| Cerebellar Hemisphere | 0.56 ± 0.25 | 0.49 ± 0.15 | 0.37 ± 0.20 |

Data are presented as mean ± SEM. Data represent total bound [$^{125}$I]-MK-801 (pmol/g tissue) measured in sections washed for 60 min, following intravenous administration of D-cycloserine (3mg/kg) to conscious rats, or vehicle (saline) to conscious and anaesthetised rats. There were no significant differences between treatment groups in any of the regions examined (ANOVA, followed by Student's *t*-test with Bonferroni correction).

## TABLE 21

## [$^{125}$I]-MK-801 BINDING RELATIVE TO CEREBELLAR LEVELS: UNWASHED SECTIONS

| STRUCTURE | [125I]-MK-801 RATIO | | |
|---|---|---|---|
| | ANAESTHETISED VEHICLE (n=6) | CONSCIOUS VEHICLE (n=6) | CONSCIOUS D-CYCLOSERINE (n=5) |
| Medial Geniculate Body | 1.36 ± 0.07 | 1.38 ± 0.06 | 1.26 ± 0.06 |
| Auditory Cortex Layer IV | 1.47 ± 0.09 | 1.32 ± 0.06 | 1.36 ± 0.05 |
| Hippocampus: CA1 | 2.14 ± 0.14 | 1.98 ± 0.09 | 2.03 ± 0.06 |
| CA3 | 2.00 ± 0.16 | 1.86 ± 0.09 | 1.84 ± 0.03 |
| Dentate Gyrus | 1.44 ± 0.08 | 1.37 ± 0.05 | 1.37 ± 0.04 |
| Hypothalamus | 1.14 ± 0.06 | 1.14 ± 0.04 | 1.08 ± 0.04 |
| Thalamus: Ventrolateral | 1.48 ± 0.10 | 1.45 ± 0.05 | 1.46 ± 0.05 |
| Posterior Cingulate Cortex | 1.44 ± 0.06 | 1.35 ± 0.06 | 1.33 ± 0.06 |
| Sensory Motor Cortex : Superficial Layers | 1.37 ± 0.06 | 1.24 ± 0.03 | 1.26 ± 0.05 |
| Deep Layers | 1.35 ± 0.07 | 1.26 ± 0.04 | 1.28 ± 0.05 |
| Lateral Septum | 1.78 ± 0.17 | 1.64 ± 0.10 | 1.60 ± 0.07 |
| Striatum | 1.29 ± 0.06 | 1.20 ± 0.04 | 1.26 ± 0.06 |
| Cerebellar Hemisphere | 1.00 ± 0.00 | 1.00 ± 0.00 | 1.00 ± 0.00 |

Data are presented as mean ± SEM ratio. Data represent ratio ([$^{125}$I]-MK-801 bound in structure/[$^{125}$I]-MK-801 bound in cerebellar hemisphere) measured in unwashed sections following intravenous administration of D-cycloserine (3mg/kg) to conscious rats, or vehicle (saline) to conscious and anaesthetised rats. There were no apparent signficant differences between treatment groups in any of the regions examined ($p>0.05$, ANOVA).

## TABLE 22

## [$^{125}$I]-MK-801 BINDING RELATIVE TO CEREBELLAR LEVELS: 15 MINUTE WASH

| STRUCTURE | [125I]-MK-801 RATIO | | |
|---|---|---|---|
| | ANAESTHETISED VEHICLE (n=6) | CONSCIOUS VEHICLE (n=6) | CONSCIOUS D-CYCLOSERINE (n=5) |
| Medial Geniculate Body | 1.67 ± 0.15 | 1.59 ± 0.09 | 1.74 ± 0.15 |
| Auditory Cortex Layer IV | 1.81 ± 0.06 | 1.50 ± 0.10 | 1.74 ± 0.22 |
| Hippocampus: CA1 | 2.85 ± 0.18 | 2.31 ± 0.19 | 3.19 ± 0.33 |
| CA3 | 2.24 ± 0.08 | 1.96 ± 0.15 | 2.42 ± 0.18 |
| Dentate Gyrus | 2.06 ± 0.14 | 1.75 ± 0.14 | 2.13 ± 0.15 |
| Hypothalamus | 1.18 ± 0.04 | 1.04 ± 0.08 | 1.19 ± 0.08 |
| Thalamus: Ventrolateral | 1.87 ± 0.08 | 1.65 ± 0.12 | 2.08 ± 0.10 |
| Posterior Cingulate Cortex | 1.85 ± 0.16 | 1.59 ± 0.12 | 1.89 ± 0.17 |
| Sensory Motor Cortex : Superficial Layers | 1.70 ± 0.10 | 1.50 ± 0.12 | 1.76 ± 0.12 |
| Deep Layers | 1.66 ± 0.09 | 1.47 ± 0.09 | 1.71 ± 0.11 |
| Lateral Septum | 1.70 ± 0.08 | 1.52 ± 0.06 | 1.73 ± 0.15 |
| Striatum | 1.66 ± 0.10 | 1.53 ± 0.08 | 1.82 ± 0.14 |
| Cerebellar Hemisphere | 1.00 ± 0.00 | 1.00 ± 0.00 | 1.00 ± 0.00 |

Data are presented as mean ± SEM ratio. Data represent ratio ([$^{125}$I]-MK-801 bound in structure/[$^{125}$I]-MK-801 bound in cerebellar hemisphere) measured in sections washed in buffer for 15 min, following intravenous administration of D-cycloserine (3mg/kg) to conscious rats, or vehicle (saline) to conscious or anaesthetised rats. There were no apparent signficant differences between treatment groups in any of the regions examined ($p>0.05$, ANOVA).

## TABLE 23

## [$^{125}$I]-MK-801 BINDING RELATIVE TO CEREBELLAR LEVELS: 30 MINUTE WASH

| STRUCTURE | [125I]-MK-801 RATIO | | |
|---|---|---|---|
| | ANAESTHETISED VEHICLE (n=6) | CONSCIOUS VEHICLE (n=6) | CONSCIOUS D-CYCLOSERINE (n=5) |
| Medial Geniculate Body | 1.74 ± 0.16 | 1.96 ± 0.16 | 1.67 ± 0.16 |
| Auditory Cortex Layer IV | 2.04 ± 0.11 | 1.69 ± 0.18 | 1.72 ± 0.20 |
| Hippocampus: CA1 | 3.31 ± 0.33 | 2.92 ± 0.23 | 3.17 ± 0.33 |
| CA3 | 2.36 ± 0.16 | 2.14 ± 0.18 | 2.25 ± 0.23 |
| Dentate Gyrus | 2.28 ± 0.13 | 1.99 ± 0.15 | 2.18 ± 0.20 |
| Hypothalamus | 1.08 ± 0.07 | 1.04 ± 0.05 | 1.12 ± 0.05 |
| Thalamus: Ventrolateral | 1.90 ± 0.18 | 1.91 ± 0.13 | 1.99 ± 0.17 |
| Posterior Cingulate Cortex | 1.88 ± 0.23 | 1.55 ± 0.08 | 1.45 ± 0.10 |
| Sensory Motor Cortex : Superficial Layers | 1.73 ± 0.19 | 1.52 ± 0.11 | 1.66 ± 0.17 |
| Deep Layers | 1.73 ± 0.17 | 1.46 ± 0.06 | 1.58 ± 0.18 |
| Lateral Septum | 1.99 ± 0.21 | 1.52 ± 0.08 | 1.51 ± 0.20 |
| Striatum | 1.80 ± 0.19 | 1.53 ± 0.05 | 1.70 ± 0.18 |
| Cerebellar Hemisphere | 1.00 ± 0.00 | 1.00 ± 0.00 | 1.00 ± 0.00 |

Data are presented as mean ± SEM ratio. Data represent ratio ([$^{125}$I]-MK-801 bound in structure/[$^{125}$I]-MK-801 bound in cerebellar hemisphere) measured in sections washed in buffer for 30 min, following intravenous administration of D-cycloserine (3mg/kg) to conscious rats, or vehicle (saline) to conscious or anaesthetised rats. There were no apparent signficant differences between treatment groups in any of the regions examined ($p>0.05$, ANOVA).

## TABLE 24

## [$^{125}$I]-MK-801 BINDING RELATIVE TO CEREBELLAR LEVELS: 60 MINUTE WASH

| STRUCTURE | [125I]-MK-801 RATIO | | |
|---|---|---|---|
| | ANAESTHETISED VEHICLE (n=6) | CONSCIOUS VEHICLE (n=6) | CONSCIOUS D-CYCLOSERINE (3mg/kg)(n=5) |
| Medial Geniculate Body | 2.44 ± 0.35 | 2.37 ± 0.31 | 2.46 ± 0.44 |
| Auditory Cortex Layer IV | 2.63 ± 0.30 | 2.03 ± 0.24 | 2.51 ± 0.49 |
| Hippocampus: CA1 | 5.08 ± 0.76 | 3.79 ± 0.50 | 4.69 ± 1.10 |
| CA3 | 3.52 ± 0.56 | 2.60 ± 0.35 | 3.30 ± 0.90 |
| Dentate Gyrus | 3.59 ± 0.55 | 2.58 ± 0.29 | 3.14 ± 0.77 |
| Hypothalamus | 1.38 ± 0.15 | 1.22 ± 0.14 | 1.31 ± 0.32 |
| Thalamus: Ventrolateral | 2.80 ± 0.43 | 2.26 ± 0.36 | 2.77 ± 0.69 |
| Posterior Cingulate Cortex | 2.45 ± 0.47 | 1.67 ± 0.14 | 2.28 ± 0.50 |
| Sensory Motor Cortex : Superficial Layers | 2.38 ± 0.30 | 1.77 ± 0.23 | 2.26 ± 0.48 |
| Deep Layers | 2.26 ± 0.25 | 1.67 ± 0.21 | 2.12 ± 0.43 |
| Lateral Septum | 2.70 ± 0.68 | 1.69 ± 0.15 | 2.06 ± 0.44 |
| Striatum | 2.25 ± 0.34 | 1.27 ± 0.16 | 2.16 ± 0.35 |
| Cerebellar Hemisphere | 1.00 ± 0.00 | 1.00 ± 0.00 | 1.00 ± 0.00 |

Data are presented as mean ± SEM ratio. Data represent ratio ([$^{125}$I]-MK-801 bound in structure/[$^{125}$I]-MK-801 bound in cerebellar hemisphere) measured in sections washed in buffer for 60 min, following intravenous administration of D-cycloserine (3mg/kg) to conscious rats, or vehicle (saline) to conscious or anaesthetised rats. There were no apparent signficant differences between treatment groups in any of the regions examined ($p>0.05$, ANOVA).

## 2.3 Focal Cerebral Ischaemia - MCA Occlusion

Following permanent MCA occlusion, ischaemic damage was observed within the territory of the occluded MCA in the ipsilateral dorsolateral cortex and neostriatum, as illustrated in Figure 8 (Methods). These areas showed the morphological characteristics of infarction (vacuolisation of the cytoplasm, swelling of the neuropil, and nuclear pyknosis). The histopathological appearance of the ischaemic brain tissue in rats treated with D-cycloserine was similar to that in vehicle-treated animals.

The effects of D-cycloserine on infarct volume and hemisphere volume 24h after permanent MCA occlusion are presented in Table 25. The volumes of ischaemic damage in both vehicle- and D-cycloserine-treated rats were calculated from densitometric measurement of the area of infarct at predetermined coronal levels throughout the brain, and knowledge of the distance between coronal levels. Hemisphere volumes ipsilateral and contralateral to MCA occlusion were similarly calculated. Areas of infarct and hemispheric areas at each of the coronal brain levels examined are illustrated in Figure 27. Intravenous administration of D-cycloserine (3mg/kg) 15 min and 255 min after MCA occlusion did not significantly alter the volume of ischaemic damage in the cerebral hemisphere (volumes of ischaemic tissue in vehicle- and D-cycloserine-treated rats were 191 ± 30$mm^3$ and 189 ± 40$mm^3$, respectively). In both vehicle- and D-cycloserine-treated animals there was no significant change in hemisphere volume following MCA occlusion, although after D-cycloserine administration there was a trend towards increased ipsilateral hemisphere volume (760 ± 19$mm^3$ vs. 642 ± 11$mm^3$ for hemispheres ipsilateral and contralateral to MCA occlusion, respectively, $p>0.05$).

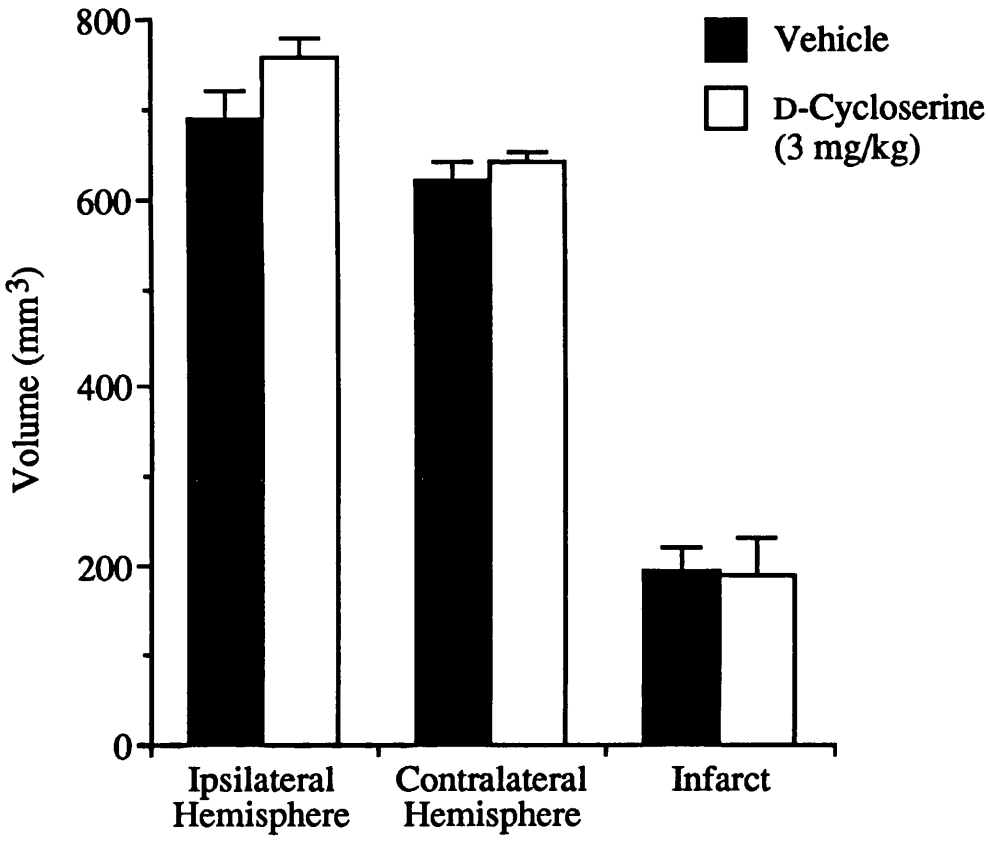


FIGURE 27: D-CYCLOSERINE AND MCA OCCLUSION

Data represent the volume of the ischaemic infarct produced by permanent middle cerebral artery (MCA) occlusion in the rat brain, and the volumes of the hemispheres ipsilateral and contralateral to MCA occlusion, following intravenous administration of D-cycloserine (3 mg/kg) or vehicle. Data presented as mean ± SEM.

D-Cycloserine had no significant effect on the volume of the ischaemic infarct, relative to vehicle-treated (control) animals. A slight tendancy towards increased hemispheric volume is evident in the hemisphere ipsilateral to occlusion in both control animals, and, more markedly, in D-cycloserine-treated rats, although there was no statistical evidence of a significant effect on hemispheric volume in either group.

## TABLE 25

## THE EFFECT OF D-CYCLOSERINE ON THE VOLUME OF ISCHAEMIC DAMAGE FOLLOWING MCA OCCLUSION

| VOLUME ($mm^3$) | VEHICLE (n=6) | D-CYCLOSERINE (3mg/kg) (n=6) |
|---|---|---|
| Infarct | 191 ± 30 | 189 ± 40 |
| Hemisphere: | | |
| Ipsilateral | 691 ± 28 | 760 ± 19 |
| Contralateral | 623 ± 22 | 642 ± 11 |
| Swelling | +67 ± 12 | +118 ± 21 |

Data are presented as mean ± SEM volume ($mm^3$). Data represent the volume of infarct produced by permanent MCA occlusion, and cerebral hemisphere volume ipsilateral and contralateral to MCA occlusion. D-cycloserine (3mg/kg) or vehicle were administered by sub-cutaneous injection 15 and 255 min after MCA occlusion. The volume of hemispheric swelling in vehicle-(controls) and D-cycloserine-treated animals is the difference between ipsilateral and contralateral hemisphere volumes within treatment groups. There were no significant differences in volumes of infarct or swelling between vehicle- or D-cycloserine-treated animals ($p>0.05$, Student's unpaired *t*-test).

## TABLE 26

## THE EFFECTS OF D-CYCLOSERINE AND NBQX ON LESION VOLUME FOLLOWING CORTICAL PERFUSION OF GLUTAMATE

| | LESION VOLUME ($mm^3$) |
|---|---|
| Vehicle (Saline) (n=8) | 20.3 ± 1.3 |
| D-Cycloserine (3mg/kg) (n=5) | 20.3 ± 2.1 |
| Vehicle (5.5% Glucose) (n=10) | 14.4 ± 0.7 |
| NBQX (30mg/kg) (n=5) | 11.1 ± 0.7* |

Data are presented as mean ± SEM volume ($mm^3$). Data represent the volumes of lesions measured 4h after onset of intracortical glutamate (0.5M) perfusion. *$p<0.05$, **$p<0.01$, significant difference relative to contemporaneous vehicle controls (ANOVA, followed by Student's unpaired *t*-test with Bonferroni correction).

## 2.4 Cortical Glutamate Neurotoxicity

### 2.4.1 General Observations

All physiological measurements are presented in Table 27. Intravenous administration of NBQX (30mg/kg x 2; 30 min before and 30 min after onset of glutamate perfusion) or D-cycloserine (3mg/kg; 30 min prior to glutamate perfusion) to halothane-anaesthetised rats had no significant effects on the measured respiratory parameters (arterial carbon dioxide tension, $pCO_2$, and oxygen tension, $pO_2$), or plasma glucose levels over the 4½h duration of the study. Rectal temperature was significantly increased following D-cycloserine administration, although the use of heating lamps during the experiment makes interpretation of drug-related temperature effects difficult. NBQX had no significant effect on temperature. Vehicle-treated control animals showed no alterations in these parameters over the experimental period.

In the anaesthetised animals, NBQX (30mg/kg) induced a moderate, sustained increase in mean arterial blood pressure throughout the period of glutamate perfusion and in the post-perfusion period, relative to levels in control animals which remained constant throughout the experiment. D-Cycloserine (30mg/kg) did not significantly alter mean arterial blood pressure during the experimental period, relative to levels in control animals.

## TABLE 27

## INTRACORTICAL GLUTAMATE PERFUSION: PHYSIOLOGICAL VARIABLES FOLLOWING INTRAVENOUS ADMINISTRATION OF D-CYCLOSERINE AND NBQX IN ANAESTHETISED RATS

| TREATMENT | GLUTAMATE PERFUSION (Min) | RECTAL TEMPERATURE (°C) | MEAN ARTERIAL BLOOD PRESSURE (mmHg) | ARTERIAL PLASMA GLUCOSE (mM) | pCO (mmHg) | pO (mmHg) |
|---|---|---|---|---|---|---|
| VEHICLE (Saline) | - 30 | 36.4 ± 0.2 | 99 ± 5 | 10.6 ± 0.5 | 40 ± 1 | 170 ± 7 |
| | 0 | 37.1 ± 0.2 | 92 ± 5 | 10.3 ± 0.5 | 38 ± 1 | 169 ± 7 |
| | 60 | 37.1 ± 0.1 | 91 ± 2 | 9.6 ± 0.7 | 38 ± 1 | 175 ± 9 |
| | 120 | 36.9 ± 0.2 | 93 ± 3 | 9.7 ± 0.7 | 36 ± 1 | 180 ± 9 |
| | 180 | 37.0 ± 0.2 | 83 ± 3 | 10.7 ± 0.5 | 34 ± 1 | 178 ± 9 |
| | 240 | 37.1 ± 0.1 | 87 ± 5 | 10.2 ± 0.4 | 37 ± 1 | 178 ± 8 |
| D-CYCLOSERINE (3mg/kg) | - 30 | 35.8 ± 0.2 | 92 ± 5 | 10.8 ± 0.9 | 39 ± 1 | 177 ± 12 |
| | 0 | 37.1 ± 0.2* | 81 ± 5 | 10.3 ± 0.6 | 37 ± 1 | 185 ± 10 |
| | 60 | 37.2 ± 0.2* | 86 ± 4 | 9.9 ± 1.1 | 39 ± 2 | 184 ± 8 |
| | 120 | 37.1 ± 0.1* | 84 ± 6 | 10.1 ± 1.1 | 39 ± 2 | 188 ± 6 |
| | 180 | 37.2 ± 0.1* | 84 ± 6 | 11.0 ± 1.3 | 35 ± 1 | 176 ± 8 |
| | 240 | 37.1 ± 0.1* | 83 ± 7 | 12.2 ± 1.7 | 37 ± 1 | 172 ± 17 |
| VEHICLE (5.5% Glucose) | - 30 | 37.0 ± 0.1 | 93 ± 2 | 9.8 ± 0.4 | 39 ± 1 | 172 ± 6 |
| | 0 | 37.2 ± 0.1 | 94 ± 3 | 9.4 ± 0.3 | 39 ± 1 | 181 ± 6 |
| | 60 | 37.0 ± 0.1 | 95 ± 3 | 9.1 ± 0.2 | 39 ± 1 | 180 ± 7 |
| | 120 | 37.1 ± 0.1 | 95 ± 2 | 9.5 ± 0.3 | 36 ± 1 | 186 ± 6 |
| | 180 | 37.1 ± 0.1 | 89 ± 2 | 10.0 ± 0.2 | 36 ± 1 | 172 ± 12 |
| | 240 | 37.0 ± 0.1 | 94 ± 2 | 10.0 ± 0.4 | 37 ± 1 | 171 ± 11 |
| NBQX (30mg/kg) | - 30 | 37.4 ± 0.2 | 98 ± 2 | 10.9 ± 0.6 | 39 ± 1 | 182 ± 5 |
| | 0 | 37.1 ± 0.2 | 102 ± 6 | 11.3 ± 1.1 | 37 ± 2 | 189 ± 3 |
| | 60 | 37.1 ± 0.2 | 115 ± 6* | 12.6 ± 2.0 | 40 ± 1 | 188 ± 4 |
| | 120 | 37.2 ± 0.1 | 113 ± 3** | 11.8 ± 1.5 | 40 ± 3 | 191 ± 7 |
| | 180 | 37.4 ± 0.4 | 107 ± 3** | 11.8 ± 1.2 | 38 ± 1 | 192 ± 12 |
| | 240 | 36.9 ± 0.1 | 110 ± 5* | 11.0 ± 0.7 | 36 ± 1 | 193 ± 11 |

Data are presented as mean ± SEM. Data represent values 30 min prior to, at the time of, and 60 min intervals after the start of glutamate perfusion. *$p<0.05$, **$p<0.01$ for statistical comparison between drug-treated and vehicle-treated (control) animals at each time point (ANOVA, followed by Student's unpaired *t*-test with Bonferroni correction).

### 2.4.2 Assessment of Histological Damage

Perfusion of 0.5M glutamate in vehicle-treated animals produced a discrete cortical lesion, as illustrated in Figure 9 (Methods). The glutamate-induced lesion in vehicle-treated animals extended approximately 2.00mm anterior and posterior to the perfusion site.

The effects of D-cycloserine (3mg/kg) and NBQX (30mg/kg) on the size of the glutamate-induced lesion are presented in Table 26. Pretreatment with D-cycloserine (3mg/kg) 30 min prior to glutamate perfusion did not significantly alter the volume of damage produced by intracortical glutamate perfusion (20.3 ± 2.1mm$^3$ and 20.3 ± 1.3mm$^3$ in D-cycloserine and vehicle-treated rats respectively). Intravenous administration of NBQX (30mg/kg) 30 min prior to, and 30 min after the start of glutamate perfusion significantly reduced the volume of glutamate-induced damage by approximately 23% (11.1 ± 0.7mm$^3$ and 14.4 ± 0.7mm$^3$ in NBQX- and vehicle-treated rats respectively ($p<0.05$). Figure 28 illustrates the areas of damaged tissue at each of the coronal brain levels examined, from which lesion volumes were calculated by knowledge of the distance between coronal levels.

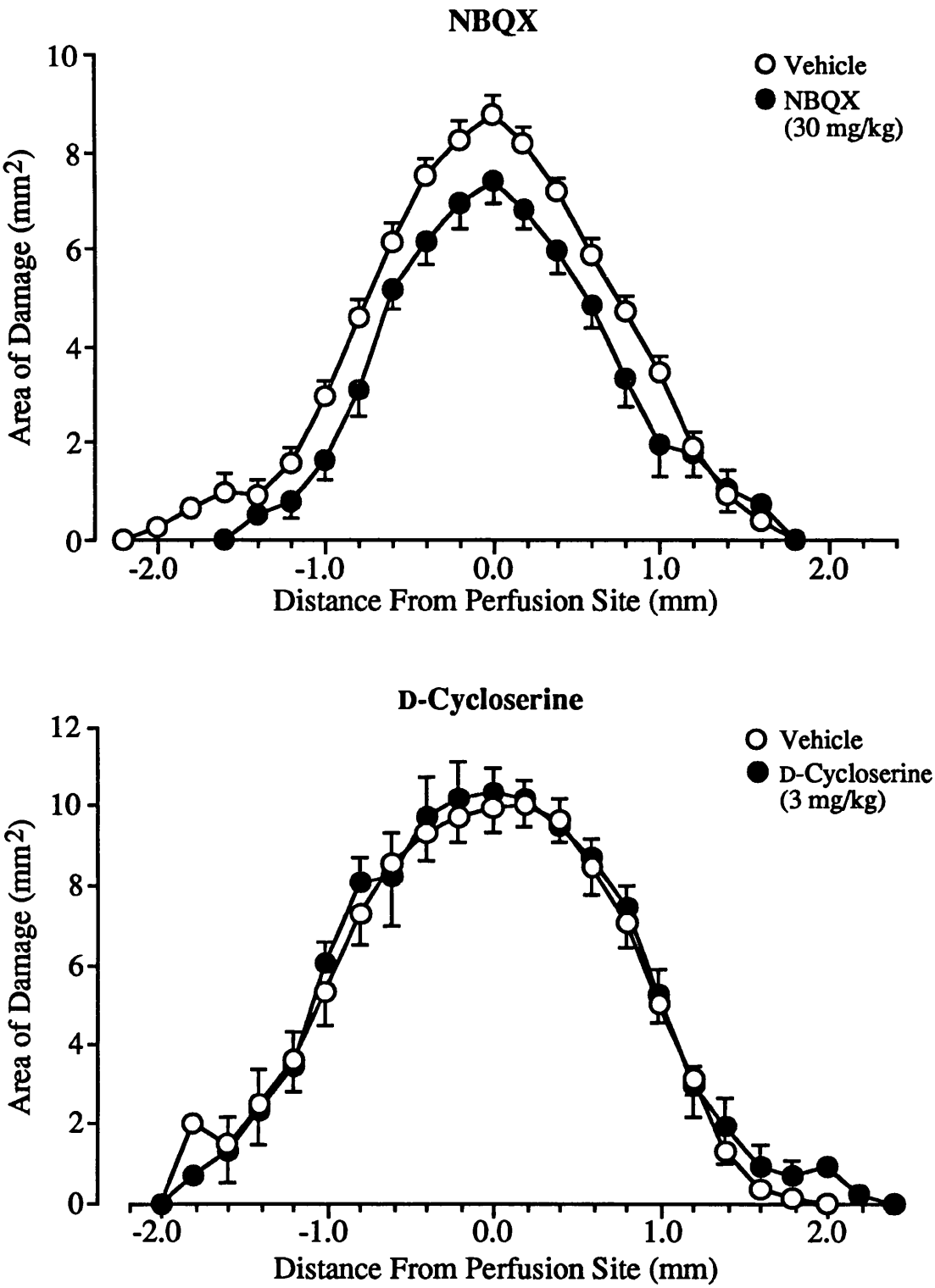


FIGURE 28: EFFECTS OF NBQX AND D-CYCLOSERINE ON GLUTAMATE-INDUCED CORTICAL DAMAGE

Graphs illustrating the effects of intravenous administration of D-cycloserine (3 mg/kg) and NBQX (30 mg/kg) on the extent of damage produced by intracortical perfusion of glutamate (0.5M) in rat brain. Points represent areas of damage in serial coronal brain sections at 200 μm intervals from the dialysis probe (0mm). Data are presented as mean ± SEM. Areas under the curves represent lesion volumes. NBQX significantly reduced the volume of glutamate-induced lesions, relative to lesion size in vehicle-treated rats ($p < 0.05$, ANOVA and t-test). D-Cycloserine did not significantly alter lesion volume.

## 3. EFFECTS OF INTRACEREBRAL BASAL FOREBRAIN MANIPULATIONS ON CEREBRAL GLUCOSE USE

The cerebral metabolic consequences of manipulating neuronal activity within the basal forebrain were investigated to gain insight into the contributions of basal forebrain neuronal populations, and in particular cholinergic neurones of the nucleus basalis magnocellularis (NBM), to integrated cerebral functional activity. Two different strategies were employed to manipulate neuronal activity:-

(i) Excitotoxic lesions of the NBM region: to assess the chronic effects of lesioning NBM efferents, including cholinergic projections to neocortex, on glucose use throughout the brain. The cerebral metabolic consequences of lesions produced by four different excitatory amino acid receptor agonists - ibotenic acid, NMDA, quisqualic acid and AMPA -were compared in the light of previous reports that of these excitotoxins AMPA shows the greatest selectivity for cholinergic magnocellular neurones. In addition, [$^3$H]-PK-11195 *in vitro* autoradiography was used to gain insight into the extent of gliosis occurring in response to excitatory amino acid lesions.

(ii) Agonist stimulation of neurones within the NBM region: to investigate the acute effects of receptor activation on cerebral glucose use. The effects of infusions of the excitatory amino acid receptor agonists NMDA and AMPA into the NBM region were compared with the cerebral metabolic consequences of infusion of the $GABA_A$ agonist muscimol.

## 3.1 Chronic Excitotoxic Basal Forebrain Lesions

### 3.1.1 General Observations

Local cerebral glucose utilisation was assessed in conscious rats 21-24 days after they had undergone unilateral infusion of ibotenic acid (0.09M), NMDA (0.09M), quisqualic acid (0.09M), AMPA (0.015M) or vehicle (saline) into the NBM region of the basal forebrain. All animals showed a reduction in body weight in the initial 24h post-operative period, but recovered to pre-operative weights within 7 days.

On the day of the [$^{14}$C]-2-deoxyglucose autoradiography procedure, all animals exhibited apparently normal behaviour. The partially restrained rats were lively and alert, with spontaneous exploratory behaviour, grooming and sniffing. The measured physiological parameters ($pCO_2$, $pO_2$, mean arterial blood pressure and plasma glucose concentration) were within acceptable limits, indicating no adverse levels of stress in the lesioned rats. Physiological measurements are presented in Table 28.

Lesion placement in the NBM region was verified in cresyl violet-stained sections from each animal. Four animals were subsequently excluded from the study on the basis of poor lesion placement.

## TABLE 28

## PHYSIOLOGICAL VARIABLES IN BASAL FOREBRAIN LESIONED RATS

| | VEHICLE | IBOTENATE | NMDA | QUISQUALATE | AMPA |
|---|---|---|---|---|---|
| Rectal Temperature (°C) | 36.9 ± 0.3 | 37.0 ± 0.1 | 37.0 ± 0.2 | 37.2 ± 0.2 | 37.4 ± 0.2 |
| Mean Arterial Blood Pressure (mmHg) | 125 ± 4 | 131 ± 3 | 130 ± 7 | 134 ± 4 | 139 ± 2 |
| Arterial Plasma Glucose (mM) | 9.0 ± 0.3 | 9.9 ± 0.5 | 9.0 ± 0.9 | 9.4 ± 0.2 | 8.6 ± 0.4 |
| $pCO_2$ (mmHg) | 42.8 ± 1.0 | 42.9 ± 1.7 | 41.7 ± 1.8 | 39.7 ± 1.1 | 42.6 ± 1.0 |
| $pO_2$ (mmHg) | 78.1 ± 2.4 | 80.8 ± 3.4 | 82.4 ± 3.0 | 79.0 ± 2.7 | 82.8 ± 4.2 |
| Number of animals | 5 | 5 | 3 | 5 | 5 |

Data are presented as mean ± SEM. Data represent values 5 min prior to commencement of the [$^{14}$C]-2-deoxyglucose procedure 21-24 days after unilateral infusions of ibotenate, NMDA, quisqualate, AMPA or vehicle into the NBM region of the basal forebrain. There were no apparent statistically significant differences between excitotoxin-infused (lesioned) and vehicle-infused (control) animals ($p>0.05$, ANOVA).

### 3.1.2 Local Cerebral Glucose Utilisation

*General*

The effects of ibotenic acid, NMDA, quisqualic acid and AMPA basal forebrain lesions on cerebral glucose use 21-24 days post-lesion are presented in Tables 29-32 (see also Figures 29, 30 and 31). The statistical design adopted *a priori* involved initial comparison between treatment groups of glucose use levels in structures in the sham-operated (contralateral) hemisphere. There were no apparent significant differences in contralateral hemisphere glucose use values between treatment groups in any of the 49 CNS regions investigated. Glucose use values in structures in the vehicle-infused (ipsilateral) and sham-operated (contralateral) hemispheres of control animals were then compared. There were no apparent statistically significant interhemispheric differences in glucose use values in control animals in any of the brain regions examined. These findings suggest that there were no trans-hemispheric effects on glucose use following excitotoxic basal forebrain lesions, and indicate that vehicle infusion had no effects on cerebral glucose use. Subsequently, glucose use values in structures in the ipsilateral (lesioned) hemisphere of excitatory amino acid-infused rats were compared with values in the corresponding region of the ipsilateral (vehicle-infused) hemisphere of control animals.

Following ibotenic acid infusion, glucose utilisation was significantly increased in the NBM, but was not significantly altered in any of the other 48 brain regions examined. Following NMDA infusion, glucose use was significantly increased in the hypothalamus, relative to levels in control animals, but was not significantly altered in any other region examined. Local rates of glucose utilisation were not significantly altered in any of the 49 CNS regions examined

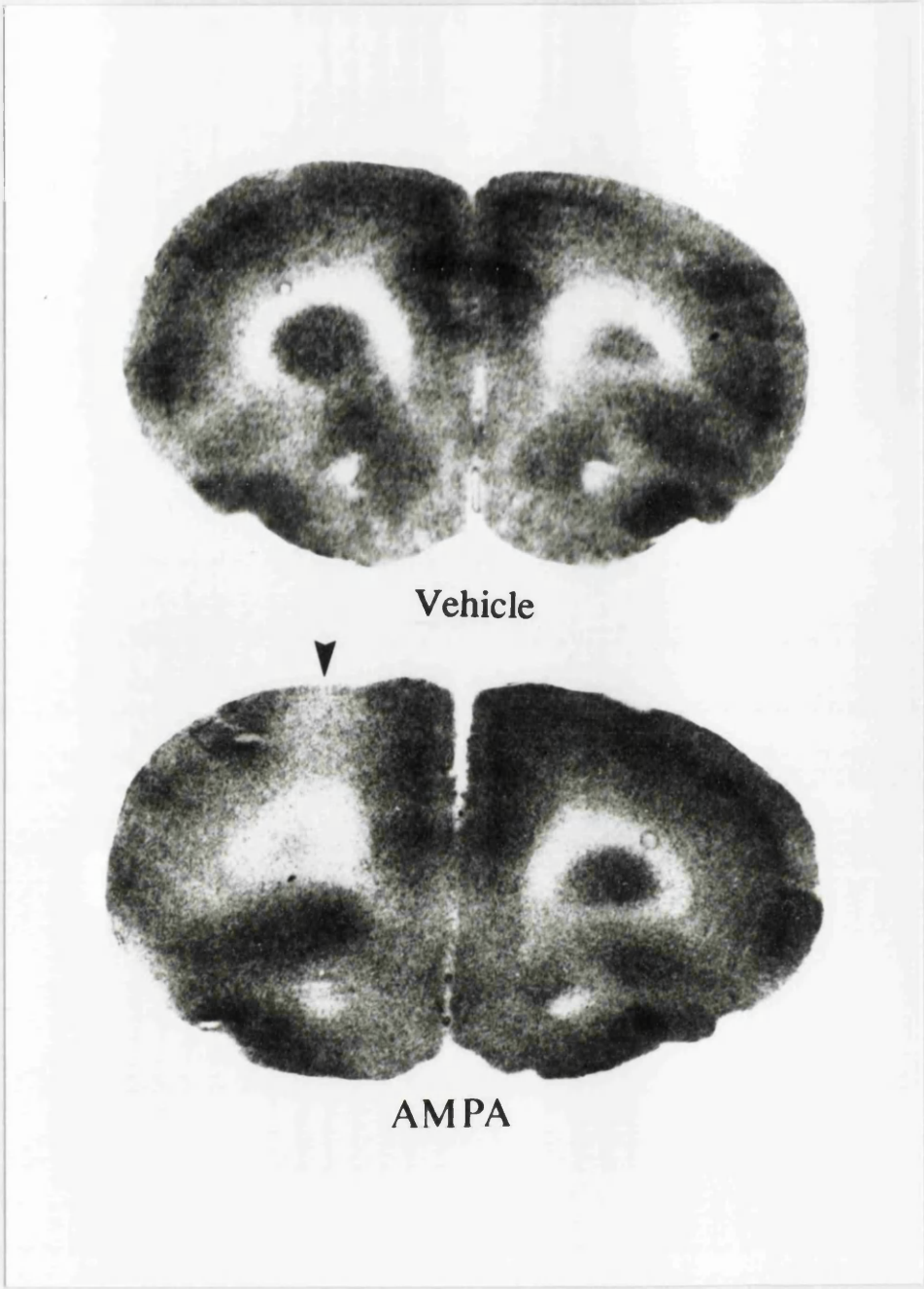


FIGURE 29: GLUCOSE USE DEPRESSION IN MEDIAL PREFRONTAL CORTEX AFTER AMPA BASAL FOREBRAIN LESIONS

Note the reduction in glucose use in the ipsilateral (left) prefrontal cortex (arrowed) after unilateral AMPA-induced lesion of the NBM region of basal forebrain, relative to cortical glucose use in the non-lesioned (right) hemisphere, and in vehicle-infused (sham) animals.

following infusions of AMPA or quisqualic acid.

It should be noted that the statistical analysis employed in the current study was extremely conservative as a consequence of the large number of treatment groups involved, involving initial analysis of variance (ANOVA) followed by independent *t*-tests with Bonferroni correction for multiple comparisons. However, insight into regions in which glucose use showed a tendency to change in response to excitotoxic lesions may be gained by examination of structures in which the analysis of variance "F" value exceeded the critical 5% probability level. Regional trends evident from such analysis are highlighted below.

*Regions Distal to Infusion Site*

Since the NBM provides the major cholinergic innervation of neocortex, any glucose use alterations in cortical regions in response to NBM lesions are of particular interest. Although there were no significant alterations in glucose utilisation in any of the cortical regions examined following infusion of any of the excitatory amino acid agonists (Table 29), a trend towards reduced glucose use was evident in frontal cortical regions following AMPA infusions. In particular, glucose use was reduced in medial prefrontal cortex, layer IV (-19%), in dorsolateral frontal cortex, layer IV (-18%) and sensory motor cortex (-19%) following AMPA lesions, as illustrated in Figures 29 and 30.

In subcortical regions, a trend towards reduced glucose use was evident in the lateral habenular nucleus following AMPA lesions (Table 31). Following NMDA infusion, glucose use was significantly increased in the hypothalamus (+20%), while a trend towards elevated glucose use was evident in the globus

pallidus in NMDA (+13%) and quisqualic acid (+19%) lesioned animals. Glucose utilisation rates in representative CNS regions are illustrated in Figures 30 and 31.

*Infusion Site*

Excitatory amino acid agonist-induced NBM lesions had marked effects on glucose use at the infusion site. Infusions of all the agonists resulted in increases in glucose utilisation in the NBM, which varied between agents in the volume of tissue in which glucose use was elevated. Volumes of tissue showing increased glucose use following each excitotoxin are presented in Table 33. The pattern of glucose use around the infusion site following AMPA, ibotenic acid and vehicle infusions is illustrated in Figure 32.

Following **vehicle, quisqualic acid** and **NMDA** infusions the volume of tissue in which glucose use was increased was negligible, being visible in only a very small area of the basal forebrain on the autoradiographic image. Increased glucose use occurred in a slightly larger volume of tissue following **AMPA** (0.25 ± 0.19mm$^3$), evident as a diffuse pattern of increased optical density in the region of the NBM and ventromedial globus pallidus. In contrast, glucose use was increased in a much larger volume of tissue following **ibotenic acid** than following any of the other agents (0.83 ± 0.37mm$^3$), producing a relatively homogenous region of elevated glucose use extending dorsally from the NBM to the striatal/pallidal border (see Figure 32). The rank ordering of agents according to the volume of tissue in which glucose use was:-

Ibotenic acid >> AMPA > NMDA > Quisqualic acid = Vehicle.

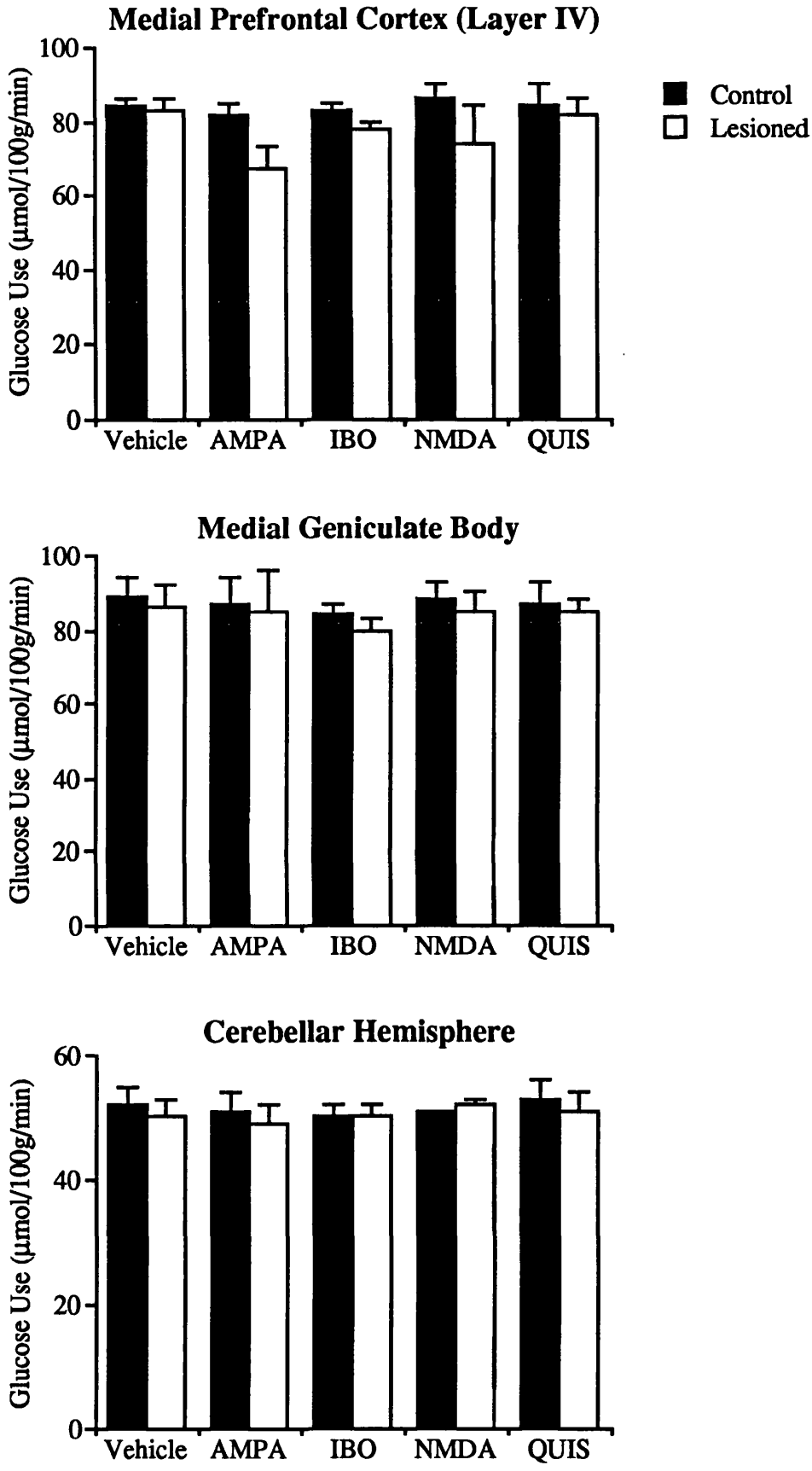


FIGURE 30: EFFECTS OF EXCITOTOXIC LESIONS ON CEREBRAL GLUCOSE USE : I

Glucose use in representative cortical, sensory and cerebellar regions (control and lesioned hemispheres) following excitotoxic lesions of the NBM. Data presented as mean ± SEM. None of the excitotoxins investigated significantly altered glucose use, but note the trend towards reduced glucose use in prefrontal cortex after AMPA lesions. *Abbreviations:* Ibo, ibotenate; Quis, quisqualate.

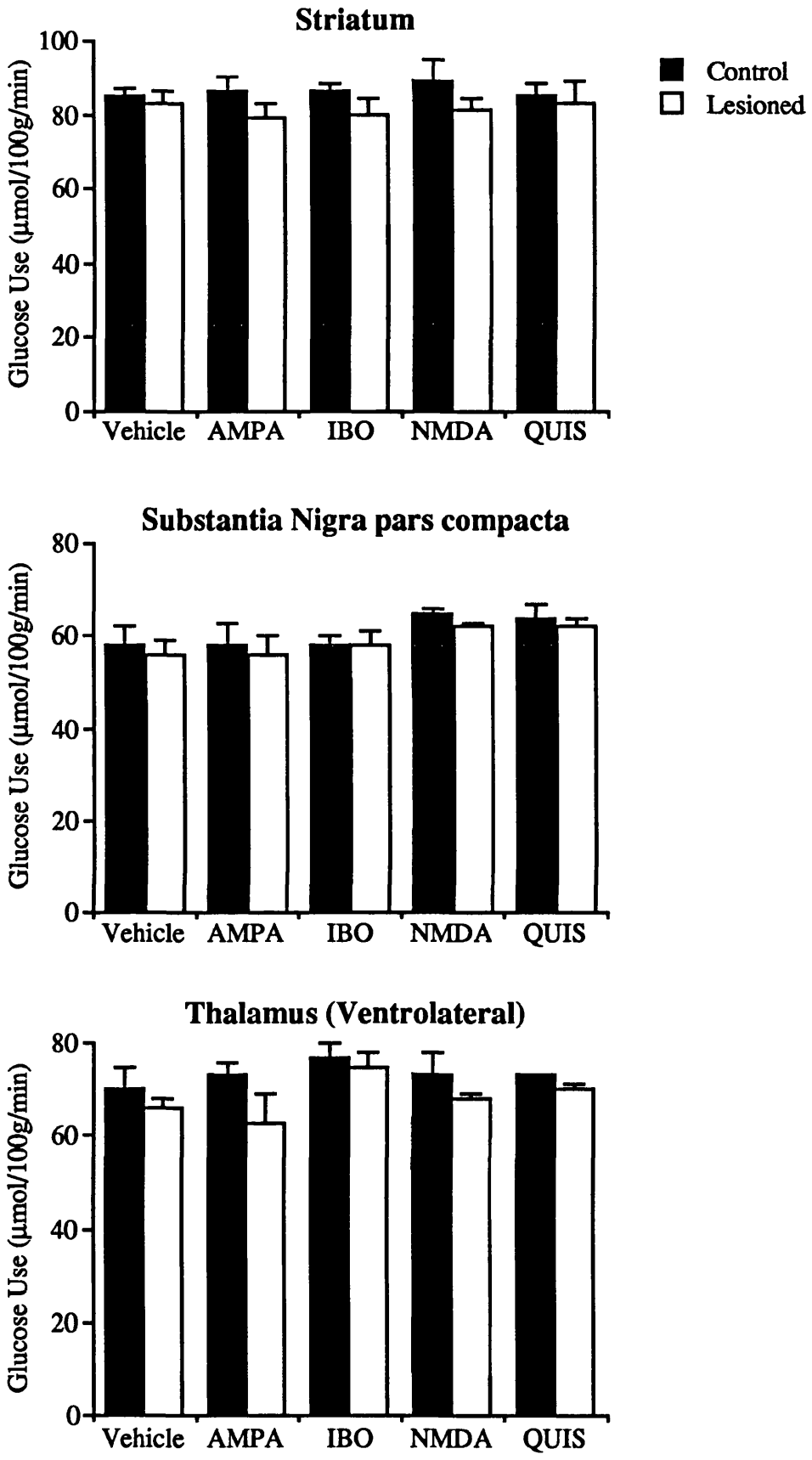


FIGURE 31: EFFECTS OF EXCITOTOXIC LESIONS ON CEREBRAL GLUCOSE USE : II

Glucose utilisation in representative extrapyramidal regions (control and lesioned hemispheres) following excitotoxic lesions of the NBM. Data presented as mean ± SEM. None of the excitotoxins investigated significantly altered glucose use in any of these regions. *Abbreviations:* Ibo, ibotenate; Quis, quisqualate.

LEGEND TO FIGURE 32:

Representative autoradiograms illustrating levels of [$^{14}$C]-2-deoxyglucose (indicative of local rates of glucose utilisation) in coronal rat brain sections 21-24 days ater vehicle ("sham"), AMPA or ibotenate infusion into the NBM region of the left hemisphere. The anatomical localisation of the infusion site is illustrated in the line diagram as the area of dark hatching, while the light hatching delineates the largest volume of tissue in which [$^{3}$H]-PK- 11195 binding increased after ibotenate infusion (see Figure 34).

Following ibotenate-induced lesions, glucose use was markedly increased in an area of tissue extending from the NBM into globus pallidus and striatum. In contrast, glucose use was increased in a small area of tissue, confined to the immediate vicinity of the infusion site, following AMPA lesions. Vehicle infusion had no apparent effect on glucose use in the basal forebrain, compared to levels in the non-infused hemisphere (right). *Abbreviations:* NBM, nucleus basalis magnocellularis; GP, globus pallidus.

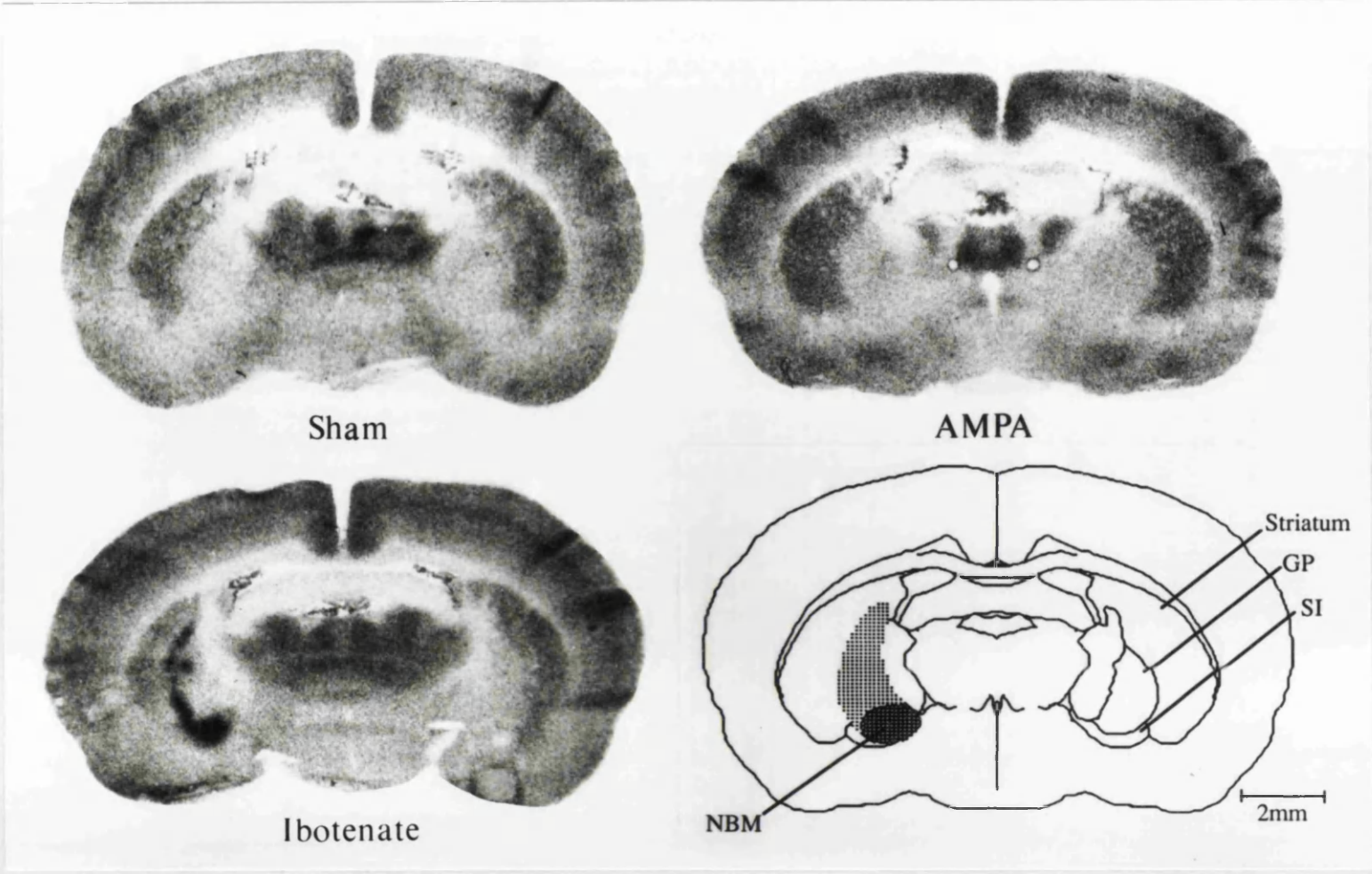


FIGURE 32: INCREASED GLUCOSE USE IN THE BASAL FOREBRAIN FOLLOWING EXCITOTOXIC LESIONS

LEGEND TO TABLES 29, 30, 31 AND 32

Data are presented as mean ± SEM local cerebral glucose utilisation (μmol/100g/min) for structures in treatment-infused (ipsilateral) and sham-operated (contralateral) hemispheres, 21-24 days after infusions of NMDA (0.09M), AMPA (0.015M), ibotenic acid (0.09M), quisqualic acid (0.09M) or vehicle into the NBM region of the ipsilateral basal forebrain. *$p<0.05$ Significant difference between glucose use values in the corresponding hemispheres of agonist- and vehicle-infused animals (ANOVA, followed by Student's unpaired *t*-test with Bonferroni correction for multiple treatment-control group comparisons).

## TABLE 29

## LOCAL CEREBRAL GLUCOSE UTILISATION 21-24 DAYS AFTER EXCITATORY AMINO ACID BASAL FOREBRAIN LESIONS: CEREBRAL CORTEX

| | IPSILATERAL | | | | | CONTRALATERAL | | | | |
|---|---|---|---|---|---|---|---|---|---|---|
| | Vehicle | AMPA | Ibotenate | NMDA | Quisqualate | Vehicle | AMPA | Ibotenate | NMDA | Quisqualate |
| | (n=5) | (n=5) | (n=5) | (n=3) | (n=5) | (n=5) | (n=5) | (n=5) | (n=3) | (n=5) |
| Prefrontal Medial: Layer IV | 83 ± 3 | 67 ± 6 | 78 ± 2 | 74 ± 10 | 82 ± 4 | 84 ± 2 | 82 ± 3 | 83 ± 2 | 86 ± 4 | 84 ± 6 |
| Frontal Dorsolateral: Layer IV | 82 ± 4 | 72 ± 8 | 83 ± 4 | 81 ± 7 | 85 ± 4 | 86 ± 2 | 87 ± 2 | 88 ± 2 | 85 ± 6 | 85 ± 4 |
| Sensory Motor:Layer IV | 86 ± 2 | 72 ± 10 | 80 ± 5 | 73 ± 17 | 81 ± 3 | 93 ± 2 | 91 ± 2 | 88 ± 4 | 89 ± 5 | 86 ± 3 |
| Parietal: Layer IV | 83 ± 4 | 83 ± 2 | 82 ± 1 | 81 ± 2 | 78 ± 2 | 86 ± 3 | 86 ± 2 | 84 ± 2 | 85 ± 2 | 83 ± 1 |
| Anterior Cingulate | 92 ± 4 | 89 ± 4 | 94 ± 2 | 90 ± 8 | 90 ± 4 | 95 ± 4 | 93 ± 7 | 95 ± 4 | 92 ± 9 | 91 ± 5 |
| Posterior Cingulate | 81 ± 5 | 85 ± 5 | 89 ± 4 | 83 ± 7 | 79 ± 4 | 80 ± 4 | 87 ± 5 | 84 ± 4 | 86 ± 8 | 79 ± 4 |
| Auditory: Layer IV | 92 ± 7 | 93 ± 9 | 99 ± 4 | 100 ± 6 | 100 ± 6 | 96 ± 8 | 95 ± 6 | 103 ± 4 | 104 ± 4 | 103 ± 6 |
| Visual: Layer IV | 91 ± 5 | 88 ± 4 | 88 ± 3 | 87 ± 3 | 93 ± 5 | 93 ± 4 | 92 ± 5 | 88 ± 3 | 92 ± 2 | 94 ± 3 |
| Occipital | 91 ± 5 | 88 ± 4 | 88 ± 3 | 87 ± 3 | 83 ± 5 | 93 ± 4 | 92 ± 5 | 88 ± 3 | 92 ± 2 | 94 ± 3 |
| Perirhinal | 79 ± 4 | 79 ± 2 | 83 ± 3 | 88 ± 1 | 85 ± 3 | 79 ± 4 | 83 ± 3 | 85 ± 4 | 90 ± 3 | 86 ± 3 |
| Entorhinal | 55 ± 4 | 55 ± 4 | 54 ± 2 | 59 ± 3 | 52 ± 3 | 53 ± 4 | 55 ± 3 | 58 ± 2 | 60 ± 3 | 53 ± 2 |

## TABLE 30

## LOCAL CEREBRAL GLUCOSE UTILISATION 21-24 DAYS AFTER EXCITATORY AMINO ACID BASAL FOREBRAIN LESIONS: EXTRAPYRAMIDAL AND OTHER MOTOR REGIONS

| | IPSILATERAL | | | | | CONTRALATERAL | | | | |
|---|---|---|---|---|---|---|---|---|---|---|
| | Vehicle | AMPA | Ibotenate | NMDA | Quisqualate | Vehicle | AMPA | Ibotenate | NMDA | Quisqualate |
| | (n=5) | (n=5) | (n=5) | (n=3) | (n=5) | (n=5) | (n=5) | (n=5) | (n=3) | (n=5) |
| Nucleus Basalis Magnocellularis (NBM) | 47 ± 2 | 69 ± 12 | 107 ± 7* | 54 ± 2 | 58 ± 4 | 45 ± 1 | 49 ± 2 | 48 ± 1 | 45 ± 1 | 50 ± 2 |
| Striatum: Dorsolateral | 83 ± 3 | 79 ± 4 | 80 ± 4 | 81 ± 3 | 83 ± 6 | 85 ± 2 | 86 ± 4 | 86 ± 2 | 89 ± 6 | 85 ± 3 |
| Nucleus Accumbens | 59 ± 3 | 61 ± 6 | 62 ± 1 | 65 ± 4 | 65 ± 3 | 64 ± 2 | 63 ± 5 | 63 ± 2 | 68 ± 6 | 66 ± 3 |
| Globus Pallidus | 47 ± 1 | 48 ± 4 | 63 ± 12 | 54 ± 3 | 58 ± 5 | 48 ± 1 | 46 ± 1 | 54 ± 2 | 50 ± 1 | 50 ± 2 |
| Thalamus:Mediodorsal | 85 ± 4 | 80 ± 5 | 81 ± 4 | 87 ± 5 | 86 ± 3 | 90 ± 2 | 92 ± 2 | 87 ± 3 | 91 ± 3 | 90 ± 2 |
| Ventrolateral | 66 ± 2 | 63 ± 6 | 75 ± 3 | 68 ± 1 | 70 ± 1 | 70 ± 5 | 73 ± 3 | 77 ± 3 | 73 ± 5 | 73 ± 0 |
| Subthalamic Nucleus | 65 ± 3 | 62 ± 3 | 61 ± 2 | 61 ± 2 | 62 ± 3 | 68 ± 3 | 68 ± 2 | 72 ± 2 | 68 ± 4 | 66 ± 3 |
| Substantia Nigra: pars compacta | 56 ± 3 | 56 ± 4 | 58 ± 3 | 62 ± 1 | 62 ± 2 | 58 ± 4 | 58 ± 5 | 58 ± 2 | 65 ± 1 | 64 ± 3 |
| pars reticulata | 53 ± 6 | 45 ± 2 | 50 ± 1 | 51 ± 1 | 51 ± 2 | 53 ± 6 | 44 ± 2 | 48 ± 1 | 51 ± 3 | 51 ± 1 |
| Dorsal Tegmental Nucleus | 86 ± 3 | 78 ± 3 | 82 ± 5 | 86 ± 4 | 80 ± 3 | 81 ± 2 | 77 ± 4 | 83 ± 4 | 85 ± 3 | 79 ± 4 |
| Red Nucleus | 64 ± 2 | 60 ± 2 | 63 ± 2 | 63 ± 5 | 67 ± 3 | 67 ± 2 | 62 ± 3 | 65 ± 2 | 66 ± 6 | 66 ± 4 |
| Pontine Nucleus | 52 ± 2 | 58 ± 5 | 59 ± 2 | 54 ± 1 | 62 ± 4 | 56 ± 2 | 59 ± 5 | 57 ± 3 | 66 ± 5 | 51 ± 4 |
| Pons | 52 ± 1 | 52 ± 2 | 52 ± 2 | 53 ± 1 | 54 ± 0 | 52 ± 1 | 54 ± 2 | 52 ± 5 | 55 ± 1 | 54 ± 1 |
| Cerebellar Hemisphere | 50 ± 3 | 49 ± 3 | 50 ± 2 | 52 ± 1 | 51 ± 3 | 52 ± 3 | 51 ± 3 | 50 ± 2 | 51 ± 0 | 53 ± 3 |

## TABLE 31

## LOCAL CEREBRAL GLUCOSE UTILISATION 21-24 DAYS AFTER EXCITATORY AMINO ACID BASAL FOREBRAIN LESIONS: LIMBIC REGIONS AND WHITE MATTER TRACTS

| | IPSILATERAL | | | | | CONTRALATERAL | | | | |
|---|---|---|---|---|---|---|---|---|---|---|
| | Vehicle | AMPA | Ibotenate | NMDA | Quisqualate | Vehicle | AMPA | Ibotenate | NMDA | Quisqualate |
| | (n=5) | (n=5) | (n=5) | (n=3) | (n=5) | (N=5) | (N=5) | (n=5) | (n=3) | (n=5) |
| Hippocampus: Molecular Layer | 63 ± 2 | 66 ± 4 | 64 ± 2 | 69 ± 2 | 69 ± 3 | 66 ± 2 | 69 ± 4 | 66 ± 1 | 73 ± 1 | 67 ± 3 |
| Dentate Gyrus | 52 ± 2 | 53 ± 3 | 55 ± 1 | 58 ± 2 | 57 ± 2 | 54 ± 2 | 55 ± 2 | 56 ± 2 | 59 ± 2 | 57 ± 4 |
| Medial Septum | 64 ± 2 | 64 ± 2 | 63 ± 3 | 66 ± 4 | 66 ± 3 | 64 ± 2 | 65 ± 2 | 64 ± 3 | 67 ± 4 | 67 ± 2 |
| Diagonal Band of Broca | 59 ± 3 | 62 ± 3 | 59 ± 2 | 67 ± 4 | 67 ± 3 | 61 ± 2 | 64 ± 3 | 62 ± 2 | 68 ± 4 | 68 ± 3 |
| Amygdala | 41 ± 3 | 39 ± 2 | 42 ± 1 | 45 ± 1 | 44 ± 1 | 44 ± 3 | 40 ± 2 | 44 ± 1 | 44 ± 1 | 43 ± 2 |
| Median Raphe Nucleus | 79 ± 3 | 80 ± 5 | 78 ± 4 | 75 ± 2 | 82 ± 5 | 78 ± 2 | 80 ± 4 | 79 ± 3 | 76 ± 1 | 83 ± 4 |
| Dorsal Raphe Nucleus | 66 ± 5 | 71 ± 4 | 67 ± 3 | 72 ± 2 | 72 ± 3 | 65 ± 4 | 72 ± 4 | 68 ± 3 | 72 ± 1 | 73 ± 4 |
| Lateral Habenular Nucleus | 98 ± 2 | 88 ± 5 | 90 ± 8 | 98 ± 6 | 95 ± 2 | 102 ± 2 | 102 ± 3 | 98 ± 3 | 99 ± 7 | 93 ± 2* |
| Medial Habenular Nucleus | 70 ± 2 | 66 ± 3 | 68 ± 3 | 73 ± 3 | 68 ± 2 | 75 ± 3 | 66 ± 3 | 70 ± 3 | 69 ± 5 | 63 ± 4 |
| Thalamus: | | | | | | | | | | |
| Anterodorsal | 84 ± 1 | 73 ± 6 | 75 ± 5 | 92 ± 11 | 86 ± 4 | 88 ± 2 | 94 ± 3 | 87 ± 2 | 91 ± 4 | 94 ± 10 |
| Anteromedial | 94 ± 2 | 100 ± 7 | 87 ± 2 | 99 ± 5 | 96 ± 3 | 97 ± 3 | 96 ± 4 | 89 ± 1 | 100 ± 4 | 100 ± 3 |
| Hypothalamus | 40 ± 2 | 41 ± 2 | 48 ± 2 | 50 ± 3* | 47 ± 3 | 44 ± 2 | 42 ± 2 | 48 ± 2 | 50 ± 2 | 47 ± 2 |
| Medial Forebrain Bundle | 62 ± 6 | 67 ± 12 | 57 ± 2 | 62 ± 4 | 59 ± 2 | 62 ± 6 | 59 ± 3 | 56 ± 1 | 61 ± 2 | 58 ± 2 |
| Genu | 33 ± 2 | 31 ± 1 | 35 ± 1 | 34 ± 3 | 35 ± 2 | 34 ± 2 | 30 ± 1 | 36 ± 1 | 34 ± 4 | 36 ± 2 |
| Cerebellar White Matter | 31 ± 1 | 34 ± 3 | 33 ± 1 | 32 ± 2 | 36 ± 3 | 34 ± 1 | 33 ± 2 | 33 ± 1 | 34 ± 3 | 33 ± 2 |

## TABLE 32

## LOCAL CEREBRAL GLUCOSE UTILISATION 21-24 DAYS AFTER EXCITATORY AMINO ACID BASAL FOREBRAIN LESIONS: PRIMARY VISUAL AND AUDITORY REGIONS

| | IPSILATERAL | | | | | CONTRALATERAL | | | | |
|---|---|---|---|---|---|---|---|---|---|---|
| | Vehicle | AMPA | Ibotenate | NMDA | Quisqualate | Vehicle | AMPA | Ibotenate | NMDA | Quisqualate |
| | (n=5) | (n=5) | (n=5) | (n=3) | (n=5) | (N=5) | (N=5) | (n=5) | (n=3) | (n=5) |
| Primary Visual System | | | | | | | | | | |
| Dorsal Lateral Geniculate Body | 96 ± 4 | 89 ± 4 | 90 ± 2 | 87 ± 4 | 85 ± 3 | 100 ± 5 | 91 ± 4 | 87 ± 2 | 91 ± 1 | 85 ± 5 |
| Superior Colliculus: | | | | | | | | | | |
| Superficial Layer | 87 ± 2 | 88 ± 7 | 83 ± 2 | 88 ± 2 | 88 ± 6 | 90 ± 1 | 88 ± 7 | 83 ± 2 | 90 ± 3 | 84 ± 5 |
| Deep Layer | 73 ± 1 | 73 ± 5 | 71 ± 2 | 72 ± 0 | 77 ± 4 | 74 ± 1 | 73 ± 4 | 68 ± 4 | 75 ± 3 | 74 ± 3 |
| Anterior Pretectal Area | 79 ± 3 | 83 ± 4 | 83 ± 2 | 85 ± 3 | 81 ± 3 | 84 ± 2 | 86 ± 3 | 84 ± 2 | 82 ± 2 | 87 ± 3 |
| Primary Auditory System | | | | | | | | | | |
| Medial Geniculate Body | 86 ± 6 | 85 ± 11 | 80 ± 3 | 85 ± 5 | 85 ± 3 | 89 ± 5 | 87 ± 7 | 84 ± 3 | 88 ± 5 | 87 ± 6 |
| Inferior Colliculus | 128 ± 5 | 122 ± 8 | 119 ± 6 | 122 ± 5 | 125 ± 4 | 130 ± 4 | 132 ± 8 | 117 ± 4 | 129 ± 3 | 124 ± 8 |
| Superior Olivary Nucleus | 111 ± 4 | 107 ± 7 | 103 ± 6 | 102 ± 1 | 98 ± 9 | 102 ± 4 | 110 ± 5 | 103 ± 7 | 96 ± 8 | 96 ± 4 |
| Cochlear Nucleus | 97 ± 6 | 101 ± 7 | 96 ± 8 | 102 ± 8 | 96 ± 9 | 103 ± 9 | 105 ± 7 | 98 ± 5 | 102 ± 6 | 92 ± 8 |
| Lateral Lemniscus | 77 ± 2 | 81 ± 7 | 74 ± 6 | 77 ± 2 | 77 ± 6 | 77 ± 2 | 83 ± 6 | 73 ± 4 | 76 ± 5 | 76 ± 2 |

## TABLE 33

## VOLUMES OF BRAIN TISSUE EXHIBITING INCREASED LOCAL CEREBRAL GLUCOSE USE AND INCREASED [$^3$H]-PK-11195 BINDING, FOLLOWING EXCITOTOXIC BASAL FOREBRAIN LESIONS

| | VOLUME / ($mm^3$) | | |
|---|---|---|---|
| | LCGU | [$^3$H]-PK-11195 | n |
| Ibotenic Acid | 0.83 ± 0.37 | 6.76 ± 1.52 | 5 |
| AMPA | 0.25 ± 0.19 | 4.64 ± 1.66 | 5 |
| NMDA | 0.20 ± 0.16 | 2.02 ± 1.29 | 3 |
| Quisqualic Acid | 0.17 ± 0.05 | 1.71 ± 0.33 | 5 |
| Vehicle | 0.16 ± 0.13 | 0.99 ± 0.55 | 5 |

Data are presented as mean ± SEM volume ($mm^3$) of brain tissue in the hemisphere ipsilateral to excitatory amino acid or vehicle infusion into the basal forebrain, exhibiting the following characteristics:

**LCGU:** Local cerebral glucose utilisation (LCGU) increased above the normal glucose utilisation level observed in vehicle-infused control animals.

**[$^3$H]-PK-11195:** [$^3$H]-PK-11195 binding above the "normal" level of binding observed in the corresponding region of vehicle-infused animals.

The excitatory amino acids infused are tabulated in decreasing order of tissue volume affected.

### 3.1.3 [$^3$H]-PK-11195 Binding

[$^3$H]-PK-11195 binds to peripheral-type benzodiazepine receptors. In the CNS these receptors are located predominantly on glial cells. Hence the pattern of [$^3$H]-PK-11195 binding in rat brain sections gives an indication of the distribution of glial cells. The pattern of total and non-specific [$^3$H]-PK-11195 binding in adjacent sections from an ibotenic acid lesioned rat is illustrated in Figure 3. Following unilateral infusions of ibotenic acid, NMDA, quisqualic acid or AMPA into the NBM region, [$^3$H]-PK-11195 binding was increased at the infusion site relative to the corresponding region in the non-infused contralateral hemisphere, as illustrated in Figure 34. The volume of tissue showing increased [$^3$H]-PK-11195 binding following infusion varied markedly between the agents infused, as shown in Table 33. Following vehicle infusion, [$^3$H]-PK-11195 binding was evident only in a small volume of tissue in the NBM region (0.99 ± 0.55mm$^3$). Similarly, after quisqualic acid and NMDA infusions, [$^3$H]-PK-11195 binding was restricted to small volumes of tissue around the infusion site (1.71 ± 0.33, and 2.02 ± 1.29mm$^3$ respectively). In contrast, [$^3$H]-PK-11195 binding was evident in considerably larger volumes of tissue following AMPA and ibotenic acid infusions (AMPA, 4.64 ± 1.66mm$^3$; ibotenic acid, 6.76 ± 1.52mm$^3$). AMPA infusion produced a diffuse pattern of [$^3$H]-PK-11195 binding in the basal forebrain, with small regions of high optical density scattered throughout the NBM and the medioventral border of the globus pallidus and the substantia innominata. In contrast, ibotenic acid infusion resulted in dense [$^3$H]-PK-11195 binding in a large region extending dorsally from the NBM to include the globus pallidus and medial striatal regions (see Figure 34). Therefore, of the excitatory

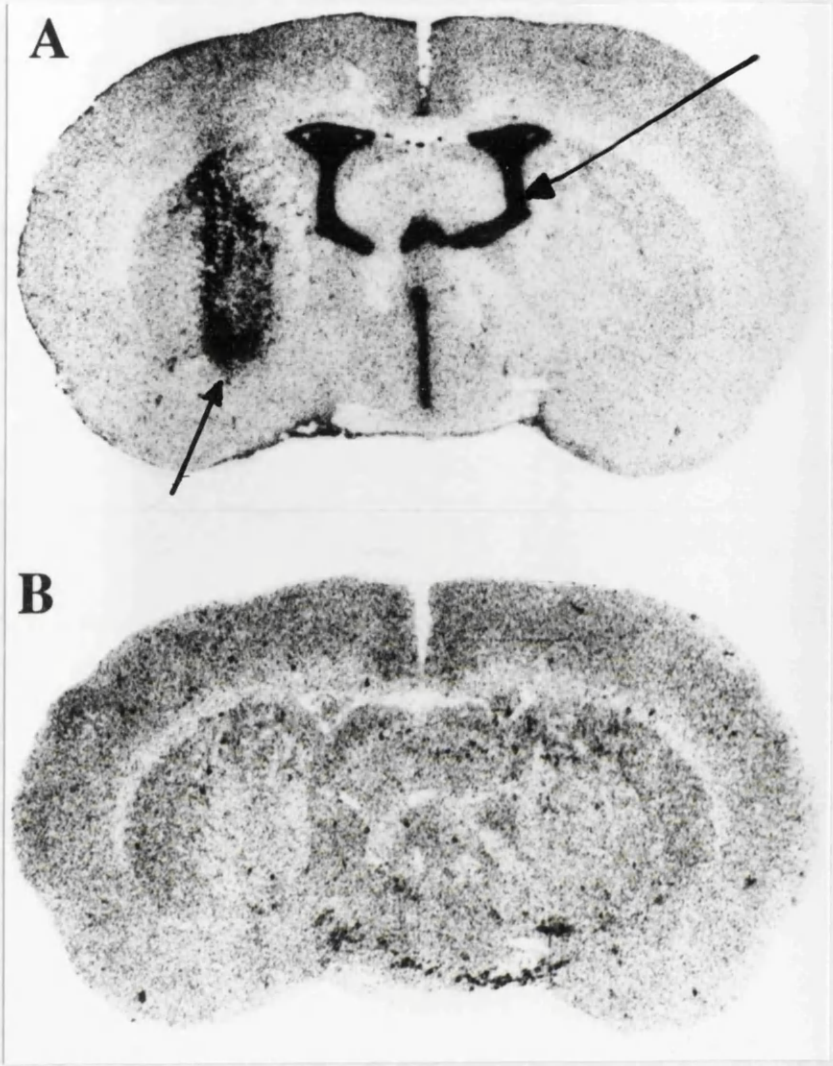


FIGURE 33: [$^3$H]-PK-11195 BINDING IN LESIONED BRAIN

Adjacent, representative brain sections illustrating A: Total, and B: Non-specific [$^3$H]-PK-11195 binding following unilateral ibotenate lesion of the NBM region of basal forebrain. Note the markedly increased [$^3$H]-PK-11195 binding around the lesion site (arrow, left), compared to levels in the non-lesioned hemisphere. In addition, high levels of [$^3$H]-PK-11195 binding are evident in the ventricles (arrow, right). These observations correspond with the known localisation of peripheral-type benzodiazepine receptors in the CNS, on glial cell and endothelial cell membranes (Benvenides et al., 1984). In contrast, non-specific [$^3$H]-PK-11195 binding is homogeneous. It should be noted that the slightly darker appearance of section B is due to a longer exposure period.

LEGEND TO FIGURE 34:

Representative autoradiograms illustrating [$^3$H]-PK-11195 binding in coronal rat brain sections 21-24 days ater vehicle ("sham"), AMPA or ibotenate infusion into the NBM region of the left hemisphere. The anatomical localisation of the infusion site is illustrated in the line diagram as the area of dark hatching, while the light hatching delineates the largest volume of tissue in which [$^3$H]-PK- 11195 binding increased after ibotenate infusion. In vehicle-infused animals,[$^3$H]-PK-11195 binding was restricted to the position of the needle tract, putatively indicative of mechanical tissue damage. Following AMPA infusion, a diffuse pattern of [$^3$H]-PK-11195 binding was evident around the infusion site in the left hemisphere. In contrast, increased levels of [$^3$H]-PK-11195 binding were evident in a large area of tissue around the infusion site following ibotenate, including NBM, globus pallidus and medial striatum. *Abbreviations:* NBM : nucleus basalis magnocellularis; GP: globus pallidus.

The sections shown are adjacent to those in Figure 32, illustrating glucose use in basal forebrain - lesioned rats.

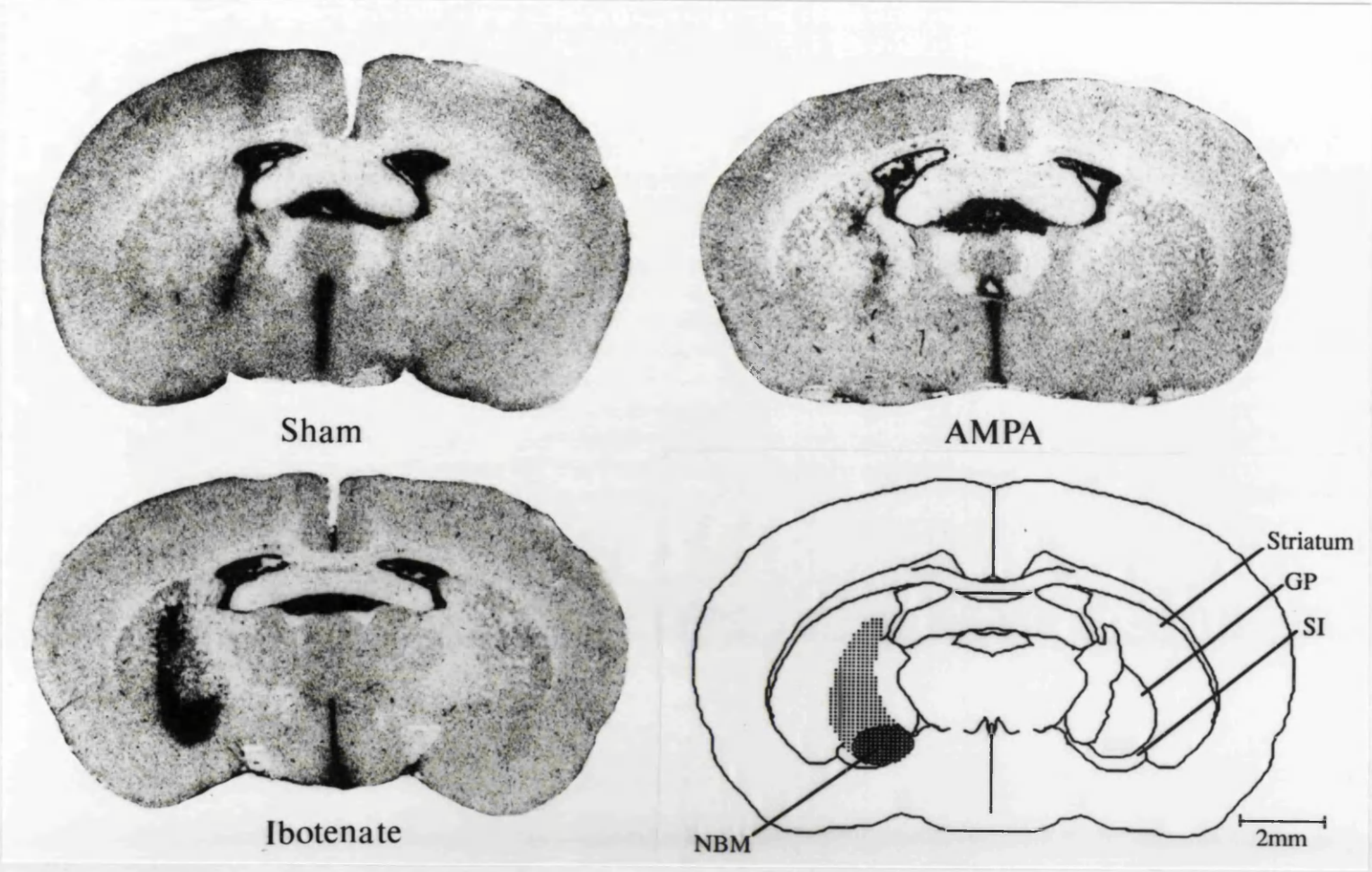


FIGURE 34: [$^3$H]-PK-11195 BINDING FOLLOWING UNILATERAL EXCITOTXIC LESIONS

amino acid agonists infused, ibotenic acid produced tissue damage furthest from the infusion site, while quisqualic acid infusion affected the smallest volume of tissue of any of the excitatory amino acids infused. Rank ordering of the volume of tissue affected by agonist in terms of volume of [$^3$H]-PK-11195 binding:-

Ibotenic acid > AMPA > NMDA > Quisqualic acid > Vehicle.

## 3.2 Acute Agonist Stimulation of the Basal Forebrain

### 3.2.1 General Observations

Local cerebral glucose utilisation was assessed in conscious rats 15 min after unilateral infusion of AMPA (0.0015M), NMDA (0.09M) or muscimol (0.03M) into the NBM region of the basal forebrain, with simultaneous vehicle infusion into the corresponding region of the contralateral hemisphere.

Intracerebral infusions of AMPA, NMDA or muscimol did not markedly alter the overt behaviour of the rats. The partially restrained rats remained lively and alert, showing normal exploratory behaviour, grooming and sniffing throughout the 1h experimental period. There were no significant alterations in the measured physiological parameters ($pCO_2$, $pO_2$, mean arterial blood pressure and plasma glucose concentration) following intracerebral infusions. All physiological measurements are presented in Table 34.

### 3.2.2 Local Cerebral Glucose Utilisation

*General*

Intracerebral infusions of NMDA, AMPA and muscimol unilaterally into the NBM region of the basal forebrain produced marked alterations in glucose

## TABLE 34

## PHYSIOLOGICAL VARIABLES FOLLOWING AGONIST INFUSIONS INTO THE BASAL FOREBRAIN OF CONSCIOUS RATS

| | TIME AFTER DRUG (min) | AMPA | NMDA | MUSCIMOL |
|---|---|---|---|---|
| Rectal Temperature (°C) | 0 | 36.9 ± 0.3 | 36.9 ± 0.4 | 37.1 ± 0.2 |
| | 50 | 36.7 ± 0.4 | 36.5 ± 0.3 | 36.7 ± 0.1 |
| Mean Arterial Blood Pressure (mmHg) | 0 | 117 ± 5 | 108 ± 8 | 126 ± 4 |
| | 50 | 106 ± 83 | 110 ± 3 | 119 ± 3 |
| Arterial Plasma Glucose (mM) | 0 | 10.2 ± 0.6 | 10.3 ± 0.4 | 9.5 ± 1.1 |
| | 50 | 13.4 ± 1.6 | 11.5 ± 1.0 | 11.8 ± 1.0** |
| $pCO_2$ (mmHg) | 0 | 45 ± 1 | 42 ± 1 | 44 ± 2 |
| | 50 | 44 ± 3 | 45 ± 3 | 39 ± 2** |
| $pO_2$ (mmHg) | 0 | 86 ± 4 | 91 ± 4 | 89 ± 4 |
| | 50 | 93 ± 6 | 97 ± 1 | 98 ± 6 |
| Number of Animals | | 6 | 5 | 5 |

Data are presented as mean ± SEM. Data represent values immediately prior to (0 min) and 50 min after unilateral infusions of AMPA, NMDA or muscimol into the NBM regions of the basal forebrain, and simultaneous infusion of vehicle into the contralateral NBM region. * $p>0.05$, **$p<0.01$ for statistical difference between values at 0 and 50 min post-infusion within each treatment group (Student's paired *t*-test).

utilisation in a number of discrete brain regions. Local rates of glucose utilisation in each of the 50 CNS regions investigated are presented in Tables 35-37.

The statistical analysis adopted *a priori* involved initial comparison of glucose use values in vehicle-infused (contralateral) hemispheres between treatment groups. Glucose use values in the vehicle-infused hemispheres did not differ significantly between the treatment groups in any of the structures investigated. Hence, statistical analysis of the effects of agonist infusions on glucose use was subsequently made by comparing glucose use values in the ipsilateral and contralateral hemispheres within each treatment group.

*Cerebral Cortex*

**AMPA** infusion produced significant reductions in glucose utilisation in ten of the 17 cortical regions investigated, 9 of which corresponded to primary projection targets of NBM efferents (medial and dorsolateral prefrontal cortex, medial frontal cortex (see Figure 35), sensory motor cortex, parietal cortex, hindlimb cortical area, anterior and posterior cingulate and retrosplenial cortex). Glucose use was also reduced in the agranular insular cortex.

**NMDA** infusion only significantly altered glucose utilisation in two cortical regions. Glucose use was reduced in ipsilateral medial prefrontal cortex (-18%). In contrast, a significant increase in glucose use was observed in medial frontal cortex, layers V-VI (+18%). Other cortical regions showed trends towards decreased glucose utilisation (with ANOVA "F" values exceeding the level required for 5% significance, but failing to reach 5% significance in the subsequent independent *t*-test with Bonferroni correction).

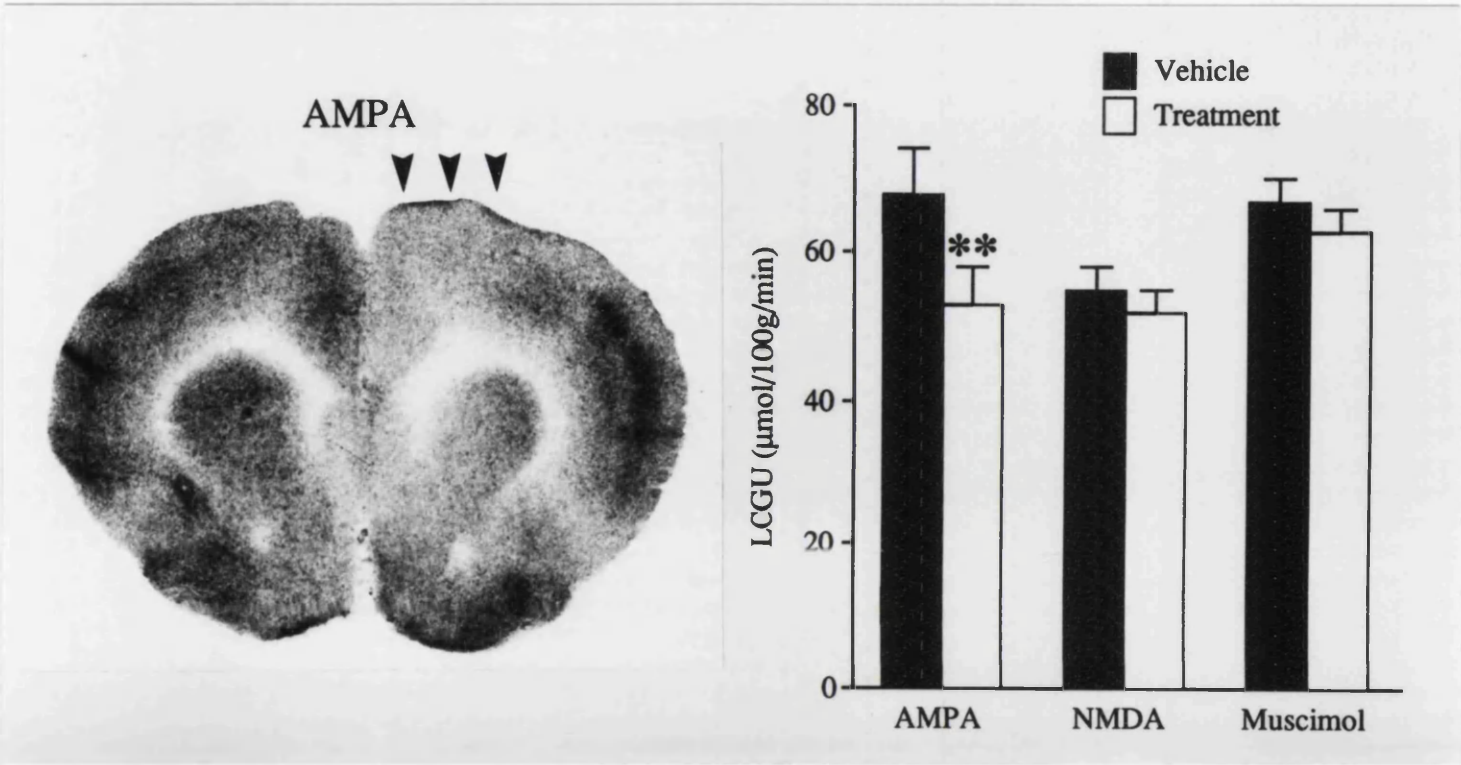


FIGURE 35: REDUCED GLUCOSE USE IN MEDIAL FRONTAL CORTEX AFTER AMPA INFUSION INTO THE BASAL FOREBRAIN

The representative autoradiogram illustrates glucose use acutely after unilateral infusion of AMPA into the NBM region of the basal forebrain. Note the reduced glucose use in the medial frontal cortex of the AMPA-infused (right) hemisphere (arrowheads) relative to the vehicle- infused (left) hemisphere.

The bar chart illustrates local cerebral glucose use (LCGU) in medial frontal cortex of vehicle- and treatment-infused hemispheres, following AMPA, NMDA and muscimol infusions into the NBM. Data presented as mean ± SEM. ** $p < 0.01$, significant difference between vehicle- and treatment-infused hemispheres (Student's paired t-test).

These regions were medial frontal, anterior cingulate and hindlimb area cortex (see Figure 35).

**Muscimol** produced significant, although very small magnitude reductions in glucose use in two cortical regions, retrosplenial (-7%) and agranular insular cortex (-4%). No other cortical regions showed any significant interhemispheric asymmetries following muscimol infusion.

*Sub-Cortical Regions*

**AMPA** induced heterogeneous alterations in glucose use in a number of sub-cortical areas (see Tables 36 and 37). Reduced glucose utilisation was observed in areas of dorsolateral and ventromedial striatum (outwith the hypermetabolic ring around the infusion site, see below) whereas in striatal and pallidal regions infringing on this hypermetabolic zone glucose use was increased. Glucose use was also altered in other sub-cortical regions which were primary or secondary projection targets of striatal/pallidal efferents. Structures showing increased functional activity included the entopeduncular nucleus (+29%), substantia nigra pars compacta (caudal, +19%) and pars reticulata (rostral +38%, caudal +39%) (see Figures 36 and 37). In contrast, glucose use was reduced in mediodorsal thalamus and nucleus accumbens (-9%). Further, AMPA infusion reduced glucose use in the ventrolateral thalamus (-15%), and produced small magnitude elevations in glucose use in the hippocampus molecular layer (+4%) and cerebellar hemisphere (+7%) (see Figures 36 and 37).

**NMDA** infusions resulted in increased glucose utilisation in a number of sub-cortical regions, including striatum, pallidum and their projection targets:-

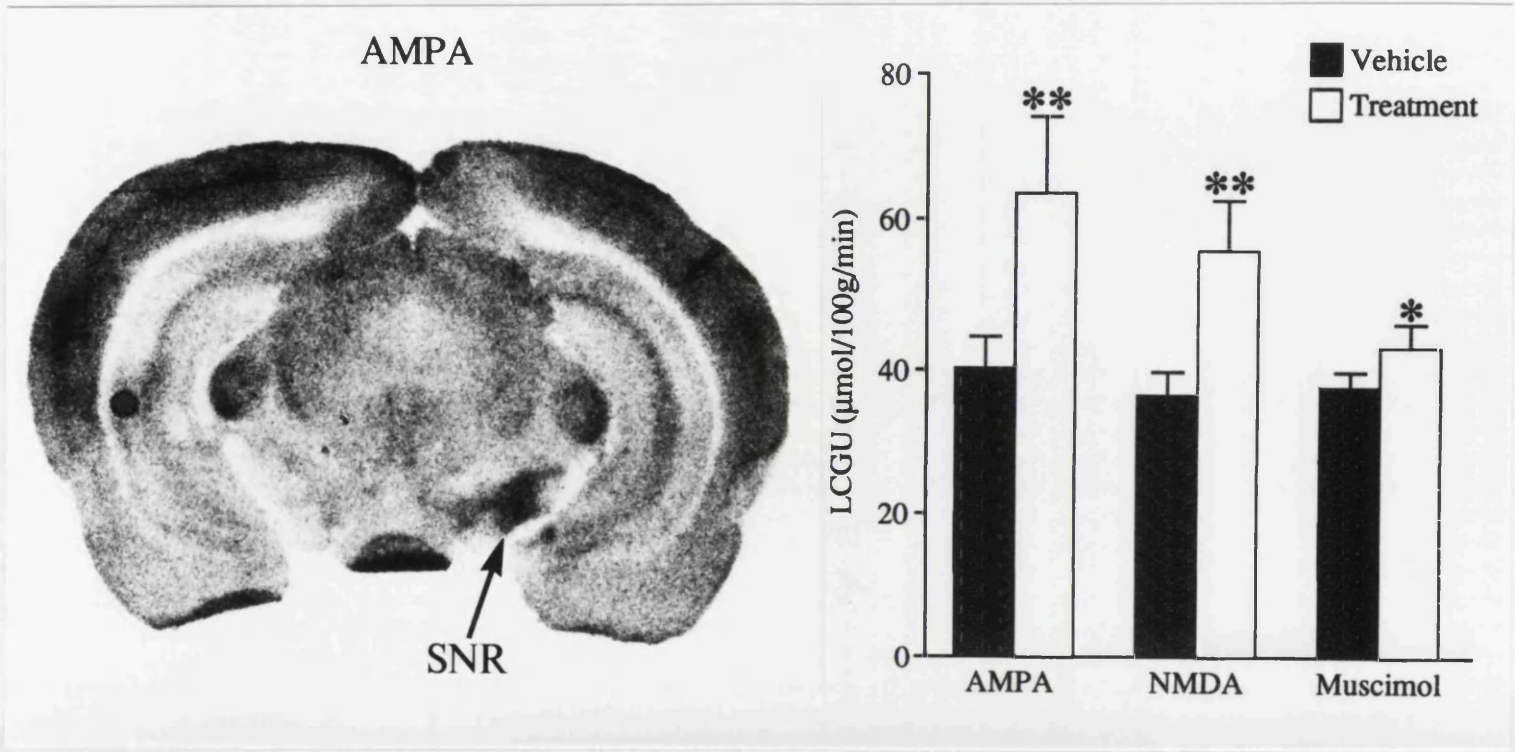


FIGURE 36: INCREASED GLUCOSE USE IN SUBSTANTIA NIGRA PARS RETICULATA AFTER AMPA INFUSION INTO THE BASAL FOREBRAIN

The representative autoradiogram illustrates glucose use acutely after unilateral infusion of AMPA into the NBM region of the basal forebrain. Note the increased glucose use in the substantia nigra pars reticulata (SNR) of the AMPA-infused (right) hemisphere (arrowed) relative to the vehicle-infused (left) hemisphere.

The bar chart illustrates local cerebral glucose use (LCGU) in substantia nigra pars reticulata of vehicle- and treatment-infused hemispheres, following AMPA, NMDA and muscimol infusions into the NBM. Data presented as mean ± SEM. * $p < 0.05$, ** $p < 0.01$, significant difference between vehicle- and treatment-infused hemispheres (Student's paired t-test).

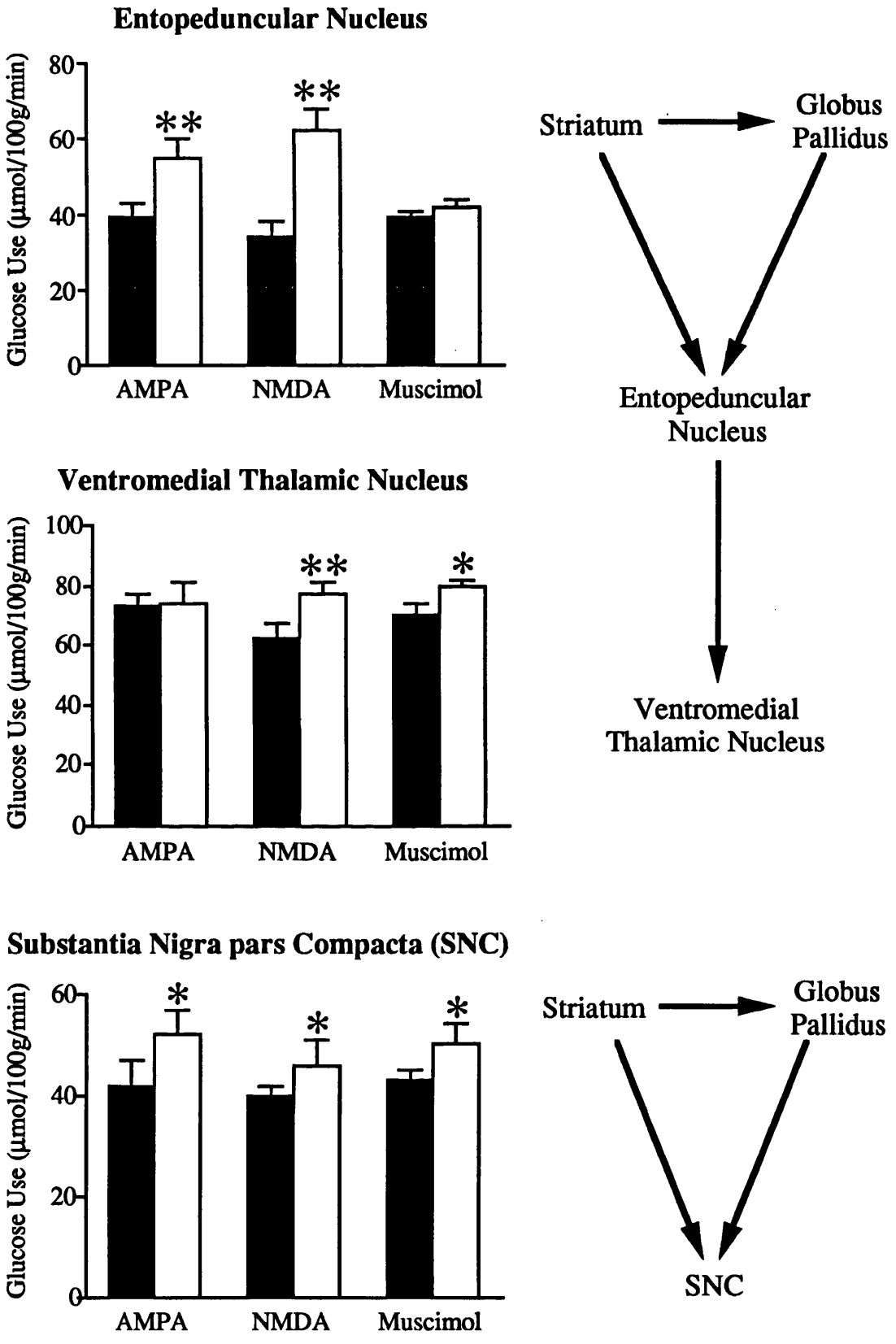


FIGURE 37: GLUCOSE USE CHANGES IN STRIATO-PALLIDAL PROJECTION TARGETS FOLLOWING AGONIST NBM INFUSIONS

Cerebral glucose utilisation in the rat acutely after unilateral AMPA, NMDA or muscimol infusions into the basal forebrain. Data are presented as mean ± SEM, in treatment-infused (■) and vehicle-infused (□) hemispheres. Agonist infusions increased glucose use in the ipsilateral hemisphere, in regions which are primary or secondary components of striato-pallidal projection pathways. * $p < 0.05$, ** $p < 0.01$, significant difference relative to glucose use in vehicle-infused hemispheres.

entopeduncular nucleus (+45%), substantia nigra pars compacta (rostral, +36%) and pars reticulata (rostral, +19%), subthalamic nucleus (+25%), ventromedial thalamus (+19%), and the lateral habenular nucleus (+16%) and in the nucleus accumbens (see Tables 30 and 31, Figures 36 and 37).

In contrast to AMPA and NMDA, **muscimol** infusion into the NBM region induced a reduction in glucose utilisation in the external segment of the globus pallidus, but did not significantly alter glucose utilisation in other pallidal or striatal regions. However, elevations in glucose use were evident in some regions corresponding to striatal/pallidal projection targets, although alterations were smaller in magnitude than those elicited by AMPA and NMDA. Increased glucose use was observed in substantia nigra pars compacta (caudal, +37%; rostral +9%) and pars reticulata (caudal +37%; rostral, +16%), (see Figures 36 and 37), subthalamic nucleus (+5%) and ventromedial thalamus (+13%). In other CNS regions, muscimol significantly elevated glucose use in the medial geniculate body (+12%), inferior colliculus (+8%) and internal capsule (+7%).

*Infusion Site*

Infusions of AMPA and NMDA into the NBM resulted in marked increases in glucose utilisation around the infusion site clearly visible from the autoradiograms in Figure 38. AMPA and NMDA produced massive increases in glucose utilisation in the NBM itself (+76% and +83%, respectively), and in a ring of tissue surrounding the infusion site which extended dorsally from the NBM to affect the striatum and globus pallidus. The extent of this zone of hypermetabolic tissue could be traced in successive brain sections,

LEGEND TO FIGURE 38:

Representative autoradiograms illustrating levels of [$^{14}$C]-2-deoxyglucose (indicative of local rates of cerebral glucose use) in the rat brain acutely after unilateral infusions of AMPA, NMDA or muscimol into the NBM region of the right hemisphere. The anatomical localisation of the infusion site is illustrated in the line diagram. AMPA and NMDA infusions produced marked increases in glucose use in a ring of tissue around the NBM in the ipsilateral hemisphere, extending into striatum and globus pallidus ("hypermetabolic" zone). Note also the reduction in glucose use in ipsilateral medial cortex following AMPA and NMDA infusions, relative to levels in the cortex of the contralateral, vehicle-infused hemisphere. In contrast, muscimol increased glucose use in only a small area within the NBM / ventromedial globus pallidus region and had no apparent effect on glucose use in cortex.

High concentrations of the [$^{14}$C] radiolabel are evident bilaterally in the dorsolateral globus pallidus of all animals. The anatomical localisation of these regions correspnds with the position of the tips of the chronically implanted guide cannulae, suggesting that the concentration of [$^{14}$C]-2-deoxyglucose in these areas results from local tissue damage caused by insertion of the injection cannulae.

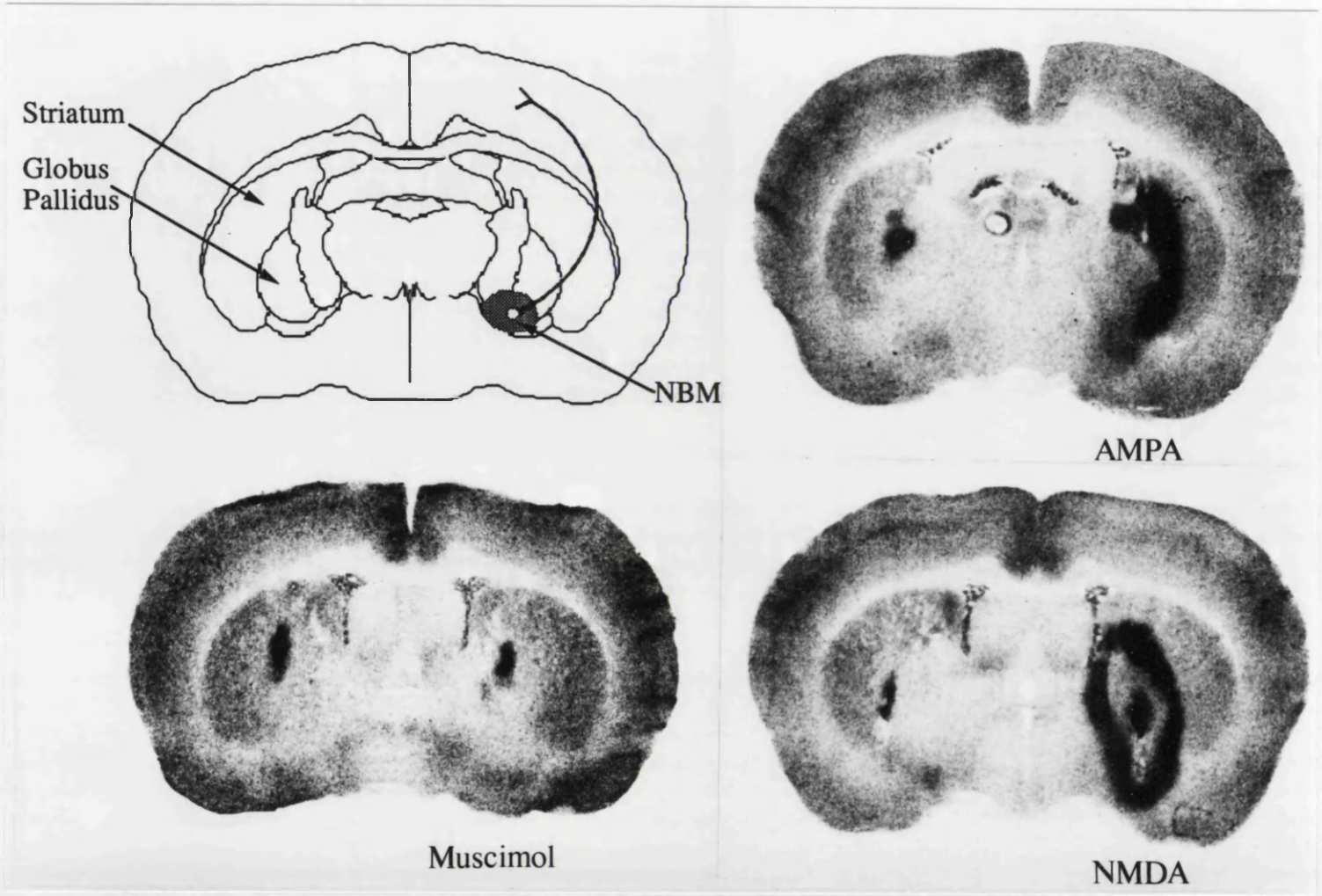


FIGURE 38: ACUTE EFFECTS OF AGONIST INFUSIONS INTO BASAL FOREBRAIN ON CEREBRAL GLUCOSE USE

extending to affect tissue ± 1.6mm and ± 1.3mm rostral and caudal to the locus of the infusion site in the NBM after infusions of NMDA and AMPA, respectively. An area of increased glucose use was also evident in the cortex around the position of the needle placement in NMDA-infused animals (see Figure 38), suggesting the possibility of NMDA back-flow up the needle tract. In contrast to the excitatory amino acid agonists, muscimol induced only a slight increase in glucose use in the NBM, restricted to a small area at the infusion site (see Figure 38).

LEGEND TO TABLES 35, 36 AND 37

Data are presented as mean ± SEM local cerebral glucose utilisation (μmol/100g/min) for structures in ipsilateral and contralateral hemispheres, acutely after unilateral infusion of NMDA (0.009M) (n=5), AMPA (0.0015M) (n=6) or muscimol (0.03mM) (n=5) into the NBM region of the ipsilateral basal forebrain. Vehicle was simultaneously infused into the corresponding region of the contralateral hemisphere. *$p<0.05$, **$p<0.01$ Significant interhemispheric differences within each treatment group (ANOVA, followed by Student's unpaired *t*-test with Bonferroni correction for multiple comparisons).

## TABLE 35

## LOCAL CEREBRAL GLUCOSE UTILISATION 1 HOUR AFTER AGONIST INFUSION INTO BASAL FOREBRAIN: CEREBRAL CORTEX

| | NMDA | | AMPA | | MUSCIMOL | |
|---|---|---|---|---|---|---|
| | IPSILATERAL | CONTRALATERAL | IPSILATERAL | CONTRALATERAL | IPSILATERAL | CONTRALATERAL |
| Prefrontal, Medial: Layer IV | 46 ± 4* | 56 ± 4 | 45 ± 4** | 62 ± 2 | 60 ± 4 | 63 ± 3 |
| Dorsolateral: Layer IV | 55 ± 3 | 58 ± 2 | 53 ± 5* | 65 ± 5 | 67 ± 3 | 68 ± 2 |
| Frontal, Medial: Layer IV | 52 ± 3 | 55 ± 3 | 53 ± 5* | 68 ± 6 | 63 ± 3 | 67 ± 3 |
| Dorsolateral: Layer IV | 65 ± 5 | 62 ± 4 | 67 ± 10 | 75 ± 6 | 74 ± 3 | 76 ± 2 |
| Frontal, Medial: Layer V-VI | 56 ± 4* | 46 ± 4 | 57 ± 7 | 56 ± 4 | 60 ± 2 | 59 ± 2 |
| Parietal: Layer IV | 63 ± 9 | 66 ± 8 | 57 ± 4* | 66 ± 6 | 66 ± 4 | 68 ± 6 |
| Hindlimb | 55 ± 2 | 60 ± 3 | 54 ± 4* | 67 ± 4 | 64 ± 4 | 65 ± 2 |
| Sensory Motor: Layer IV | 71 ± 7 | 64 ± 3 | 55 ± 5** | 69 ± 6 | 73 ± 5 | 73 ± 5 |
| Anterior Cingulate | 56 ± 4 | 63 ± 4 | 54 ± 3** | 73 ± 4 | 69 ± 4 | 74 ± 3 |
| Posterior Cingulate | 64 ± 3 | 66 ± 1 | 64 ± 2** | 75 ± 3 | 69 ± 4 | 73 ± 4 |
| Retrosplenial | 60 ± 3 | 60 ± 2 | 67 ± 3* | 77 ± 5 | 62 ± 5* | 67 ± 4 |
| Auditory, Layer IV | 73 ± 5 | 78 ± 5 | 75 ± 9 | 81 ± 12 | 89 ± 4 | 86 ± 4 |
| Visual, Layer IV | 54 ± 3 | 56 ± 3 | 73 ± 5 | 72 ± 4 | 67 ± 3 | 66 ± 2 |
| Piriform | 72 ± 3 | 69 ± 5 | 76 ± 6 | 73 ± 8 | 76 ± 4 | 76 ± 3 |
| Perirhinal | 44 ± 2 | 46 ± 4 | 63 ± 19 | 66 ± 18 | 53 ± 2 | 52 ± 1 |
| Entorhinal | 47 ± 5 | 43 ± 6 | 44 ± 5 | 49 ± 3 | 44 ± 3 | 41 ± 1 |
| Agranular Insular | 44 ± 3 | 46 ± 3 | 46 ± 2* | 54 ± 4 | 53 ± 3* | 55 ± 3 |

## TABLE 36

## LOCAL CEREBRAL GLUCOSE UTILISATION 1 HOUR AFTER AGONIST INFUSION INTO BASAL FOREBRAIN: EXTRAPYRAMIDAL REGIONS

| | NMDA | | AMPA | | MUSCIMOL | |
|---|---|---|---|---|---|---|
| | IPSILATERAL | CONTRALATERAL | IPSILATERAL | CONTRALATERAL | IPSILATERAL | CONTRALATERAL |
| Nucleus Basalis Magnocellularis (NBM) | 77 ± 14* | 42 ± 6 | 76 ± 17 | 43 ± 3 | 45 ± 6 | 43 ± 3 |
| Striatum: Rostral, Dorsolateral | 80 ± 19 | 57 ± 6 | 61 ± 5** | 66 ± 5 | 63 ± 2 | 64 ± 3 |
| Rostral, Ventromedial | 65 ± 5* | 54 ± 4 | 55 ± 4* | 61 ± 5 | 57 ± 3 | 61 ± 4 |
| Caudal | 60 ± 10 | 48 ± 6 | 58 ± 4 | 57 ± 7 | 58 ± 3 | 58 ± 3 |
| Nucleus Accumbens: Core | 55 ± 6* | 46 ± 6 | 52 ± 3* | 57 ± 3 | 57 ± 1 | 59 ± 2 |
| Ventromedial | 54 ± 5* | 46 ± 3 | 48 ± 4 | 51 ± 5 | 52 ± 2 | 54 ± 2 |
| Globus Pallidus: External Segment | 60 ± 8* | 36 ± 3 | 59 ± 6 | 47 ± 3 | 44 ± 2** | 50 ± 2 |
| Internal Segment | 68 ± 9** | 37 ± 5 | 64 ± 4* | 48 ± 7 | 48 ± 7 | 52 ± 6 |
| Ventral Pallidum | 104 ± 21* | 38 ± 4 | 65 ± 13 | 44 ± 5 | 43 ± 3 | 43 ± 3 |
| Thalamus: Mediodorsal | 71 ± 7 | 73 ± 6 | 70 ± 2* | 76 ± 3 | 73 ± 4 | 73 ± 4 |
| Ventrolateral | 60 ± 6 | 61 ± 6 | 52 ± 3* | 61 ± 2 | 56 ± 1 | 58 ± 2 |
| Ventromedial | 77 ± 4** | 62 ± 5 | 74 ± 7 | 73 ± 4 | 80 ± 2* | 70 ± 4 |
| Subthalamic Nucleus | 73 ± 3** | 55 ± 4 | 62 ± 5 | 54 ± 4 | 56 ± 2** | 53 ± 2 |
| Substantia Nigra Pars Reticulata: (Rostral) | 56 ± 7* | 36 ± 3 | 64 ± 10* | 40 ± 4 | 43 ± 3* | 37 ± 2 |
| (Caudal) | 69 ± 17 | 40 ± 3 | 70 ± 10 | 43 ± 4 | 56 ± 4** | 41 ± 3 |
| Substantia Nigra Pars Compacta: (Rostral) | 54 ± 3** | 44 ± 2 | 60 ± 11 | 45 ± 5 | 48 ± 1** | 44 ± 1 |
| (Caudal) | 46 ± 5 | 40 ± 2 | 52 ± 5* | 42 ± 4 | 56 ± 4* | 41 ± 3 |
| Entopeduncular Nucleus | 62 ± 6** | 34 ± 4 | 55 ± 5** | 39 ± 4 | 42 ± 2 | 39 ± 2 |

## TABLE 37

## LOCAL CEREBRAL GLUCOSE UTILISATION 1 HOUR AFTER AGONIST INFUSION INTO BASAL FOREBRAIN: LIMBIC AND SENSORY MOTOR REGIONS

| | NMDA | | AMPA | | MUSCIMOL | |
|---|---|---|---|---|---|---|
| | IPSILATERAL | CONTRALATERAL | IPSILATERAL | CONTRALATERAL | IPSILATERAL | CONTRALATERAL |
| Hippocampus: Molecular Layer | 50 ± 2 | 49 ± 2 | 52 ± 4* | 50 ± 4 | 58 ± 3 | 54 ± 2 |
| Medial Septum | 46 ± 4 | 45 ± 4 | 51 ± 3 | 50 ± 4 | 51 ± 2 | 51 ± 2 |
| Amygdala | 52 ± 15 | 35 ± 4 | 37 ± 1 | 38 ± 1 | 35 ± 1 | 35 ± 1 |
| Lateral Habenular Nucleus | 95 ± 12* | 80 ± 9 | 88 ± 5 | 82 ± 3 | 91 ± 3 | 94 ± 5 |
| Medial Habenular Nucleus | 58 ± 8 | 58 ± 10 | 54 ± 5 | 55 ± 6 | 54 ± 3 | 56 ± 3 |
| Thalamus: Anteriodorsal | 75 ± 3 | 71 ± 3 | 80 ± 5 | 82 ± 4 | 77 ± 3 | 77 ± 3 |
| Anteriomedial | 69 ± 3 | 70 ± 4 | 82 ± 5 | 84 ± 5 | 81 ± 5 | 79 ± 5 |
| Hypothalamus | 35 ± 3 | 34 ± 3 | 40 ± 3 | 41 ± 4 | 38 ± 1 | 39 ± 1 |
| Dorsal Lateral Geniculate Body | 70 ± 6 | 70 ± 5 | 70 ± 4 | 69 ± 5 | 72 ± 3 | 69 ± 2 |
| Superior Colliculus: Superficial Layer | 58 ± 2 | 58 ± 4 | 67 ± 4 | 67 ± 6 | 62 ± 3 | 64 ± 2 |
| Deep Layer | 61 ± 3 | 59 ± 2 | 59 ± 3 | 58 ± 5 | 61 ± 2 | 59 ± 2 |
| Anterior Pretectal Area | 75 ± 3 | 69 ± 3 | 66 ± 4 | 71 ± 4 | 66 ± 0 | 66 ± 2 |
| Medial Geniculate Body | 67 ± 6 | 70 ± 4 | 65 ± 7* | 68 ± 8 | 76 ± 3** | 68 ± 2 |
| Inferior Colliculus | 116 ± 6 | 117 ± 5 | 107 ± 7 | 107 ± 10 | 116 ± 6* | 107 ± 4 |
| Cerebellar Hemisphere | 42 ± 2 | 44 ± 5 | 46 ± 3* | 43 ± 3 | 41 ± 2 | 40 ± 2 |
| Cerebellar White Matter | 27 ± 3 | 28 ± 3 | 29 ± 3 | 27 ± 2 | 28 ± 2 | 28 ± 1 |
| Internal Capsule | 32 ± 3 | 27 ± 4 | 30 ± 3 | 29 ± 3 | 30 ± 1** | 28 ± 1 |

# CHAPTER IV

# DISCUSSION

## 1. FUNCTIONAL CONSEQUENCES OF AMPA RECEPTOR BLOCKADE

The cellular functions and energy requirements of cerebral tissue components are intimately related. Since neuronal energy requirements are met by oxidative catabolism of glucose, measurements of local rates of glucose utilisation provide direct insight into regional levels of functional activity within the CNS.

Glutamate is the major excitatory neurotransmitter within the CNS, its neurotransmitter action being mediated by a group of post-synaptic excitatory amino acid receptors of which four classes - NMDA, AMPA, kainate and metabotropic have been characterised to date. Glutamate also possesses neurotoxic properties, which has led to the implication of a role for glutamate in the pathogenesis of a number of neurodegenerative disorders. Consequently, the contributions of glutamate receptor subtypes to cerebral functional activity in normal and pathological conditions are of great interest. [$^{14}$C]-2-Deoxyglucose autoradiography provides a means to map *in vivo* functional events following manipulations of specific glutamate receptor populations, as these are reflected by alterations in local rates of cerebral glucose utilisation. In the past, studies involving inhibition of receptor activity have been particularly fruitful in revealing anatomical pathways associated with certain receptor populations. Alterations in rates of glucose metabolism in discrete brain regions after systemic administration of competitive and non-competitive NMDA antagonists have shed light on the polysynaptic pathways modulated by NMDA receptor activity, and on the modes of action of different NMDA antagonist classes (Nehls et al., 1988; Chapman et al., 1989; Kurumaji et al., 1989; McCulloch and Iversen, 1991).

The NMDA receptor has to date been the most intensively studied of the glutamate receptor subtypes due to the availability of several potent NMDA antagonists, while research into non-NMDA receptor subtypes has until recently been restricted by the lack of selective, centrally active antagonists. In the present thesis, the [$^{14}$C]-2-deoxyglucose *in vivo* autoradiography technique has been used to assess the effects of two recently developed potent AMPA receptor antagonists, NBQX and LY-293558, on cerebral glucose utilisation.

Systemic administration of both NBQX (10, 30 and 100mg/kg) and LY-293558 (10, 30 and 100mg/kg) produced marked, anatomically widespread, dose-dependent reductions in glucose utilisation throughout the brain. The metabolic depressant effects observed after administration of the highest doses of NBQX and LY-293558 (100mg/kg) were so great that cerebral glucose use was reduced by up to 68% in a number of brain regions, with reductions of greater than 50% seen predominantly in auditory, cortical and limbic structures. No elevations in glucose use were observed in the fifty regions investigated following any dose of either agent.

In view of the known pharmacologies of these two agents, the metabolic depression induced by NBQX and LY-293558 appears to be attributable to blockade of glutamatergic AMPA receptors (Sheardown et al., 1990; Ornstein et al., 1993). NBQX and LY-293558 both potently inhibit [$^{3}$H]-AMPA binding in rat cortical membranes ($IC_{50}$ values of 0.15μM and 1.35μM, respectively) and reduce AMPA-evoked depolarizations in the rat cortical slice preparations. In addition, both exhibit markedly higher affinity for AMPA rather than kainate receptors (approximately 30-50 fold), but have minimal

affinity for the NMDA receptor subtype. While NBQX has negligible affinity for the NMDA receptor *in vitro* or *in vivo*, LY-293558 does show low affinity for the NMDA receptor recognition site *in vitro*, but has been found to have no effect on NMDA-induced lethality *in vivo*, even at concentrations up to 100 fold greater than the $ED_{50}$ for AMPA-mediated effects (Sheardown et al., 1990; Ornstein et al., 1993). The essentially similar effects of NBQX and LY-293558 on local cerebral glucose use observed in the present study, in terms of the nature, magnitude and anatomical pattern of responses, therefore appear to reflect the comparable pharmacologies of these two agents.

Despite the broad similarity in regional responses to NBQX and LY-293558, results indicated subtle differences in sensitivity in the effects of the two agents on glucose use in certain CNS regions (evident from visual inspection of the autoradiograms (see Figures 14 and 15) and corroborated by marked differences in the values of the ranking function, "*f* ", for the two agents in a small number of regions). The use of the "*f* " ranking function (for arithmetic derivation see Methods, Section 2.2.2) provides a means of assimilating all the information available from the dose-response relationships for each agent in each of the 50 regions investigated, and provides a valuable approach for comparing and contrasting the anatomical patterns of glucose use alterations evoked by different drug treatments. The pharmacological utility of the "*f* " ranking function has previously been illustrated by its ability to separate the cerebral functional effects of the benzodiazepine diazepam, from those of the GABA agonists muscimol and THIP (Kelly et al. 1986). In the present study, correlation analysis of regional *f* values for

NBQX and LY-293558 indicates that glucose use in thalamo-cortical and primary auditory systems is more sensitive to LY-293558 than NBQX (illustrated in Figure 20). In other CNS regions LY-293558 and NBQX appear to be more or less equipotent, or regions exhibit marginally greater susceptibility to NBQX. The clustering of the "*f*" function data into two well accepted functional systems (thalamo-cortical and primary auditory areas) suggests that this phenomenon is not a random numerical artefact, but implies that functional heterogeneity may exist between different AMPA antagonists. Due to the reported high specificity of both NBQX and LY-293558 for the AMPA receptor subtype, and low affinity for other excitatory amino acid receptor subtypes, it appears unlikely that this heterogeneity reflects actions on other receptor populations. While pharmacological studies have not as yet provided strong support for the existence of AMPA receptor subtypes, recent molecular biological evidence of multiple non-NMDA glutamate receptor subunits (Keinanen et al., 1990) indicates there is undoubtedly diversity amongst AMPA receptors which might underly the observed heterogeneous functional consequences of NBQX and LY-293558.

In one of the 50 regions investigated, the superficial layer of the superior colliculus, glucose use was not significantly altered by any dose of either NBQX or LY-293558 (see Figure 15), despite reports of moderate levels of AMPA receptors in this region (Chalmers and McCulloch, 1991). The reason for this lack of response to AMPA blockade is unclear, but may reflect contributions of other transmitter systems to functional activity in this region.

At first sight, the overall patterns of glucose use reductions seen throughout the brain following either NBQX or LY-293558 administration appear to reflect the distribution of receptors in the CNS, since areas in which glucose use was markedly depressed following AMPA receptor blockade, including cortical, hippocampal and thalamic regions, largely correspond to regions in which high densities of AMPA binding sites have been demonstrated in previous autoradiographic and *in situ* hybridization studies (Monaghan et al., 1984; Rainbow et al., 1984; Olsen et al., 1987; Sato et al., 1993). However, closer inspection reveals a number of discrepancies which contradict this view. Firstly, the laminar pattern of glucose use seen in the cortex of control animals, with highest glucose use in layer IV (which is conserved following both NBQX and LY-293558 administration), does not correspond with the reported topography of AMPA binding sites which are located predominantly in outer cortical layers. Most notably, the greatest magnitude reductions in glucose use seen in the present study occurred in auditory regions, despite reports of only relatively moderate AMPA binding site densities in these areas. However, electrophysiological evidence indicates that non-NMDA receptors mediate most of the excitatory input to auditory nuclei (Zhou and Parks, 1991), perhaps explaining the massive impact AMPA receptor blockade has on functional activity in these regions. Further, comparison of the $f$ values generated in the present study for 16 discrete brain regions, with the corresponding reported concentrations of AMPA binding sites (taken from Monaghan et al., 1984) indicates that there is no correlation between the concentration of AMPA receptors in a given region with that region's glucose use response to AMPA blockade by either

LEGEND TO FIGURE 39:

The relationship between the responsiveness of glucose utilisation in 16 brain regions to NBQX or LY-293558, and [$^3$H]-AMPA binding site concentrations in the same regions. Each data point represents the "*f* " value generated from analysis of the entire dose-response curve of a single structure in reponse to NBQX or LY-293558, and specific [$^3$H]-AMPA binding site densities reported in an autoradiographic ligand binding study by Monaghan *et al.* (1984). Values were compared using Pearson's product-moment correlation analysis. Examination of the respective correlation coefficients, *r*, indicates that in the regions studied there is little or no evidence of an association between the concentrations of AMPA receptors and the observed metabolic response to either NBQX ($r = 0.286$) or LY-293558 ($r = 0.0$).

The regions examined were : parietal cortex, frontal cortex (layers I-III, IV and V-VI), lateral and medial geniculate bodies, globus pallidus, dorsolateral striatum, hippocampus CA1, dentate gyrus, entorhinal cortex, lateral habenular nucleus, hypothalamus, olfactory tubercle, cerebellar hemisphere (molecular layer) and cerebellar white matter.

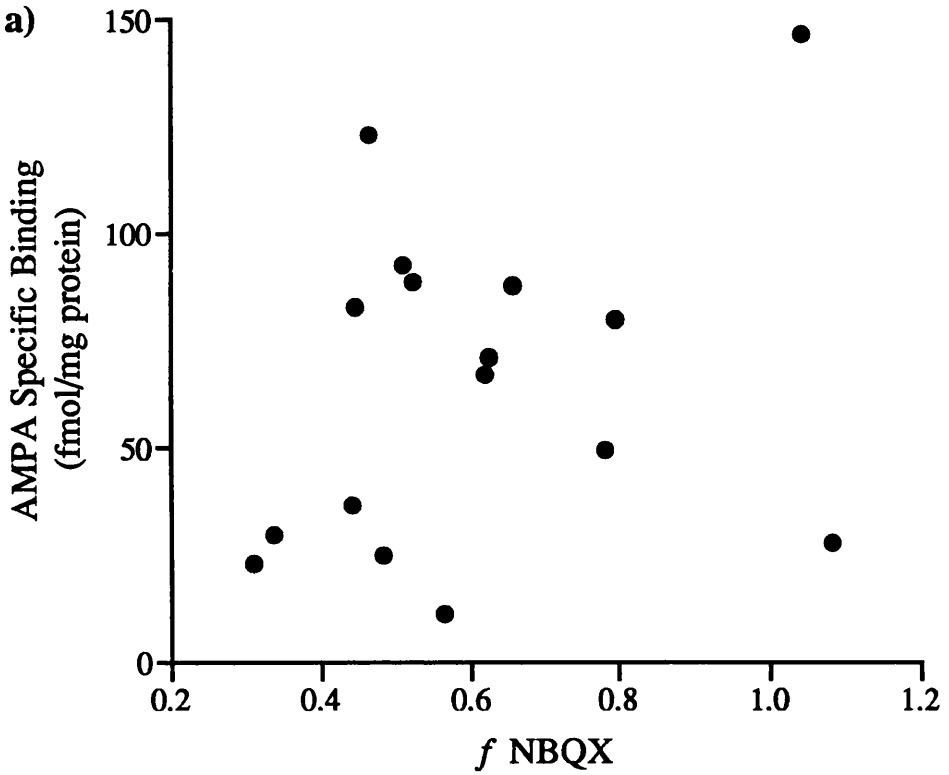


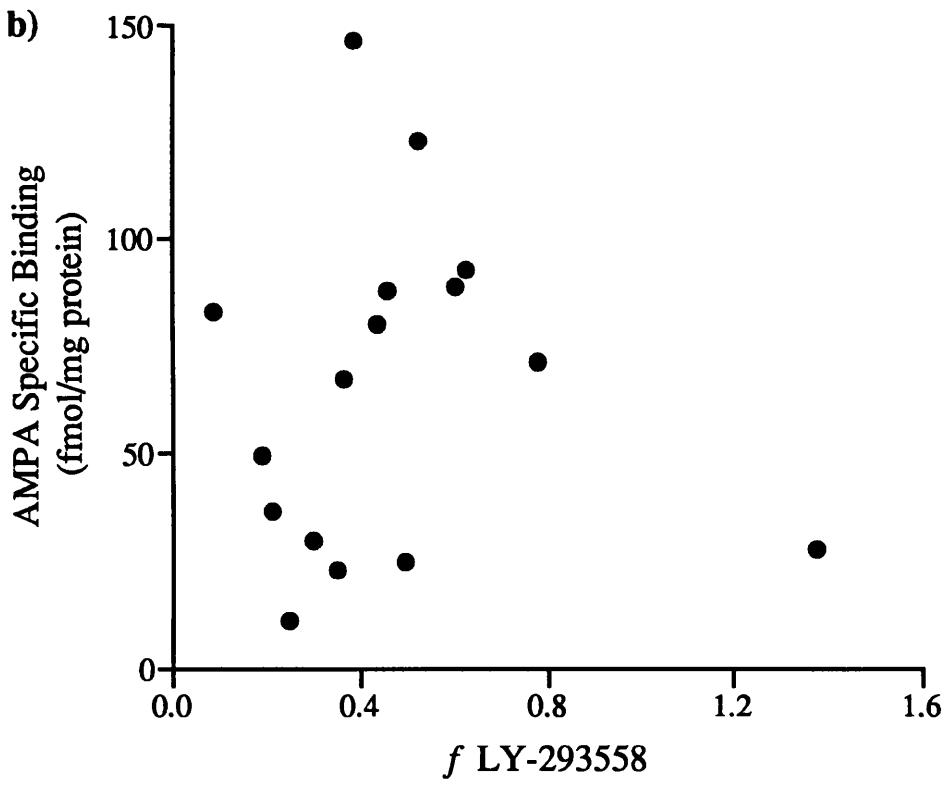


FIGURE 39: RELATIONSHIP BETWEEN [$^3$H]-AMPA BINDING SITE DENSITIES AND *f* VALUES FOR GLUCOSE USE AFTER NBQX OR LY-293558

NBQX or LY-293558 (see Figure 39). It therefore appears that the topography of cerebral glucose use alterations produced by NBQX or LY-293558 more likely reflect the distribution of regions functionally associated with AMPA receptor-mediated activity.

It should be noted that, in a small number of regions, the alterations in glucose use seen in the present study following NBQX (10 and 30mg/kg) contrast with a previous report of the cerebral metabolic effects of this drug. Suzdak and Sheardown (1992) reported selective increases in rates of glucose use in the lateral habenular nucleus, raphe nuclei, superior and inferior colliculus 75 min after systemic administration of NBQX (3-30mg/kg) to conscious rats, whereas in the present study glucose use was either significantly decreased, or showed a trend towards a reduction in these regions. An explanation for these discrepancies is not immediately obvious although a number of factors may contribute, such as the experimental protocol employed, and the timing of the procedure in view of the extremely short plasma half life of NBQX ($t_{\frac{1}{2}}$ = 30 min; Gill, 1992).

The extent of the metabolic depression seen following LY-293558 and NBQX is similar, both in magnitude and in the widespread anatomical distribution, to glucose use reductions previously reported following administration of other CNS depressants, such as barbiturates (Crane et al., 1978; Hodes et al., 1985), GABA agonists (Kelly and McCulloch, 1982: Kelly et al. 1986), and certain inhalation anaesthetics including chloral hydrate, thiopental and halothane (Sokoloff et al., 1977; Shapiro et al., 1978; Grome and McCulloch, 1983). However, although many pharmacological interventions produce reductions in glucose use, the magnitude of the effects

seen with AMPA antagonists in the present study has only been observed previously following doses of barbiturates which produce complete electrocortical silence (Crane et al., 1978). Despite the general similarities between glucose use alterations produced by AMPA antagonists and other CNS depressants, some dissimilarities exist. For example, whereas AMPA antagonists markedly reduce glucose use in limbic regions, barbiturates have been reported to induce only moderate reductions in these areas (15-30%) at doses which maximally depress glucose use in thalamocortical areas (by 50 - 60%). These observations are particularly pertinent in light of reports that barbiturates putatively have an inhibitory action at AMPA receptors in the CNS (Simmonds and Horne, 1988), but the anomalies may be explained by recent reports that the barbiturates thiopental, phenobarbital and pentobarbital exert their actions at the kainate, rather than AMPA, non-NMDA receptor subtype (Frandsen et al., 1990; Zeman and Lodge, 1991).

Examination of the "$f$ " ranking analysis has also highlighted anomalies between the effects of AMPA antagonists and GABA agonists. Comparison of $f$ values following AMPA antagonist administration with previously reported $f$ values generated from a dose-response study of the effects of the $GABA_A$ agonist muscimol (Kelly et al., 1986), suggest inter-regional disparities between the consequences of AMPA receptor blockade and stimulation of inhibitory GABAergic systems within the CNS. The differences between the two classes of CNS depressants are highlighted by the lack of association between $f$ values for muscimol and either NBQX ($r$ = 0.164) or LY-293558 ($r$ = 0.224) treated rats, as illustrated in Figure 40.

LEGEND TO FIGURE 40:

The relationship between the responsiveness of glucose utilisation in 36 brain regions to NBQX or LY-293558 and muscimol. Each data point represents the "*f* " values generated from analysis of the entire dose-response curve of a single structure in reponse to NBQX or LY-293558, and to muscimol. The "*f* " values for the dose-dependent effects of the $GABA_A$ agonist muscimol were taken from a previous [$^{14}$C]-2-deoxyglucose autoradiographic study by Kelly *et al.* (1986). "*f* " values were compared using Pearson's product-moment correlation analysis. Examination of the respective correlation coefficients, *r*, indicates that in the regions studied there is a low degree of association between the observed metabolic responses to muscimol and those to either NBQX ($r = 0.164$) or LY-293558 ($r = 0.224$)

The regions examined were : cortical regions (frontal and sensory motor (layers I-III, IV and V-VI), prefrontal, parietal, visual, auditory and posterior and anterior cingulate), lateral geniculate body, superior colliculus (superficial and deep layers), globus pallidus, substantia nigra *pars compacta* and *pars reticulata*, hippocampus molecular layer, dentate gyrus, entorhinal cortex, lateral and medial habenulae, mammillary body, median raphe nucleus, ventrolateral and mediodorsal thalamus, subthalamus, hypothalamus, inferior colliculus, superior olivary nucleus, cochlear nucleus, medial geniculate body, cerebellar nuclei, cerebellar hemisphere (molecular layer) and cerebellar white matter,.

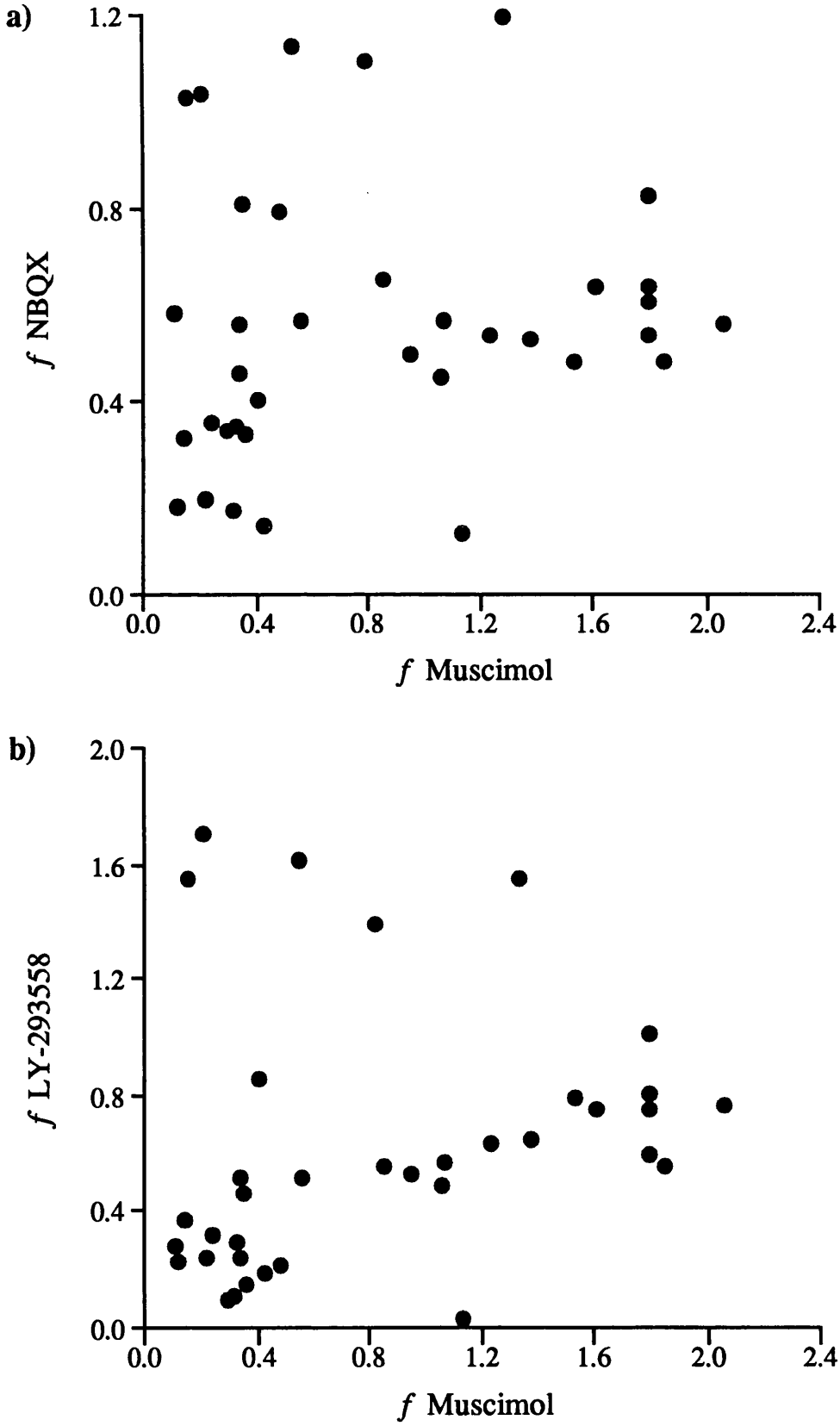


FIGURE 40: RELATIONSHIP BETWEEN *f* VALUES FOR CNS DEPRESSANTS

Following the observations in the present study of marked respiratory depression after administration of both NBQX (30 and 100mg/kg) and LY-293558 (30 and 100mg/kg), concomitant with the widespread depression in glucose utilisation, the possibility arises that the physiological effects of the drugs may affect cerebral energy metabolism resulting in altered glucose utilisation. However, from examination of the effects of hypoxic and hypercapnic conditions on cortical glucose utilisation reported by Borgström et al. (1976), it seems unlikely that the alterations in arterial oxygen tension ($pO_2$) and carbon dioxide tension ($pCO_2$) in the present study are of a large enough magnitude to account for the massive reductions in glucose use. Borgström and colleagues (1976) reported that hypoxia producing an 80% reduction in arterial $pO_2$ for 15 min did not significantly alter the cerebral metabolic rate for glucose. In contrast, hypercapnia producing an increase in arterial $pCO_2$ from 38 ± 1 to 85 ± 2mmHg resulted in an approximate 30% reduction in cortical glucose use. In the present study, the highest doses of NBQX or LY-293558 (100mg/kg) increased arterial $pCO_2$ by only approximately 25% of the increase reported by Borgström et al. (1976), from 40 ± 1 to 50 ± 1 and 56 ± 4mmHg following NBQX and LY-293558, respectively. Therefore, the respiratory depressant effects of NBQX and LY-293558 do not appear to be responsible for the glucose use reductions in the present study.

In view of the capacity of AMPA antagonists to inhibit neuronal excitation, NBQX and LY-293558 might have been predicted to induce global glucose use depression throughout the CNS. Dynamic alterations in glucose use reflect predominantly energy-demanding activity in axonal terminals of

polysynaptic neuronal pathways. Since non-NMDA receptor activation is thought to mediate glutamate-induced neuronal excitation under normal conditions (see MacDermott and Dale, 1987), blockade of AMPA-mediated excitatory events should result in decreased energy demanding activity in axonal terminals of polysynaptic neuronal pathways (see McCulloch, 1982). Thus, the ubiquity of glutamate-excitable neurones and widespread distribution of AMPA receptors throughout the CNS (Monaghan et al., 1984; Rainbow et al., 1984; Cotman et al., 1987; Collingridge and Lester, 1989) may explain the extensive functional depression seen following NBQX and LY-293558. However, as is illustrated in Figure 41, the patterns of glucose use alterations seen in the present study contrast strikingly with those induced by NMDA receptor antagonists which might also, at the most simplistic level, have been expected to reduce neuronal excitability and hence depress function. Instead, systemic administration of competitive and non-competitive NMDA antagonists has been found to produce heterogeneous alterations in glucose use. Non-competitive NMDA antagonists such as MK-801 and phencyclidine (PCP) markedly increase glucose use in anatomical components of the limbic system (in particular posterior cingulate and entorhinal cortices, hippocampus, mamillary body, substantia nigra *pars compacta* and *pars reticulata*), while moderately reducing glucose use in neocortex and the inferior colliculus (Weissman et al., 1987; Nehls et al., 1988; Kurumaji et al., 1989; McCulloch and Iversen, 1991). In contrast, while non-competitive NMDA antagonists produce largely similar patterns of altered glucose use, competitive antagonists display heterogeneous effects on glucose use. For example, CPP and AP7 induce few overt glucose use changes, whereas CPP-

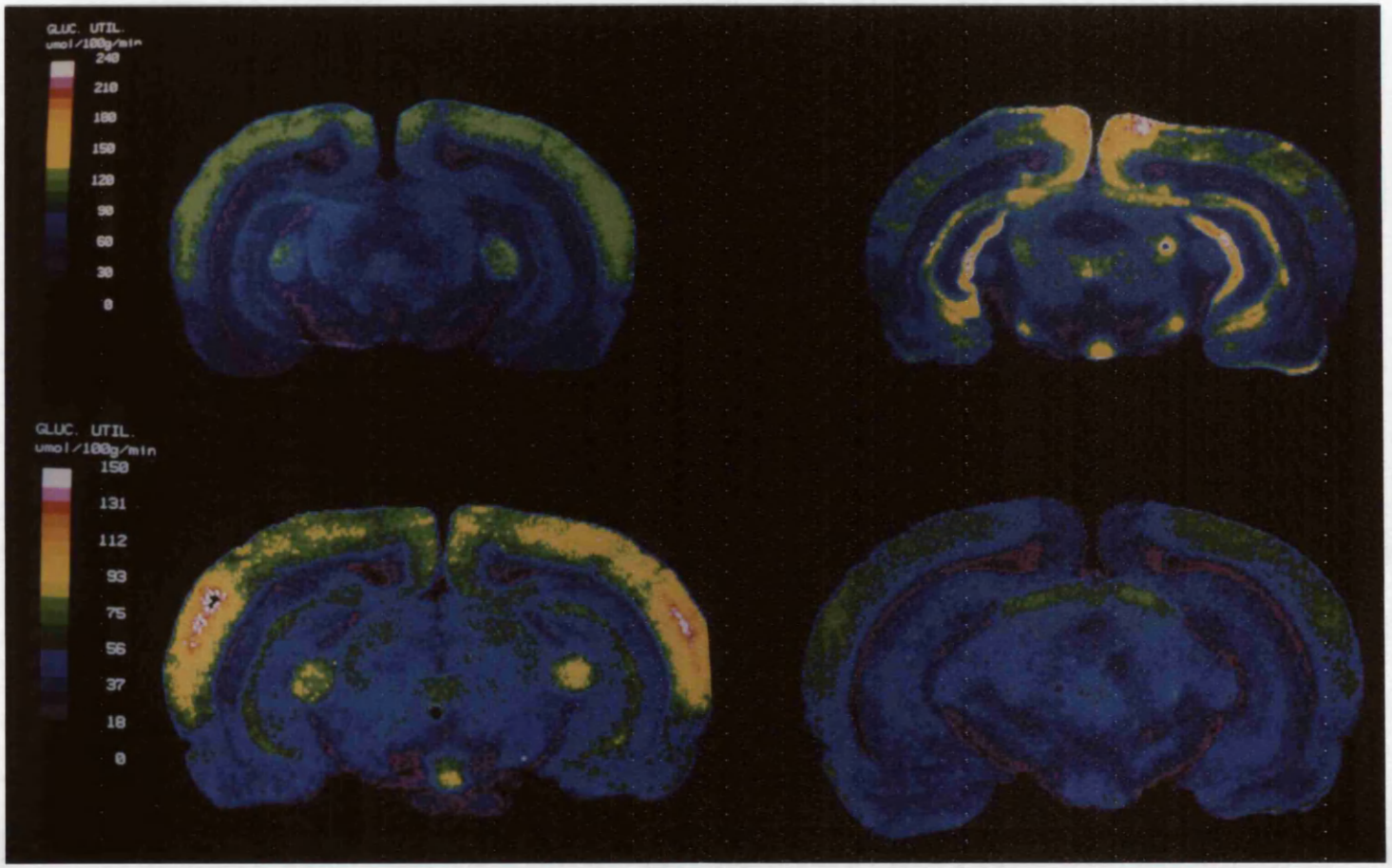


FIGURE 41: HETEROGENEOUS EFFECTS OF AMPA AND NMDA RECEPTOR BLOCKADE ON GLUCOSE USE

Representative colour-coded autoradiograms, at the level of the medial geniculate body / superior colliculus, following intravenous administration of :- TOP: MK-801 (0.5 mg/kg; right) or vehicle (left); BOTTOM: LY-293558 (30 mg/kg; right) or vehicle (left). The colour bars denote rates of glucose utilisation. Note the marked increase in glucose use in limbic regions (posterior cingulate cortex, hippocampus) following MK-801, relative to control levels. In contrast, widespread glucose use depression is evident following LY-29355, except in the superior colliculus superficial layer.

ene reduces glucose use in sensory regions including auditory and visual structures, while not markedly affecting glucose use in limbic regions (Chapman et al., 1989; Kurumaji et al., 1989; Inglis et al., 1992). In addition, the AP7 analogue CGP-39551 (2-amino-4-methyl-5-phosphono-3-pentanoic acid 1-ethyl ester), a potent orally active competitive NMDA antagonist, induces large increases in glucose use in limbic, extrapyramidal, and olfactory regions, but does not affect sensory regions (Chapman et al., 1991).

The basis for the differences in metabolic responses to NMDA and AMPA receptor blockade are not yet fully understood, although differences appear to reflect divergent mechanisms of actions between the drug classes. For example, the hypermetabolic sequelae of non-competitive NMDA antagonists such as MK-801 are thought to reflect the use-dependent nature of non-competitive receptor inhibition, which leads to potentiation of blockade in areas of high glutamatergic activity (Kurumaji et al., 1989). In contrast, competitive NMDA and AMPA receptor antagonists will be competitively and readily displaced by the endogenous agonist during intense glutamatergic activity.

The contrasting patterns of glucose use alterations produced by NMDA antagonists and the AMPA antagonists NBQX and LY-293558 may have some bearing on the clinical utility of these drugs as anti-ischaemic agents. Overwhelming evidence that NMDA antagonists are potent neuroprotectants led to a role in the management of ischaemic injury being proposed (for review see McCulloch and Iversen, 1991). However, observations of marked focal increases in glucose utilisation in components of the limbic system after administration of NMDA antagonists such as MK-801, PCP and CGS-19755

have led to major concern about the safety of these drugs, since metabolic changes in areas such as the posterior cingulate cortex following NMDA antagonist administration have been shown to precede (and may contribute to) the appearance of pathomorphological changes in neurones, such as cytosolic swelling and vacuolisation (Olney et al., 1989, 1991; Hargreaves et al., 1993). In addition, hypermetabolic sequelae in limbic regions have been suggested to be involved in the psychotomimetic properties of NMDA antagonists such as PCP. The absence of any focal elevations in glucose use following systemic administration of AMPA antagonists, as demonstrated in the present study, therefore suggests that the morphological changes associated with NMDA antagonists are an unlikely consequence of AMPA antagonist administration.

In the present investigation the dose range studied encompassed the range over which the AMPA antagonists NBQX and LY-293558 have been demonstrated to be neuroprotective against glutamate-mediated excitotoxicity and ischaemic cell death both *in vitro* (Choi, 1991) and *in vivo*. Significant reductions in the size of ischaemic lesions produced by middle cerebral artery (MCA) occlusion in the rat have been seen after dual administration of NBQX (30mg/kg) pre- and post-occlusion up to 60 min apart (Buchan et al., 1991; Gill et al., 1992), while in experimental models of global ischaemia 3 injections of NBQX (30mg/kg) within 30 min are typically required to significantly reduce neuronal injury (Sheardown et al., 1990, 1993; Buchan et al., 1991; Diemer et al., 1992). In addition, NBQX (30mg/kg) is neuroprotective against the delayed neuronal death seen in the hippocampus following transient forebrain ischaemia even when administered up to 24h after the initial insult,

and under circumstances in which NMDA antagonists are ineffective (Buchan et al., 1991; Buchan and Pulsinelli, 1991; Diemer et al., 1992; Nellgard and Wieloch, 1992; Sheardown et al., 1993). It should be noted that this neuroprotective dose of NBQX (30mg/kg) was the lowest dose found to significantly depress glucose use in any of the CNS regions investigated in the present study.

The impact of the novel AMPA antagonist LY-293558 on ischaemic neuronal death has not yet been investigated as extensively as NBQX. However, an initial study in a model of focal cerebral ischaemia in the cat indicates that LY-293558 (15mg/kg) is neuroprotective at lower doses than NBQX (Bullock et al., 1993). In corollary, in the present thesis LY-293558 (10mg/kg) significantly reduced glucose use in seven of the 50 regions examined, whereas NBQX (10mg/kg) did not significantly alter glucose use in any regions.

In conclusion, the observations of almost global reductions in glucose utilisation following AMPA receptor blockade by systemic administration of NBQX and LY-293558, taken together with previous reports of their neuroprotective properties under conditions of ischaemia and glutamate-induced excitotoxicity, indicate that the use of AMPA antagonists as potential therapeutic agents for the management of cerebral ischaemia in man is unlikely to be complicated by concerns over adverse hypermetabolic CNS sequelae, in contrast to the effects of NMDA antagonists. However, it should be noted that there are a number of factors which may restrict the clinical utility of NBQX and LY-293558. These include the low solubility of NBQX in aqueous media and its poorly defined penetration of the blood-brain barrier

(Gill, 1992), reports of precipitation of NBQX in renal tubercles, together with the evidence from the present study of CNS and respiratory depression following systemic administration of neuroprotective doses of NBQX (30 and 100mg/kg) and LY-293558 (30 and 100mg/kg).

## 2. NMDA RECEPTOR MANIPULATION

The NMDA subtype of excitatory amino acid receptors is believed to play an important role in processes of learning and memory. Activation of NMDA receptors has been linked with the mechanism of long-term potentiation (LTP) which is hypothesised to be intrinsic to learning and memory (Collingridge and Bliss, 1987). Competitive and non-competitive NMDA receptor antagonists have been found to block induction of LTP in both the hippocampus and cortex, while the competitive NMDA antagonist AP5 has been shown to impair learning of cognitive tasks in rats (Morris et al., 1986; Danysz et al., 1988). It has therefore been suggested that compounds which enhance glutamatergic transmission at the NMDA receptor, such as agonists interacting with the NMDA receptor-associated glycine site, may facilitate learning and memory in pathological conditions involving impaired cognitive function, such as Alzheimer's disease (AD). This proposal has gained further support following a report that glycine stimulation of [$^3$H]-MK-801 binding at the NMDA receptor channel site is reduced in the cerebral cortex of Alzheimer's disease patients (Procter et al., 1989). Observations that full NMDA transmitter site agonists and glycine site agonists may exacerbate NMDA receptor-mediated neurotoxicity, and can produce convulsions, have led to glycine site partial agonists such as D-cycloserine being proposed as

putative cognitive enhancers.

D-Cycloserine is a partial agonist at the strychnine-insensitive glycine regulatory site on the NMDA receptor (Hood et al., 1989; Watson et al., 1990; Emmett et al., 1991). This compound, which has been in clinical use as an antibiotic for a number of years, was initially identified as a potential cognitive enhancer following observations that it readily crosses the blood-brain barrier and is centrally active (Mandell and Sardt, 1990). D-Cycloserine has subsequently been found to improve performance of learning and memory tasks in rodents (Handelman et al., 1988; Monahan et al., 1989; Flood et al., 1992), and has been shown in rats to reverse the impairments produced in learning tasks by hippocampal lesions (Schuster and Schmidt, 1992), or by treatment with the muscarinic antagonist scopolamine (Sirviö et al., 1992). In postmortem studies, Chessell and colleagues (1991) have demonstrated that D-cycloserine can potentiate NMDA receptor activation, which has been shown to be impaired in cortical neurones of AD patients (Procter et al., 1991). Consistent with the partial agonist profile of D-cycloserine, Chessel et al. (1991) reported that D-cycloserine (0.1-100μM) enhanced [$^{3}$H]-MK-801 binding in AD cortex homogenates, producing a maximal stimulation of 64% of the response induced by glycine alone. At higher concentrations (>100μM), D-cycloserine exhibited antagonist properties, producing a marked reduction in [$^{3}$H]-MK-801 binding.

In the current thesis, experiments have been performed in rats to try to further characterise the actions of D-cycloserine *in vivo*. Quantitative [$^{14}$C]-2-deoxyglucose and [$^{125}$I]-MK-801 autoradiographic techniques were employed to investigate the dose-dependent effects of D-cycloserine on local

cerebral glucose use, and the effects of a putative agonist concentration of D-cycloserine (3mg/kg) on NMDA receptor activation, respectively. In addition, the effects of D-cycloserine (3mg/kg) on glutamate-induced neurotoxicity were investigated in models of focal cerebral ischaemia (MCA occlusion), and in a model of cortical glutamate neurotoxicity. The proposed agonist dose of D-cycloserine (3mg/kg), employed in these studies was determined from previous reports of potentiation of NMDA receptor-mediated responses *in vivo*, including observations of enhanced learning in behavioural tests (Handelman et al., 1988; Monahan et al., 1989), and increased NMDA receptor-mediated cGMP turnover in mouse cerebellum (Emmett et al., 1991).

*Local Cerebral Glucose Utilisation*

D-Cycloserine (0.3, 3 or 30mg/kg) had no significant effects on cerebral glucose use in conscious rats, in any of the 51 CNS regions investigated. Since behavioural and biochemical studies have previously indicated enhanced functional activity within the brain following systemic administration of D-cycloserine within the range of 1-10mg/kg (Handelman et al., 1988; Monahan et al., 1989b; Wood et al., 1989; Emmett et al., 1991), the results of the present study suggest that the [$^{14}$C]-2-deoxyglucose technique is insensitive to any subtle effects on cerebral metabolism which may be associated with the functional consequences of D-cycloserine, within the dose range examined. However, examination of the dose-response curves for D-cycloserine (Figures 21 and 22) reveals a striking degree of similarity, within regions, between glucose use values for each concentration investigated, with very few regions showing any trends towards alterations in glucose use, and a small degree of

variance at each dose. This observation suggests that it is unlikely that any insensitivity in the [$^{14}$C]-2-deoxyglucose method is masking biologically relevant glucose use alterations evoked by D-cycloserine. It should be taken into consideration that regional glucose use values reflect overall rates of glucose utilisation in a given structure, but do not allow spatial resolution at the cellular level. Hence, dynamic metabolic changes in one neuronal population within a structure may be counterbalanced by opposite changes in another population within the same region, resulting in no apparent glucose use change overall. Another factor which may influence outcome is the timing of the glucose utilisation measurement relative to drug administration. In the present study, the [$^{14}$C]-2-deoxyglucose procedure was initiated 15 min after intravenous injection of D-cycloserine. The profile of [$^{14}$C]-2-deoxyglucose uptake from circulating plasma into brain tissue, as described by Sokoloff and colleagues (1977), indicates that [$^{14}$C]-2-deoxyglucose is rapidly extracted from plasma in a concentration-dependent manner, so that the bulk of the injected bolus is taken up from the plasma within the first 15 min after intravenous injection (as illustrated in Figure 42). Hence glucose use measurements reflect predominantly [$^{14}$C]-2-deoxyglucose uptake in the first 15 min of the 45 min measurement period. In the behavioural studies of the effects of D-cycloserine, learning tasks were assessed over the initial 30 min period post-drug administration (Handelman et al. 1988; Monahan et al., 1989b). Hence the period over which [$^{14}$C]-2-deoxyglucose uptake was measured after D-cycloserine administration is consistent with the experimental period employed in behavioural tests, and with measurements of cerebellar cGMP activity assayed 30 min post-drug (Emmett et al., 1991).

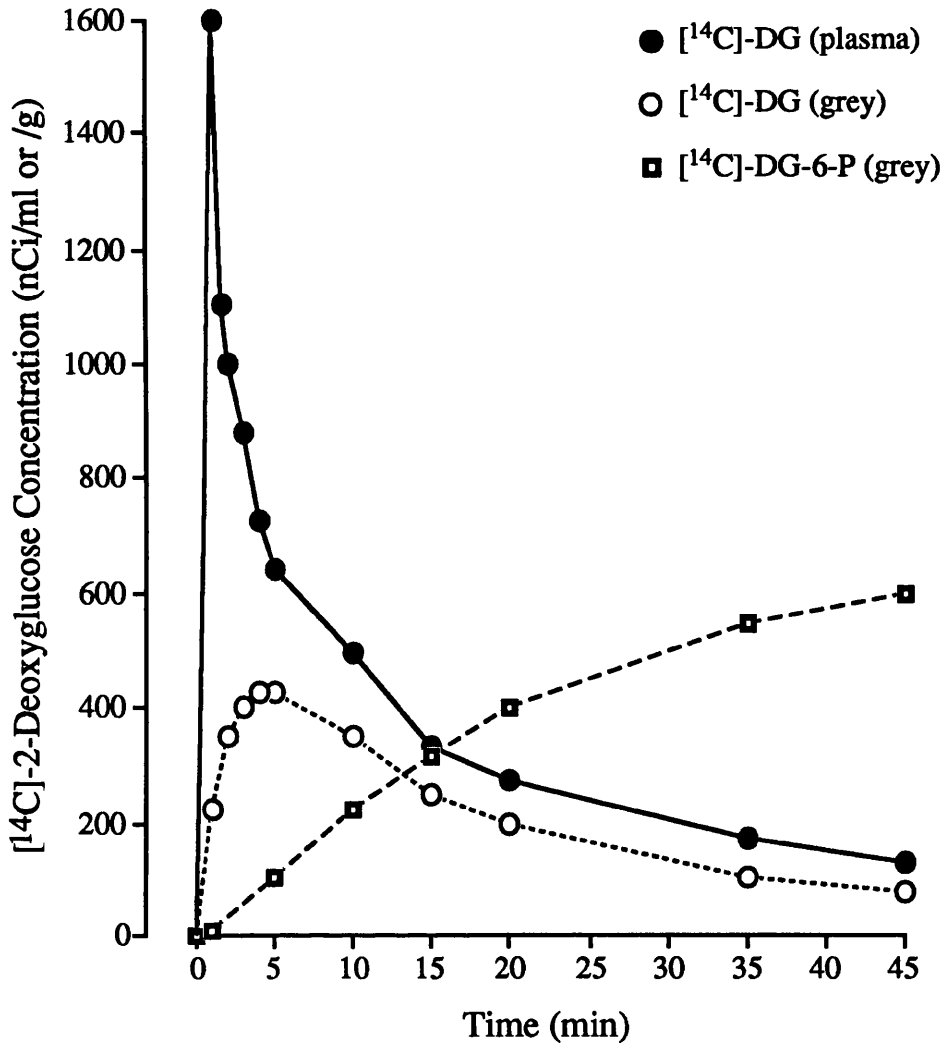


FIGURE 42: [$^{14}$C]-2-DEOXYGLUCOSE UPTAKE FROM ARTERIAL PLASMA

Graphical representation of the time courses of [$^{14}$C]-2-deoxyglucose ([$^{14}$C]-DG) concentrations in arterial plasma and grey matter, and [$^{14}$C]-2-deoxyglucose-6-phosphate ([$^{14}$C]-DG-6-P) concentration in grey matter, over the 45 min experimental period following an intravenous pulse of 50 μCi [$^{14}$C]-2-deoxyglucose at time 0 min (after Sokoloff et al., 1977). The plasma curve was derived from measurements of plasma [$^{14}$C]-2-deoxyglucose concentrations. Tissue concentrations are average levels calculated from the plasma curve and the mean values of the rate constants for the operational equation for the procedure, $k_1$*, $k_2$* and $k_3$*, for 15 grey matter regions in the conscious rat (see Sokoloff et al., 1977).

Note the rapid extraction of [$^{14}$C]-2-deoxyglucose from the circulating arterial blood over the first 15 min after intravenous injection. In excess of 75% of the isotope has been taken up from the plasma within 15 min of injection.

It therefore appears unlikely that the timing of the experimental protocol in the present study would mask any cerebral metabolic effects of D-cycloserine.

Although the [$^{14}$C]-2-deoxyglucose *in vivo* autoradiography technique has previously proved to be a potent tool for investigating the cerebral metabolic consequences of numerous pharmacological and physiological manipulations, there are examples of pharmacological agents with known actions on function which do not markedly affect cerebral glucose utilisation. For instance, intravenous administration of the prostaglandin synthesis inhibitor indomethacin has previously been shown to have no significant effect on glucose use in the CNS, despite evidence that corresponding doses of indomethacin significantly reduce cerebral blood flow and inhibit cerebral prostaglandin synthesis (McCulloch et al., 1982a). Since neurochemical and electrophysiological evidence indicates that prostaglandins are involved in synaptic transmission, affecting adenylate cyclase activity and cell firing rates in a number of brain regions, it is of interest that modulation of their functional activity by indomethacin is not reflected by changes in glucose use. These observations further support the implication from the present study that assessment of cerebral glucose utilisation by [$^{14}$C]-2-deoxyglucose technique does not adequately reflect the cerebral functional sequelae of D-cycloserine administration.

*[ $^{125}$I]-MK-801 Binding*

The density and distribution of [$^{125}$I]-MK-801 binding sites *in vivo* is thought to reflect the extent of NMDA receptor activation, since MK-801 can

only gain access to its binding site when the NMDA channel is open, during receptor activation. McCulloch et al. (1992) have previously demonstrated that the use of [$^{125}$I]-MK-801 technique to map the distribution of activated NMDA receptors in the brain is optimally exploited under circumstances of abnormal NMDA receptor activation, such as during an ischaemic insult when extracellular glutamate levels are markedly elevated. Hence, it was hypothesised that an agonist dose of D-cycloserine (3mg/kg) might potentiate NMDA receptor activation, resulting in elevated levels of [$^{125}$I]-MK-801 binding in the CNS. [$^{125}$I]-MK-801 binding site densities were predicted to be highest in CNS regions rich in NMDA receptors, in particular hippocampal regions CA1 and CA3 (Monaghan et al., 1985). In the present study, the effect of D-cycloserine (3mg/kg) on [$^{125}$I]-MK-801 binding in conscious rats was compared with levels of [$^{125}$I]-MK-801 binding in conscious and halothane-anaesthetised control (vehicle-treated) rats. D-Cycloserine did not significantly alter [$^{125}$I]-MK-801 binding densities in any of the 13 brain regions examined, relative to either control group. The pattern of [$^{125}$I]-MK-801 binding measured by this *in vivo* autoradiographic technique was similar to the previously reported distribution of NMDA receptors determined in *in vitro* autoradiographic methods, with highest levels in hippocampal regions, in particular CA1, and lowest levels in the hypothalamus and cerebellum.

*Glutamate-Induced Neurotoxicity*

Following the apparent lack of effect of a putative agonist dose of D-cycloserine (3mg/kg) on [$^{3}$H]-MK-801 binding *in vivo* and the

ineffectiveness of D-cycloserine (0.3, 3 and 30mg/kg) on local cerebral glucose use, it was decided to further investigate the effects of D-cycloserine (3mg/kg) on glutamate-mediated events under pathological conditions. Two experimental models were used to investigate glutamate excitotoxicity *in vivo*: permanent middle cerebral artery (MCA) occlusion, and intracortical perfusion of glutamate. In the light of previous *in vivo* demonstrations of agonist properties of this dose of D-cycloserine (3mg/kg) (Handelman et al., 1988; Monahan et al., 1989b; Emmett et al., 1991), and reports of the intrinsic involvement of NMDA receptor activity in the neurotoxic actions of glutamate (see Choi, 1987), D-cycloserine might have been predicted to exacerbate the effects of glutamate, via potentiation of NMDA receptor activity, in both models of neurotoxic damage. However, neither the volume of ischaemic damage produced by permanent MCA occlusion or the volume of neuronal damage produced by cortical glutamate perfusion, were significantly altered following systemic administration of D-cycloserine.

The MCA occlusion experimental model of focal cerebral ischaemia allows assessment of drug actions on glutamate-mediated neurotoxic events *in vivo*, in a model closely resembling the effects of stroke injury in the CNS. Using this model, the *in vivo* neuroprotective properties of a number of excitatory amino acid receptor antagonists, such as MK-801 and NBQX, have previously been demonstrated. The lack of efficacy of D-cycloserine in this model may simply reflect the concentration of D-cycloserine, or alternatively, the experimental protocol employed (D-cycloserine was administered 15 min and 255 min after onset of ischaemia). However, perhaps the most likely explanation for the lack of efficacy of D-cycloserine

in this model is the possibility of saturation of the glycine site *in vivo* by endogenous glycine, which will be discussed in greater detail later.

In contrast to the MCA occlusion model, the cortical glutamate perfusion model of glutamate-induced neuronal damage facilitates investigation of the effects of systemic drug administration on the neurotoxic actions of glutamate in a model which is uncomplicated by factors which may contribute to the mechanism of ischaemic injury, such as reduced blood flow. Retrograde dialysis of glutamate (0.5M) into the cerebral cortex in rats produces a discrete, well-defined and reproducible lesion within the cortex. In the present study, systemic administration of D-cycloserine (3mg/kg) had no effect on the size of the glutamate-induced lesion. There are a number of possible explanations for this lack of response to D-cycloserine. The first concerns the integrity of the procedure. In order to verify the utility of the glutamate perfusion model as a representative model of excitatory amino acid receptor-mediated events *in vivo*, the effects of the AMPA antagonist NBQX were investigated in the same model. NBQX has previously been shown to ameliorate glutamate-mediated neuronal damage in both global and focal models of ischaemic damage (minimum neuroprotective dose: 30mg/kg) (Buchan et al., 1991a; Gill et al., 1992). Consequently, NBQX (30mg/kg) was found to significantly reduce the volume of neuronal damage in the glutamate perfusion model by approximately 25% (see Figure 28).

The effects of other agents which putatively modulate glutamatergic activity have also been investigated previously in this model of cortical neurotoxicity, summarised in Figure 43 (see also Fujisawa et al., 1993). Systemic administration of the non-competitive NMDA antagonist MK-801,

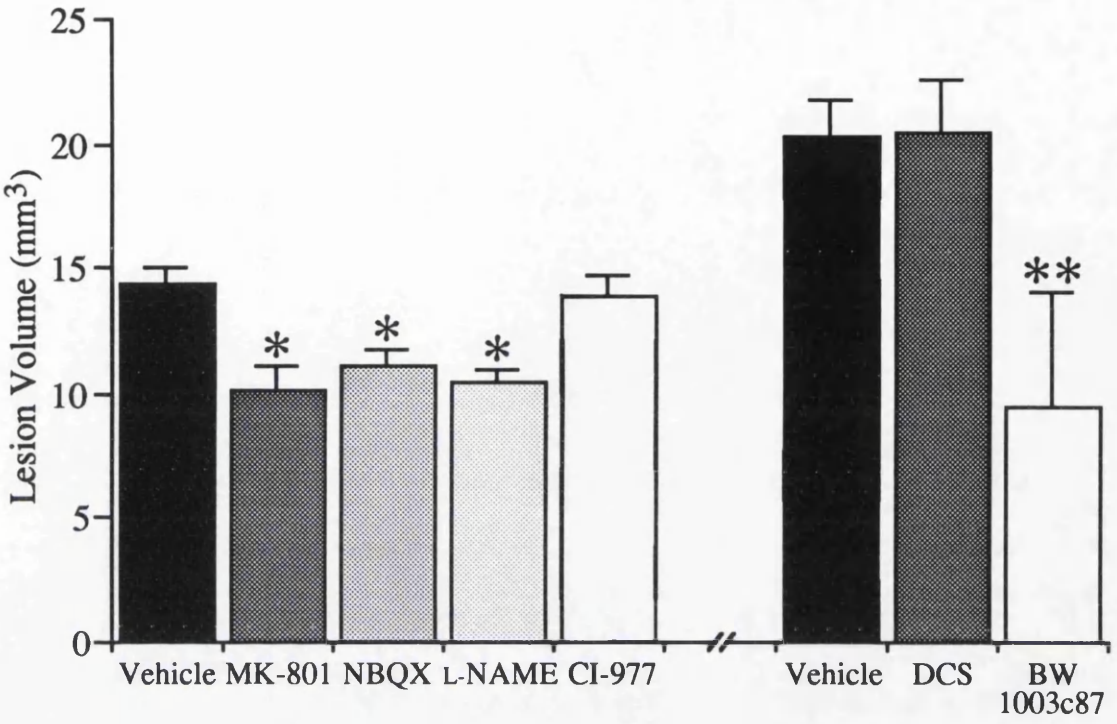


FIGURE 43: THE EFFECTS OF GLUTAMATERGIC MANIPULATION ON CORTICAL NEURONAL DAMAGE

The effects of systemic administration of previously reported neuroprotective doses of MK-801 (0.5mg/kg; NMDA antagonist), NBQX (2 x 30mg/kg; AMPA antagonist), L-NAME (10mg/kg; nitric oxide synthase inhibitor) and CI-977 (2 x 0.3mg/kg; kappa opioid antagonist) on the extent of neuronal damage produced by intra-cortical glutamate (0.5M) perfusion, were investigated relative to the lesion volume in vehicle (5.5% glucose) - treated rats . In a separate study, the effects of D-cycloserine (3mg/kg; NMDA receptor glycine site partial agonist) and BW-1003c87 (20mg/kg; sodium channel blocker) were investigated in the same model, relative to vehicle (saline) - treated animals. Data are presented as mean ± SEM, * $p < 0.05$, ** $p < 0.01$ statistical difference relative to the appropriate vehicle group (ANOVA, followed by Student's unpaired t-test).

Agents which modify glutamate-mediated events via post-synaptic actions (*ie.* MK-801, NBQX, L-NAME and possibly BW-1003c87) produced marked reductions in the volume of neuronal damage in the cortex. In contrast, neither the pre-synaptic glutamate release inhibitor CI-977 or the putative agonist dose of D-cycloserine significantly altered lesion volume (see also Fujisawa et al., 1993).

or the nitric oxide synthase inhibitor L-nitroarginine methyl ester (L-NAME), significantly reduced lesion volume in this model. In contrast, two agents which putatively inhibit presynaptic release of endogenous glutamate, the kappa opioid agonist CI-977 (enadoline) and the sodium channel blocker BW-1003c87, had conflicting effects on lesion volume. CI-977 did not alter the volume of the lesion induced by exogenous glutamate, as might have been predicted from the proposed presynaptic site of action of this drug. However, BW-1003c87 significantly reduced the volume of glutamate-induced damage by approximately 50%. These results suggest that although the neuroprotective actions of both CI-977 and BW-1003c87 against ischaemic neuronal injury have been proposed to be mediated by presynaptic inhibition of glutamate release, a post-synaptic component of BW-1003c87 activity may contribute to its neuroprotective effect. Overall, these results indicate that the cortical glutamate neurotoxicity model is sensitive to compounds acting at post-synaptic excitatory amino acid receptors.

*Lack of Efficacy of D-Cycloserine In Vivo*

A number of factors may contribute to the apparent lack of effect of D-cycloserine in the *in vivo* experimental paradigms investigated in this thesis, including the concentrations of D-cycloserine employed, possible saturation of the glycine regulatory site *in vivo*, or the statistical design of the experiments.

The concentrations of D-cycloserine employed in the present studies were selected on the basis of doses previously reported to have agonist properties *in vivo*. Handelman et al. (1988) and Monahan et al. (1989b) reported that

intraperitoneal injection of D-cycloserine injections of 3mg/kg, and 0.3, 3 and 10mg/kg respectively, enhanced performance in behavioural tests of learning. Further, Emmett et al. (1991) have demonstrated agonist effects of D-cycloserine (1.25, 5 and 10mg/kg) on the rate of NMDA receptor-mediated cGMP turnover in mouse cerebellum, following sub-cutaneous administration. Consequently, in the present thesis, the investigation of the effects of D-cycloserine on local cerebral glucose use employed a dose range of 0.3 - 30mg/kg (incorporating putative agonist doses of D-cycloserine), while D-cycloserine (3mg/kg) was used to study the effects of agonist stimulation of the NMDA receptor on [$^{125}$I]-MK-801 binding *in vivo*, and on glutamate-induced neurotoxicity *in vivo*. It is therefore of interest that these functionally active doses of D-cycloserine had no effect on the parameters measured in this thesis. However, it should be noted that the route of drug administration and timing of the measurement period may influence the detected effects of the drug. In addition, that concentrations of D-cycloserine which possess agonist properties seem to vary according to the experimental paradigm involved. With reference to this last point, three studies of dose-dependent behavioural effects of D-cycloserine have recently been reported which describe differential agonist doses of D-cycloserine. Flood et al. (1992) reported that subcutaneous administration of 10, 20 and 30mg/kg D-cycloserine significantly improved memory retention in a cognitive test in mice, while doses of 2.5, 5, 40 and 50mg/kg were ineffective. In a water maze task assessing cognitive function in mice, D-cycloserine (0.3 and 1mg/kg) improved the learning deficit induced by scopolamine, but D-cycloserine (3mg/kg) had no effect (Sirviö et al., 1992). Further, Schuster et al. (1992) demonstrated

that D-cycloserine (12mg/kg) enhanced performance in a spatial learning task in hippocampus-lesioned rats, following intraperitoneal administration (no other doses were investigated in this study). Therefore, it is possible that the concentration range of D-cycloserine employed in the present thesis were inadequate to optimally reflect the effects of D-cycloserine in the experimental paradigms investigated.

A critical factor influencing the efficacy of D-cycloserine *in vivo* is the extent of occupancy of the NMDA glycine site by endogenous glycine. Glycine site saturation could account for the lack of effect of D-cycloserine on cerebral glucose use, [$^{125}$I]-MK-801 binding, and on glutamate-induced lesions. Previous microdialysis studies have indicated that concentrations of endogenous glycine in extracellular fluid within the brain are sufficient to saturate the glycine site (Butcher et al., 1990), which might explain the inability of exogenously added D-cycloserine to potentiate NMDA receptor activity. However, evidence of enhanced performance in behavioural tests by D-cycloserine (Monahan et al., 1989b) suggests that there is some capacity for potentiation of NMDA receptor activity *in vivo*. In addition, the distribution of a recently cloned neurone-specific glycine transporter in the brain indicates that this transporter is expressed in regions with a high density of NMDA receptors, including the cortex and hippocampus (Smith et al., 1993). Therefore, since this transporter putatively regulates extracellular glycine levels, it has been suggested that there may be some capacity for modulation of NMDA-receptor mediated synaptic transmission within regions containing high concentrations of the transporter, including hippocampal regions (for review see Kemp and Leeson, 1993).

Another complicating factor in the analysis of D-cycloserine's central action *in vivo* is that, as a consequence of its partial agonist properties, D-cycloserine may antagonise ligand binding at the glycine site in circumstances of glycine site saturation by an endogenous ligand (Hood et al., 1989). Thus, under conditions in which extracellular glycine concentrations are elevated, such as during MCA occlusion, the systemic administration of a putative agonist dose of D-cycloserine may conversely antagonise NMDA receptor-mediated events. It is therefore possible that the lack of effect of D-cycloserine on infarct size in the MCA occlusion model may be due to an overall "cancelling out" of agonist and antagonist effects of the drug. Alternatively, the massive release of glutamate into the extracellular space during ischaemia may be so great that its effects are largely unaffected by a relatively trivial modulation of the NMDA receptor. Similarly, attempting to enhance NMDA receptor activity by D-cycloserine stimulation of the glycine site during cortical glutamate perfusion may also be futile, in view of reports that excessive NMDA receptor stimulation provokes glycine release to above saturating levels (Fadda et al., 1988; Hood et al., 1990).

The overwhelming impression gained from the studies performed in this thesis to investigate the *in vivo* actions of D-cycloserine is that the experimental paradigms employed are insensitive to the cerebral functional effects of this agent. In order to gain further insight into the sensitivities of the four approaches used, *post hoc* power analysis was used to calculate the magnitude of effect which would be detected as a statistically significant alteration in each of the four studies. The calculated detectable effect for each paradigm is presented in Table 38, based on the group sizes and variance of measurement in representative regions within control groups.

## TABLE 38

## D-CYCLOSERINE STUDIES: METHODOLOGICAL ASSESSMENT

| VARIABLE PARAMETER | MEAN ± SEM (n) | DETECTABLE EFFECT |
|---|---|---|
| Glucose Use (Frontal Cortex) | 89 ± 4 (6) | 18% |
| [125I]-MK-801 Binding (Hippocampus CA1) | 1.74 ± 0.38 (6) | 86% |
| MCA Occlusion (Infarct Size) | 1.91 ± 30 (6) | 62% |
| Cortical Lesion (Lesion Size) | 20.3 ± 1.3 (5) | 25% |

*Post hoc* power analysis, based on group size (n) and variance within control groups, using representative data from studies reported in this thesis. "Detectable effect" is the minimum change required to elicit a statistically significant response in a 2-tailed analysis of the parameters outlined, employing the simplest experimental design of 1 control group and 1 treatment group. $\alpha = 5\%$, $\beta = 80\%$.

Cohen (1977)

Power analysis assesses the likelihood of Type 2 (false negative) errors occurring within a statistical analysis. *Post hoc* power analysis of the data set generated in a given experiment gives an indication of the magnitude of change which would be detected as a statistically significant alteration. the "detectable effect" calculated in Table 38 is based on the change required to achieve a probability value of $p<0.05$ with 80% power in a simple statistical comparison between two groups, such as an independent *t*-test, using the experimental designs employed in the studies outlined in this thesis. The results indicate that local cerebral glucose use is the most sensitive of the measures which were used to assess the *in vivo* effects of D-cycloserine, capable of detecting small magnitude (18%) changes. Similarly, the cortical glutamate perfusion model is sensitive to relatively small magnitude effects. In contrast, in the MCA occlusion model, and especially in the [$^{125}$I]-MK-801 autoradiography procedure, power is very weak with the group sizes used (62% and 86% respectively), indicating a realistic possibility of false negative results which must be considered when assessing the experimental results. However, in order to be able to detect any significant effects of D-cycloserine using these two techniques (set arbitrarily at 20% changes), power analysis based on the variance observed in the present studies indicates that group sizes of 59 for MCA occlusion and 115 for [$^{125}$I]-MK-801 autoradiography should be used.

## 3. BASAL FOREBRAIN INTERVENTIONS

Cholinergic neurotransmission in the cerebral cortex and hippocampus is implicated in processes of learning and memory. In Alzheimer's disease (AD), in which mnemonic function is impaired, learning and memory deficits have been correlated with depleted levels of cholinergic markers in the cerebral cortex (Bartus et al., 1982; Fibiger, 1991; Price et al. 1991). The nucleus basalis of Meynert (nbM), within the basal forebrain, has been identified as the primary extrinsic source of acetylcholine (ACh) in the cerebral cortex (Lehmann et al., 1980; Johnston et al., 1981; Bigl et al., 1982). Hence, reports of neuronal loss in the NBM of AD patients (Whitehouse et al., 1982) have resulted in the proposition that nbM cholinergic dysfunction is critically involved in the etiology of AD (Richardson and Delong 1988).

The contribution of cortical cholinergic deafferentation to memory impairment has been investigated experimentally in the rat, by lesioning efferent projections arising from the nucleus basalis magnocellularis (NBM, homologous to the nbM in man). In the absence of a specific cholinergic neurotoxin, excitatory amino acid agonists have been widely used to produce axon-sparing lesions of basal forebrain neurones, including NBM projections. However, there are a number of problems inherent to the use of excitotoxins. Primarily, due to the diffuse distribution of magnocellular cholinergic neurones of the NBM throughout the basal forebrain (and in particular in dorsal globus pallidus), excitatory amino acids will destroy both cholinergic and non-cholinergic neurones in the basal forebrain, provided they have receptors for these agonists. Ibotenic acid, in particular, induces widespread cell death throughout the basal forebrain.

Investigations of the effects of basal forebrain lesions on cognitive function have, to date, centred on assessment of altered behaviour in tests of learning, memory and attention. In conjunction with observations of differential reductions in cortical cholinergic markers, such as choline acetyl transferase (ChAT) activity, these behavioural studies provide evidence of a dissociation in the effects of NMDA and non-NMDA receptor agonists on NBM neurones (Dunnett et al., 1987; Etherington et al., 1987; Robbins et al. 1989 a and b; Connors and Thal, 1991; Page et al., 1991). The AMPA receptor agonists quisqualic acid and, in particular, AMPA appear to be much more selective for cholinergic NBM neurones than NMDA ibotenate or KA (see Table 3; for review see Dunnett et al., 1991). In view of these reports, and in the light of PET studies which have demonstrated glucose use and oxygen use depression in the cortex of AD patients (Frackowiak et al., 1981; McGeer et al., 1986), the effects of excitotoxic basal forebrain lesions on local cerebral glucose use in the conscious rat have been assessed in the conscious rat, as an alternative index of functional activity in the brain.

In the present study, the consequences of ibotenic acid, NMDA, quisqualic acid and AMPA-induced NBM lesions on cerebral glucose use were compared. In contrast to behavioural and neurochemical studies, autoradiographic assessment of glucose use by the [$^{14}$C]-2-deoxyglucose technique provides a non-subjective method for analysing functional changes, as these are reflected by alterations in the cerebral metabolic rate for glucose, in all components of the CNS simultaneously. Previous [$^{14}$C]-2-deoxyglucose studies have investigated the effects of ibotenic acid and KA-induced NBM lesions on glucose use in the rat (London et al., 1984; Lamarca

and Fibiger, 1984; Orzi et al., 1988), however the effects of AMPA and quisqualic acid-induced lesions have not previously been reported. In addition, the acute cerebral metabolic effects of NMDA and AMPA infusions into the NBM region were also assessed.

*Chronic Effects of Excitotoxic Lesions*

Local rates of cerebral glucose utilisation were assessed 21-24 days after unilateral injections of ibotenate, NMDA, quisqualate or AMPA into the NBM region of the basal forebrain. The agonist concentrations, injection volumes, and stereotactic coordinates of the injection sites employed in the present study reflected the injection protocols used by Dunnett and colleagues in previous lesioning studies, in which deficits in cognitive or attentional function have been reported at a similar time point post-lesion (Dunnett et al., 1987; Robbins et al., 1989 a and b; Page et al., 1991). Due to the cryostat processing of cerebral tissue in the present study, necessitated by the [$^{14}$C]-2-deoxyglucose technique, it was not possible to assess cortical ChAT levels in the same animals in which glucose use was measured. However, evidence from previous studies using the same lesioning paradigms indicates marked cortical ChAT deficits at this time point (-30-40% after unilateral ibotenate and NMDA infusions, approximately -50% after quisqualate, and -70% after AMPA) (Dunnett et al., 1987; Robbins et al., 1989a and b; Page et al., 1991).

In spite of reports from numerous studies of sustained functional depression 3 weeks after excitotoxic lesions (i.e. cortical ChAT depletion and behavioural impairments), significant alterations in glucose use were observed

in only 2 of the 51 CNS regions investigated after infusions of any of the agonists into the NBM region. Glucose use was increased relative to control levels in ipsilateral NBM after ibotenate, and ipsilateral hypothalamus after NMDA (although the glucose use increase seen in the hypothalamus of NMDA-treated rats was slight and there was no evidence of interhemispheric glucose use differences in these animals, questioning the biological significance of this apparent change). It should be noted that the statistical approach employed in the present study was extremely conservative, due to the application of a Bonferroni correction factor to compensate for the large number of vehicle/treatment group comparisons. This approach largely rules out the possibility of Type I (or "false positive") statistical errors, but increases the chance of Type II or "false negative" errors. Setting a significance level of $p<0.05$ in any statistical analysis represents setting an arbitrary cut off point for putatively "real" biological changes, and means that 1 in 20 statistical comparisons might be wrongly assigned. Due to the large number of comparisons involved in the present study, with 5 treatment groups, a Bonferroni correction factor was employed in the statistical analysis to reduce the number of random false positive results. However, this conservative approach risks masking some small magnitude, but potentially biologically relevant, changes in glucose use. Therefore, it is of interest to examine the trends in glucose use alterations observed after ibotenate, NMDA, quisqualate and AMPA lesions. In order to do this it was decided to scrutinise the data with regard to regions in which glucose use changes generated a probability value of $p<0.05$ in the independent *t*-test analysis prior to application of the Bonferroni correction factor.

The most striking alterations in glucose use were seen at the infusion site in the NBM region of the basal forebrain, where all four excitatory amino acid agonists studied induced increases in glucose utilisation. These hypermetabolic effects were most marked following ibotenate and AMPA lesions, which produced massive increases in glucose use in sub-cortical regions in close proximity to the NBM (i.e. in striatum and globus pallidus). In contrast, glucose use was marginally increased in only a small volume of tissue after NMDA and quisqualate infusions. The reason for this increased metabolic activity at the lesion site is not certain, however it is possible that elevated levels of glucose use may be due to the energy-demanding processes of reactive gliosis. Examination of the pattern of [$^{3}$H]-PK-11195 binding around the lesion site (which labels peripheral-type benzodiazepine receptors, predominantly associated with glial cells in brain tissue) indicates marked glial proliferation in a large volume of tissue around the infusion site following ibotenate and AMPA lesions. However, the contribution of increased metabolism in glial cells cannot be conclusively linked with increased glucose use at the infusion site, in view of the fact that there was no evidence in any animals of increased glucose use in the vicinity of the needle tract through the cortex, despite increased [$^{3}$H]-PK-11195 binding in the same region (see Figures 32 and 34). Moreover, comparison of [$^{14}$C]-2-deoxyglucose autoradiograms with [$^{3}$H]-PK-11195 binding patterns in adjacent sections indicates that the regions in which glucose use was markedly elevated were restricted to the core of the gliotic tissue, as is evident from examination of Figures 32 and 34 . However, observations that astrocytes initially accumulate around the periphery of lesioned tissue and gradually

infiltrate into the core (see Logan and Berry, 1993) support the suggestion that reactive gliosis may still be occurring in the lesion core 3 weeks post-lesion. Alternatively, the increased glucose use in the lesion core may reflect the consequences of tissue damage on the kinetic parameters of deoxyglucose uptake in the NBM region.

Cholinergic neurones of the NBM region project topographically to neocortex. Hence, lesioning NBM efferents might be predicted to result in reduced metabolic activity in the terminal projection zones in cortex. In the present study, glucose utilisation in frontal cortical regions innervated by NBM efferents was not significantly altered by any of the excitotoxic lesions. However, metabolic depression was evident in ipsilateral prefrontal cortex following AMPA lesions and trends towards glucose use reductions were also seen in frontal and sensory motor cortex after AMPA. Reductions in glucose use in prefrontal and sensory motor cortex were also evident following NMDA, although of smaller magnitude than AMPA-induced decrements. Although these cortical glucose use changes failed to reach statistical significance with the statistical analysis employed in this study, these observations are particularly pertinent in view of the biochemical and behavioural evidence that AMPA receptors appear to show a much greater degree of co-localisation with cholinergic NBM neurones than NMDA receptors. The results of this study also highlight the lack of selectivity of ibotenic acid for cholinergic neurones within the basal forebrain, ibotenic acid lesions having no effect on cortical glucose use despite consistently producing the largest volumes of tissue damage of the four excitotoxins investigated. This observation is consistent with reports that ibotenic acid lesions produce cognitive deficits

which can be replicated by disruption of cholinergic innervation of the hippocampus and cortical regions outwith the NBM projection field, which originate from more rostral segments of the basal forebrain cholinergic system (i.e. the medial septum and diagonal band of Broca (Dunnett et al., 1991).

This study demonstrates that chronic excitotoxic lesions of the NBM region of the basal forebrain only minimally affect integrated functional activity in the CNS, as assessed by the measurement of local rates of cerebral glucose use. Although cortical glucose use measurements hint at a separation in the effects of AMPA-induced lesions from those of ibotenate, NMDA and quisqualate, the results from this study provide no conclusive evidence to support suggestions of differential contributions of excitatory amino acid receptor subtypes to cholinergic activity in the NBM. In the light of evidence of sustained cortical cholinergic dysfunction and cognitive impairment after excitotoxic basal forebrain lesions (Bartus et al., 1982; Arendash et al., 1987; Dunnett et al., 1987; Etherington et al., 1987; Robbins et al., 1989a), the lack of cerebral metabolic changes 3 weeks post-lesion may be accounted for by compensatory functional adaptation within both cholinergic and non-cholinergic neuronal populations in the brain. Therefore, in order to further investigate whether glucose use measurements provide any insight into the putative dissociation between NMDA and non-NMDA receptor-mediated events in the basal forebrain, it was decided to investigate the cerebral metabolic consequences of stimulating cholinergic neurones in the NBM via pharmacological modulation of excitatory amino acid receptor activity.

*Acute Agonist Stimulation in the Basal Forebrain*

Local rates of glucose use were mapped throughout the brain acutely after stimulation of NMDA or non-NMDA receptor subtypes within the basal forebrain by NBM infusions of NMDA or AMPA, respectively. The acute metabolic consequences of putatively inhibiting cholinergic neuronal activity in the NBM region were also investigated, following manipulation of the GABAergic input to cholinergic NBM neurones by the $GABA_A$ agonist muscimol.

Unilateral infusions of NMDA and AMPA into the basal forebrain NBM region induced widespread, heterogeneous alterations in cerebral glucose use in a number of regions in the ipsilateral hemisphere. The anatomical patterns of glucose use changes seen after agonist infusions into the basal forebrain revealed activity in well-organised anatomical pathways, involving changes in discrete brain regions which could be grouped largely into three areas: the infusion site, anatomically associated cortical regions, and a number of anatomically or functionally related sub-cortical regions. In contrast, glucose use alterations following muscimol were largely restricted to ipsilateral sub-cortical regions.

In the vicinity of the infusion site at the NBM, NMDA and AMPA induced a massive increase in glucose use in a band of tissue forming a ring of "hypermetabolism", approximately 1.5mm radius around the NBM region. This area of markedly enhanced metabolic activity affected a region of tissue extending dorsally from the NBM into striatum and globus pallidus, and rostally and caudally from the infusion site, as is illustrated following NMDA infusion in Figure 44. At the centre of the hypermetabolic ring, a region of

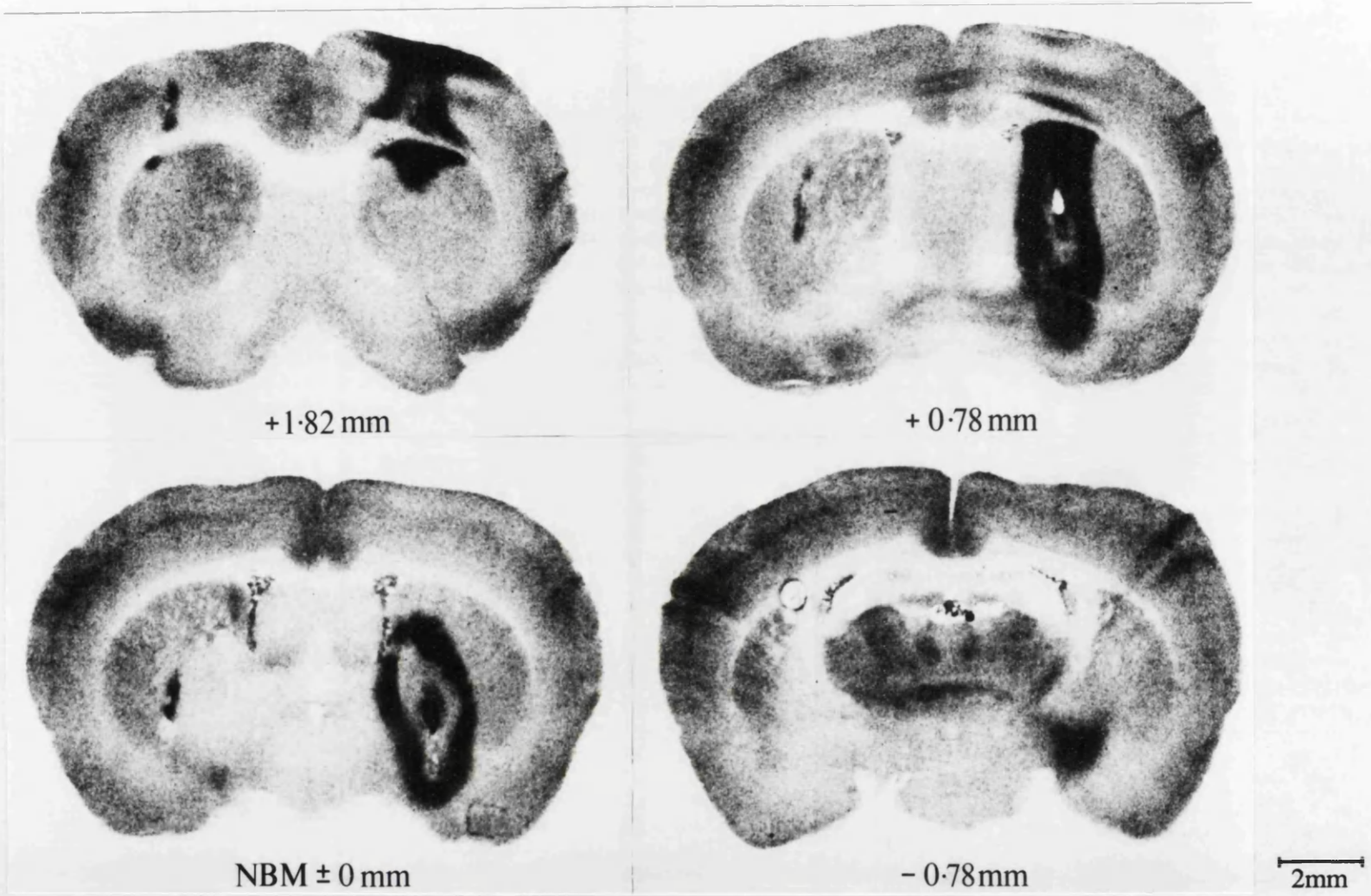


FIGURE 44: EXTENT OF HYPERMETABOLIC RESPONSE TO NMDA INFUSON

Representative autoradiograms, from the same animal, illustrating glucose use acutely after unilateral infusion of NMDA into the NBM basal forebrain region (right hemisphere). Excessively increased glucose use, relative to levels in the vehicle-infused (left) hemisphere, is evident in brain regions rostral (+1.82 and + 0.78mm) and caudal (-0.78mm) to the infusion site (NBM ± 0mm). Note the increased glucose use around the needle tract in the cortex (+1.82mm).

unaltered glucose use (relative to the contralateral hemisphere) was evident in each animal examined. It is postulated that the perimeter of the hypermetabolic zone reflects the extent of spread of AMPA and NMDA over the 60 min period post-injection. The extent of spread of a given infusate within the brain depends on a number of factors, including the infusate's molecular weight, valency and lipophilicity, and is therefore difficult to estimate. However, the position of the hypermetabolic ring in the present study is reasonably consistent with the extent of spread of dyes following intracerebral injection, previously reported by Myers (1966).

The patterns of glucose use around the infusion site appear to reflect the concentration profile of the excitotoxins, with the highest concentration at the core of the infusion site, and the lowest at the periphery. Under normal conditions, dynamic alterations in glucose utilisation predominantly reflect changes in metabolic activity in neurone terminals (see Kurumaji et al., 1993). Therefore, the fact that glucose use is unaltered at the core of the infusion site does not necessarily mean that neuronal activity in this region is unaffected by the infusates. Conversely, the marked glucose use reductions seen in the cerebral cortex following AMPA and NMDA infusions imply a marked reduction in energy demand in the cortex due to reduced terminal activity. Since the NBM provides the major extrinsic cholinergic innervation of the neocortex, it appears likely that the metabolic depression seen in cortex may be due to desensitization of cell bodies at the infusion site, as a result of overstimulation of NMDA or AMPA receptors by excessively high concentrations of the excitatory amino acids. In contrast, it is unlikely that the hypermetabolic response in the striatum and globus

pallidus following NMDA and AMPA infusions reflects increased activity in NBM projection terminals, since, while trivial projections from the NBM cannot be ruled out, there is no evidence to date from anatomical or physiological studies of a biologically important projection from the NBM to these regions.

It is of interest that the massive increase in glucose use observed in the hypermetabolic zone closely resembles the glucose use elevations seen in the ischaemic penumbra following MCA occlusion, and at the perimeter of cortical lesions produced by glutamate perfusion (Ginsberg, 1990; Landolt et al. 1992). Two possible explanations for this hypermetabolic response are, firstly, massively enhanced presynaptic terminal activity (in an attempt to remove the excitotoxins from the synaptic cleft), or alternatively, abnormally high levels of metabolic activity in neuronal cell bodies. Therefore, at the perimeter of the region of excitotoxin spread, neurones appear to be exposed to concentrations of excitotoxins sufficient to stimulate metabolic activity to abnormal levels, but insufficient to desensitize cells within the period of exposure.

At first sight the fact that AMPA reduced glucose use in 10 of the 17 cortical regions examined, in contrast to the 2 cortical regions in which glucose use was depressed by NMDA, suggests that AMPA is much more selective for cholinergic NBM neurones than NMDA. However, examination of the absolute rates of glucose use in NMDA-treated rats reveals that in a number of other ipsilateral frontal cortical regions, such as frontal and parietal cortex, glucose use levels closely resemble those seen in the corresponding regions of AMPA-infused animals (for example, see Figure 35).

However, further investigation suggests that the apparent paucity of statistically significant glucose use changes in cortex following NMDA-infusion may reflect the statistical design employed in this study. The statistical analysis, determined *a priori*, initially involved comparison of glucose use values in the contralateral (vehicle-infused) hemisphere between treatment groups, to try to identify any interhemispheric drug effects. Trends towards reduced glucose use following NMDA were evident in a number of contralateral cortical regions, including frontal and parietal cortex, although no statistically significant differences were identified between glucose use levels in the three treatment groups in any of the 50 contralateral regions investigated. The effects of NMDA, AMPA and muscimol infusions on glucose use in the ipsilateral hemisphere were then analysed by comparison of glucose use values in ipsilateral and contralateral hemispheres within treatment groups. Therefore, although the observed trends towards reduced glucose use in contralateral frontal cortical regions following NMDA infusion were not large enough to reach statistical significance, they may have been sufficient to mask ipsilateral glucose use reductions in the subsequent inter-hemispheric statistical analysis.

The cause of the apparent glucose use depression in the contralateral cortex after NMDA infusion is not clear. However, the observation that no glucose use alterations were evident in the contralateral hemisphere of AMPA- or muscimol-treated animals implies that this effect is not associated with vehicle infusion into the basal forebrain. In addition, changes in contralateral glucose use in NMDA-infused rats were confined to frontal cortical areas, suggesting that these alterations do not reflect global

functional depression by NMDA, but rather are directly associated with the local effects of NMDA infusion, possibly due to cortico-cortical communication or trans-callosal spread of the infusate. These hypotheses are supported by visual inspection of the autoradiograms which indicate an area of hypermetabolism around the needle tract in ipsilateral cortex of NMDA-treated rats, suggesting the possibility of back flow of NMDA up the needle tract which may have influenced cortical neuronal activity (see Figure 44).

In contrast to NMDA and AMPA, muscimol did not markedly alter glucose use at the infusion site, in regions around the infusion site such as the striatum or globus pallidus, or in any cortical regions directly innervated by NBM efferents. These results suggest that muscimol has no effect on cholinergic neurones in the NBM. This apparent lack of responsiveness to muscimol could be interpreted to reflect an inadequate dose of muscimol, although the concentration of muscimol employed in this study has previously been found to alter cognitive and attentional function following unilateral infusion into the basal forebrain (Muir et al., 1992b). In addition, muscimol infusion altered glucose use in other brain regions, for example reducing glucose use in cingulate cortex and agranular insular cortex. These metabolic alterations may result indirectly from the stimulatory effects of muscimol on neuronal activity in thalamic nuclei, such as the ventromedial thalamus which sends afferent projections to the agranular insular cortex (Guildin and Markowitsh, 1983), and cingulate cortex (Vogt et al., 1981).

Increased glucose use was observed in a number of subcortical regions acutely after infusions of AMPA, NMDA and muscimol into the basal

forebrain. Regions affected included the substantia nigra pars compacta and reticulata, the subthalamic nucleus, the entopeduncular nucleus and the ventromedial thalamic nucleus. The common factor between these regions, which are not directly innervated by NBM projections, is that all are primary or secondary components of polysynaptic projection pathways originating in the globus pallidus or striatum, as is illustrated in Figure 45. Thus, subcortical regions in which glucose use is altered correspond with regions receiving efferent projections arising from the zone of hypermetabolism induced by NMDA and AMPA infusions (see Figure 46). The effects of muscimol, in contrast, are less clear cut. Glucose use was largely unaltered in the vicinity of the infusion site and no elevations in glucose use were observed in striatum or pallidum following muscimol. In spite of these observations, and the fact that there is no evidence to date of a major GABAergic subcortical projection from the basal forebrain, glucose use was increased in striato-pallidal projection targets following muscimol infusions into the NBM. These effects of muscimol are reminiscent of the consequences of muscimol injection directly into the striatum (Kelly and McCulloch, 1984).

Muscimol is postulated to indirectly modulate cholinergic neuronal activity in the NBM via activation of inhibitory GABAergic neurones which synapse on magnocellular NBM neurones (Muir et al., 1992b). The inhibitory nature of GABAergic neurones may, superficially, suggest that stimulation of GABAergic pathways will inhibit functional activity in target structures, and hence reduce glucose use. However, synaptic transmission in inhibitory pathways still requires terminal activity, and therefore the increases in

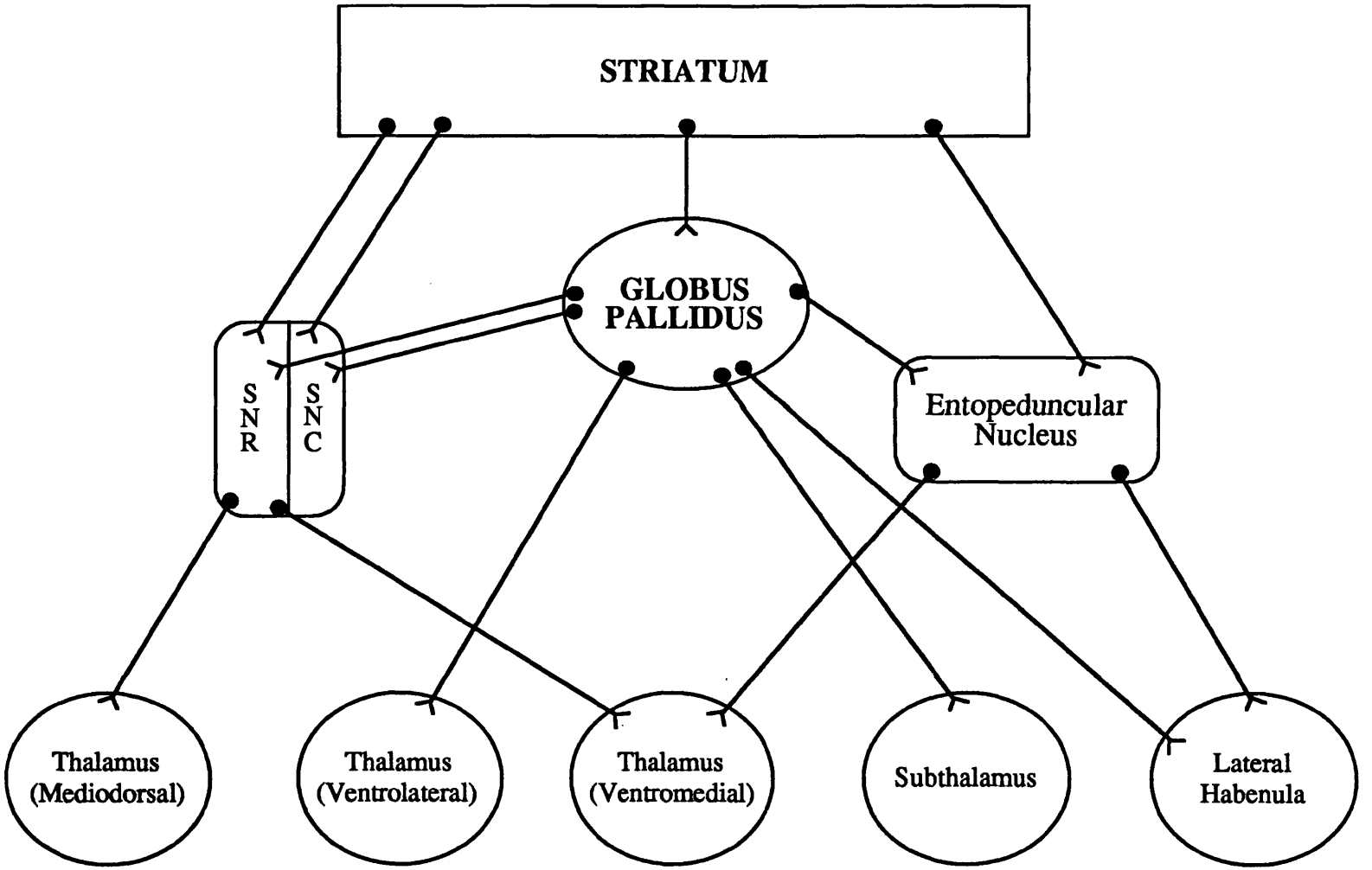


FIGURE 45: SCHEMATIC REPRESENTATION OF MAJOR SUB-CORTICAL STRIATO-PALLIDAL PROJECTIONS

Sub-cortical components of striato-pallidal efferent projection pathways in which glucose use was altered after infusions of AMPA, NMDA or muscimol into the NBM. (After Hattori et al., 1975; Carter and Fibiger, 1978; Van der Kooy et al., 1980; Gerfen, 1985: Haber et al., 1985).

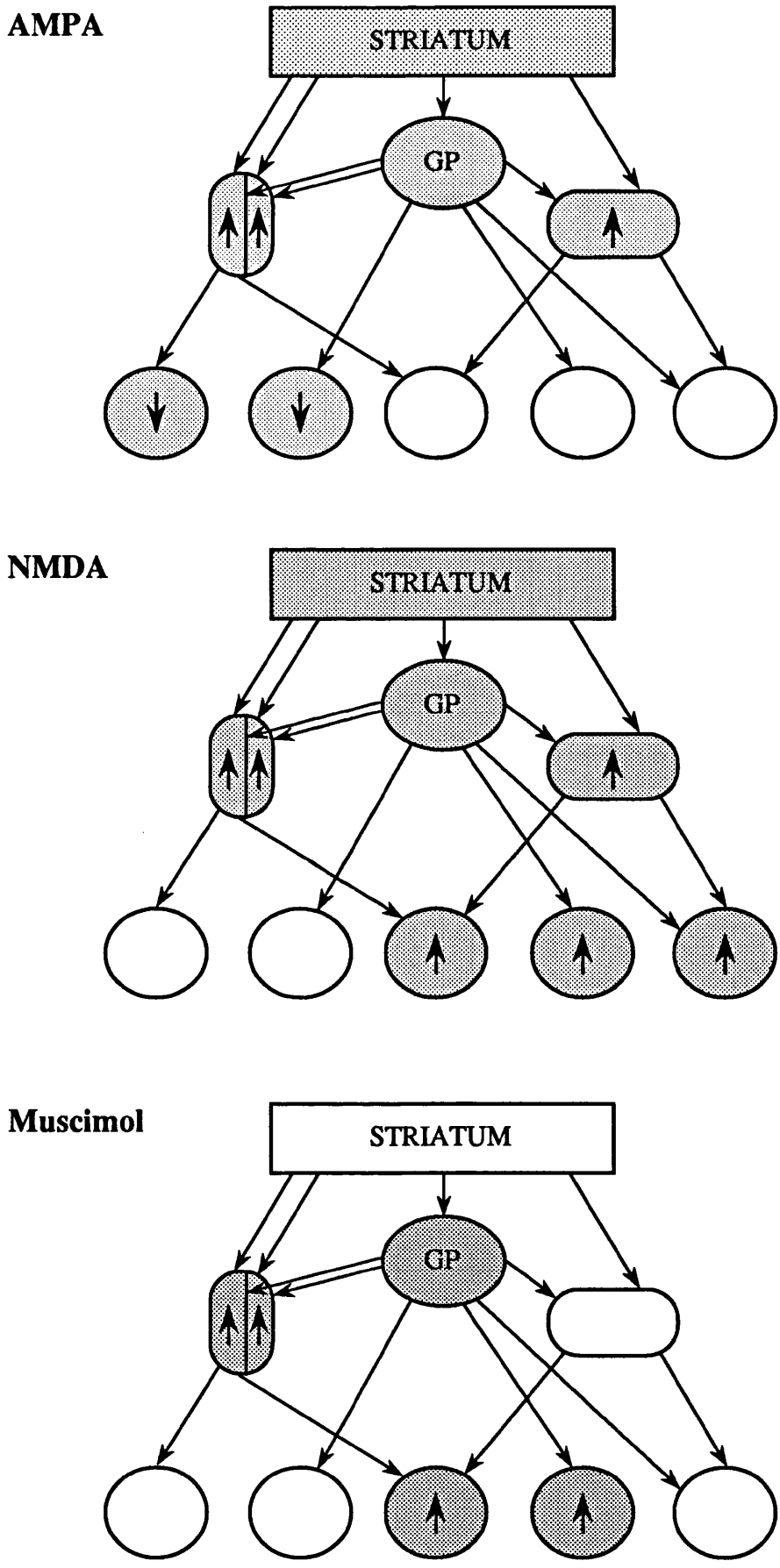


FIGURE 46: SUMMARY OF AGONIST EFFECTS IN THE STRIATOPALLIDAL PROJECTION FIELD

Schematic representation of the effects of agonist NBM infusion of AMPA, NMDA or muscimol on cerebral glucose use in sub-cortical regions of the ipsilateral hemisphere. Symbols correspond to regions as illustrated in Figure 45. Shading indicates regions in which glucose use was significantly increased ( ↑ ) or decreased ( ↓ ).

glucose use seen in sub-cortical regions after muscimol may simply be indicative of activity in GABAergic projection pathways. The lack of a hypermetabolic response in the striatum and pallidum following muscimol does not rule out the possibility of muscimol spread to affect striato-pallidal regions, but suggests that concentrations of muscimol in these regions are insufficient to abnormally affect the metabolic rate in cell bodies. However, the concentrations of muscimol in striatum and globus pallidus may still be sufficient to enhance terminal activity in striato-pallidal efferents. An alternative hypothesis is that muscimol may overstimulate GABAergic neurones around the infusion site, resulting in desensitization of GABAergic neurones and subsequent disinhibition of sub-cortical projection pathways in which activity is normally suppressed by GABAergic input.

It should be noted that the experimental protocol employed, including the concentration, volume and stereotactic placement of infusions, will greatly influence the outcome of studies involving intracerebral interventions. This point is underlined by the disparities in reports of cortical ChAT depletion following NBM lesions by different experimenters, outlined previously in Table 3. Since the aim of the present study, to compare the effects of different basal forebrain manipulations on cerebral glucose use, arose from observations of a dissociation in the effects of different excitatory amino acid receptor agonists in behavioural studies reported by Muir and colleagues, the experimental design used in the present study closely resembled that of Muir et al. (1992b, and personal communication). In investigations of the acute effects of unilateral basal forebrain infusions on acquisition of a conditional visual discrimination task (a learning test), and

on a five-choice serial reaction time task (an attention test), Muir and colleagues have found that NMDA (0.09M) and AMPA (0.0015M) impaired performance in the attentional task (but not the learning task), while doses 10 fold lower did not affect performance in the same task (Muir, personal communication). Similarly, muscimol (0.03mM) was the lowest dose found to impair performance in both the attentional and learning tasks. Therefore, the same concentrations were used in the present study of local cerebral glucose use (10 fold lower than the minimum doses found to chronically impair performance in the same behavioural tests, performed by the same investigators, 3 weeks post-lesion). In addition, the measurement period in the [$^{14}$C]-2-deoxyglucose study was selected to reflect the assessment period employed in the behavioural tests.

The present study has demonstrated overwhelmingly that the acute cerebral metabolic consequences of NBM infusions of NMDA, AMPA and muscimol are not restricted solely to the NBM and functionally associated areas, but also have a profound effect on activity in sub-cortical regions not directly associated with the infusion site. Rather, sub-cortical glucose use changes appear to reflect an action of the infusates on neurones in the striatum and globus pallidus. These observations have important consequences for the interpretation of deficits seen in behavioural tests of cognitive function following agonist infusions, since it is evident that the behavioural deficits reported after NMDA, AMPA and muscimol cannot be attributed to an action solely on cholinergic NBM neurones. Further, the effects of the infusates on striato-pallidal neurones, with concomitant alterations in metabolic activity in a number of thalamic nuclei associated with movement

control, suggest that deficits in performance of behavioural tasks following NBM manipulations are not necessarily representative of cognitive or attentional impairments, but may also reflect impaired ability to perform a given task.

*Functional Plasticity Following Basal Forebrain Interventions*

The acute and chronic effects of basal forebrain manipulations on glucose use imply that although metabolic activity in the brain is strikingly altered immediately after excitatory amino acid infusions into the basal forebrain, the cerebral metabolic sequelae are transient - glucose use returning to basal levels within 3-4 weeks in areas distal to the infusion site. Since the cortex is the primary projection target for cholinergic NBM efferents, the metabolic recovery seen in cortex after excitotoxic basal forebrain lesions is of particular interest, in view of the concomitant neuronal loss in the NBM, reports of persistent deficits in neurochemical cholinergic markers in the cortex, and sustained learning the memory impairment (Arendash et al., 1987; Orzi et al., 1988; for review see Dunnett et al., 1991). In addition, a number of other studies have also reported biphasic effects of NBM lesions on glucose utilisation, with initial reductions in cortical glucose evident 3 or 4 days post-lesion, recovering to basal levels within 4 weeks despite sustained ChAT deficits (ibotenate lesion: London et al., 1984; Lamarca and Fibiger, 1984; KA lesion: Orzi et al., 1988; electrocoagulation: Kiyosawa et al., 1989; Yamaguchi et al., 1990).

A number of mechanisms may contribute to metabolic recovery, all of which implicate compensation or adaptation to deafferentation. One possible

explanation is cholinergic reinnervation of the cortex by neuronal sprouting, either from residual intact neurones in the NBM, from the contralateral NBM, or from other cholinergic neuronal populations such as intrinsic cortical neurones. However, evidence of sustained long-term depression in cortical ChAT activity following unilateral NBM lesions in rat and baboon studies makes cholinergic reinnervation appear unlikely (London et al., 1984; Kiyosawa et al., 1989). Nevertheless, this possibility cannot be ruled out in the light of reports that deficits in other biochemical markers of cholinergic function, such as acetylcholinesterase (AChE) activity, do not necessarily parallel the long-term ChAT deficits (Bartus et al, 1985).

Other mechanisms which may contribute to metabolic recovery include possible adaptation within cholinergic projection fields to increase the sensitivity of intact neurones to AChE, or alternatively to increase the densities of post-synaptic receptors (McKinney and Coyle, 1982). Alterations in other neurotransmitter systems in the cortex have also been reported following basal forebrain lesions in the rat, including GABA, 5-HT and peptidergic systems (Arendash et al., 1987), suggesting the possibility of transynaptic reorganization in damaged tissue. Further hypotheses include the possibility of indirect compensatory effects of NBM lesions on cortical metabolic activity via NBM-thalamic connections, or recovery of damage to non-cholinergic neurones in the NBM (for review see Kiyosawa et al., 1989). Metabolic recovery appears to be a general phenomenon in deafferentated cortex, cortical glucose use recovery has also been observed for example after orbital enucleation (Chalmers and McCulloch, 1991). In addition, metabolic recovery has been witnessed following unilateral sub-cortical

lesions, for example hippocampal glucose use recovery following medial septum lesions in rats despite a persistent decrease in AChE activity (Harrell and Davis, 1984). In contrast, Motohashi et al., (1986) have reported that deafferentation of the dorsal raphé by habenula lesions does not result in metabolic recovery. These observations infer that the capacity of a region for functional recovery will be inherently dependent on the magnitude and specificity of the denervation involved, and on the nature of the extrinsic innervation of the deafferented region.

The results presented in this thesis suggest that the [$^{14}$C]-2-deoxyglucose autoradiographic method is insensitive to subtle functional changes at chronic time points post-lesion, putatively due to the masking of altered metabolic activity in one transmitter system by compensation in another. This leads to the suggestion that perhaps only pharmacological or behavioural challenge will be able to shed light on the long-term functional consequences of excitatory amino acid receptor manipulations in the basal forebrain. In addition, these results of apparent functional plasticity contrast with the reported chronic, sustained deficits in cortical metabolic activity in Alzheimer's patients (Frackowiak et al., 1981; McGeer et al., 1986), leading to speculation that decreased cortical glucose utilisation in AD is not related to degeneration of the nbM-cortical projection.

The investigations into the effects of different basal forebrain manipulations on local cerebral glucose use in this thesis were prompted by suggestions of a dissociation in the effects of NMDA and non-NMDA agonists on basal forebrain cholinergic neurones. However, the proposition that AMPA receptors are co-localised with basal forebrain cholinergic neurones

to a greater extent than other glutamatergic receptor subtypes is supported only to a limited extent by the results of the present glucose use studies. The most obvious observation from these studies is that excitatory amino agonist infusions into the basal forebrain acutely alter glucose utilisation in numerous brain regions, which are not restricted solely to the NBM and its cortical projection targets. The nature and magnitude of the effects of NMDA, AMPA and muscimol on metabolic activity in sub-cortical regions suggest that functional alterations in these areas may influence animals' performances in behavioural tasks, thus complicating interpretation of behavioural studies of the effects of basal forebrain interventions on cognitive function.

## 4. OVERVIEW

The 2-deoxyglucose autoradiography technique has been proved to be a potent tool in neuroscience research, providing a unique opportunity to localise and quantify alterations in metabolic demand associated with CNS challenge (Sokoloff, 1981; Kurumaji et al., 1993). The utility of this procedure is based on the close coupling which has been demonstrated to exist between functional activity and energy consumption in the CNS, and is enhanced by the capacity of the technique to measure local rates of glucose utilisation simultaneously in discrete regions throughout the CNS in conscious animals. Consequently, [$^{14}$C]-2-deoxyglucose *in vivo* autoradiography has been widely used to investigate the cerebral metabolic consequences of pathological, physiological and pharmacological challenge in experimental animals, and the technique has been adapted to allow non-invasive metabolic mapping in man using positron emission tomography (PET). Cerebral glucose

use studies have been found to be particularly beneficial in mapping the global patterns of dynamic metabolic alterations, such as the acute action of drugs in the brain, or the massive functional disturbances occurring in acute pathological states, such as during an ischaemic insult (see Ginsberg, 1990). As a result, the contributions of numerous neurotransmitter systems within the brain to cerebral functional activity have been investigated using the [$^{14}$C]-2-deoxyglucose technique in combination with a variety of techniques to manipulate receptor activity, such as systemic drug administration, direct intracerebral administration of receptor agonists or antagonists, or lesioning specific projection pathways within the brain.

Due to glutamate's critical role in the CNS as the major excitatory neurotransmitter, and it's involvement in excitotoxic processes within the brain, the effects of glutamate receptor manipulations on local rates of glucose use have been extensively investigated (for review see Kurumaji et al., 1993). Studies have revealed that antagonist manipulation of excitatory amino acid receptor subtypes generally yields more information about the location of glutamate-mediated events within the CNS than agonist administration, exemplified by the selective nature of glucose use responses to intravenous administration of kainic acid, (Cellik et al., 1979), compared to the widespread effects of NMDA or AMPA receptor blockade (Kurumaji et al., 1989a and the present study). These discrepancies appear to reflect both the ubiquitous distribution of glutamate in the CNS and the importance of its role as an excitatory neurotransmitter in integrated functional activity,and suggest that exogenous agonist stimulation of an excitatory amino acid receptor subtype will have little or no dynamic impact on neuronal

activity under normal conditions, whereas inhibition of transmission at post-synaptic glutamatergic receptors has a dramatic effect on functional activity in polysynaptic pathways. This is supported by the results of the present studies, in which putative agonist stimulation of NMDA receptors by D-cycloserine had no effect on cerebral glucose use, while the AMPA receptor antagonists NBQX and LY-293558 produced almost global metabolic depression.

In other excitatory transmitter systems the metabolic responses to systemic agonist and antagonist administration appear to be more heterogeneous. For example, enhancement of central cholinergic transmission by systemic administration of oxotremorine, a muscarinic receptor agonist, results in pronounced elevations in glucose use in a number of brain regions, and principally in structures involved in motor function such as motor cortex, the globus pallidus, subthalamic nucleus, nigro-striatal system and cerebellum (see Kurumaji et al., 1993). In contrast, inhibition of cholinergic activation by the muscarinic antagonist scopolamine selectively alters glucose use, resulting in metabolic depression in a small number of regions, while increasing glucose metabolism in the cerebellar vermis and the reticular formation (Helén and London, 1984). Manipulations of inhibitory neurotransmitter systems have also indicated diversity amongst different transmitter systems in terms of the localisation and nature of their effects on functional activity in the brain. For instance, whereas manipulation of dopaminergic systems by both agonists or antagonists produce extremely highly regionally-specific glucose use alterations, responses to GABA receptor stimulation are widespread, as has been discussed previously (see Introduction,

Section 3.1.1; see also McCulloch, 1982).

The pattern of dynamic events acutely following intracerebral injection of agents is generally markedly different from the cerebral metabolic consequences of systemic administration. This is highlighted by the pronounced glucose use alterations seen, in the present study, following infusion of excitatory amino acid agonists into the NBM region of the basal forebrain. Local rates of cerebral glucose utilisation were altered in regions corresponding to the projection fields of the NBM, and of striatum and globus pallidus. Hence, following administration of agents which are capable of modifying dynamic neuronal activity, assessment of alterations in local rates of glucose utilisation provides insight not only into the location of specific receptor subtypes within the brain, but moreover into functional pathways in which activity is influenced by specific receptor manipulations.

In contrast to the acute effects of basal forebrain receptor manipulations, chronic excitotoxic NBM lesions appear to have no effect on cerebral glucose use, putatively due to functional plasticity in deafferentated regions (London et al., 1984; Orzi et al., 1988; Kiyosawa et al., 1989; and present study). However this lack of effect of chronic lesions on glucose metabolism is not characteristic of all lesion paradigms. For example, following chronic, unilateral excitotoxic lesions of the striatum with kainic acid, resulting in interruption of predominantly GABAergic striatofugal projections, pronounced increases in glucose use have been observed in the primary projection targets of striatal efferents - the ipsilateral globus pallidus and substantia nigra pars reticulata (Kelly et al., 1982). In these structures the striatal projection represents the major afferent input. Therefore, the

chronic metabolic sequelae of neuronal lesions appear to depend on the region lesioned and its structural and functional association with other brain regions.

In conclusion, the results of the present local cerebral glucose use studies in rat brain have highlighted some of the strengths and weaknesses of using the [$^{14}$C]-2-deoxyglucose technique to gain insight into functional events *in vivo*. It is clear from the cerebral metabolic sequelae of the excitatory amino acid receptor-mediated events outlined in these studies that this autoradiographic technique is maximally exploited in situations in which there is capacity for dynamic modulation of neuronal activity, such as during excitatory amino acid receptor blockade. However, meaningful interpretation of local alterations in rates of cerebral glucose utilisation following receptor manipulations critically requires consideration of the anatomical distribution of receptors, in conjunction with an appreciation of functional pathways within the CNS in which activity is influenced by these receptor populations. The development of quantitative *in vitro* ligand binding autoradiography techniques has provided a means of mapping the distributions of receptors and receptor subtypes within the CNS, while *in vivo* ligand binding procedures, such as [$^{125}$I]-MK-801 *in vivo* autoradiography, facilitate enhanced characterisation of the functional status of receptor populations in the normal brain, and under conditions of CNS challenge. Therefore, the application of other techniques in parallel with assessment of cerebral glucose use, such as quantitative *in vitro* and *in vivo* binding autoradiography, or biochemical, electrophysiological or histological investigation of the consequences of receptor manipulation, augments understanding of the contribution of neurotransmitter systems to integrated functional activity within the CNS.

## REFERENCES


Abdul-Ghani, A.S., Bradford, H.F., Cox, D.W. and Dodd, P.R. (1979) Peripheral sensory stimulation and the release of transmitter amino acids in vivo from specific regions of cerebral cortex. *Brain Research*, **171**, 55-66.

Abe, T., Sugihara, H., Nawa, H., Shigemoto, R., Mizuno, N. & Nakanishi, S. (1992) Molecular characterization of a novel metabotropic glutamate receptor mGluR5 coupled to inositol phosphate/$Ca^{2+}$ signal transduction. *Journal of Biological Chemistry*, **267**, 13361-13368.

Abele, A.E., Scholz, K.P., Scholz, W.K. & Miller, R.J. (1990) Excitotoxicity induced by enhanced excitatory neurotransmission in cultured hippocampal pyramidal neurones. *Neuron*, **2**, 413-419.

Ackermann, R.F., Finch, D.M., Babb, T.L. & Engel Jr., J. (1984) Increased glucose metabolism during long-duration recurrent inhibition of hippocampal pyramidal cells. *Journal of Neuroscience*, **4**, 251-264.

Aebischer, B., Frey, P., Haerter, H.P., Herrling, P.L., Mueller, W., Olverman, H.J. & Watkins, J.C. (1989) Synthesis and NMDA-antagonistic properties of the enantiomers of CPP and the unsaturated analogue CPP-ene. *Helv. Chim. Acta*, **72**, 1043-1051.

Agrawal, S.G. & Evans, R.H. (1986) The primary afferent depolarizing action of kainate in the rat. *British Journal of Pharmacology*, **87**, 345-355.

Arendash, G.W., Millard, W.J., Dunn, A.J. & Meyer, E.M. (1987) Long-term neuropathological and neurochemical effects of nucleus basalis lesions in the rat. *Science*, **238**, 952-956.

Arendt, T., Allen, Y., Marchbanks, R.M., Schugens, M.M., Sinden, J., Lantos, P.L. & Gray, J.A. (1989) Cholinergic system and memory in the rat: effects of chronic ethanol, embryonic basal forebrain brain transplants and excitotoxic lesions of cholinergic basal forebrain projection system. *Neuroscience*, **33**, 435-462.

Ascher, P. & Nowak, L. (1987) Electrophysiological studies of NMDA receptors. *Trends in Neurosciences*, **10**, 284-288.

Ascher, P. & Nowak, L. (1988a) Quisqualate- and kainate-activated channels in mouse central neurones in culture. *Journal of Physiology*, **399**, 227-246.

Ascher, P. & Nowak, L. (1988b) The role of divalent cations in the *N*-methyl-D-aspartate responses of mouse central neurones in culture. *Journal of Physiology*, **399**, 247-266.

Astrup, J., Sørensen, P.M. & Sørensen, H.R. (1981) Oxygen and glucose consumption related to $Na^+$-$K^+$ transport in canine brain. *Stroke*, **12**, 726-730.

Barbour, B., Brew, H. & Attwell, D. (1988) Electrogenic glutamate uptake in glial cells is activated by intracellular potassium. *Nature*, **335**, 433-435.

Barbour, B., Szatkowski, M., Ingledew, N. & Attwell, D. (1989) Arachidonic acid induces a prolonged inhibition of glutamate uptake into glial cells. *Nature*, **342**, 918-920.

Bartus, R.T., Dean III, R.L., Beer, B. & Lippa, A.S. (1982) The cholinergic hypothesis of geriatric memory dysfunction. *Science*, **217**, 408-417.

Bartus, R.T., Flicker, C., Dean, R.L., Pontecorvo, M., Figueiredo, J.C. & Fisher, S.K. (1985) Selective memory loss following nucleus basalis lesions: long term behavioural recovery despite persistent cholinergic deficiences. *Pharmacology, Biochemistry and Behaviour*, **23**, 125-135.

Bashir, Z.I., Bartolotto, Z.A., Davies, C.JH., Berretta, N., Irving, A.J., Seal, A.J., Henley, J.M., Jane, D.E., Watkins, J.C. & Collingridge, G.L. (1993) Induction of LTP in the hippocampus needs synaptic activation of glutamate metabotropic receptors. *Nature*, **363**, 347-350.

Beal, M.F., Kowall, N.W., Ellison, D.W., Mazurek, M.F., Swartz, K.J. & Martin, J.B. (1986) Replication of the neurochemical characteristics of Huntington's disease by quinolinic acid. *Nature*, **321**, 168-171.

Beckstead, R.M., Domesick, V.B. & Nauta, W.J.H. (1979) Efferent connections of the substantia nigra and ventral tegmental area in the rat. *Brain Research*, **175**, 191-217.

Bekkers, J.M. & Stevens, C.F. (1993) NMDA receptors at excitatory synapses in the hippocampus: test of a theory of magnesium block. *Neuroscience Letters*, **156**, 73-77.

Ben-Ari, Y., Aniksztejn, A. & Bregestovski, P. (1992) Protein kinase C modulation of NMDA currents: an important link for LTP induction. *Trends in Neurosciences*, **15**, 333-339.

Benavides, J., Fage, D., Carter, C. & Scatton, B. (1987) Peripheral type benzodiazepine binding sites are a sensitive indirect index of neuronal damage. *Brain Research*, **421**, 167-172.

Benavides, J., Quarteronet, D., Imbault, F., Malgouris, C., Uzan, A., Renault, C., Dubroeucq, M.C., Gueremy, C. & Le Fur, G. (1983) Labelling of "peripheral-type" benzodiazepine binding sites in the rat brain by using [$^3$H]PK 11195, an isoquinoline carboxamide derivative: kinetic studies and autoradiographic localization. *Journal of Neurochemistry*, **41**, 1744-1750.

Benveniste, H., Drejer, J., Schousboe, A. & Diemer, N.H. (1984) Elevation of the extracellular concentrations of glutamate and aspartate in rat hippocampus during transient cerebral ischemia monitored by intracerebral microdialysis. *Journal of Neurochemistry*, **43**, 1369-1374.

Bettler, B., Egebjerg, J., Sharma, G., Pecht, G., Hermansborgmeyer, I., Mou, C., Stevens, C.F. & Heinemann, S. (1992) Cloning of a putative glutamate receptor - A low affinity kainate-binding subunit. *Neuron*, **8**, 257-265.

Bigl, V., Woolf, N.J. & Butcher, L.L. (1982) Cholinergic projections from the basal forebrain to frontal, parietal, temporal, occipital and cingulate cortices: A combined fluorescent tracer and acetylcholinesterase analysis. *Brain Research Bulletin*, **8**, 729-749.

Bleakman, D., Chard, P.S. Foucart, S. & Miller, R.J. (1991) Block of neuronal $Ca^{2+}$ influx by the antiischemic agent TA-3090. *Journal of Pharmacology and Experimental Therapeutics*, **259**, 430-438.

Bonhaus, D.W., Burge, B.C. & McNamara, J.O. (1987) Biochemical evidence that glycine allosterically regulates an NMDA receptor coupled ion channel. *European Journal of Pharmacology*, **142**, 489-490.

Borgström, L., Norberg, K. & Siesjö, B.K. (1976) Glucose consumption in rat cerebral cortex in normoxia, hypoxia and hypercapnia. *Acta Physiologica Scandinavia*, **96**, 569-574.

Bosley, T.M., Woodhams, P.L., Gordon, R.D. & Balazs, R. (1983) Effects of anoxia on the stimulated release of amino acid neurotransmitters in the cerebellum in vitro. *Journal of Neurochemistry*, **40**, 189-201.

Bowery, N.G., Wong, E.H.F & Hudson, A.L. (1988) Quantitative autoradiography of [$^3$H]-MK-801 binding sites in mammalian brain. *British Journal of Pharmacology*, **93**, 944-954.

Bredt, D.S. & Snyder, S.H. (1989) Nitric oxide mediates glutamate-linked enhancement of cGMP levels in the cerebellum. *Proceedings of the National Academy of Sciences, U.S.A.*, **86**, 9030-9033.

Brierley, J.B. & Graham, D.I. (1984) Hypoxia and vascular disorders of the central nervous system. In *Greenfield's Neuropathology*, ed. Adams, J.H., Corsellis, J.A.N., Duchen, L.W., pp.125-207, John Wiley & Sons Inc., New York.

Bristow, D.R., Bowery, N.G. & Woodruff, G.N. (1986) Light microscopic autoradiographic localisation of [$^3$H]glycine and [$^3$H]strychnine binding sites in rat brain. *European Journal of Pharmacology*, **126**, 303-307.

Brorson, J.R., Bleakman, D., Chard, P.S. & Miller, R.J. (1992) Calcium directly permeates kainate/alpha-amino-3-hydroxy-5-methyl-4-isoxazole propionic acid receptors in cultured cerebellar Purkinje neurons. *Molecular Pharmacology*, **41**, 603-608.

Brorson, J.R., Bleakman, D., Gibbons, S.J. & Miller, R.J. (1991) The properties of intracellular $Ca^{2+}$ stores in cultured rat cerebellar neurons. *Journal of Neuroscience*, **11**, 4024-4043.

Brown, A.W. & Brierley, J.B. (1972) Anoxic-ischaemic cell change in rat brain light microscopic and fine-structural observations. *Journal of Neurological Sciences*, **16**, 59-84.

Brown, L.L. & Wolfson, L.I. (1978) Apomorphine increases glucose utilization in the substantia nigra, subthalamic nucleus, and corpus striatum of rat. *Brain Research*, **140**, 188-193.

Browne, S.E., Horsburgh, K., Dewar, D. & McCulloch, J. (1991) D-[$^3$H]-aspartate binding does not locate glutamate-releasing neurones in the retino-fugal projection: an autoradiographic comparison with [$^3$H]cyclohexyladenosine binding. *Molecular Neuropharmacology*, **1**, 129-133.

Buchan, A.M., Li, H., Cho, S. & Pulsinelli, W.A. (1991a) Blockade of the AMPA receptor prevents CA1 hippocampal injury following severe but transient forebrain ischemia in adult rats. *Neuroscience Letters*, **132**, 255-258.

Buchan, A., Li, H. & Pulsinelli, W.A. (1991b) The N-methyl-D-aspartate antagonist, MK-801, fails to protect against neuronal damage caused by transient severe forebrain ischaemia in adult rats. *The Journal of Neuroscience*, **11**, 1049-1056.

Buchan, A.M. & Pulsinelli, W.A. (1990) Septo-hippocampal deafferentation protects CA1 neurons against ischemic injury. *Brain Research*, **512**, 7-14.

Bullock, R., Graham, D.I. & McCulloch, J. (1993) The neuroprotective effect of the AMPA receptor antagonist LY-293558 in focal cerebral ischemia in the cat. *Journal of Cerebral Blood Flow and Metabolism*, (in press).

Bullock, R., Kuroda, Y., Teasdale, G.M. & McCulloch, J. (1992) Prevention of post-traumatic excitotoxic brain damage with NMDA antagonist drugs: A new strategy for the nineties. *Acta Neurochir.*, **55**, 49-55.

Burke, S.P. & Nadler, J.V. (1988) Relgulation of glutamate and aspartate release from slices of the hippocampal CA1 area: effects of adenosine and baclofen. *Journal of Neurochemistry*, **51**,1541-1551.

Burnashev, N., Monyer, H., Seeburg, P.J. & Sakmann, B. (1992) Divalent ion permeability of AMPA receptor channels is dominated by the edited form of a single subunit. *Neuron*, **8**, 189-198.

Butcher, S.P., Bullock, R., Graham, D.I. & McCulloch, J. (1990) Correlation between amino acid release and neuropathologic outcome in rat brain following middle cerebral artery occlusion. *Stroke*, **21**, 1727-1733.

Carter, D.A. & Fibiger, H.C. (1978) The projections of the entopeduncular nucleus and globus pallidus in rat as demonstrated by autoradiography and horseradish peroxidase histochemistry. *The Journal of Comparative Neurology*, **177**, 113-124.

Casamenti, F., Deffenu, G., Abbamondi, A.L. & Pepeu, G. (1986) Changes in cortical acetylcholine output induced by modulation of the nucleus basalis. *Brain Research Bulletin*, **16**, 689-695.

Celik, G., Graham, D.I., Kelly, P.A.T. & McCulloch, J. (1982) Kainic acid adminstration and the relationship between local cerebral glucose utilization and local blood flow, In: *Cerebral Blood Flow: Effects of Nerves and Neurotransmitters*, ed. Heistad, D.D. & Marcus, M.L., pp.249-255, Elsevier North Holland.

Chalmers, D.T., Dewar, D., Graham, D.I., Brooks, D.N. & McCulloch, J. (1990) Differential alterations of cortical glutamatergic binding sites in senile dementia of the Alzheimer type. *Proceedings of the National Academy of Sciences, U.S.A.*, **87**, 1352-1356.

Chalmers, D.T. & McCulloch, J. (1991) Selective alterations in glutamate receptor subtypes after unilateral orbital enucleation. *Brain Research*, **540**, 255-265.

Chapman, A.G., Graham, J.L., Swan, J.H. & Meldrum, B.S. (1991) Regional cerebral glucose utilization in rat brain following the administration of CGP 39551, a competitive NMDA antagonists. *Journal of Cerebral Blood Flow and Metabolism*, **11**, (Suppl. 2), S226.

Chapman, A.G., Swan, J.H. & Meldrum, B.S. (1989) Enhanced glucose utilization in pyriform cortex of rats induced by the competitive NMDA antagonist AP7. *Journal of Cerebral Blood Flow and Metabolism*, **9**, (Suppl. 1), S310.

Chen, M., Bullock, R., Graham, D.I., Frey, P., Lowe, D. & McCulloch, J. (1991) Evaluation of a competitive NMDA antagonist (D-CPPene) in feline focal cerebral ischemia. *Annals of Neurology*, **30**, 62-70.

Chessell, I.P., Procter, A.W., Francis, P.T. & Bowen, D.M. (1991) D-cycloserine, a putative cognitive enhancer, facilitiates activation of the N-methyl-D-aspartate receptor-ionophore complex in Alzheimer brain. *Brain Research*, **565**, 345-348.

Choi, D.W., (1987) Ionic dependence of glutamate neurotoxicity. *The Journal of Neuroscience*, **7**, 369-79.

Choi, D.W. (1990) Methods for antagonizing glutamate neurotoxicity. *Cerebrovascular Brain Metabolism Reviews*, **2**, 105-147.

Choi, D.W. (1991) Excitotoxicity. In *Excitatory Amino Acid Antagonists*, ed. Meldrum, B.S., pp.216-236, Oxford: Blackwell.

Cohen, J. (1977) Statistical power analysis for the behavioral sciences, rev. ed., New York: Academic Press.

Clineschmidt, B.V., Martin, G.E. & Bunting, P.R. (1982) Anticonvulsant activity of (+)-5-methyl-10,11-dihydro-5H-dibenzo[a,d]cyclohepten-5,10-imine maleate (MK-801), a substance with potent anticonvulsant, central sympathomimetic, and apparent anxiolytic properties. *Drug Development Research*, **2**, 123-134.

Collingridge, G.L. & Bliss, T.V.P. (1987) NMDA receptors - their role in long-term potentiation. *Trends in Neurosciences*, **10**, 288-294

Collingridge, G.L., Kehl, S.J. & McLennan, H. (1983) Excitatory amino acids in synaptic transmission in the Schaffer collateral-commissural pathway of the rat hippocampus. *Journal of Physiology*, **334**, 33-46.

Collingridge, G.L. & Lester, R.A.J. (1989) Excitatory amino acid receptors in the vertebrate central nervous system. *Pharmacological Reviews*, **40**, 143-210.

Collins, G.G.S. (1980) Release of endogenous amino acid neurotransmitter candidates from rat olfactory cortex slices: possible regulatory mechanisms and the effects of pentobarbitone. *Brain Research*, **190**, 517-528.

Collins, R.C., McCandless, D.W. & Wagman, I.L. (1987) Cerebral glucose utilization: comparison of [$^{14}$C]-deoxyglucose and [6-$^{14}$C]glucose quantitative autoradiography. *Journal of Neurochemistry*, **49**, 1564-1570.

Cotman, C.W., Flatman, J.A., Ganong, A.H. & Perkins, M.N. (1986) Effects of excitatory amino acid antagonists on evoked and spontaneous excitatory potentials in guinea-pig hippocampus. *Journal of Physiology*, **378**, 403-415.

Cotman, C.W., Foster, A. & Lanthorn, T. (1981) An overview of glutamate as a neurotransmitter. In *Glutamate as a Neurotransmitter*, ed. DiChiara, G., Gessa, G.L., pp.1-27, Raven Press, New York.

Cotman, C.W. & Iversen, L.L. (1987) Excitatory amino acids in the brain -focus on NMDA receptors. *Trends in Neurosciences*, **10**, 263-265

Cotman, C.W., Monaghan, D.T., Ottersen, O.P. & Storm-Mathisen, J. (1987) Anatomical organization of excitatory amino acid receptors and their pathways. *Trends in Neurosciences*, **7**, 273-280.

Cowburn, R., Hardy, J., Roberts, P. & Briggs, R. (1988) Presynaptic and postsynaptic glutamatergic function in Alzheimer's disease. *Neuroscience Letters*, **86**, 109-113.

Coyle, J.T. & Schwarcz, R. (1976) Lesion of striatal neurones with kainic acid provides a model for Huntington's chorea. *Nature*, **263**, 244-246.

Crane, P.D., Braun, L.D., Cornford, E.M., Cremer, J.E., Glass, J.M. and Oldendorf, W.H. (1978) Dose dependent reduction of glucose utilization by pentobarbital in rat brain. *Stroke*, **9**, 12-18.

Cudennec, A., Duverger, D., Nishikawa, T., McRae-Degueurce, A., MacKenzie, E.T. & Scatton, B. (1988a) Influence of ascending serotonergic pathways on glucose use in the conscious rat brain. I. Effects of electrolytic or neurotoxic lesions of the dorsal and/or medial raphé nucleus. *Brain Research*, **444**, 214-226.

Cudennec, A., Duverger, D., Serrano, A., Scatton, B. & MacKenzie, E.T. (1988b) Influence of ascending serotonergic pathways on glucose use in the conscious rat brain. II. Effects of electrical stimulation of the rostral raphé nucleus. *Brain Research*, **444**, 227-246.

Curtis, D.R. & Johnston, G.A. (1974) Amino acid transmitters in the mammalian central nervous system. *Ergeb-Physiol.*, **69**, 97-188.

Curtis, D.R., Phillis, J.W. & Watkins, J.C. (1960) The chemical excitation of spinal neurones by certain acidic amino acids, *Journal of Physiology*, **150**, 656-682.

D'Angelo, E., Rossi, P. & Garthwaite, J. (1990) Dual-component NMDA receptor currents at a single central synapse. *Nature*, **346**, 467-469.

Danysz, J.T., Wroblewski, J.T. & Costa, E. (1988) Learning impairment in rats by N-methyl-D-aspartate receptor antagonists. *Neuropharmacology*, **27**, 653-656.

Dawson, V.L., Dawson, T.M., Bartley, D.A., Uhl, G.R. & Snyder, S.H. (1993) Mechanisms of nitric oxide-mediated neurotoxicity in primary brain cultures. *The Journal of Neuroscience*, **13**, 2651-2661.

Dawson, V.L., Dawson, T.M., London, E.D., Bredt, D.S. & Snyder, S.H. (1991) Nitric oxide mediates glutamate neurotoxicity in primary cortical cultures. *Proceedings of the National Academy of Sciences, U.S.A.*, **88**, 6368-6371.

DeBoni, U. & Crapper-McLachlan, D.R. (1985) Controlled induction of paired helical filaments of the Alzheimer type in cultured human neurons, by glutamate and aspartate. *Journal of Neurological Sciences*, **68**, 105-118.

Dewar, D., Chalmers, D.T., Graham, D.I. & McCulloch, J. (1991) Glutamate metabotropic and AMPA binding sites are reduced in Alzheimer's disease: an autoradiographic study of the hippocampus. *Brain Research*, **553**, 58-64.

Dewar, D. & McCulloch, J. (1992) Mapping functional events in the CNS with 2-deoxyglucose autoradiography; In *Quantitative Methods in Neuroanatomy*, ed. Stewart, M.G., pp.57-84, John Wiley & Sons, Chichester.

Diaz-Gierra, M.J., Sanches-Prieto, J., Bosca, L., Pocock, J., Barrie, A. & Nicholls, D. (1988) Phorbol ester translocation of protein kinase C in guinea-pig synaptosomes and the potentiation of calcium-dependent glutamate release. *Biochim. Biophys. Acta*, **970**, 157-165.

DiChiara, G. & Gessa, G.L. (1981) *Glutamate as a Neurotransmitter*, New York: Raven Press.

Diemer N.H., Jörgensen M.B., Johansen, F.F., Sheardown M. and Honoré T. (1992) Protection against ischemic hippocampal CA1 damage in the rat with a new non-NMDA antagonist, NBQX. *Acta Neurologica Scandinavia*, **86**, 45-49.

Dienel, G. (1984) Regional accumulation of calcium ion in post-ischemic rat brain. *Journal of Neurochemistry*, **43**, 913-925.

Do, K.Q., Herrling, P.L., Streit, P., Turski, W.A. & Cuenod, M. (1986) *In vitro* release and electrophysiological effects *in situ* of homocysteic acid, an endogenous *N*-methyl-(D)-aspartic acid agonist, in the mammalian striatum. *The Journal of Neuroscience*, **6**, 2226-22234.

Drejer, J., Benveniste, H., Diemer, N.H. & Schousboe, A. (1985) Cellular origin of ischemia-induced glutamate release from brain tissue in vivo and in vitro. *Journal of Neurochemistry*, **45**, 145-151.

Dumuis, A., Sebben, M., Haynes, L., Pin, J.-P. & Bockaert, J. (1988) NMDA receptors activate the arachidonic acid cascade system in striatal neurones. *Nature*, **336**, 68-70.

Dunnett, S.B., Everitt, B.J. & Robbins, T.W. (1991) The basal forebrain-cortical cholinergic system: interpreting the functional consequences of excitotoxic lesions. *Trends in Neurosciences*, **14**, 494-500.

Dunnett, S.B., Whishaw, I.Q., Jones, G.H. & Bunch, S.T. (1987) Behavioural, biochemical and histochemical effects of different neurotoxic amino acids injected into nucleus basalis magnocellularis of rats. *Neuroscience*, **20**, 653-669.

Emmett, M.R., Mick, S.J., Cler, J.A., Rao, T.S., Iyengar, S. & Wood, P.L. (1991) Actions of D-cycloserine at the *N*-methyl-D-aspartate-associated glycine receptor site *in vivo*. *Neuropharmacology*, **30**, 1167-1171.

Etherington, R., Mittleman, G. & Robbins, T.W. (1987) Comparative effects of nucleus basalis and fimbria-fornix lesions on delayed matching and alteration tests of memory. *Neuroscience Research Communications*, **1**, 135-143.

Everitt, B.J., Robbins, T.W., Evenden, J.L., Marston, H.M., Jones, G.H. & Sirkia, T.E. (1987) The effects of excitotoxic lesions of the substantia innominata, ventral and dorsal globus pallidus on the acquisition and retention of a conditional visual discrimination: implications for cholinergic hypotheses of learning and memory. *Neuroscience*, **22**, 441-469.

Fadda, E., Danysz, W., Wroblewski, J.T. & Costa, E. (1988) Glycine and D-serine increase the affinity of *N*-methyl-D-aspartate sensitive glutamate-binding sites in rat brain synaptic-membranes. *Neuropharmacology*, **27**, 1183-1185.

Faden, A.I. & Simon, R.P. (1988) A potential role for excitotoxins in the pathophysiology of spinal cord injury. *Annals of Neurology*, **23**, 623-626.

Ffrench-Mullen, J.M.H., Koller, K., Zaczek, R., Coyle, J.J., Hori, N. & Carpenter, D.O. (1985) *N*-acetylaspartylglutamate: possible role for the neurotransmitter of the lateral olfactory tract. *Proceedings of the National Academy of Sciences, U.S.A.*, **82**, 3897-3900.

Fibiger, H.C. (1991) Cholinergic mechanisms in learning, memory and dementia: a review of recent evidence. *Trends in Neurological Sciences*, **14**, 220-223.

Flicker, C., Dean, R.L., Watkins, D.L., Fisher, S.K. & Bartus, R.T. (1983) Behavioural and neurochemical effects following neurotoxic lesions of a major cholinergic input to the cerebral cortex in the rat. *Pharmacology, Biochemistry and Behaviour*, **18**, 973-981.

Flood, J.F., Morley, J.E. & Lanthorn, T.H. (1992) Effect on memory processing by D-cycloserine, an agonist of the NMDA/glycine receptor. *European Journal of Pharmacology*, **221**, 249-254.

Fonnum, F. (1984) Glutamate: a neurotransmitter in mammalian brain. *Journal of Neurochemistry*, **41**, 1-11.

Foster, A.C. & Fagg, G.E. (1984) Acidic amino acid binding sites in mammalian neuronal membranes: their characteristics and relationship to synaptic receptors. *Brain Research Reviews*, **7**, 103-164.

Foster, A.C., Gill, R. & Woodruff, G.N. (1988) Neuroprotective effects of MK-801 in vivo: selectivity and evidence for delayed degeneration mediated by NMDA receptor activation. *Journal of Neuroscience*, **8**, 4745-4754.

Foster, A.C. & Kemp, J.A. (1989) Glycine maintains excitement. *Neurobiology*, **338**, 377-378.

Frandsen, A., Quistoff, B. & Schousboe, A. (1990) Phenobarbital protects cerebral cortex neurones against toxicity induced by kainate but not by other excitatory amino acids. *Neuroscience Letters*, **111**, 233-238.

Fujisawa, H., Dawson, D., Browne, S.E., Mackay, K.B., Bullock, R. & McCulloch, J. (1993a) Pharmacological modification of glutamate neurotoxicity in vivo. *Brain Research* **629**, 73-78.

Fujisawa, H., Landolt, H., Macrae, I.M. & Bullock, R. (1993b) Glutamate neurotoxicity in vivo: The effect of ischaemia and ionic concentrations in extracellular fluid. *Journal of Cerebral Blood Flow and Metabolism*, **13** (Suppl.1), S784.

Garthwaite, J. (1991) Glutamate, nitric oxide and cell-cell signalling in the nervous system. *Trends in Neurosciences*, **14**, 60-67.

Garthwaite, J. & Garthwaite, G. (1990) Mechanisms of excitatory amino acid neurotoxicity in rat brain slices. In *Excitatory Amino Acids and Neuronal Plasticity*, ed. Ben-Ari, Y., pp.505-518, Plenum Press, New York.

Geddes, J.W., Chang-Chui, H., Cooper, S.M., Lott, I.T. & Cotman, C.W. (1986) Density and distribution of NMDA receptors in the human hippocampus in Alzheimer's disease. *Brain Research*, **399**, 156-161.

Gerfen, C.R. (1985) The neostriatal mosaic. I. Compartmental organization of projections from the striatum to the substantia nigra in the rat. *The Journal of Comparative Neurology*, **236**, 454-476.

Giffard, R.G., Monyer, H., Christine, C.W. & Choi, D.W. (1990) Acidosis reduces NMDA receptor activation, glutamate neurotoxicity, and oxygen-glucose deprivation neuronal injury in cortical cultures. *Brain Research*, **506**, 339-342.

Gill, R. (1992) Neuroprotective studies of excitatory amino acid antagonists in focal cerebral ischaemia in the rat, (Thesis) University of London.

Gill, R., Brazell, C., Woodruff, G.N. & Kemp, J.A. (1991) The neuroprotective action of dizocilpine (MK-801) in the rat middle cerebral artery occlusion model of focal ischaemia. *British Journal of Pharmacology*, **103**, 2030-2036.

Gill, R., Foster, A.C. & Woodruff, G.N. (1987) Systemic administration of MK-801 protects against ischemia-induced hippocampal neurodegeneration in the gerbil. *The Journal of Neuroscience*, **7**, 3343-3349.

Gill, R., Foster, A.C. & Woodruff, G.N. (1989) Neuroprotective actions of MK-801 in rat global ischaemia model. *Journal of Cerebral Blood Flow and Metabolism*, **9**, (Suppl.1), S629.

Gill, R., Nordholm, L. & Lodge, D. (1992) The neuroprotective actions of 2,3-dihydroxy-6-nitro-7-sulfamoyl-benzo(F)quinoxaline (NBQX) in a rat focal ischaemia model. *Brain Research*, **580**, 35-43.

Ginsberg, M.D. (1990) Local metabolic responses to cerebral ischaemia. *Cerebrovascular Brain Metabolism Reviews*, **2**, 58-93.

Ginsberg, M.D., Dietrich, D.W. & Busto, R. (1987) Coupled forebrain increases of local cerebral glucose utilization and blood flow during physiologic stimulation of a somatosensory pathway in the rat: demonstration by double-label autoradiography. *Neurology*, **37**, 11-19.

Gjedde, A. (1982) Calculation of cerebral glucose phosphorylation from brain uptake of glucose analogus *in vivo*: a re-examination. *Brain Research Reviews*, **4**, 237-274.

Graham, S.H., Chen, J., Sharp, F.R. & Simon, R.P. (1993) Limiting ischemic injury by inhibition of excitatory amino acid release. *Journal of Cerebral Blood Flow and Metabolism*, **13**, 88-97.

Granata, A.R. & Reis, D.J. (1983) Release of [$^3$H]L-glutamic acid (L-glu) and [$^3$H]D-aspartic acid (D-asp) in the area of nucleus tractus solitarius in vivo produced by stimulation of the vagus nerve. *Brain Research*, **259**, 77-93.

Greenamyre J.T. (1986) The role of glutamate in neurotransmission and in neurologic disease. *Archives of Neurology*, **43**, 1058-1063.

Greenamyre J.T., Penney, J.B., D'Amato, C.J. & Young, A.B. (1987) Dementia of the Alzheimer's type: changes in hippocampal L-[$^3$H]glutamate binding. *Journal of Neurochemistry*, **48**, 543-551.

Grome, J.J. & McCulloch, J. (1983) The effects of apomorphine upon local cerebral glucose utilization in conscious rats and in rats anaesthetized with chloral hydrate. *Journal of Neurochemistry*, **40**, 569-576.

Guildin, W.O. & Markowitsch, H.J. (1983) Cortical and thalamic afferent connections on the visular and adjacent cortex of the rat. *The Journal of Comparative Neurology*, **215**, 135-153.

Habner, S.N., Groenewegen, H.J., Grove, E.A. & Nauta, W.J.H. (1985) Efferent connections of the ventral pallidum: evidence of a dual striato pallidofugal pathway. *The Journal of Comparative Neurology*, **235**, 322-335.

Hagberg, H., Lehman, A., Sandberg, M., Nyström, B., Jacobson, I. & Hamberger, A. (1985) Ischemia-induced shift of inhibitory and excitatory amino acids from intra- to extracellular compartments. *Journal of Cerebral Blood Flow and Metabolism*, **5**, 413-419.

Grotta, J. (1994) Safety and tolerability of the glutamate antagonist CGS19755 in acute stroke patients. *Stroke*, 25 (Suppl.), 52, 255.

Haldeman, S. & McLennan, H. (1972) The antagonist action of glutamic acid diethyl ester towards amino acid-induced and synaptic excitations of central neurones. *Brain Research*, **45**, 393-400.

Hamberger, A., Berthold, C.-H., Karlsson, B. et al. (1983) Extracellular GABA, glutamate and glutamine in vivo: Perfusion dialysis of the rabbit hippocampus. In *Glutamine, Glutamate and GABA in the Central Nervous System*, ed. Hertz, L., Kvamme, E., McGeer, E.G. et al., pp.473-491, Alan R. Liss Inc., New York.

Handelmann, G.E., Mueller, L.L. & Cordi, A.A. (1988) Glycinergic compounds facilitate memory formation and retrieval in rats. *Society for Neuroscience Abstracts*, **14**, 101.5.

Hargreaves, R.J., Rigby, M., Smith, D., Hill, R.G. and Iversen, L.L. (1993) Competitive as well as uncompetitive N-methyl-D-aspartate receptors antagonists affect cortical neuronal morphology and cerebral glucose metabolism. *Neurochemical Research*, **18**, 1263-1269.

Harrell, L.E. & Davis, J.N. (1984) Cholinergic denervation of the hippocampal formation does not produce long-term changes in glucose metabolism. *Experimental Neurology*, **85**, 128-138.

Hattori, T., Fibiger, H.C. & McGeer, P.L. (1975) Demonstration of a pallido-nigral projection innervating dopaminergic neurons. *The Journal of Comparative Neurology*, **162**, 487-504.

Hawkins, R.A. & Miller, A.L. (1987) Deoxyglucose-6-phosphate stability in vivo and the deoxyglucose method. *Journal of Neurochemistry*, **49**, 1941-1949.

Hawkins, R.A., Miller, A.L., Cremer, J.E. & Veech, R.L. (1974) Measurement of the rate of glucose utilization by rat brain *in vivo*. *Journal of Neurochemistry*, **23**, 917-923.

Hayashi, T. (1954) Effects of sodium glutamate on the nervous system. *Keio Journal of Medicine*, **3**, 183-192.

Headley, P.M. & Grillner, S. (1990) Excitatory amino acids and synaptic transmission: the evidence for a physiological function. *Trends in Pharmacological Sciences*, **11**, 205-211

Helén, P. & London, E.D. (1984) Muscimol-scopolamine interactions in the rat brain: study with 2-deoxy-D-[1-$^{14}$C]glucose. *The Journal of Neuroscience*, **4**, 1405-1413.

Hodes, J.E., Soncrant, T.T., Larson, D.M., Carlson, S.G. & Rappoport, S.I. (1985) Selective changes in local cerebral glucose utilization induced by phenobarbital in the rat. *Anesthesiology*, **63**, 633-639.

Hollman, M., Hartley, M. & Heinemann, S. (1992) $Ca^{2+}$-permeability of KA-AMPA gated glutamate channels depends on subunit composition. *Science*, **252** 851-853.

Hollmann, M., O'Shea-Greenfield, A., Rogers, S.W. & Heinemann, S. (1989) Cloning by functional expression of a member of the glutamate receptor family. *Nature*, **342**, 643-648.

Holopainen, I., Enkrist, M.O.K. & Akerman, K.E.O. (1989) Glutamate receptor agonists increase intracellular $Ca^{2+}$ independently of voltage gated $Ca^{2+}$ channels in rat cerebellar granule cells. *Neuroscience Letters*, **98**, 57-62.

Honey, C.R., Miljkovic, Z. & MacDonald, J.F. (1985) Ketamine and phencyclidine cause a voltage-dependent block of responses to L-aspartic acid. *Neuroscience Letters*, **61**, 135.

Honoré, T., Davies, S.N., Drejer, J., Fletcher, E.J., Jacobson, P., Lodge, D. & Nielsen, F.E. (1988) Quinoxalinediones: Potent competitive non-NMDA glutamate receptor antagonists. *Science*, **241**, 701-703.

Honoré, T., Drejer, J. & Nielsen, M. (1986) Calcium discriminates two [$^{3}$H]kainate binding sites with different molecular target sizes in rat cortex. *Neuroscience Letters*, **65**, 47-52.

Honoré, T., Laurisden, J. & Krogsgaard-Larsen, P. (1982) The binding of [$^3$H]-AMPA, a structural analogue of glutamic acid, to rat brain membranes. *Journal of Neurochemistry*, **38**, 173-178.

Hood, W.F., Compton, R.P. & Monahan, J.B. (1989) D-Cycloserine: a ligand for the *N*-methyl-D-aspartate coupled glycine receptor has partial agonist characteristics. *Neuroscience Letters*, **98**, 91-95.

Hood, W.F., Compton, R.P. & Monahan, J.B. (1990) *N*-methyl-D-aspartate recognition site ligands modulate activity at the coupled glycine recognition site. *Journal of Neurochemistry*, **54**, 1040-1046.

Huettner, J.E. & Bean, B.P. (1988) Block of *N*-methyl-D-aspartate-activated current by the anticonvulsant MK-801: selective binding to open channels. *Proceedings of the National Academy of Sciences, U.S.A.*, **85**, 1307-1311.

Hyman, B.T., VanHoesen, G.W. & Damasio, A.R., (1987) Alzheimer's disease: Cell-specific pathology isolates the hippocampal formation. *Science*, **225**, 1168-1170.

Iino, M., Ozawa, S. & Tsuzuki, K. (1990) Permeation of calcium through excitatory amino acid receptor channels in cultured rat hippocampal neurones. *Journal of Physiology*, **424**, 151-165.

Inglis, F.M., Macrae, I.M., Bullock, R. & McCulloch, J. (1991) The effects of the competitive NMDA antagonist D-CPP-ene, on cerebral glucose use in the rat. *Journal of Cerebral Blood Flow and Metabolism*, **11**, (Suppl. 2), S307.

Jansen, K.L.R., Dragunow, M. & Faull, R.L.M. (1989a) [$^3$H]Glycine binding sites, NMDA and PCP receptors have similar distributions in the human hippocampus: an autoradiographic study. *Brain Research*, **482**, 174-178.

Jansen, K.L.R., Dragunow, M. & Faull, R.L.M. (1989b) Excitatory amino acid receptors in the human cerebral cortex: a quantitative autoradiographic study comparing the distributions of [$^3$H]TCP, [$^3$H]glycine, L-[$^3$H]glutamate, [$^3$H]AMPA and [$^3$H]kainic acid binding sites. *Neuroscience*, **32**, 589-607.

Johnson, J.W. & Ascher, P. (1987) Glycine potentiates the NMDA response in cultured mouse brain neurons. *Nature*, **325**, 529-531.

Johnston, G.A.R., Lodge, D., Bornstein, J.C. & Curtis, D.R. (1980) Potentiations of L-glutamate and L-aspartate excitation of cat spinal neurons by the steroisomers of *threo*-d-hydroxyaspartate. *Journal of Neurochemistry*, **34**, 241-243.

Johnston, M.V., McKinney, M. & Coyle, J.T. (1981) Neocortical cholinergic innervation: A description of extrinsic and intrinsic components in the rat. *Experimental Brain Research*, **43**, 159-172.

Jorgensen, M.B., Johansen, F.F. & Diemer, N.H. (1987) Removal of the entorhinal cortex protects hippocampal CA-1 neurons from ischemic damage. *Acta Neuropathologica*, **73**, 189-194.

Kadekaro, M., Vance, W.H., Terrell, M.L., Gary Jr., H., Eisenberg, H.M. & Sokoloff, L. (1987) Effects of antidromic stimulation of the ventral root on glucose utilization in the ventral horn of the spinal cord in the rat. *Proceedings of the National Academy of Sciences, U.S.A.*, **48**, 5492-5495.

Kanai, Y., Smith, C.P. & Hediger, M.A. (1993) The elusive transporters with a high affinity for glutamate. *Trends in Neurosciences*, **9**, 365-370.

Kauer, J.S. & Cinelli, A.R. (1993) Are there structural and functional modules in the vertebrate olfactory bulb? *Microscopic Research Techniques*, **24**, 157-167.

Keinanen, K., Wisden, W., Sommer, B., Werner, P., Herb, A., Verdoom, T.A., Sakmann, B. & Seeburg, P.H. (1990) A family of AMPA-selective glutamate receptors. *Science*, **249**, 556-560.

Kelly, P.A.T., Ford, I. & McCulloch, J. (1986) The effect of diazepam upon local cerebral glucose use in the conscious rat. *Neuroscience*, **19**, 257-265.

Kelly, P.A.T., Graham, D.I. & McCulloch, J. (1982) Specific alterations in local cerebral glucose utilization following striatal lesions. *Brain Research*, **233**, 157-172.

Kelly, P.A.T. & McCulloch, J. (1982) Effects of the putative GABAergic agonists, muscimol and THIP, upon local cerebral glucose utilisation. *Journal of Neurochemistry*, **39**, 613-624.

Kelly, P.A.T. & McCulloch, J. (1984) Extrastriatal circuits activated by intrastriatal muscimol: A [$^{14}$C]2-deoxyglucose investigation. *Brain Research*, **292**, 357-366.

Kelly, P.A.T. & McCulloch, J. (1987) Cerebral glucose utilization following striatal lesions: the effects of the GABA agonist, muscimol, and the dopaminergic agonist, apomorphine. *Brain Research*, **425**, 290-300.

Kemp, J.A., Foster, A.C. & Wong, E.H.F. (1987) Non-competitive antagonists of excitatory amino acid receptors. *Trends in Neurosciences*, **10**, 294-298.

Kemp, J.A. & Leeson, P.D. (1993) The glycine site of the NMDA receptor - five years on. *Trends in Pharmacological Sciences*, **14**, 20-25.

Kennedy, C., Des Rosiers, M.H., Jehle, J.W., Reivich, M., Sharp, F. & Sokoloff, L. (1975) Mapping of functional neural pathways by autoradiographic survey of local metabolic rate with [$^{14}$C]deoxyglucose. *Science*, **187**, 850-853.

Kessler, M., Terramani, T., Lynch, G. & Baudry, M. (1989) A glycine site associated with *N*-methyl-D-aspartic acid receptors: characterization and identification of a new class of antagonists. *Journal of Neurochemistry*, **52**, 1319-1328.

Kety, S.S. (1960) I. Blood-tissue exchange methods. Theory of blood-tissue exchange and its application to measurement of blood flow. In *Methods in Medical Research*, ed. Bruner, H.D., Vol. 8, pp.223-227, The Year Book Publishers Inc., Chicago.

Kety, S.S. & Schmidt, C.F. (1948) The nitrous oxide method for the quantitative determination of cerebral blood flow in man: theory, procedure and normal values. *Journal of Clinical Investigation*, **27**, 476-483.

Kiyosawa, M., Baron, J.-C., Hamel, E., Pappata, S., Duverger, D., Riche, D., Mazoyer, B., Naquet, R. & MacKenzie, E. (1989) Time course of effects of unilateral lesions of the nucleus basalis of Meynert on glucose utilization by the cerebral cortex. *Brain*, **112**, 435-455.

Kleckner, N.W. & Dingledine, R. (1988) Requirement for glycine in activation of NMDA-receptors expressed in *Xenopus oocytes*. *Science*, **241**, 835-837.

Koh, J.-Y. & Choi, D.W. (1988) Cultured striatal neurons containing NADPH-diaphorase or acetylcholinesterase are selectively resistant to injury by NMDA receptor agonists. *Brain Research*, **446**, 374-378.

Kozlowski, M.R. & Marshall, J.F. (1980) Plasticity of [$^{14}$C]2-deoxy-D-glucose incorporation into neostriatum and related structures in response to dopamine neurone damage and apomorphine replacement. *Brain Research*, **197**, 167-183.

Krebs, H.A. (1935) Metabolism of amino acids. IV. Synthesis of glutamine from glutamic acid and ammonia and the enzymic hydrolysis of glutamine in animal tissue. *Biochemical Journal*, **29**, 1951-1969.

Krogsgaard-Larsen, P., Honoré, T., Hansen, J.J., Curtis, D.R. & Lodge, D. (1980) New class of glutamate agonist structurally related to ibotenic acid. *Nature*, **284**, 64-66.

Kurumaji, A., Dewar, D. & McCulloch, J. (1993) Metabolic mapping with deoxyglucose autoradiography as an approach for assessing drug action in the central nervous system. In *Imaging Drug Action in the Brain*, ed. London, E.D., pp.207-246, CRC Press.

Kurumaji, A. & McCulloch, J. (1990a) Effects of MK-801 upon local cerebral glucose utilisation in conscious rats following unilateral lesion of caudal entorhinal cortex. *Brain Research*, **531**, 72-82.

Kurumaji, A. & McCulloch, J. (1990b) Effects of unilateral intrahippocampal injection of MK-801 upon local cerebral glucose utilisation in conscious rats. *Brain Research*, **518**, 342-346.

Kurumaji, A., Nehls, D.G., Park, C.K. & McCulloch, J. (1989) Effects of NMDA antagonists MK-801 and CPP, upon local cerebral glucose use. *Brain Research*, **496**, 268-284.

Kusumoto, K., Mackay, K.B. & McCulloch, J. (1992) The effects of the kappa-opioid receptor agonist CI-977 in a rat model of focal cerebral ischaemia. *Brain Research*, **576**, 147-151.

Kutsuwada, T., Kashiwabuchi, N., Mori, H., Sakimura, K., Kushiya, E., Araki, K., Meguro, H., Masaki, H., Kumanishi, T., Arakawa, M. & Mishina, M. (1992) Molecular diversity of the NMDA receptor channel. *Nature*, **358**, 36-41.

Lafon-Cazal, M., Pietri, S., Culcasi, M. & Bockaert, J. (1993) NMDA-dependent superoxide production and neurotoxicity. *Nature*, **364**, 535-537.

Lamarca, M.V. & Fibiger, H.C. (1984) Deoxyglucose uptake and choline acetyltransferase activity in cerebral cortex following lesions of the nucleus basalis magnocellularis, *Brain Research*, **307**, 366-369.

Landau, W.M., Freygang Jr., W.H., Rowland, L.P., Sokoloff, L. & Kety, S.S. (1955) The local circulation of the living brain: values in the unanesthetized and anesthetized cat. *Trans. American Neurological Asociation*, **80**, 125-129.

Landolt, H., Bullock, R., Fujisawa, H., McCulloch, J. & Miller, S. (1993) Glutamate diffusion characteristics determine neurotoxicity in the rat brain: $^{14}C$ glutamate autoradiography. *Journal of Cerebral Blood Flow and Metabolism*, **13**, (Suppl. 1), S753.

Lanthorn, T.H., Ganong, A.H. & Cotman, C.W. (1984) 2-Amino-4-phosphonobutyrate selectively blocks mossy fiber-CA3 responses in guinea pig but not rat hippocampus. *Brain Research*, **290**, 174-178.

Lehmann, J., Nagy, J.I., Atmadja, S. & Fibiger, H.C. (1980) The nucleus basalis magnocellularis: The origin of a cholinergic projection to the neocortex of the rat. *Neuroscience*, **5**, 1161-1174.

Lester, R.A.J., Clements, J.D., Westbrook, G.L. & Jahr, C.E. (1990) Channel kinetics determine the time course of NMDA receptor-mediated synaptic currents. *Nature*, **346**, 565-567.

Lester, R.A.J., Tong, G. & Jahr, C.E. (1993) Interactions between the glycine and glutamate binding sites of the NMDA receptor. *Journal of Neuroscience*, **13**, 1088-1096.

Lindvall, O. & Björklund, A. (1979) Dopaminergic innervation of the globus pallidus by collaterals from the nigrostriatal pathway. *Brain Research*, **172**, 169-173.

Linn, C.P. & Christensen, B.N. (1992) Excitatory amino acid regulation of intracellular $Ca^{2+}$ in isolated cat fish core horizontal cells measured under voltage and concentration damp conditions. *The Journal of Neuroscience*, **12**, 2156-2164.

Lipton, S.A., Choi, Y.-B., Pan, Z.-H., Lei, S.Z., Chen, H.-S.V., Sucher, N.J., Loscalzo, J., Singel, D.J. & Stamler, J.S. (1993) A redox-based mechanism for the neuroprotective and neurodestructive effects of nitric oxide and related nitroso-compounds. *Nature*, **364**, 626-632.

Lodge, D. & Johnson, K.M. (1990) Noncompetitive excitatory amino acid receptor antagonists. *Trends in Pharmacological Sciences*, **11**, 81-86.

Logan, A. & Berry, M. (1993) Transforming growth factor-$\beta_1$ and basic fibroblast growth factor in the injured CNS. *Trends in Pharmacological Sciences*, **14**, 337-343.

Loiacono, R.E. & Beart, P.M. (1992) Hippocampal lesions induced by microinjection of the nitric oxide donor nitroprusside. *European Journal of Pharmacology*, **216**, 331-333.

London, E.D. (1993) *Imaging Drug Action in the Brain*, CRC Press.

London, E.D., McKinney, M., Dam, M., Ellis, A. & Coyle, J.T. (1984) Decreased cortical glucose utilization after ibotenate lesion of the rat ventromedial globus pallidus. *Journal of Cerebral Blood Flow and Metabolism*, **4**, 381-390.

Lucas, D.R. & Newhouse, J.P. (1957) The toxic effect of sodium L-glutamate on the inner layers of the retina. *AMA Archives of Opthalmology*, **58**, 193-201.

MacDermott, A.B. & Dale, N. (1987) Receptors, ion channels and synaptic potentials underlying the integrative actions of excitatory amino acids. *Trends in Neurosciences*, **10**, 280-288.

MacDermott, A.B., Mayer, M.L., Westbrook, G.L., Smith, S.J. & Barker J.L. (1986) NMDA-receptor activation increases cytoplasmic calcium concentration in cultured spinal cord neurones. *Nature*, **321**, 519-522.

MacDonald, J.F. & Nowak, L.M. (1990) Mechanisms of blockade of excitatory amino acid receptor channels. *Trends in Pharmacological Sciences*, **11**, 167-172.

Malenka, R.C., Kauer, J.A., Zucker, R.S. & Nicholl, R.A. (1988) Postsynaptic calcium is sufficient for potentiation of hippocampal synaptic transmission. *Science*, **242**, 81-84.

Mandeil, G.L. & Sande, M.A. (1990) Drugs used in the chemotherapy of tuberculosis and leprosy. In *The Pharmacological Basis of Therapeutics*, Eight Edition, ed. Gilman, A.G., Rall, T.W., Nies, A.S., Taylor, P., pp.1156-1157, Pergamon Press.

Mann, D.M.A. (1988) Neuropathological and neurochemical aspects of Alzheimer's disease. In *Handbook of Psychopharmacology, Vol. 20*, ed. Iversen, L.L., Iversen, S.D. & Snyder, S.H., pp.1-67, Plenum Press.

Maragos, W.F., Greenamyre, J.T., Penney, J.B. & Young, A.B. (1987) Glutamate dysfunction in Alzheimer's disease: an hypothesis. *Trends in Neurosciences*, **10**, 65-68.

Maragos, W.F., Penney, J.B. & Young, A.B. (1988) Anatomic correlation of NMDA and [$^3$H]TCP labelled receptors in rat brain. *Journal of Neuroscience*, **8**, 493-501.

Marchi, M., Bocchieri, P., Garbarino, L. & Raiteri, M. (1989) Muscarinic inhibition of endogenous glutamate release from rat hippocampus synaptosomes. *Neuroscience Letters*, **96**, 229-234.

Massieu, L., Thedinga, K.H., McVey, M. & Fagg, G.E. (1993) A comparative analysis of the neuroprotective properties of competitive and uncompetitive *N*-methyl-D-aspartate receptor antagonists *in vivo*: implications for the process of excitotoxic degeneration and its therapy. *Neuroscience*, **55**, 883-892.

Mayer, M.L. & Vyklicky Jr., L. (1989) The action of zinc on synaptic transmission and neuronal excitability in cultures of mouse hippocampus. *Journal of Physiology*, **415**, 351-365.

Mayer, M.L. & Westbrook, G.L. (1987a) The physiology of excitatory amino acids in the vertebrate central nervous system. *Progress in Neurology*, **28**, 197-276.

Mayer, M.L. & Westbrook, G.L. (1987b) Permeation and block of N-methyl-D-aspartic acid receptor channels by divalent cations in mouse cultured central neurons. *Journal of Physiology*, **394**, 501-527.

Mayer, M.L. & Miller, R.J. (1990) Excitatory amino acid receptors: regulation of neuronal $[Ca^{2+}]_i$ and other second messengers. *Trends in Pharmacological Sciences*, **11**, 254-260.

Mayer, M.L., Vyklicky, L. & Clements, J. (1989) Regulation of NMDA receptor desensitization in mouse hippocampal neurons by glycine. *Nature*, **338**, 425-427.

McCulloch, J. (1992) Excitatory amino acid antagonists and their potential for the treatment of ischaemic brain damage in man. *British Journal of Clinical Pharmacology*, **34**, 106-114.

McCulloch, J. (1982) Mapping functional alterations in the CNS with [$^{14}$C]deoxyglucose; In *Handbook of Psychopharmacology*, ed. Iversen, L.L., Iversen, S.D. & Snyder, S.H., Vol. 15, pp.321-410, New York:Plenum Press.

McCulloch, J., Bullock, R. and Teasdale, G.M. (1991) Excitatory amino acid antagonists: opportunities for the treatment of ischaemic brain damage in man. In *Excitatory Amino Acid Antagonists*, ed. Meldrum, B.S., pp.287-326, Blackwell/Oxford.

McCulloch, J. & Iversen, L.L. (1991) Autoradiographic assessment of the effects of N-methyl-D-aspartate (NMDA) receptor antagonists in vivo. *Neurochemical Research*, **16**, 897-916.

McCulloch, J., Kelly, P.A.T., Grome, J.J. & Pickard, J.D. (1982a) Local cerebral circulatory and metabolic effects of indomethacin. *American Journal of Physiology*, **243**, H416-H423.

McCulloch, J., Savaki, H.E., McCulloch, M.C., Jehle, J. & Sokoloff, L. (1982b) The distribution of alterations in energy metabolism in the rat brain produced by apomorphine. *Brain Research*, **243**, 67-80.

McCulloch, J., Savaki, H.E. & Sokoloff, L. (1982c) Distribution of effects of haloperidol on energy metabolism in the rat brain. *Brain Research*, **243**, 81-90.

McCulloch, J., Savaki, H.E., McCulloch, M.C. & Sokoloff, L. (1980) Retina-dependent activation by apomorphine of metabolic activity in the superficial layer of the superior colliculus. *Science*, **207**, 313-315.

McCulloch, J., Wallace, M.C., Laurie, D., Angerson, W.J., Burns, H.D. & Gibson, R.E. (1992) Imaging activation in the NMDA receptor complex with $^{125}$Iodo-MK-801; In *Pharmacology of Cerebral Ischemia*, ed. Krieglstein, J. & Oberpichler-Schwenk, H., pp.59-63, Wissenschaftliche Verlagsgesellschaft mbH Stuttgart.

McGeer, P.L., Kamo, H., Harrop, R., McGeer, E.G., Martin, W.R.W., Pate, B.D. & Li, D.K.B. (1986) Comparison of PET, MRI and CT with pathology in a proven case of Alzheimer's disease. *Neurology*, **36**, 1569-1574.

McGeer, E.G. &. McGeer, P.L. (1976) Duplication of biochemical changes of Huntington's chorea by intrastriatal injections of glutamic and kainic acids. *Nature*, **263**, 517-519.

McKinney, M. & Coyle, J.T. (1982) Regulation of neocortical muscarinic receptors: effects of drug treatment and lesions. *The Journal of Neuroscience*, **2**, 97-105.

McLennan, H. & Lodge, D. (1979) The antagonists of amino acid-induced excitatory of spinal neurones in the cat. *Brain Research*, **169**, 83-90.

McMahon, H.T. & Nicholls, D.G. (1990) The relationship between cytoplasmic free Ca2+ and the release of glutamate from synaptosomes. *Biochemistry Society Transactions*, **18**, 375-377.

McMahon, H.T. & Nicholls, D.G. (1991) Transmitter glutamate release from isolated nerve terminals: evidence for biphasic release and triggering by localized Ca2+. *Journal of Neurochemistry*, **56**, 86-94.

Meister, A. (1979) Biochemistry of glutamate, glutamine and glutathione. In *Advances in Biochemistry and Physiology: Glutamic Acid*, ed. Keller, Jr., L.J., Garanti, S., Kane, M.R., Reynolds, W.A. & Wurtman, R.J., pp.64-84, Raven Press, New York.

Meldrum, B. (1990) Protection against ischaemic neuronal damage by drugs acting on excitatory neurotransmission. *Cerebrovascular Brain Metabolism Reviews*, **2**, 27-57.

Meldrum, B. & Garthwaite, J. (1990) Excitatory amino acid neurotoxicity and neurodegenerative disease. *Trends in Pharmacological Sciences*, **11**, 379-387.

Miller R.J., Brorson, J.R., Bleakman, D. & Chard, P.S. (1992) Glutamate receptors in the regulation of neuronal $Ca^{2+}$; In *Pharmacology of Cerebral Ischemia*, ed. Krieglstein, J. and Oberpichler-Schwenk, H., pp.3-11, Wissenschaftliche Verlagsgesellschaft mbH Stuttgart.

Miyaoka, M., Shinohara, M., Batipps, M., Pettigrew, K.D., Kennedy, C. & Sokoloff, L. (1979) The relationship between the intensity of the stimulus and the metabolic responses in the visual system of the rat. *Acta Neurologica Scandinavia*, **60**, (Suppl. 72), 16-17.

Monaghan, D.T., Bridges, R.J. & Cotman, C.W. (1989) The excitatory amino acid receptors: their classes, pharmacology, and distinct properties in the function of the central nervous system. *Annual Review of Pharmacology and Toxicology*, **29**, 365-402.

Monaghan, D.T. & Cotman, C.W. (1982) The distribution of [$^3$H] kainic acid binding sites as determined by autoradiography. *Brain Research*, **191**, 387-403.

Monaghan, D.T. and Cotman, C.W. (1985) Distribution of N-methyl-D-aspartate-sensitive L-[$^3$H]glutamate-binding sites in rat brain. *Journal of Neuroscience*, **5**, 2909-2919.

Monaghan, D.T., Olverman, H.J., Nguyen, L., Watson, J.C. & Cotman, C.W. (1988) Two classes of *N*-methyl-D-aspartate recognition sites: differential distribution and differential regulation by glycine. *Proceedings of the National Academy of Sciencies, U.S.A.*, **85**, 9836-9840.

Monaghan, D.T., Yao, D. & Cotman C.W. (1984a) Distribution of [$^3$H]AMPA binding sites in rat brain as determined by quantitative autoradiography. *Brain Research*, **324**, 160-164.

Monaghan, D.T., Yao, D., Olverman, H.J., Watkins, J.C. & Cotman, C.W. (1984b) Autoradiography of D-2-[$^3$H]amino-5-phosphonopentanoate binding sites in rat brain. *Neuroscience Letters*, **52**, 253-258.

Monahan, J.B., Corpus, V.M., Hood, W.F., Thomas, J.W. & Compton, R.P. (1989a) Characterization of a [$^3$H]glycine recognition site as a modulatory site of the *N*-methyl-D-aspartate receptor complex. *Journal of Neurochemistry*, **53**, 370-375.]

Monahan, J.B., Handelmann, G.E., Hood, W.F. & Cordi, A.A. (1989b) D-Cycloserine, a positive modulator of the N-methyl-D-aspartate receptor, enhances performance of learning tasks in rats. *Pharmacology, Biochemistry & Behavior*, **34**, 649-653.

Monyer, H., Sprengel, R., Scoepfer, R., Herb, a., Higuchi, M., Lomeli, H., Burnashev, N., Sakmann, B. & Seeburgh, P.H. (1992) Heteromeric NMDA receptors: molecular and functional distinction of subtypes. *Science*, **256**, 1217-1221.

Morad, M., Dichter, M. & Tang, C.M. (1988) The NMDA activated current in hippocampus neurons is highly sensitive to $[H^+]_o$. *Society for Neuroscience Abstracts*, **14**, 791.

Mori, K., Schmidt, K., Jay, T., Palombo, E., Nelson, T., Lucignani, G., Pettigrew, K., Kennedy, C. & Sokoloff, L. (1990) Optimal duration of experimental period in measurement of local cerebral glucose utilization with the deoxyglucose method. *Journal of Neurochemistry*, **54**, 307-319.

Moriyoshi, K., Masu, M., Ishii, T., Shigemoto, R., Mizuno, N. & Nakanishi, S. (1991) Molecular cloning and characterization of the rat NMDA receptor. *Nature*, **354**, 31-37.

Morris, R.G.M., Anderson, E., Lynch, G.S. & Baudry, M. (1986) Selective impairment of learning and blockade of long-term potentiation by an N-methyl-D-aspartate receptor antagonist, AP5. *Nature*, **319**, 774-776.

Motohashi, N., Nishikawa, T., Scatton, B. & Mackenzie E.T. (1986) Temporal effects of habenular lesions on glucose utilization in the anterior raphé nuclei of the rat. *Neuroscience Letters*, **67**, 245-250.

Muir, J.L., Dunnett, S.G., Robbins, T.W. & Everitt, B.J. (1992a) Attentional functions of the forebrain cholinergic systems: effects of intraventricular hemicholinium, physostigmine, basal forebrain lesions and intracortical grafts on a multiple-choice serial reaction time task. *Experimental Brain Research*, **89**, 611-622.

Muir, J.L., Robbins, T.W. & Everitt, B.J. (1992b) Disruptive effects of muscimol infused into the basal forebrain on conditional discrimination and visual attention: differential interactions with cholinergic mechanisms. *Psychopharmacology*, **107**, 541-550.

Murphy, S.N. & Miller, R.J. (1989) Regulation of $Ca^{++}$ influx into striatal neurons by kainic acid. *Journal of Pharmacology and Experimental Therapeutics*, **249**, 184-193.

Myers, R.D. (1966) Injections of solutions into cerebral tissue: relation between volume and diffusion. *Physiology and Behaviour*, **1**, 171-174.

Naito, S. & Ueda, T. (1985) Characterization of glutamate uptake into synaptic vesicles. *Journal of Neurochemistry*, **44**, 99-109.

Nedergaard, M. (1988) Mechanisms of brain damage in focal cerebral ischaemia. *Acta Neurologica Scandinavia*, **77**, 81-101.

Nehls, D.G., Kurumaji, A., Park, C.K. & McCulloch, J. (1988) Differential effects of competitive and non-competitive N-methyl-D-aspartate antagonists on glucose use in the limbic system. *Neuroscience Letters*, **91**, 204-210.

Nellgard, B. & Wieloch, T. (1992) Postischemic blockade of AMPA but not NMDA receptors mitigates neuronal damage in the rat brain following transient severe cerebral ischemia. *Journal of Cerebral Blood Flow and Metabolism*, **12**, 2-11.

Nelson, T., Dienel, G.A., Mori, K., Cruz, N.F. & Sokoloff, L. (1987) Deoxyglucose-6-phosphate stability in vivo and the deoxyglucose methods: response to comments of Hawkins and Miller. *Journal of Neurochemistry*, **49**, 1949-1960

Nicholls, D.G. (1989) Release of glutamate and aspartate from isolated nerve terminals. *Journal of Neurochemistry*, **52**, 331-341.

Nicholls, D.G. (1993) Ion channels and the regulation of neurotransmitter glutamate release. *Biochemical Society Transactions*, **21**, 53-58.

Nicholls, D. & Attwell, D. (1990) The release and uptake of excitatory amino acids. *Trends in Pharmacological Sciences*, **11**, 462-468.

Nowicki, J.P., Duval, D., Poignet, H. & Scatton, B. (1991) Nitric oxide mediates neuronal death after focal cerebral ischaemia in the mouse. *European Journal of Pharmacology*, **204**, 339-340.

Ogura, A., Akita, K. & Kudo, Y. (1990) Non-NMDA receptors mediated cytoplasmic $Ca^{2+}$ elevation in cultured hippocampal neurons. *Neuroscience Research*, **9**, 103-113.

Olney, J.W. (1969) Brain lesions, obesity, and other disturbances in mice treated with monosodium glutamate. *Science*, **164**, 719-721.

Olney, J.W. (1971) Glutamate-induced neuronal necrosis in the infant mouse hypothalamus. An electron microscopic study. *Journal of Neuropathology and Experimental Neurology*, **30**, 75-90.

Olney, J.W. & de Gubbareff, T. (1978) The fate of synaptic receptors in the kainate-lesioned striatum. *Brain Research*, **140**, 340-343.

Olney, J.W., Fuller, T. & de Gubbareff, T. (1979) Acute dendrotoxic changes in the hippocampus of kainate treated rats. *Brain Research*, **176**, 91-100.

Olney, J.W., Labruyere, J. and Price, M.T. (1989) Pathological changes induced in cerebrocortical neurons by phencyclidine and related drugs. *Science*, **244**, 1360-1362.

Olney, J.W., Labruyere, J., Wang, G., Wozniak, D.F., Price, M.T. & Sesma, M.A. (1991) NMDA antagonist neurotoxicity: mechanism and prevention. *Science*, **254**, 1515-1518.

Olsen, R.W., Szamraj, O. & Houser, C.R. (1987) [$^3$H]AMPA binding to glutamate receptor subpopulations in rat brain. *Brain Research*, **402**, 243-254.

Olverman, H.J., Monaghan, D.T., Cotman, C.W. & Watkins, J.C. (1986) [$^3$H]CPP, a new competitive ligand for NMDA receptors. *European Journal of Pharmacology*, **131**, 161-162.

Onodera, H, Sato, G. & Kogure, K. (1986) Lesions to Schaffer collaterals prevent ischemic death of CA1 pyramidal cells. *Neuroscience Letters*, **68**, 169-174.

Ornstein, P.L., Arnold, M.B., Augenstein, N.K., Lodge, D., Leander, J.D. and Schoepp, D.D. (1993) 3SR,4aRS,6RS,8aRS-6-(2-(1H-tetrazol-5-yl)ethyl)-decahydroisoquinoline-3-carboxylic acid: A structurally novel, systemically active, competitive AMPA receptor anatgonist. *Journal of Medical Chemistry*, **36**, 2046-2048.

Orzi, F., Diana, G., Casamenti, F., Palombo, E. & Fieschi, C. (1988) Local cerebral glucose utilization following unilateral and bilateral lesions of the nucleus basalis magnocellularis in the rat. *Brain Research*, **462**, 99-103.

Ottersen, O.P. & Storm-Mathisen, J. (1984) Glutamate- and GABA-containing neurons in the mouse and rat brain, as demonstrated with a new immunocytochemical technique. *The Journal of Comparative Neurology*, **229**, 374-392.

Ottersen, O.P. & Storm-Mathisen, J. (1987) Localization of amino acid neurotransmitters by immunocytochemistry. *Trends in Pharmacological Sciences*, **10**, 250-255.

Ozawa, S., Iino, M. & Tsuzuki, K. (1991) Two types of kainate response in cultured rat hippocampal neurons. *Journal of Neurophysiology*, **66**, 2-11.

Page, K.J., Everitt, B.J., Robbins, T.W., Marston, H.M. & Wilkinson, L.S. (1991) Dissociable effects on spatial maze and passing avoidance acquisition and retention following AMPA and ibotenic acid-induced excitotoxic lesions of the basal forebrain in rats: differential dependence on cholinergic neuronal loss. *Neuroscience*, **43**, 457-72.

Pan, Z.Z., Tong, G. & Jahr, C.E. (1993) A false transmitter at excitatory synapses. *Neuron*, **11**, 85-91.

Park, C.K., McCulloch, J., Kang, J.K. & Choi, C.R. (1991) Comparison of competitive and non-competitive NMDA antagonists in focal cerebral ischaemia in rats. *Journal of Cerebral Blood Flow and Metabolism*, **11**, S299.

Park, C.K., Nehls, D.G., Graham, D.I., Teasdale, G.M. & McCulloch, J. (1988a) Focal cerebral ischaemia in the cat: Treatment with the glutamate antagonist MK-801 after induction of ischemia. *Journal of Cerebral Blood Flow and Metabolism*, **8**, 757-762.

Park, C.K., Nehls, D.G., Graham, D.I., Teasdale, G.M. & McCulloch, J. (1988b) The glutamate antagonist MK-801 reduces focal ischemic brain damage in the rat. *Annals of Neurology*, **24**, 543-551.

Paxinos, G. & Watson, C. (1986) *The Rat Brain in Stereotaxic Coordinates.* Second Edition, Academic Press.

Pedata, F., Lo Cente, G., Sorbi, S., Marconcini-Pepeu, I. & Pepeu, G. (1982) Changes in high affinity choline uptake in rat cortex following lesions of the magnocellular forebrain nuclei. *Brain Research*, **233**, 359-367.

Peinado, J.M. & Mora, F. (1986) Glutamic acid as putative transmitter of the interhemispheric corticocotical connections in the rat. *Journal of Neurochemistry*, **47**, 1598-1603.

Pellegrini-Giampietro, D., Zukin, R.S., Bennett, M., Cho, S. & Pulsinelli, W. (1993) Switch in glutamate receptor subunit gene expression following global ischemia in rats. *Proceedings of the National Academy of Sciences, U.S.A.*, (in press).

Peng, C.T. (1977) Sample preparation in liquid scintillation. *Radiochemistry Centre Reviews*, **17**.

Perry, E.K., Perry, R.H., Blessed, G. & Tomlinson, B.E. (1978) Changes in brain cholinesterases in senile dementia of the Alzheimer type. *Neuropathology and Applied Neurobiology*, **4**, 273-277.

Potashner, S.J. (1978) The spontaneous and electrically evoked release, from slices of guinea-pig cerebral cortex, of endogenous amino acids labelled via metabolism of D-[U-14C]glucose. *Journal of Neurochemistry*, **31**, 177-186.

Procter, A.W., Palmer, A.M., Francis, P.T., Lowe, S.L., Neary, D., Murphy, E., Doshi, R. & Bowen, D.M. (1988) Evidence of glutamatergic denervation and possible abnormal metabolism in Alzheimer's disease. *Journal of Neurochemistry*, **50**, 790-802.

Procter, A.W., Stratmann, G.C., Francis, P.T., Lowe, S.L., Bertolucci, P.H.F. & Bowen, D.M. (1991) Characterisation of the glycine modulatory site of the *N*-methyl-D-aspartate receptor-ionophore complex in human brain. *Journal of Neurochemistry*, **56**, 299-310.

Procter, A.W., Wong, E.H.F., Stratmann, G.C., Lowe, S.L. & Bowen, D.M. (1989) Reduced glycine stimulation of [$^3$H]MK-801 binding in Alzheimer's disease. *Journal of Neurochemistry*, **53**, 698-704.

Pulsinelli, W.A., Brierley, J.B. & Plum, F. (1982) Temporal profile of neuronal damage in a model of transient forebrain ischemia. *Annals of Neurology*, **11**, 491-498.

Pulsinelli, W., Pellegrini-Giampietro, D., Zukin, S., Bennett, M. & Cho, S. (1992) AMPA receptors: their *in vivo* role in selective ischemic necrosis of CA1 hippocampal neurons. In *Pharmacology of Cerebral Ischemia*, ed. Krieglstein, J. & Oberpichler-Schwenk, H., pp.53-58, Wissenschaftliche Verlagsgesellschaft mbH Stuttgart.

Rainbow, T.C., Wieczorek, C.M. & Halpain, S. (1984) Quantitative autoradiography of binding sites for $^{3}$H-AMPA, a structural analogue of glutamic acid. *Brain Research*, **309**, 173-177.

Ransom, T.W. & Stec, N.L. (1988) Cooperative modulation of [$^{3}$H]MK-801 binding to the N-methyl-D-aspartate receptor-ion channel complex by L-glutamate, glycine and polyamines. *Journal of Neurochemistry*, **51**, 830-836.

Raymond, L.A., Blackstone, C.D. & Huganir, R.L. (1993) Phosphorylation of amino acid neurotransmitter receptors in synaptic plasticity. *Trends in Neurosciences*, **16**, 147-153.

Regan, R.F. & Choi, D.W. (1991) Glutamate neurotoxicity in spinal cord cell culture. *Neuroscience*, **43**, 585-591.

Reynolds, I.J. & Miller, R.J. (1988) [$^{3}$H]MK801 binding to the NMDA receptor/ionophore complex is regulated by divalent cations: evidence for multiple regulatory sites. *European Journal of Pharmacology*, **151**, 103-112.

Reynolds, I.J. & Miller, R.J. (1989) Ifenprodil is a novel type of N-methyl-D-aspartate receptor antagonist: interaction with polyamines. *Molecular Pharmacology*, **36**, 758-765.

Reynolds, I.J., Murphy, S.N. & Miller, R.J. (1988) [$^3$H]Labeled MK-801 binding to the excitatory amino acid receptor complex from rat brain is enhanced by glycine. *Proceedings of the National Academy of Sciences, U.S.A.*, **84**, 7744-7748.

Ribak, C.E., Vaughn, J.E. & Roberts, E. (1980) GABAergic nerve terminals decrease in the substantia nigra following hemitransections of the striatonigral and pallidonigral pathways. *Brain Research*, **192**, 413-420.

Richardson, R.T. & DeLong, M.R. (1988) A reappraisal of the functions of the nucleus basalis of Meynert, *Trends in Neurological Sciences*, **11**, 264-267.

Robbins, T.W., Everitt, B.J., Ryan, C.N., Marston, H.M., Jones, G.H. & Page, K.J. (1989a) Comparative effects of ibotenic acid- and quisqualic acid-induced lesions of the substantia innominata on attentional function in the rat: further implications for the role of the cholinergic neueons of the nucleus basalis in cognitive processes. *Behavioural Brain Research*, **35**, 221-240.

Robbins, T.W., Everitt, B.J., Ryan, C.N., Marston, H.M., Jones, G.H. & Page, K.J. (1989b) Comparative effects of quisqualic and ibotenic acid-induced lesions of the substantia innominata and globus pallidus on the acquisition of a conditional visual discrimination: differential effects on cholinergic mechanisms. *Neuroscience*, **28**, 337-352.

Roberts, E. &. Frankel, D. (1950) γ-Aminobutyric acid in brain: its formation from glutamic acid. *Journal of Biological Chemistry*, **187**, 55-63.

Rogawski, M.A. (1993) Therapeutic potential of excitatory amino acid antagonists: channel blockers and 2,3-benzodiazepines. *Trends in Pharmacological Sciences*, **14**, 325-331.

Rogers, J. & Morrison, J.H. (1985) Quantitative morphology and regional laminar distributions of senile plaques in Alzheimer's disease. *Journal of Neuroscience*, **5**, 2801-2808.

Rothman, S.M. & Olney, J.W. (1986) Glutamate and the pathophysiology of hypoxic-ischemic brain damage. *Annals of Neurology*, **19**, 105-111.

Rothman, S.M. & Olney, J.W. (1987) Excitotoxicity and the NMDA receptor. *Trends in Neurosciences*, **10**, 299-302.

Sacaan, A.I. & Johnson, K.M. (1990) Characterization of the stimulatory and inhibitory effects of polyamines on [$^3$H]N-(1-[thienyl]cyclohexyl) piperidine binding to the N-methyl-D-aspartate receptor ionophore complex. *Molecular Pharmacology*, **37**, 572-577.

Sakurada, O., Kennedy, C., Jehle, J., Brown, J.D., Carbin, G.L., Sokoloff, L. (1978) Measurement of local cerebral blood flow with iodo[$^{14}$C]antipyrine, *American Journal of Physiology*, **234**, H59-H66.

Sakurai, S.Y., Cha, J.-H.J., Penney, J.B. & Young, A.B. (1991) Regional distribution and properties of [$^3$H]MK-801 binding sites determined by quantitative autoradiography in rat brain. *Neuroscience*, **40**, 533-543.

Sakurai, S.Y., Penney, J.B. & Young, A.B. (1993) Regionally distinct *N*-methyl-D-aspartate receptors distinguished by quantitative autoradiography of [$^3$H]MK-801 binding in rat brain. *Journal of Neurochemistry*, **60**, 1344-1353.

Salt, T.E. (1989) Modulation of NMDA receptor-mediated responses by glycine and D-serine in the rat thalamus *in vivo*. *Brain Research*, **481**, 403-406.

Sarter, M., Bruno, J.P. & Dudchenko, P. (1990) Activating the damaged basal forebrain cholinergic system: tonic stimulation versus signal amplification. *Psychopharmacology*, **101**, 1-17.

Sato, K., Kiyama, H. & Tohyama, M. (1993) The differential expression patterns of messenger RNAs encoding non-*N*-methyl-D-aspartate glutamate receptor subunits (GluR1-4) in the rat brain. *Neuroscience*, 52, 515-539.

Savaki, H.E., Macpherson, H. & McCulloch, J. (1982) Alterations in local cerebral glucose utilization during hemorrhagic hypotension in the rat. *Circulation Research*, **50**, 633-644.

Schoepp, D.D. & Conn, P.J. (1993) Metabotropic glutamate receptors in brain function and pathology. *Trends in Pharmacological Sciences*, **14**, 13-20.

Schousboe, A., Westergaard, N. & Hertz, L. (1993) Neuronal-astrocytic interactions in glutamate metabolism. *Biochemical Society Transactions*, **21**, 49-53.

Schuier, F., Orzi, F., Suda, S., Lucignani, G., Kenney, C. & Sokoloff, L. (1990) Influence of plasma glucose concentration on lumped constant of the deoxyglucose method: Effects of hyperglycemia in the rat. *Journal of Cerebral Blood Flow and Metabolism*, **10**, 765-773.

Schuster, G.M. & Schmidt, W.J. (1992) D-Cycloserine reverses the working memory impairment of hippocampal-lesioned rats in a spatial learning task. *European Journal of Pharmacology*, **224**, 97-98.

Schwartz, W.J., Smith, C.B., Davidsen, L., Savaki, H.E., Sokoloff, L., Mata, M., Fink, D.J. and Gainer, H. (1979) Metabolic mapping of functional activity in the hypothalamo-neurohypophyseal system of the rat. *Science*, **205**, 723-725.

Scott, R.H., Sutton, K.G. & Dolphin, A.C. (1993) Interactions of polyamines with neuronal ion channels. *Trends in Neurosciences*, **4**, 153-160.

Seeburg, P.H. (1993) The molecular biology of mammalian glutamate receptor channels. *Trends in Neurosciences*, **16**, 359-365.

Shapiro, H.M., Greenberg, J.H., Reivich, M., Ashmead, G. & Sokoloff, L. (1978) Local cerebral glucose uptake in awake and halothane-anesthetized primates. *Anesthesiology*, **48**, 97-103.

Sheardown, M.J., Nielsen, E.Ø., Hansen, A.J., Jacobsen, P. & Honoré, T. (1990) 2,3-Dihydroxy-6-nitro-7-sulphamoyl-benzo(F)quinoxaline: A neuroprotectant for cerebral ischemia. *Science*, **247**, 571-574.

Sheardown, M.J., Suzdak, P.D. & Nordolm, L. (1993) AMPA, but not NMDA, receptor antagonism is neuroprotective in gerbil global ischaemia, even when delayed 24 h. *European Journal of Pharmacology*, **236**, 347-353.

Siesjö, B.K. (1978) *Brain Energy Metabolism*, John Wiley & Sons.

Siesjö, B.K. (1988) Historical overview. Calcium, ischemia, and death of brain cells. *Annals of the New York Academy of Sciences*, **522**, 638-661.

Siesjö, B.K. (1992) Pathophysiology and treatment of focal cerebral ischaemia. *Journal of Neurosurgery*, **77**, 169-184.

Siesjö, B.K. & Bengtsson, F. (1989) Calcium fluxes, calcium antagonists, and calcium-related pathology in brain ischemia, hypoglycemia, and spreading depression: a unifying hypothesis. *Journal of Cerebral Blood Flow and Metabolism*, **9**, 127-140.

Siesjö, B.K., Memezawa, H. & Smith, M.L. (1991) Neurocytotoxicity: pharmacological implications. *Fundamental Clinical Pharmacology*, **5**, 755-767.

Simmonds, M.A. & Horne, A.L. (1988) Barbiturates and excitatory amino acid interactions. In *Excitatory Amino Acids in Health and Disease*, ed. Lodge, D., pp.219-236, John Wiley and Sons, Chichester.

Simon, R. & Shiraishi, K., (1990) *N*-methyl-D-aspartate antagonist reduces stroke size and regional glucose metabolism. *Annals of Neurology*, **27**, 606-611.

Simon, R.P., Swan, J.H., Griffiths, T. & Meldrum, B.S. (1984) Blockade of *N*-methyl-D-aspartate receptors may protect against ischemic damage in the brain. *Science*, **226**, 850-852.

Singh, L., Oles, R.J. & Tricklebank, M.D. (1990) Modulation of seizure susceptibility in the mouse by the strychnine-insensitive glycine recognition site of the NMDA receptor/ion channel complex. *British Journal of Pharmacology*, **99**, 285-288.

Sirvio, J., Ekonsalo, T., Riekkinen Jr., P., Lahtinen, H. & Riekkinen Sr. P. (1992) D-cycloserine, a modulator of the N-methyl-D-aspartate receptor, improves spatial learning in rats treated with muscarinic antagonist. *Neuroscience Letters*, **146**, 215-218.

Smith, S.E., Dürmüller, N. & Meldrum, B.S. (1991) The non-N-methyl-D-aspartate receptor antagonists, GYKI 52466 and NBQX are anticonvulsant in two animal models of reflex epilepsy. *European Journal of Pharmacology*, **201**, 179-183.

Smith, S.E. and Meldrum, B.S. (1992) Cerebroprotective effect of a non-N-methyl-D-aspartate antagonist GYKI 52466, after focal ischemia in the rat. *Stroke*, **23**, 861-864.

Snell L.D., Morter, R.S. & Johnson, K.M. (1987) Glycine potentiates *N*-methyl-D-aspartate-induced [$^3$H]TCP binding to rat cortical membranes. *Neuroscience Letters*, **83**, 313-317.

Snyder, S.H. & Bredt, D.S. (1991) Nitric oxide as a neuronal messenger. *Trends in Pharmacological Sciences*, **12**, 125-128.

Sofroniew, M.V. & Pearson, R.C.A. (1985) Degeneration of cholinergic neurons in the basal nucleus following kainic or N-methyl-D-aspartic acid application to the cerebral cortex in the rat. *Brain Research*, **339**, 186-190.

Sokoloff, L., Reivich, M., Kennedy, C., Des Rosiers, M.H., Patlak, C.S., Pettigrew, K.D., Sakurada, O. & Shinohara, M. (1977) The [$^{14}$C]deoxyglucose method for the measurement of local cerebral glucose utilisation. Theory, procedure and normal values in the conscious and anaesthetised albino rat. *Journal of Neurochemistry*, **28**, 897-916.

Sokoloff, L. (1981) Localization of functional activity in the central nervous system by the measurement of glucose utilization with radioactive deoxyglucose. *Journal of Cerebral Blood Flow and Metabolism*, **1**, 7-36.

Sommer, B. & Seeburg, P.H. (1992) Glutamate receptor channels: novel properties and new clones. *Trends in Pharmacological Sciences*, **13**, 291-296.

Soncrant, T.T., Holloway, H.W., Horwitz, B., Rapoport, S.I. & Lamour, Y.A. (1992) Effects of nucleus basalis magnocellularis ablation on local brain glucose utilization in the Rat: Functional brain reorganization. *European Journal of Neuroscience*, **4**, 653-662.

Sprosen, T.S. & Woodruff, G.N. (1990) Polyamines potentiate NMDA induced whole-cell currents in cultured striatal neurons. *European Journal of Pharmacology*, **179**, 477-478.

Stone, T.W. (1979) Amino acids as neurotransmitters of corticofugal neurons in the rat: a comparison of glutamate and aspartate. *British Journal of Pharmacology*, **67**, 545-551.

Stone, T.W. & Burton, N.R. (1988) NMDA receptors and ligands in the vertebrate CNS. *Progress in Neurobiology*, **30**, 333-368.

Sugihara, H., Moriyoshi, K., Ishii, T., Masu, M. & Nakanishi, S. (1992) Structures and properties of seven isoforms of the NMDA receptor generated by alternative splicing. *Biochemical and Biophysiological Research Communications*, **185**, 826-832.

Sugiyama, H., Ito, I. & Hirono, C. (1987) A new type of glutamate receptor linked to inositol phospholipid metabolism. *Nature*, **325**, 531-533.

Suzdak, P.D. & Sheardown, M.J. (1992) The effect of the specific AMPA receptor antagonist NBQX upon local cerebral glucose utilization in the rat. *Society for Neuroscience Abstracts*, **412.2**.

Tamura, A., Graham, D.I., McCulloch, J. & Teasdale, G.M. (1981a) Focal cerebral ischaemia in the rat: I. Description of technique and early neuropathological consequences following middle cerebral artery occlusion. *Journal of Cerebral Blood Flow and Metabolism*, **1**, 53-60.

Tamura, A., Graham, D.I., McCulloch, J. & Teasdale, G.M. (1981b) Focal cerebral ischemia in the rat: 2. Regional cerebral blood flow determined by [$^{14}$C]iodoantipyrine autoradiography following middle cerebral artery occlusion, *Journal of Cerebral Blood Flow and Metabolism*, **1**, 61-69.

Tarnawa, I., Engberg, I. & Flatman, J.A. (1990) GYKI 52466, an inhibitor of spinal reflexes is a potent quisqualate antagonist. In *Amino Acids: Chemistry, Biology and Medicine*, ed. Lubec, G. & Rosenthal, G.A., pp.538.

Taxt, T. & Storm-Mathisen, J. (1984) Uptake of D-aspartate and L-glutamate in excitatory axon terminals in hippocampus: autoradiographic and biochemical comparison with gamma-aminobutyrate and other amino acids in normal rats and in rats with lesions. *Neuroscience*, **11**, 79-100.

Thomas, J.W., Hood, W.F., Monagan, J.B., Contreras, P.C. & O'Donohue, T.L. (1988) Glycine modulation of the phencyclidine binding site in mammalian brain. *Brain Research*, **442**, 396-398.

Thomson, A.M., Walker, V.E. & Flynn, D.M. (1989) Glycine enhances NMDA-receptor mediated synaptic potentials in neocortical slices. *Nature*, **338**, 422-424.

Toga, A.W. & Collins, R.C. (1981) Metabolic response of optic centers to visual stimuli in the albino rat: anatomical and physiological considerations. *Journal of Comparative Neurology*, **199**, 443-464.

Tombaugh, G.D. & Sapolsky, R.M. (1990) Mild acidosis protects hippocampal neurons from injury induced by oxygen and glucose deprivation. *Brain Research*, **506**, 343-345.

Tremblay, E., Ottersen, O.P., Rovira, C. & Ben-Ari, Y. (1983) Intra-amygdaloid injections of kainic acid: regional metabolic changes and their relation to the pathological alterations. *Neuroscience*, **8**, 299-315.

Trifilleti, R.R. (1992) Neuroprotective effects of $N^G$-nitro-L-arginine in focal stroke in the 7-day-old rat. *European Journal of Pharmacology*, **218**, 197-198.

Unnerstall, J.R. & Wamsley, J.K. (1983) Autoradiographic localization of high affinity [$^3$H]kainic acid binding sites in the rat forebrain. *European Journal of Pharmacology*, **83**, 361-371.

Van Der Kooy, D. & Carter, D.A. (1981) The organization of the efferent projections and striatal afferents of the entopeduncular nucleus and adjacent areas in the rat. *Brain Research*, **211**, 15-36.

Van Harreveld, A. (1959) Compounds in brain extracts causing spreading depression of cerebral cortical activity and contraction of crustacean muscle. *Journal of Neurochemistry*, **3**, 300-315.

Verdoorn, T.A., Burnashev, N., Monyer, H., Seeburg, P.H. & Sakmann, B. (1991) Structural determinants of ion flow through recombinant glutamate receptor channels. *Science*, **252**, 1715-1718.

Vigé, X., Carreau, A., Scatton, B. & Nowicki, J.P. (1993) Antagonism by $N^G$-nitro-L-arginine of L-glutamate-induced neurotoxicity in cultured neonatal rat cortcial neurons. Prolonged application enhances neuroprotective efficacy. *Neuroscience*, **55**, 893-901.

Vogt, B.A., Rosene, D.L. & Peters, A. (1981) Synaptic termination of thalamic and callosal afferents in cingulate cortex of the rat. *The Journal of Comparative Neurology*, **201**, 265-283.

Wallace, M.C., Teasdale, G.M. & McCulloch, J. (1992) Autoradiographic analysis of $^3$H-MK-801 (dizocilpine) *in vivo* uptake and *in vitro* binding after focal cerebral ischemia in the rat. *Journal of Neurosurgery*, **76**, 127-133.

Watkins, J.C., Krogsgaard-Larsen, P. & Honoré, T. (1990) Structure-activity relationships in the development of excitatory amino acid receptor agonists and competitive antagonists. *Trends in Pharmacological Sciences*, **11**, 25-33.

Watson, G.B., Bolanowski, M.A., Baganoff, M.P., Deppeler, C.L. & Lanthorn, T.H. (1990) D-Cycloserine acts as a partial agonist at the glycine modulatory site of the NMDA receptor expressed in *Xenopus* oocytes. *Brain Research*, **510**, 158-160.

Weil-Malherbe, H. (1950) Significance of glutamic acid for the metabolism of nervous tissue. *Physiology Reviews*, **30**, 549-568.

Weissman, A.D., Dam, M. and London, E.D. (1987) Alterations in local cerebral glucose utilization induced by phencyclidine. *Brain Research*, **435**, 29-40.

Wenk, G.L. (1984) Pharmacological manipulations of the substantia innominata-cortical cholinergic pathway. *Neuroscience Letters*, **51**, 99-103.

Wenk, G.L., Markowska, A.L. & Olton, D.S. (1989) Basal forebrain lesions and memory: Alterations in neurotensin, not acetylcholine, may cause amnesia. *Behavioral Neuroscience*, **103**, 765-769.

Wenk, G.L. & Olton, D.S. (1984) Recovery of neocortical cholineacetyltransferase activity following ibotenic acid injection into the nucleus basalis of Meynert in rats. *Brain Research*, **293**, 184-186.

Westbrook, G.L. & Mayer, M.L. (1987) Micromolar concentrations of Zn2+ antagonize NMDA and GABA responses of hippocampal neurons. *Nature*, **328**, 640-643.

Whitehouse, P.J., Price, D.L., Struble, R.G., Clark, A.W. & Coyle, J.T. (1982) Alzheimer's disease and senile dementia: loss of neurons in the basal forebrain. *Science*, **215**, 1237-1239.

Wieloch, T., Gustafsson, I. & Westerberg, E. (1989) The NMDA antagonist, MK-801, is cerebro-protective in situations where some energy production prevails but not under conditions of complete energy deprivation. *Journal of Cerebral Blood Flow and Metabolism*, **9**, (Suppl. 1), S6.

Wieloch, T., Lindvall, O., Blomquist, P. & Gage, F.H. (1985) Evidence for amelioration of ischaemic neuronal damage in the hippocampal formation by lesions of the perforant path. *Neurology Research*, **7**, 24-26.

Wong, E.H.F., Knight, A.R. & Ransom, R. (1987) Glycine modulates [$^3$H]-MK-801 binding to the NMDA receptor in rat brain. *European Journal of Pharmacology*, **142**, 487-488.

Wood, P.L. (1985) Pharmacological evaluation of GABAergic and glutamatergic inputs to the nucleus basalis-cortical and septal-hippocampal cholinergic projections. *Canadian Journal of Physiology and Pharmacology*, **64**, 325-328.

Wood, P.L., Emmett, M.R., Rao, T.S., Mick, S., Cler, J. & Iyengar, S. (1989) In vivo modulation of the *N*-methyl-D-aspartate receptor complex by D-serine: Potentiation of ongoing neuronal activity as evidenced by increased cerebellar cyclic GMP. *Journal of Neurochemistry*, **53**, 979-981.

Wooten, G.F. & Collins, R.C. (1980) Regional brain glucose utilization following intrastriatal injections of kainic acid. *Brain Research*, **201**, 173-184.

Yamaguchi, T., Kunimoto, M., Pappata, S., Chavoix, C., Brouillet, E., Riche, D., Mazière, M., Naquet, R., MacKenzie, E.T. & Baron, J.-C. (1990) Effects of unilateral lesion of the nucleus basalis of Meynert on brain glucose utilization in callosotomized baboons: A PET study. *Journal of Cerebral Blood Flow and Metabolism*, **10**, 618-623.

Yeh, G.C., Bonhaus, D.W. & McNamara, J.O. (1990) Evidence that zinc inhibits *N*-methyl-D-aspartate receptor-gated ion channel activation by noncompetitive antagonism of glycine binding. *Molecular Pharmacology*, **38**, 14-19.

Young, A.B & Fagg, G.E. (1990) Excitatory amino acid receptors in the brain: membrane binding and receptor autoradiographic approaches. *Trends in Pharmacological Sciences*, **11**, 126-133.

Zaborszky, L., Heimer, L., Eckenstein, F. & Leranth, C. (1986) GABAergic input to cholinergic forebrain neurons: an ultrastructural study using retrograde tracing of HRP and double immunolabelling. *Journal of Comparative Neurology*, **250**, 282-295.

Zeman, S. & Lodge, D. (1991) Barbiturates selectively reduce depolarising responses to kainate rather than those to AMPA in neonatal rat spinal cord *in vitro*. *British Journal of Pharmacology*, **104**, suppl., 335P.

Zheng, F. & Gallagher, J.P. 1992) Metabotropic glutamate receptors are required for the induction of long-term potentiation. *Neuron*, **9**, 163-172.

Zhou, N. & Parks, T.N. (1991) Pharmacology of excitatory amino acid neurotransmission in nucleus laminaris of the chick. *Hearing Research*, **52**, 195-200.

Zorumski, C.F., Yamada, K.A., Price, M.T. & Olney, J.W. (1993) A benzodiazepine recognition site associated with the non-NMDA glutamate receptor. *Neuron*, **10**, 61-67.

## LIST OF PUBLICATIONS

### DEFINITIVE PAPERS

Browne, S.E. & McCulloch, J. (1993) AMPA receptor antagonists and local cerebral glucose utilization in the conscious rat. *Brain Research*, (in press).

Fujisawa, H., Dawson, D., Browne, S.E., Mackay, K.B., Bullock, R. & McCulloch, J. (1993) Pharmacological modification of glutamate neuroxicity *in vivo*. *Brain Research*, (in press).

Browne, S.E., Horsburgh, K., Dewar, D. & McCulloch, J. (1991) D-[$^3$H]-aspartate binding does not locate glutamate-releasing neurones in the retino-fugal projection: an autoradiographic comparison with [$^3$H]cyclohexyladenosine binding. *Molecular Neuropharmacology*, **1**, 129-133.

Browne, S.E., Muir, J.L., Everitt, B., Robbins, T.W. & McCulloch, J. (1993) Manipulations of excitatory amino acid receptors in the basal forebrain: Effects on local cerebral glucose utilisation (in preparation).

### ABSTRACTS

Browne, S.E., Page, K.J., Everitt, B.J., Robbins, T.W. & McCulloch, J. (1992) An *in vivo* assessment of functional consequences of basal forebrain excitotoxic lesions in the rat using [$^{14}$C]2-deoxyglucose autoradiography. *Neuroscience Letters*, **42**, Suppl., S37.

Browne, S.E., Muir, J., Everitt, B.J., Robbins, T.W. & McCulloch, J. (1992) The acute effects of infusions of AMPA, NMDA and muscimol into the basal forebrain on cerebral function in the rat. *British Journal of Pharmacology*, **107**, 56P.

Browne, S.E., Horsburgh, K., Dewar, D. & McCulloch, J. (1991) An autoradiographic comparison of D-[$^3$H]aspartate and [$^3$H]cyclohexyladenosine binding in the rat visual system after orbital enucleation. *British Journal of Pharmacology*, **102**, 285P.

Browne, S.E., Horsburgh, K., Dewar, D. & McCulloch, J. (1991) D-[$^3$H]-aspartate binding does not map glutamate terminals in the rat visual system - an autoradiographic study. *Journal of Cerebral Blood Flow and Metabolism*, **11** Suppl. 2, S599.

Browne, S.E. & Macrae, I.M. (1993) An autoradiographic study of changes in glucose use in rat brain stem following a hypotensive dose of rilmenidine or BHT-933. *Society for Neuroscience Abstracts*, **19**, 133.3.

Mackay, K.B., Browne, S.E. & McCulloch, J. (1993) Modulation of glutamate mechanisms with enadoline and NBQX: local cerebral glucose utilization in the rat. *Journal of Cerebral Blood Flow and Metabolism*, **13** Suppl. 1, S786.

Fujisawa, H., Bullock, R., Dawson, D., Browne, S., Mackay, K.B. & McCulloch, J. (1993) Pharmacological intervention in a new *in vivo* model of glutamate neurotoxicity. *Second International Neurotrauma Symposium*, **2**, P57.